Technical Report

TR-11-06

Alternative buffer material

Status of the ongoing laboratory investigation of reference materials and test package 1

Daniel Svensson, Svensk Kärnbränslehantering AB

Ann Dueck, Ulf Nilsson, Siv Olsson, Torbjörn Sandén
Clay Technology AB

Sara Lydmark, Sara Jägerwall, Karsten Pedersen
Microbial Analytics Sweden AB

Staffan Hansen, LTH Lund University

July 2011

Svensk Kärnbränslehantering AB
Swedish Nuclear Fuel
and Waste Management Co

Box 250, SE-101 24 Stockholm
Phone +46 8 459 84 00

ISSN 1404-0344
SKB TR-11-06

Alternative buffer material

Status of the ongoing laboratory investigation of reference materials and test package 1

Daniel Svensson, Svensk Kärnbränslehantering AB

Ann Dueck, Ulf Nilsson, Siv Olsson, Torbjörn Sandén
Clay Technology AB

Sara Lydmark, Sara Jägerwall, Karsten Pedersen
Microbial Analytics Sweden AB

Staffan Hansen, LTH Lund University

July 2011

Keywords: Bentonite, Mineralogy, Swelling pressure, Hydraulic conductivity, Unconfined compression test, Iron-bentonite, Iron, X-ray diffraction.

A pdf version of this document can be downloaded from www.skb.se.

Abstract

Bentonite clay is part of the Swedish KBS-3 design of final repositories for high level radioactive waste. Wyoming bentonite with the commercial name MX-80 (American Colloid Co) has long been the reference for buffer material in the KBS-3 concept. Extending the knowledge base of alternative buffer materials will make it possible to optimize regarding safety, availability and cost. For this reason the field experiment Alternative Buffer Material (ABM) was started at Äspö Hard Rock Laboratory during 2006. The experiment includes three medium-scale test packages, each consisting of a central steel tube with heaters, and a buffer of compacted clay. Eleven different clays were chosen for the buffers to examine effects of smectite content, interlayer cations and overall iron content. Also bentonite pellets with and without additional quartz are being tested. The buffer in package 1 had been subjected to wetting by formation water and heating for more than two years (at 130°C for ~ 1 year) when it was retrieved and analyzed. The main purposes of the project were to characterise the clays with respect to hydro-mechanical properties, mineralogy and chemical composition and to identify any differences in behaviour or long term stability. The diversity of clays and the heater of steel also make the experiment suitable for studies of iron-bentonite interactions. This report concerns the work accomplished up to now and is not to be treated as any final report of the project.

Reference clays

The hydro-mechanical standard tests (water content as delivered, free swelling, liquid limit and grain density) showed the large diversity of the materials included in the ABM project. The liquid limit varies between 68% (Friedland) up to 545% (MX-80). There was also a clear difference between the different materials regarding the grain density. Eight of the tested materials had a grain density between 2,678 and 2,753 kg/m^3 while three of the materials (Asha, Rokle and Friedland) had a grain density between 2,828 and 2,940 kg/m^3.

Most clays had a rather high CEC values which is typical for bentonites. Friedland and Callovo-Oxfordian was much lower in CEC which is compatible with their different mineralogy. The extractable amount of sulphate and chloride was not negligible. Ikosorb, Friedland and Asha 505 had 0.2–0.3 wt% chloride. MX-80, IbecoSeal, Deponit CA-N and Friedland had 0.3–0.5 wt% sulphate, the most likely source is gypsum which is a water soluble hydrated calcium sulphate. Fluoride and bromide are very low in all cases. Elevated amounts of Mn in Rokle indicate possible presence of undetected Mn-phase. Rather high Si in Calcigel and Rokle (compared to Kunigel that is low but high in quartz) possibly indicates the presence of amorphous silica.

The chemical data and evolved gas analysis confirmed the variety in the clays regarding e.g. iron content. Kunigel with only 1.9 wt% Fe_2O_3 can be compared to Asha 505 and Rokle with 12.2 and 13.7 wt% respectively. Organic carbon was low in most cases, but higher in Callovo-Oxfordian (0.7) and Friedland (0.5) wt%. The total sulfur content was very low (< 0.2 wt%) in Rokle, Ikosorb, Febex, Calcigel, Asha 505, low (< 0.5 wt%) in MX80, Ibecoseal and Kunigel, and higher in Friedland (0.53) and Callovo-oxfordian (0.68). X-ray diffraction was used to show the variability in the crystalline phases of the clays. Most clays were found to be dominated by dioctahedral smectites. Two dimensional diffraction data was also presented to illustrate difficulties in milling the mineral grains appropriately.

A drastic difference in microbial abundance between the examined materials was observed; Kunigel V1 was close to sterile while Friedland and Ibeco Seal M-90 contained high numbers of all microbes examined. It was found that 200–84,000 g^{-1} aerobic microbes were present in ten of the eleven dry materials, while Kunigel V1 lacked detectable aerobic microorganisms. Iron reducers were detected in all examined materials, ranging from 10 (in Kunigel V1) to 8,000 g^{-1} (in Ibeco Seal M-90). Autotrophic acetogens was detected in the range of 20–60 g^{-1} in the Febex, Friedland and Ibeco Seal materials, and below 10 g^{-1} in the other materials examined. Sulphate reducers were detected in the range of 10–90 g^{-1} in Asha 505, Calcigel, Deponit CA-N, Febex, Friedland and Ibeco Seal M-90,

and was below 10 g^{-1} in the other materials. In addition, the temperature tolerance of sulphide- and acetate-producing microorganisms in the dry clays was studied. The dominant part of sulphate reducers and acetogens in the materials thrived in the thermophilic temperature range and grew faster at 50°C than at 20°C. A correlation between produced acetate and sulphide was observed, suggesting that acetogenesis boosted the sulphate-reducing populations in the clay mineral systems. The studies showed that dry clay is a very potent media for long term survival of both aerobic, anaerobic and thermophilic microbes and as it seems from phylogenetic studies, not spore-formers only.

Clays from ABM package 1

At excavation, the water content, dry density, and degree of saturation were determined for all the different types of clays. The degree of saturation was very close to 100% in all samples.

Hydraulic conductivity and swelling pressures were determined on MX-80, Asha 505 and Deponit CAN. No difference was seen in hydraulic conductivity between samples from the field experiment and the corresponding reference materials. However, a significant decrease in swelling pressure was seen on Asha 505 and Deponit CAN. The largest deviation was noticed on samples from the innermost part, which was also the warmest part during the experiment. One explanation for the registered decrease in swelling pressure may be that there has been a significant redistribution of cations in the test package and this may have influenced the physical properties of the clays. Mechanical properties were determined by unconfined compression tests on MX-80, Asha and Deponit CAN. Reduced strain, i.e. less strain compared to reference specimens, was observed on re-saturated specimens of all three materials from the field experiment. Regarding maximum deviator stress and compared to reference material no large deviations was seen on specimens of MX-80 and Deponit CAN while a decreased maximum deviator stress was seen on Asha specimens and especially on specimens taken from the innermost position. Unconfined compression tests were also run on air-dried, ground, re-compacted and re-saturated material of MX-80, Asha and Deponit CAN from the field experiment. Those tests showed strain of the same size or larger than observed on the reference specimens while the maximum deviator stress was of the same size.

Eleven blocks of different clays were analyzed for exchangeable cations and water-soluble salts. In addition, the cation exchange capacity (CEC), the mineralogy and the chemical composition were determined for the bulk of MX-80, Calcigel, Asha 505 and Deponit CAN.

The distribution of chloride indicated that the wetting with groundwater resulted in laterally and vertically smoothed and almost constant concentrations. In contrast, the sulfate distribution displayed no consistent pattern, but some blocks had a sulfate maximum at the heater, along with depletion in the peripheral parts, indicating a lateral transfer of sulfate.

The test conditions also resulted in significant changes in the exchangeable cation pool. Whereas lateral gradients within the blocks were insignificant, a vertical gradient in the relative cation distribution had developed, dividing the package into an upper, Ca-dominated, and a lower, Na-dominated part. The distribution of acid soluble carbon indicated carbonate dissolution close to the heater in the carbonate-bearing bentonites. Furthermore, the iron content had increased in several of the blocks, suggesting that iron released by corrosion of the steel had been incorporated into the bentonite matrix.

All four blocks examined displayed a deficit in magnesium in the peripheral parts and a more or less distinct gradient towards to the heater. The XRD-data for random powders provided no evidence of any significant change of the smectite structure in any of the four blocks examined. Supplementary analyses of clay fractions are, however, necessary for more detailed evaluations.

It was found that mesophilic aerobic bacteria were present in the range of 10^2–10^3 g^{-1}wet weight (gww^{-1}) in Asha 505, Deponit CA-N and MX-80. All other bacteria were below detection in the materials in the test package 1. Thus, the results in this report show that bacteria with potential corrosive or buffer degradation properties were present in the raw bentonites and how the same mostly failed to survive after in-situ incubation at high swelling pressure and temperatures exceeding 90°C.

Sammanfattning

Bentonitlera används som buffertmaterial i SKBs KBS-3 metod för slutförvaring av använt kärnbränsle. Wyomingbentonit med det kommersiella namnet MX-80 (American Colloid Co) har länge använts som standardlera för bufferten, men för att optimera säkerhet, tillgänglighet samt kostnader behöver man mer kunskap om andra bentonitsorter. Av denna anledning startades fältförsöket Alternativa Buffertmaterial (ABM) 2006 på Äspölaboratoriet. Elva olika leror av varierande sammansättning och genes inkluderades i försöket, dels som kompakterade ringar och dels som pelletsfyllda burar. Centralvärmaren i försöket är av järn vilket gör försöket lämpligt för studier av interaktionen mellan metalliskt järn och bentonit.

Delförsöket ABM 1 avbröts 2009. Bufferten hade då varit utsatt för bevätning med grundvatten och förhöjd temperatur i mer än två år (130°C under c:a ett år). Denna rapport inkluderar resultat som uppnåtts till dags datum och ska inte ses som en slutrapport för projektet.

Referensleror

Bestämningarna av vattenkvot vid leverans, fri svällning, flytgräns och korndensitet visade stor variation mellan de olika material som ingår i ABM projektet. Flytgränsen varierade mellan 68% (Friedland) och 545% (MX-80). En tydlig skillnad noterades i korndensitet hos de olika materialen. Åtta av de testade materialen hade en korndensitet mellan 2 678 och 2 753 kg/m^3 medan tre av materialen (Asha, Rokle och Friedland) hade en korndensitet mellan 2 828 och 2 940 kg/m^3. Repeterbarheten av katjonutbyteskapaciteten (CEC) var tämligen god mellan olika mättillfällen och mellan olika laboranter. De flesta lerorna hade relativt höga CEC värden vilket är typiskt för bentonitleror. För att på ett så korrekt sätt som möjligt jämföra två prover med varandra bör de undersökas vid ett och samma tillfälle av en och samma laborant. Bulkkemi data bekräftade skillnader mellan lerornas varierande innehåll. Järninnehållet varierade från 1,9 vikt% Fe_2O_3 i Kunigel till 13,7 vikt% i Rokle leran. Innehållet av organiskt kol var lågt i de flesta lerorna med undantag av Callovo-oxfordian (0,7 %) och Friedland (0,5 %). Med röntgendiffraktion (XRD) kunde lerornas kristallina huvudkomponenter bestämmas. De flesta lerorna dominerades av dioktahedriska smektitmineral.

Leror från fältförsöket ABM 1

Vid upptaget bestämdes vattenkvot, torrdensitet och vattenmättnadsgrad på prover tagna från alla materialtyperna. Vattenmättnadsgraden var väldigt nära 100 % för alla materialen.

Den hydrauliska konduktiviteten och svälltrycket bestämdes på materialen MX-80, Asha och Deponit CAN. Ingen skillnad kunde noteras i hydraulisk konduktivitet mellan prover tagna från fältförsöket och prover tagna från respektive referensmaterial. Däremot kunde en tydlig minskning i svälltryck observeras hos Asha och Deponit CAN i prover från fältförsöket. Störst avvikelse noterades hos prover som tagits från den innersta delen av bufferten som utsatts för varmast förhållande under fältförsöket. En förklaring till minskningen i svälltryck kan vara den stora omfördelning av katjoner som ägt rum inom försökspaketet under försökstiden vilket kan ha påverkat de fysikaliska egenskaperna hos de aktuella materialen.

De mekaniska egenskaperna hos MX-80, Asha och Deponit CAN bestämdes med enaxliga tryckförsök. Minskade töjningar, det vill säga mindre töjningar än hos motsvarande referensprover, observerades på de prover som tagits från fältförsöket och därefter vattenmättats. Den maximala deviatorspänning hos proverna av MX-80 och Deponit CAN avvek däremot inte från motsvarande referensprover medan minskad maximal deviatorspänning kunde observeras hos prover av Asha och då speciellt på prover som tagits från de innersta positionerna.

Enaxliga tryckförsök utfördes dessutom på prover från samma tre materialtyper men som torkats, malts, återkompakterats och därefter vattenmättats. Resultat från dessa försök visade samma eller större töjningar vid brott jämfört med motsvarande referensprover medan den maximala deviatorspänningen var av samma storleksordning som hos referensproverna.

Vattenlösliga salter och utbytbara katjoner bestämdes i elva block av olika leror. Utöver dessa analyser bestämdes katjonbyteskapacitet (CEC), mineralogisk och kemisk sammansättning för bulkprov av MX-80, Calcigel, Asha och Deponit CAN. De ursprungliga skillnaderna i bentoniternas kloridhalt hade utjämnats under fältförsöket, då bentoniterna mättats med grundvatten. Även sulfat hade omfördelats och i vissa block sågs en anrikning närmast värmaren, medan ytterdelen av blocken förlorat sulfat. Försöksbetingelserna resulterade också i väsentligt ändrade proportioner mellan de utbytbara katjonerna, varigenom de ursprungliga skillnaderna mellan lerorna slätats ut. Istället hade en tydlig vertikal gradient utbildats inom bufferten – bentoniterna i övre delen var Ca-dominerade medan bentoniterna i nedre delen var Na-dominerade. Närmast värmaren av stål hade flera av blocken förhöjda järnhalter samtidigt som tydliga färgförändringar kunde ses i leran. Vidare hade karbonathaltiga bentoniter förlorat en del karbonat närmast värmaren. Magnesium, å andra sidan, uppvisade ett underskott i blockens yttre del och en mer eller mindre tydlig koncentrationsgradient mot värmaren. Några strukturella förändringar hos smektiten kunde inte påvisas vid röntgendiffraktionsanalys av oorienterade bulkprov. En mer detaljerad utvärdering av lermineralstrukturer kräver dock kompletterande röntgenundersökningar av orienterade preparat före och efter diagnostiska förbehandlingar.

Contents

1 Introduction

Bentonite clay is part of the Swedish KBS-3 design for final repositories of high level radioactive waste. In the KBS-3 design copper canisters will work as corrosion resistant containers of the waste when placed at approximately 500 m depth in crystalline rock. Between the canister and the rock, compacted bentonite blocks are emplaced as buffer material in order to minimize water flow and transport between the rock and the canister. The swelling pressure of the clay will keep the canister in place and the microbiological activity low, while the plasticity of the clay should be high enough not to transfer any force from the rock in case of rock displacements.

The MX80 bentonite from American Colloid Co (Wyoming) has long been the reference for buffer material in the KBS-3 concept. Extending the knowledge base of alternative buffer materials will make it possible to optimise regarding safety, availability and cost. For this reason the field experiment Alternative Buffer Material was started at Äspö Hard Rock Laboratory during 2006. Eleven different clays have been chosen to examine effects of smectite content, interlayer cations and overall iron content. Also bentonite pellets with and without additional quartz are being tested. The main purposes of the project are to characterise the mineralogical content of the clays and to identify any differences in behaviour or long term stability. Recent research (Lantenois et al. and Carlson et al.) indicates that the bentonite buffer is sensitive to the presence of metallic iron. This is of high importance since the copper canisters in the KBS-3 concept have an iron insert and iron is also present in other parts of the repository as rock reinforcement etc. The diversity of clays and the more repository like conditions of the experiment (compacted clay, non-powdered source of metallic iron, swelling pressure from the clay, large scale, in situ at repository depth, natural water from the bedrock) will give some important results in the field of iron-bentonite interactions.

This experiment is an SKB project with several international partners collaborating in the part of laboratory experiments and analysis.

This report concerns the work accomplished to this point and is not to be treated as any final report of the project.

2 Objectives

2.1 General

The laboratory program was designed to determine important properties such as:

- The amount of smectites.
- The mineralogy of the bentonites.
- The content of carbon, organic carbon and sulfur.
- Microbiological organisms (types and amounts).
- Cation exchange capacity.
- Cations and anions present in the clays.
- Iron redox chemistry.
- Hydro-mechanical properties of the buffer.

The large number of clays included in the project makes it impractical to study them all at equal level of detail. Hence in some cases only some of the clays have been selected for analysis. In order to perform the oxygen sensitive iron redox analysis a new sampling procedure was developed.

2.2 Mineralogical stability

One of the most important properties of the buffer material is its mineralogical stability over time in order to enable the long term functioning of the buffer. The long term stability of Wyoming montmorillonite in contact with a copper canister is studied in another SKB project named LOT. The identified potential processes in LOT are divided into:

1. Smectite to illite conversion.
2. Dissolution and neoformation of accessory minerals.
3. Cation exchange.
4. Salt transport.

In the ABM project the same processes are studied on a variety of clays. Additionally an iron heater is present instead of copper. As metallic iron is much less stable in the repository environment compared to copper some additional potential processes needs to be added:

5. Iron corrosion product build-up.
6. Iron-bentonite interaction.

According to literature the corrosion and/or its products seem to in some cases react with the clay minerals creating new non-swelling minerals (Lantenois 2005).

The most probable scenarios of iron-bentonite interaction:

- Formation of ion exchanged iron-montmorillonite.
- Reduction of the iron in the octahedral sheet of the montmorillonite structure, possibly coupled to dehydroxylation (reversible or irreversible).
- Dissolution and/or transformation of the montmorillonite.
- Formation of corrosion products with possible cementation of the buffer.

All scenarios will probably affect the buffer performance to some extent. The rate and degree of destabilisation of the smectite seems to depend on the nature of the smectite (dioctahedral/trioctahedral, counter ion and Fe^{III}-content) (Lantenois 2005). The effect of the iron reduction might have a negative impact on the hydraulic conductivity and the swelling properties. The cation fixation capacity has been noticed to increase (Khaled and Stucki 1991).

2.3 Microbiology

Special emphasis is put on the abundance and identity of aerobic heterotrophs and anaerobic sulphate and iron reducers and autotrophic acetogens, because of their abilities to affect the KBS-3 type of storages for nuclear waste in different ways.

The microbiological work as well as the reporting was divided in two parts: (i) reference materials including all clays, and (ii) MX80, DepCAN and Asha 505 samples from package 1. The reports are available in appendix 1–2.

2.4 Iron corrosion

Metallic iron is not thermodynamically stable in the repository ($E^0 < 0$ V) hence corrosion products will form and interaction with the buffer must be considered. The corrosion and the iron-bentonite interaction depends on several factors such as the redox potential, the temperature, the pH, the solutes and the composition of the buffer and its minerals. But also other less obvious factors may be important such as the buffer density, temperature gradients, transport rates, microbes etc.

Iron corrosion in the absence of bentonite

The initial step in anaerobic corrosion takes place as follows:

$$Fe(s)+2H_2O \rightleftharpoons Fe^{2+}+2\ OH^-+H_2(g)$$

If any oxygen is present the following reaction will follow:

$$Fe(OH)_2(s)+½\ O_2(g) \rightleftharpoons Fe(OH)_3(s)$$

If carbonic acid is available, carbonates may precipitate:

$$HCO_3^-+OH^- \rightleftharpoons CO_3^{2-}+H_2O(I)$$

$$CO_3^{2-}+M^{2+} \rightleftharpoons MCO_3(s)$$

If carbonic acid is absent, $Fe(OH)_2$ will precipitate, which is stable in the absence of oxygen at low temperatures. At higher temperatures (> 373 K) it will convert to the thermodynamically more favoured magnetite phase. The reaction is also possible at lower temperatures but is then much slower. The following reaction is known as the Schikorr reaction:

$$3Fe(OH)_2(s) \rightleftharpoons Fe_3O_4(s)+H_2(g)+2H_2O(I)$$

This possible build-up of magnetite and other corrosion products can passivate the iron surface and hence decrease the corrosion rate.

2.5 Physical properties

The buffer has various requirements on the physical properties such as swelling pressure, hydraulic conductivity and stiffness or plasticity. These properties are investigated in a selection of three materials: MX-80, DepCAN and Asha 505. Both re-compacted samples and drilled samples are used in order to distinguish between such things as irreversible changes due to mineralogical alteration or reversible changes such as potential micro structural texture. These properties are expressed as a function of the compacted density of the buffer.

3 Buffer materials

3.1 General

The ABM tests includes eleven different materials which have been compacted to blocks, installed in the field tests and exposed to high temperature and saturated by formation water. This chapter gives a short description of the materials regarding country of origin, the main content of clay minerals and also the commercial name and abbreviations. A photo showing the materials as delivered is provided in Figure 3-1.

3.2 Description of the different materials

- **Asha 505** produced by Ashapura Minechem Co.is the commercial name of natural Na-bentonite that is quarried in the Kutch area, 60–80 km from the ports of Kandla and Mandvi on the north-west-coast of India. The bentonite is associated with the basaltic Deccan Trap rocks of Tertiary age and formed through hydrothermal alteration of volcanic ash in saline water (Shah 1997). The bentonite occurs in scattered pockets or layers within the basaltic rocks, with thicknesses ranging from a few meters up to 30 meters. Due to the high content of secondary iron oxides the color is normally dark reddish brown but there are also light colored variants low in iron.
- **Calcigel** is the commercial name of a natural Ca-bentonite produced from selected Bavarian bentonites by Süd-Chemie AG. The bentonites are quarried in the triangle between Mainburg, Moosburg and Landshut in southern Germany, where the most important commercial deposits in Germany are located. Most of the Bavarian bentonite deposits occur as scattered, rather thin ($\leq$ 3 m) lenses or layers in sedimentary sequences of late Miocene marls and tuffaceous sands, and are believed to have formed by *in situ* alteration of acid vitreous tuff, originating from the volcanic activity in the Carpathian Mountains (Süd-Chemie 2011). The bentonite quality varies from relatively pure montmorillonite (up to 70%) to material with rather much kaolinite, mica and quartz.
- The **Callovo-Oxfordian** (COX) sedimentary formation in the eastern part of the Paris basin was selected by Andra to host the French underground laboratory in the Meuse/Haute-Marne region. This macroscopically homogeneous Jurassic formation (~150–160 Ma) of argillites is ~130 m thick and has a burial depth of more than 400 m below the ground surface in the region. The rock formation was selected because it's potential ability to act as barrier to radionuclide migration from the storage to the environment due to a very low hydraulic conductivity and large vertical extension on either side of the laboratory level. Quartz and calcite globally represent approximately 50% of the bulk rock, whereas clay minerals, including mixed-layers as well as discrete smectite, illite, kaolinite and chlorite, represent 40–45% (Claret et al. 2004).
- IBECO **Deponit CA-N** is the commercial name of a natural calcium bentonite mined by S&B Industrial Minerals S.A. The bentonite is quarried in the north-eastern part of the island of Milos, Greece, where some of the economically most important bentonite deposits in Europe are concentrated. The island of Milos is located in the central part of the South Aegean active volcanic arc. Pyroclastic tuffs and lavas of andesitic to rhyolitic compositon are the main parent rocks of the bentonite, which forms irregular bodies within the pyroclastics (Kelepertsis 1989). The volcanic rocks have yielded K-Ar ages in the range 3.5–0.09 m.y. Based on isotope data, Decher et al. (1996) conclude that the bentonite formation is a result of hydrothermal reactions between the permeable volcanic rocks and percolating groundwater heated during volcanic activity, although there is some disagreement about the genesis e.g. Christidis et al. (1995).

- The **FEBEX** bentonite is a Mg-Ca bentonite extracted from the Cortijo de Archidona deposit in the southern part of Serrata de Nijar in Almería, Spain. The deposit has been exploited by the major Spanish bentonite producer, Minas de Gádor S.A (now Süd-Chemie Espana). Conditioning of the bentonite at the quarry/factory has been strictly mechanical. According to Caballero et al (2005) the bentonites in Cortijo de Archidona are alteration products of rhyodacitic glasses and ignimbrites. Radiometric dating of the volcanic events indicates ages of 15 to 7 Ma. The FEBEX bentonite (also called S-2 or Serrata clay) had been chosen as reference bentonite by ENRESA before the start of the FEBEX project (Full-scale Engineered Barriers Experiment), among others because of the homogenous nature and very high montmorillonite content (ENRESA 1998). The subordinate amount of accessory minerals includes quartz, cristobalite, plagioclase and calcite.
- The **Friedland** clay is quarried near the town of Neubrandenburg, NE Germany, and is a sedimentary clay formed in a shallow marine basin during the Eocene (57–35 million years ago). This clay is not a bentonite according to strict terminology and the mineralogy is complex, reflecting the mixture of detrital material derived through erosion of the pre-existing weathering mantle, tephra fall-outs and mineral neoformation during early diagenesis (Henning and Kasbohm 1998). The quarried deposit is massive and homogeneous with a thickness up to 140 m.
- **Ikosorb Ca White** (actual commercial name: IBECO RWC White) is a Ca, Mg, Na bentonite, characterized by an high Montmorillonite content (> 80%), a low sulphur content (< 0.1%) and an off-white color which is related to a low content of iron in the smectite clay minerals. The subordinate amount of accessory minerals includes quartz, mica, ct-opal and feldspar. The bentonite is mined in Morocco in the Mount Tidienit area, where rhyolithic pyroclastic rocks related to a rhyodacitic intrusive body of Pliocene/Pre-Pliocene age have been altered to bentonite (Martin-Vivaldi 1962).
- **Ibeco Seal M-90** (actual commercial name: IBECO RWN) is a natural sodium bentonite, characterized by a high Montmorillonite content (> 80%) and a low sulphur content (< 0.1%), produced by S&B Industrial Minerals A in the Askana region in Georgia/CIS. The subordinate amount of accessory minerals includes quartz, illite and mica. The bentonite is derived from andesite-trachyte pyroclastic rocks of Jurassic to Tertiary age. There are several theories for the formation of the bentonite ranging from weathering or hydrothermal alteration to submarine alteration as described by Grim and Güven (1978).
- **Kunigel V1** is the commercial name of a sodium bentonite produced by Kunimine Industries Co., Ltd., Japan. The bentonite is quarried in under-ground mines in the Tsukinuno district, northern part of Japan, which is the largest bentonite production area in Japan. The Tsukinuno formation consists of stratified bodies of bentonitized felsic tuff beds intercalated in sedimentary hard shale and mudstone of Miocene age (Takagi 2005). There are more than 30 bentonite layers in the mining area, ranging in thickness from centimeters to several meters. The Tsukinuno bentonite is composed of Na smectite with subordinate quartz, feldspars, illite, calcite, and zeolite.
- The Wyoming bentonite **MX-80**, produced by American Colloid Co., is a blend of several natural sodium dominated bentonite horizons, dried and milled to millimeter-sized grains. The Wyoming bentonite occurs as layers in marine shales, and is widespread and extensively mined, not only in Wyoming but also in parts of Montana and South Dakota. The bentonite formed through alteration of rhyolitic tephra deposited in ancient Mowry Sea basin during the Createceous, more than 65 million years ago (Slaughter and Earley 1965). There are strong evidence that the tephra altered in contact with the Mowry seawater (Elzea and Murray 1989, 1990), but palaeosalinity and palaeoredox conditions within the semi-restricted basin varied spatially and through time, which explains that the smectite composition varies both stratigraphically and laterally.

- The **Rokle** deposit within the north Bohemian volcanic areas NW of Prague, is one of the economically most important deposits in the Czech Republic. The deposit is part of a series of argillised volcanoclastic accumulations of Tertiary age, formed in shallow lacustrine basins within the stratovolcano complex of Doupovské Mountains (Konta 1986). The lens-shaped bentonite body has a maximum thickness of c. 40 m. The volcanic glass is completely altered to smectite, but flakes of biotite, which is a primary constituent of the basaltic magma, are relatively frequent. The bentonite is highly variable in colour, ranging from olive-gray to yellow/red due to the admixture of secondary iron and manganese oxides.

In addition to the blocks manufactured of the materials described above, four special "blocks" were manufactured to each of the three test packages installed. These blocks consist of cages made of steel frames which then have been wrapped with fiber cloth. The cages contains granulate made of Mx-80 and a mixture of 70% MX-80 and 30% quartz respectively. The construction is described in detail in the ABM installation report (Eng et al. 2007).

Figure 3-1. *Photo showing the different materials in the ABM test.*

4 Experiment description

4.1 General

4.1.1 Principals

The experiment layout is similar to the Swedish KBS-3 concept with a copper canister surrounded by clay situated in crystalline bedrock at approximately 500 m depth. The differences are mainly the scale and that the simulated canister is made of steel instead of copper. The experiment consists of three test-packages which are placed in three separate vertical bore holes drilled in granitic rock. Each test package consists of a central steel tube including heaters on the inside, ring shaped bentonite blocks and in addition also some instruments. The bentonite is during test time exposed to conditions similar to the KBS-3 concept except for the temperature which is higher, 130°C compared to 90°C. The higher temperature will accelerate the alteration processes.

All three test packages were prepared in order to use an artificial water saturation system. The outermost slot between bentonite blocks and rock was filled with sand in which titanium pipes, perforated with drilled holes at different levels, are placed. The pipes are connected to a water tank which can be pressurized.

This chapter provides an overview of the experiment design regarding test package design, instrumentation and system for artificial saturation. In addition to this, the design and installation of the three test packages also is described in a report (Eng et al. 2007).

4.1.2 Experimental configuration

The test packages were originally planned to be retrieved after about one, three, and five years test duration at maximum temperature. The one year and the five year packages were heated from test start but the heating of the three year package was started when the bentonite was judged to be fully water saturated.

All three packages are wetted by natural water from fractures in the rock. In addition the one and three years tests also are artificially wetted by the installed wetting system. An overview of the test program is provided in Table 4-1.

Table 4-1. Test program for the Alternative Buffer Material project.

Test no.	Test duration	Max temp.	Artificial wetting	Remark
1	1 year	130°C	Yes	
2	3 years	130°C	Yes	Heating starts after saturation
3	5 years	130°C	No	

4.2 Test site

4.2.1 General

The Alternative Buffer Material, ABM, experiment is located in the TASQ tunnel at the –450 meter level at Äspö HRL, see Figure 4-1. A niche, NASQ, is excavated on the eastern side of the tunnel and the three test holes are placed here. The rock consists of Äspö diorite and greenstone. The tunnel holds quite many water bearing fractures further in but these are avoided in the test niche which is rather dry.

4.2.2 Test holes

The three test holes have a diameter of 300 mm and a depth of about 3.2 m. Water inflow measurements were made and showed similar results for all three holes, about 0.06 l/min. The test holes are named KQ0032G01, KQ0036G01 and KQ0040G01 according to the SKB borehole ID system.

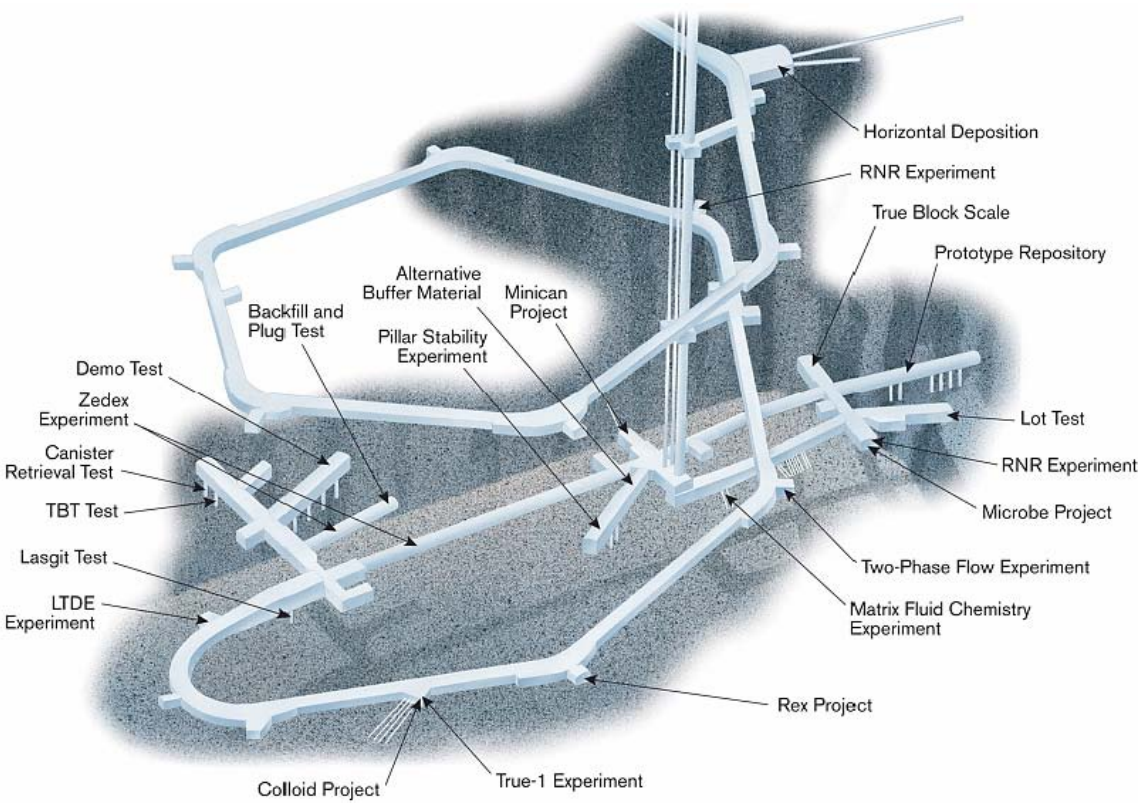

Figure 4-1. *Test sites in the lower part of the Äspö HRL. The ABM test is located in the TASQ tunnel.*

4.3 Test packages

4.3.1 General

The principal design of a test package is shown in Figure 4-2. The design is similar to the Swedish KBS-3 concept with a central canister surrounded by highly compacted bentonite blocks. The packages were put together above the test holes and then lowered down in the rock.

4.3.2 Central tubes

The central tubes containing heaters are made of carbon steel, P235TR1. The tubes have a length of about four meters and an outer diameter of 108 mm. In order to facilitate installation and to be able to put together a complete test package, a steel plate is welded on the bottom.

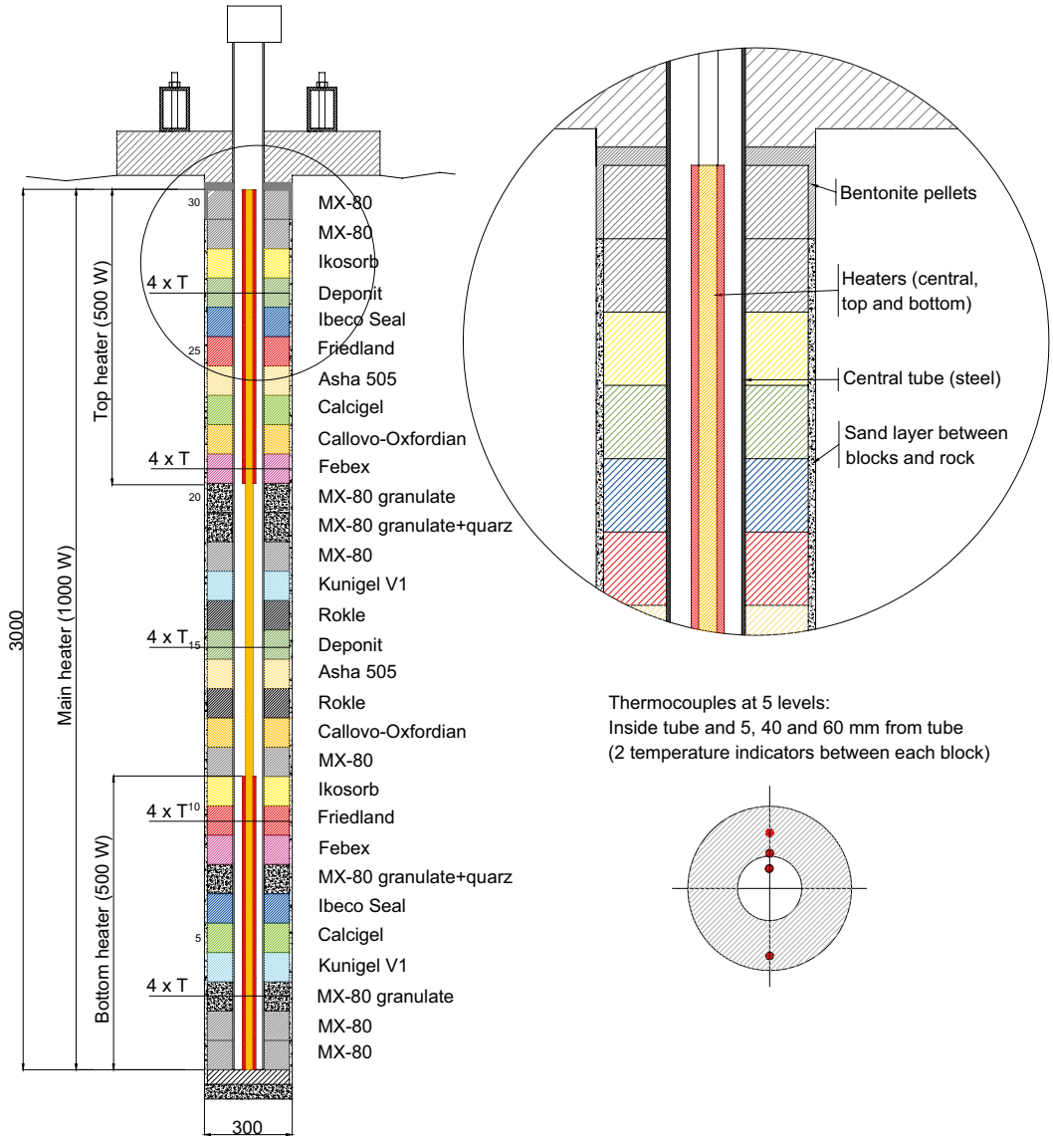

Figur 4-2. *Schematic view of the test layout for the ABM experiment. The drawing shows the block positions in test package 1, the thermocouple positions and the heaters.*

4.3.3 Heaters

Three heaters are installed in each of the test packages. There is one central heater (1,000 W), one heater at the top (500W) and one at the bottom (500 W). The effect of each heater can be adjusted separately which makes it possible to get an even temperature along the test package. The heaters are placed inside the central steel tube which is favorable in case of failure, since the damaged heater can be lifted up and a new installed very easily.

4.3.4 Blocks

All bentonite blocks used in the test were compacted in a special mould with a pressure of 100 MPa. The compaction technique was based on experiences from previous SKB projects concerning block production (Johannesson et al. 1995). The blocks have a slight axial conical shape and chamfered edges between mantle and end sides. In order to produce blocks of good quality it was also necessary to use a small amount of grease. The grease reduces the friction and facilitates de-moulding. The grease used contained an additive of molybdenum disulfide, MoS_2.

The blocks were compacted with the as-delivered water content and granule size except for the Callovo –Oxfordian and the Asha material. The Callovo-Oxfordian material was delivered as hard rock shards and was crushed down to a maximum grain size of five mm by use of sledge hammer, jaw crusher and finally a roller mill. The Asha material was delivered with a water content of 26.6% and was before compaction dried to a water content of about 13%. All manufactured blocks were after compaction weighed and measured, see data provided in Table 4-2.

In addition to the blocks manufactured of the different bentonite materials, four special “blocks” were manufactured. These blocks consist of cages made of steel frames which then have been wrapped with fiber cloth. The cages contains granulate made of Mx-80 and a mixture of 70% MX-80 and 30% quartz respectively. The construction is described in detail in the ABM installation report (Eng et al. 2007). An information report regarding the granulated materials is provided in Appendix 1.

Table 4-2. Data for blocks used in ABM test package 1.

Block no.	Material	m g	dy mm	Dy mm	Di mm	h1 mm	h2 mm	h3 mm	w %	Bulk density kg/m³	Dry density kg/m³
1	MX-80	10,639	276.6	280.0	110.1	100.1	99.5	100.0	14.1	2,091	1,833
2	MX-80	10,636	276.6	280.0	110.3	100.1	100.5	100.5	13.4	2,082	1,835
3	MX-80 granulate	-	280.0	280.0	110.0	100.0	100.0	100.0	-	1,243	-
4	Kunigel V1	10,858	276.7	280.4	110.5	98.8	99.1	98.8	8.0	2,154	1,994
5	Calcigel	10,189	276.8	280.4	110.6	99.8	99.7	100.3	7.1	2,000	1,868
6	Ibeco Seal M-90	10,736	276.0	279.6	110.1	100.0	99.9	99.9	14.8	2,118	1,846
7	MX-80 granulate+quarz	-	280.0	280.0	110.0	100.0	100.0	100.0	-	1,282	-
8	Febex	10,541	276.5	280.1	110.1	101.1	101.3	101.6	14.8	2,042	1,778
9	Friedland	11,709	276.5	280.6	110.2	101.0	101.1	101.0	5.7	2,271	2,149
10	Ikosorb	10,681	275.8	279.4	110.0	99.4	99.1	99.4	15.5	2,124	1,839
11	MX-80	10,639	276.2	280.1	110.2	100.1	100.3	100.2	13.6	2,088	1,839
12	Callovo-Oxfordian	11,455	276.7	280.2	110.3	102.0	102.2	102.1	2.7	2,201	2,143
13	Rokle	11,706	276.4	281.2	110.0	116.8	116.6	116.7	10.5	1,958	1,772
14	Asha 505	11,023	276.7	280.2	110.1	100.7	100.6	100.7	13.2	2,147	1,896
15	Deponit CA-N	10,561	276.7	279.1	110.1	101.1	101.0	101.2	18.6	2,057	1,735
16	Rokle	10,695	277.6	281.1	109.1	107.0	107.4	107.7	10.6	1,931	1,746
17	Kunigel V1	10,842	276.1	280.1	110.1	98.5	98.6	99.5	9.1	2,157	1,977
18	MX-80	10,595	276.5	280.1	110.3	100.9	100.5	100.6	13.5	2,067	1,822
19	MX-80 granulate+quarz	-	280.0	280.0	110.0	100.0	100.0	100.0	-	1,243	-
20	MX-80 granulate	-	280.0	280.0	110.0	100.0	100.0	100.0	-	1,282	-
21	Febex	10,569	276.2	280.1	110.1	100.5	100.6	100.7	14.7	2,065	1,801
22	Callovo-Oxfordian	11,462	276.7	280.4	110.3	101.5	101.6	101.7	2.7	2,212	2,154
23	Calcigel	10,230	276.4	280.0	110.4	98.1	98.6	98.8	6.9	2,043	1,911
24	Asha 505	10,992	276.7	280.3	110.4	100.8	101.1	100.9	13.2	2,136	1,887
25	Friedland	11,716	276.2	280.5	110.5	100.6	100.5	100.7	5.8	2,288	2,162
26	Ibeco Seal M-90	10,776	276.4	280.0	110.2	100.1	100.2	100.2	15.1	2,114	1,836
27	Deponit CA-N	10,582	276.1	279.4	109.9	102.1	102.3	102.1	18.3	2,041	1,725
28	Ikosorb	10,693	275.8	279.1	109.6	99.6	99.7	99.8	16.0	2,118	1,826
29	MX-80	10,640	276.9	279.6	110.0	100.5	100.6	100.7	13.8	2,076	1,824
30	MX-80	10,455	276.2	280.0	110.2	89.2	98.0	98.2	14.0	2,163	1,898

4.4 Instrumentation

4.4.1 General

The three ABM test packages are sparsely instrumented. The main objectives with the test series are to expose the different bentonite materials to conditions similar to a repository and to adverse conditions with respect to temperature. This means that measurements of the temperature distribution in the test packages are important.

The test program includes that the heating of test package two should not start before the bentonite was judged to be saturated. In order to get a rough estimation of how the saturation proceeded, this package was equipped with four relative humidity sensors.

The instrumentation is described in detail in an installation report (Eng et al. 2007).

4.4.2 Thermocouples

Twenty thermocouples were installed in each of the test packages. The thermocouples are of type K and the shield of the sensors is made of cupronickel in order to withstand the tough conditions in the test holes. The thermocouples in test package one and three are positioned in block number 3, 9, 15, 21 and 27, see Figure 4-2. The thermocouples in test package two are positioned in block numbers 3, 9, 15, 22 and 28.

Four thermocouples are positioned at each level, one inside the steel tube and three in the buffer. The thermocouples in the buffer are positioned at different radial distance from the heater, 5, 40 and 60 mm.

4.4.3 Temperature indicators

Two temperature indicators were installed on the surface of each block, one sensor was placed three cm from the heater and one was placed three cm from the outer surface. The indicators are of offline type, which means that the sensors can only be read after retrieval. The sensors indicate the highest temperature they have been exposed to. The innermost sensors have a temperature interval of 121 to 160°C in eight steps and the outermost 77 to 116° also in eight steps.

4.4.4 Relative humidity

The relative humidity sensors in test package two were positioned in block numbers 3, 9, 22 and 28. The sensors were installed in predrilled holes in the blocks about five cm down from the block surface and at a radial distance from the heater of 3 cm.

The relative humidity sensors were delivered by Vaisala Oyj. Before installation the sensors were encapsulated in special housings in order to protect them physically.

4.5 Artificial wetting system

All three test packages were prepared in order to use an artificial water saturation system. The outermost slot between bentonite blocks and rock was filled with sand in which titanium tubes, d=6 mm, were placed. The sand will serve as a filter and distribute water around the outer mantle surface. Four titanium tubes were installed in each of the test packages. They are connected two and two underneath the bottom buffer block, which makes it possible to flush the system if needed. Holes were drilled in the titanium tubes every ten cm (test package 1) and every meter (test package 2 and 3). In order to avoid sand to enter or clog the small holes, a perforated plastic “sock” was pulled over the pipes. The pipes are connected to a water tank which can be pressurized.

As mentioned in Section 4.1, only test package 1 and 2 have been artificially wetted from test start.

5 Field operation, test package 1

5.1 General

The assembly and installation of the test parcels are described in an installation report (Eng et al. 2007). Immediately after installation, all instruments were connected to a data logger and the registration of data was started. The artificial wetting (test package one and two) and the heating (test package one and three) was started three days after installation.

5.2 Heating

The heating of test package one was started 2006-12-07, i.e. three days after installation. The power was increased in steps, see Figure 5-1. During the increase of power the achieved temperature was controlled in order to get as even temperature profile as possible along the whole test package, see Figure 5-2 to 5-4.

During the test period, there have been some problems with the artificial water saturation system; see Section 5.4, which made it necessary to decrease the temperature for some periods in order to avoid boiling. The bentonite has been exposed for the maximum temperature for about one year.

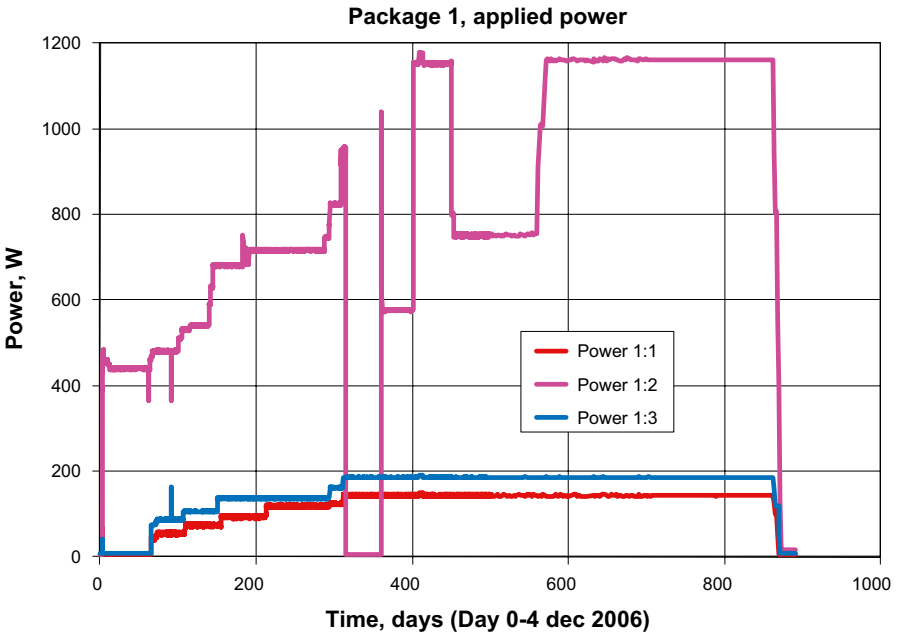

Figure 5-1. *Applied power in test package 1 plotted vs. time.*

5.3 Temperature measurements

The registered temperature data for the five levels is presented in Figure 5-2 and 5-3. The number of measuring points is limited but the registered data gives a fairly good picture of the temperature distribution in the test package. Figure 5-4 shows the temperature distribution in test package one in November 2008 (after 710 days test).

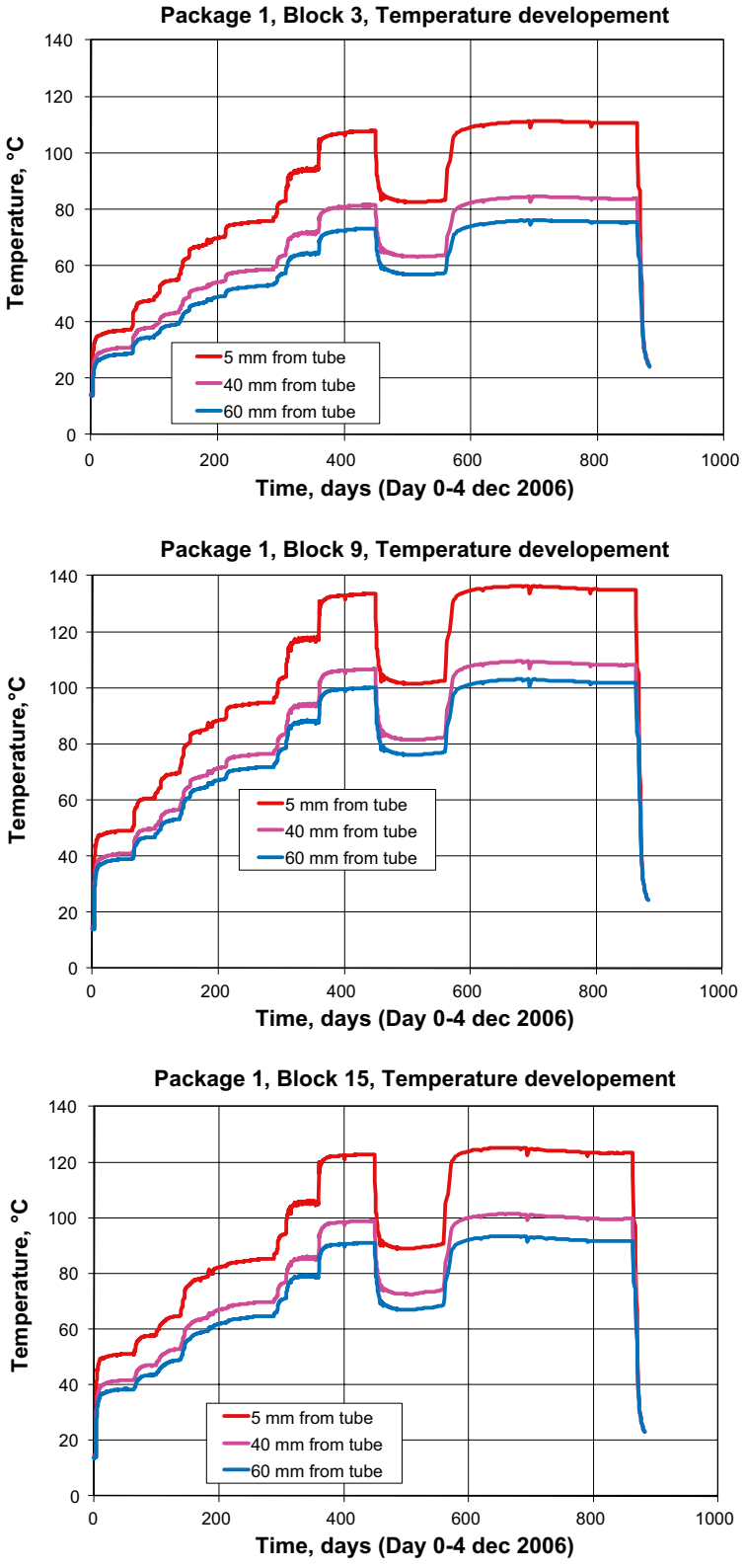

Figure 5-2. Temperature measurements from block three, nine and fifteen, plotted vs. time. Block number three is the third block from bottom of the test package.

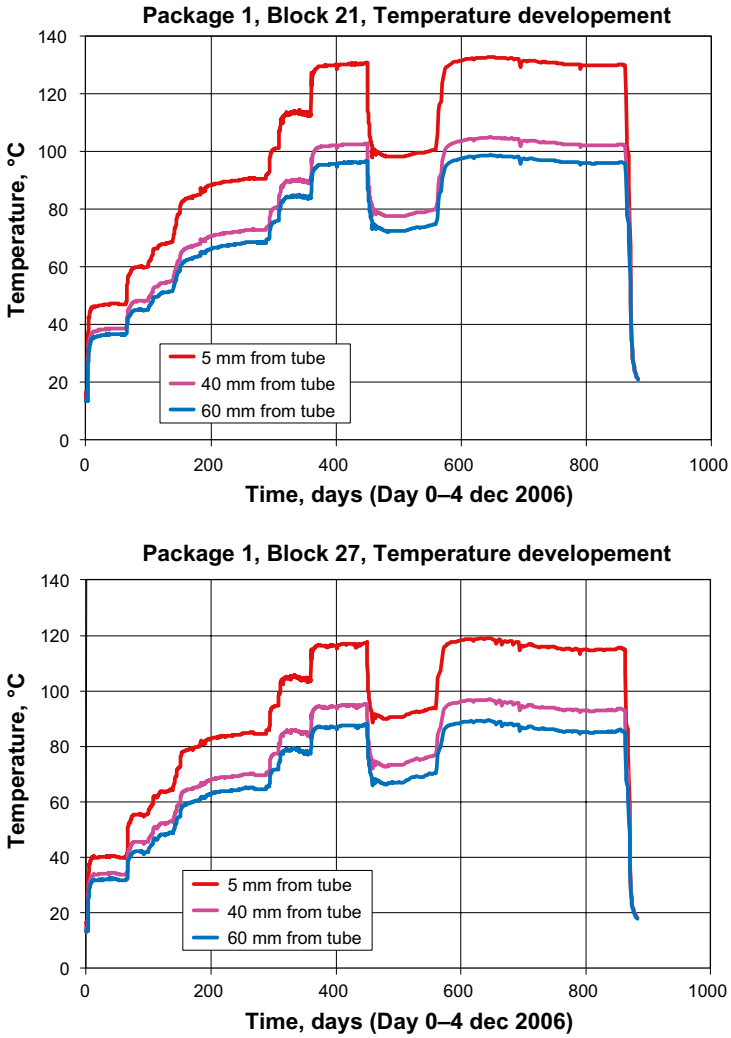

Figure 5-3. *Temperature measurements from block twenty-one and twenty-seven plotted vs. time.*

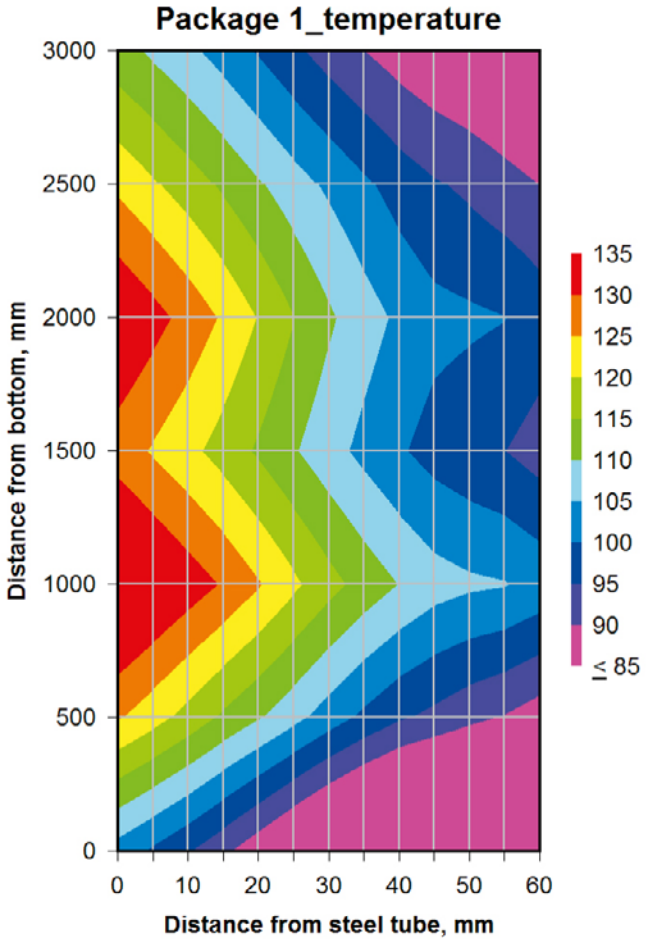

Figure 5-4. *Temperature distribution in the 60 mm closest to the heater in test package 1, november 2008 after about 710 days test duration. The horizontal scale is magnified.*

5.4 Artificial water saturation

The water supply to test package 1 and 2 started three days after installation and at the same time as the increase of temperature was started, see Figure 5-5. During the artificial saturation of test package 1 the following actions and decisions were made:

- During the first 50 days the inflow rate was very high (about 850 litres were injected) and in order to avoid strong erosion of the installed bentonite during long time the inflow was stopped for a period of about four months.
- After about four months a water pressure of 1.3 bars was applied and this was then increased in steps up to 2.7 bars. At this pressure the water inflow increased again and it was decided that again decrease the pressure. In order to avoid boiling at the intended test temperature (130°C), 2.7 bar absolute pressure is needed. The applied pressure during the test period was about 1.7 bars which is enough to prevent boiling up to 117°C.
- In order to discover where the water flowing took place; a small test was made day 721. The valve feeding test package 2 was closed for about eight hours but this did not have any impact on the water consumption. The leakage therefore appears to be linked to test package 1.
- The termination of test package 1 was done after 881 days. Before termination the heat was shut down day 863 and the artificial water saturation day 872.

The composition of the water used for the artificial saturation was made 2009-10-07 within the Äspö HRL campaigns and the results are given in Table 5-1.

Table 5-1. Main elements in the water supply. The water is taken from bore hole KA2598A.

Na (mg/l)	K (mg/l)	Ca (mg/l)	Mg (mg/l)	HCO_3 (mg/l)	CL (mg/l)	SO_4 (mg/l)	SO_4_S (mg/l)	BR (mg/l)	F (mg/l)	Si (mg/l)	PH (pH unit)
2,470.0	12.4	2,560.0	64.8	51.7	8,580.0	483.0	171.0	59.0	1.5	6.3	7.33

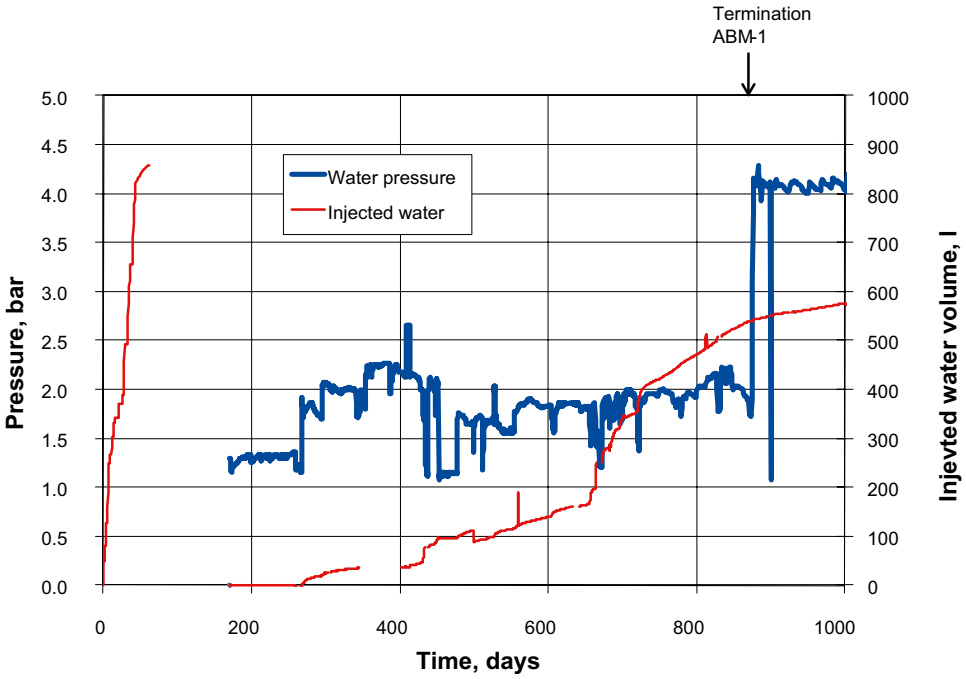

Figure 5-5. *Applied water pressure and injected water volume plotted vs. time.*

5.5 Termination of test package 1

In order to facilitate the termination of the experiment, the heater power was closed 2009-04-15, about three weeks before the uplifting. The artificial water saturation system was closed nine days later, 2009-04-24.

The test package was released by seam-drilling (d=89 mm) the rock around the package giving a rock cover of about 150 to 200 mm, see Figure 5-6. After finishing the seam-drilling two core-drilled holes with a diameter of 300 mm were drilled at one side. In these holes wire sawing equipment was installed which was used in order to release the rock column in the bottom.

The core drilling showed that the rock was rather fractured at some levels which could cause problems when lifting up the package. In order to keep the package together it was covered with boards and then surrounded by straps. The lifting of the package was made by positioning three wires with loops around the package and outside the boards. The wires were used as lassos i.e. when lifting in the free end the loops were stretched harder around the package. The free ends of the wires were led through a special cap placed on the central steel tube. The lifting of the test package was made by a lorry with a crane, see Figure 5-7. The test package was then placed on the flatbed of the lorry and transported up to the ground.

The test package was lifted up 2009-05-04.

Figure 5-6. *Photo showing the released test package. After the seam-drilling, two core drilled holes with a diameter of 300 mm were drilled in order to make it possible to install the wire-sawing equipment and saw off the rock column in the bottom.*

Figure 5-7. *The test package was lifted up in one piece. In order to avoid pieces from falling off during the handling, the test package was surrounded by boards and straps.*

5.6 Division and material handling in field

5.6.1 General

Immediately after retrieval of the test package, the work with division of the rock column and uncovering the bentonite blocks was started. The rock was at some levels rather fractured which facilitated the dismantling, see Figure 5-8.

The intention was to make a rough division in field and save the fine division for the laboratory. The rough division was made by sawing up parcels containing of one to four bentonite blocks complete with the inner steel tube which also was sawed, see Figure 5-9. The sawing of both bentonite and steel was made with a special alligator saw.

Some of the blocks were very fragile and in order to keep the bentonite together they were supported by plastic straps, see Figure 5-9. The four special "blocks" that consisted of a steel cage filled with pellets were treated so that they after the rough division were placed in between two other blocks.

The parcels were placed in sacks of alumina laminate, see Figure 5-10, which were evacuated and welded together. The sacks were then placed in air tight barrels and transported to the laboratory where the fine division was made.

5.6.2 Handling of instruments

After retrieval, a function test was made with the thermocouples that were possible to save (13 out of 20 thermocouples); some were destroyed during the dismantling. The function tests were made by placing them in boiling water and register the measured temperature. The measured temperature was for all 13 tested thermocouples between 98.4 to 99.3 degrees.

The temperature indicators, see Section 4.4, were all completely destroyed and it was impossible to read anything on them.

Figure 5-8. *Parts of the rock cover was rather fractured.*

Figure 5-9. *Some blocks were very fragile and in order to keep them together during the cutting, they were supported by plastic straps.*

Figure 5-10. *The parcels containing bentonite blocks were placed in sacks of alumina laminate which were evacuated welded together and then placed in air tight barrels.*

5.7 Division and material handling in laboratory

The different participating organizations had in advantage given whishes regarding which blocks they were interested in and how the material should be protected during transport, see compilation in Figure 5-11.

The fine division was made by use of a band saw and also by manually cutting and sawing. All pieces were directly after division, again placed in alumina laminate which were evacuated and welded together. Some pieces were, according to the instructions from the receiver placed in either a slight overpressure of argon (Andra) or in nitrogen (Posiva).

Splitting of Package 1, ABM (wishes)

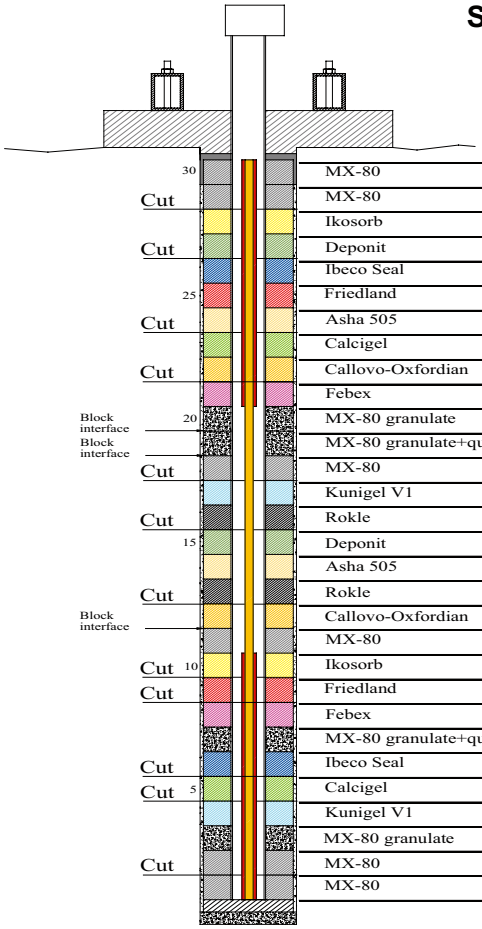

	SKB	Andra	BGR	GRS	JAEA	Nagra	Posiva	RAWRA	AECL	MICANS
MX-80						Yes				
MX-80										
Ikosorb										
Deponit		Yes								
Ibeco Seal										
Friedland										
Asha 505										
Calcigel			Yes 1							
Callovo-Oxfordian		Yes								
Febex		Yes						Yes		
MX-80 granulate	Yes					Yes	Yes		Yes	
MX-80 granulate+quarz						Yes			Yes	
MX-80									Yes	
Kunigel V1			Yes 2		Yes					
Rokle	Yes							Yes		
Deponit	Yes	Yes	Yes 3				Yes			Yes
Asha 505	Yes		Yes 4				Yes			Yes
Rokle			Yes 5					Yes		Yes
Callovo-Oxfordian	Yes	Yes							Yes	
MX-80	Yes	Yes	Yes 6				Yes		Yes	Yes
Ikosorb	Yes		Yes 7							Yes
Friedland	Yes		Yes 8				Yes			Yes
Febex		Yes	Yes 9					Yes		Yes
MX-80 granulate+quarz	Yes									
Ibeco Seal	Yes		Yes 10							Yes
Calcigel	Yes									Yes
Kunigel V1					Yes					
MX-80 granulate	Yes					Yes	Yes			
MX-80	Yes					Yes	Yes			
MX-80	Yes	Yes					Yes			

Amount and requirement of material needed:

SKB Approximately 1/8 of a block, as a piece ("tårtbit") from outer part to inner part. Air should be removed and the piece should be sealed in plastic bag possibly in inert atmosphere.

RAWRA (CTU) Approximately 2 kg (1/6?, min. 1.5 kg) of a block, as a piece from outer part to inner part. Air should be removed and the piece should be sealed in plastic bag.
after discussion with RAWRA, the "RAWRA wish" for Kunigel and Asha samples seems like a mistake - we (RAWRA/ CTU) are interested in Rokle and FEBEX (as noticed in the attachement). As I informed earlier, we offer some more capacity for swelling pressure and permeability measurement on some other samples (depending on deadline for results etc. :)).

BGR As far as we understood each block is divided into 8 parts? Actually we are a little bit afraid of the possible effect of the sensors. Therefore, we´d like to ask for pieces of each block being far apart from the sensors (if possible).

POSIVA Approximately 1/2 of each block, as a piece from outer part to inner part. The parcel should be split in oxygen-free conditions. The pieces should be sealed in the transportation vessels (to be submitted). The air should be removed from the vessels by nitrogen flushing.

Andra a. Half of each block of Callovo-Oxfordian + approximately 1/4 of Deponit, Febex and MX80. Air should be removed and the piece should be sealed in a double plastic bag with a pressure of argon about 1.5 bar (just above the atmospheric pressure)
b. Analyses planned: bulk chemistry analysis, XRD, TEM, SEM, microstrucural study of the clay minerals, FTIR spectrophotometry, CEC, XPS analyses, microstructure and water status
c. we are interested also by the chemical evolution of steel in contact with the clay at high temperature. So if it's possible we would like a piece of the steel liner. Sample should be sealed in a double plastic bag with a pressure of argon about 1.5 bar (just above the atmospheric pressure).
d. We are interested also to be in field during the dismantling . Is it possible ? If not, thank you to give a copy of the logbook and photos

AECL **A sample from blocks 11 (MX-80) and 12 (COx), attached to each other such that the block-block interface is preserved** if possible, and that would **cover the whole block from the heater to the rock** such that we can do 7 analyses for the presence of microbes:

11 MX-80 bulk (middle of block)
11 MX-80 heater-block interface
11 MX-80 rock/sand-block interface
11/12 MX-80-COx Interface
12 Cox-bulk (middle of block)
12 COx-heater-block interface
12 COx-rock/sand-block interface

Samples from blocks 18, 19 and 20 attached to each other such that block-block interfaces are preserved, and covering the whole block from the heater to the rock. We would do 5 analyses:

18 MX-80 bulk (middle of block)
19 MX-80 granulate + quartz bulk (middle of material)
18/19 MX-80 - MX granulate+ quartz - interface (if possible)
20 MX-80 granulate bulk (middle of material)
19/20 MX-80 granulate + quartz - MX-80 granulate - interface

We would also like to receive an archived sample of MX-80 granulate and MX-80 granulate + quartz because we did not ask for those last year and we would like to have some sort of benchmark analysis for microbial content.

We would like the samples sent to us in a cooler with some icepacks, by courier. This has been done before from Sweden, with the CRT samples.

These 14 analyses will give us information about microbial survival and culturabilty in the bulk of MX-80, MX-80-granulate, MX-80 granulate + quartz and COx clay and at many material interfaces of interest.

MICANS One piece per material. Max temperature gradient.

Figure 5-11. *The figure show which blocks the different participating organizations was mainly interested in.*

6 Hydro-mechanical tests

6.1 General

After termination of test parcel one, material from the different blocks have been tested and analyzed. The tests were aimed to discover possible changes in physical properties, mineralogy and microstructure compared to the reference material.

Some mineralogical properties were investigated for all materials (eleven different buffer materials) while the tests aiming to investigate the physical properties were focused on three materials which are of higher interest for SKB i.e. MX-80, Asha 505 and Deponit CAN. The following physical properties have been investigated:

- Standard laboratory tests (all eleven reference materials).
- Water content and density (all installed blocks).
- Swelling pressure (MX-80, Asha 505 and Deponit CAN).
- Hydraulic conductivity (MX-80, Asha 505 and Deponit CAN).
- Stress-strain-strength (MX-80, Asha 505 and Deponit CAN).

The preliminary results from the tests are described in the following sections.

6.2 Material and denominations

Totally thirty blocks were installed in each of the ABM test packages. After termination of test package one, see Chapter 5, the air-tight barrels containing parcels with buffer blocks, were transported to Clay Technology AB in Lund. In order to receive suitable samples for tests and analyses, the division of each block was done with a band-saw. After the division, all samples cut out, were again placed in new alumina sacks which were evacuated and welded together as soon as possible in order to prevent drying and exposing to air.

The denominations of the different block positions were made according to the following example (see Figure 6-1 and 6-2):

AB108AS3b

AB ABM-material.
1 Test package number.
08 Block number (counted from the bottom of the package, see Figure 6-2).
A Vertical level in the block.
S Direction of compass in the test hole.
3 Radial distance in centimeter from the inner mantel surface to the center of the sample.
b Bulk material (alternative c = clay fraction).

Due to the test layout of the ABM experiment with blocks made of different materials in contact with each other, and in order to avoid that the tests were made with mixed material, the sampling have been done in the B level in the investigated blocks.

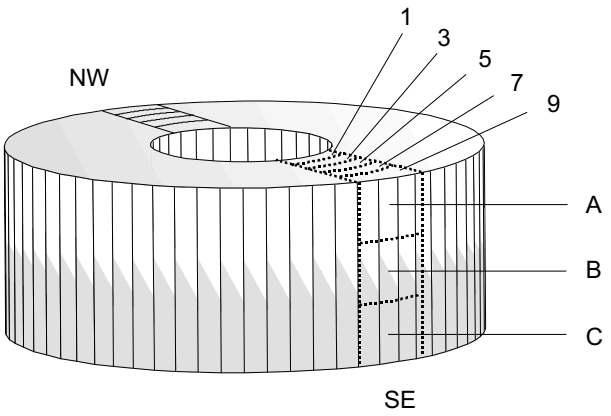

Figure 6-1. *Schematic block division. SE and NW denote the direction of compass in the test hole, figures denote the center of the samples expressed in centimeters from the inner mantel surface of the block and A, B and C denotes the vertical position in the blocks.*

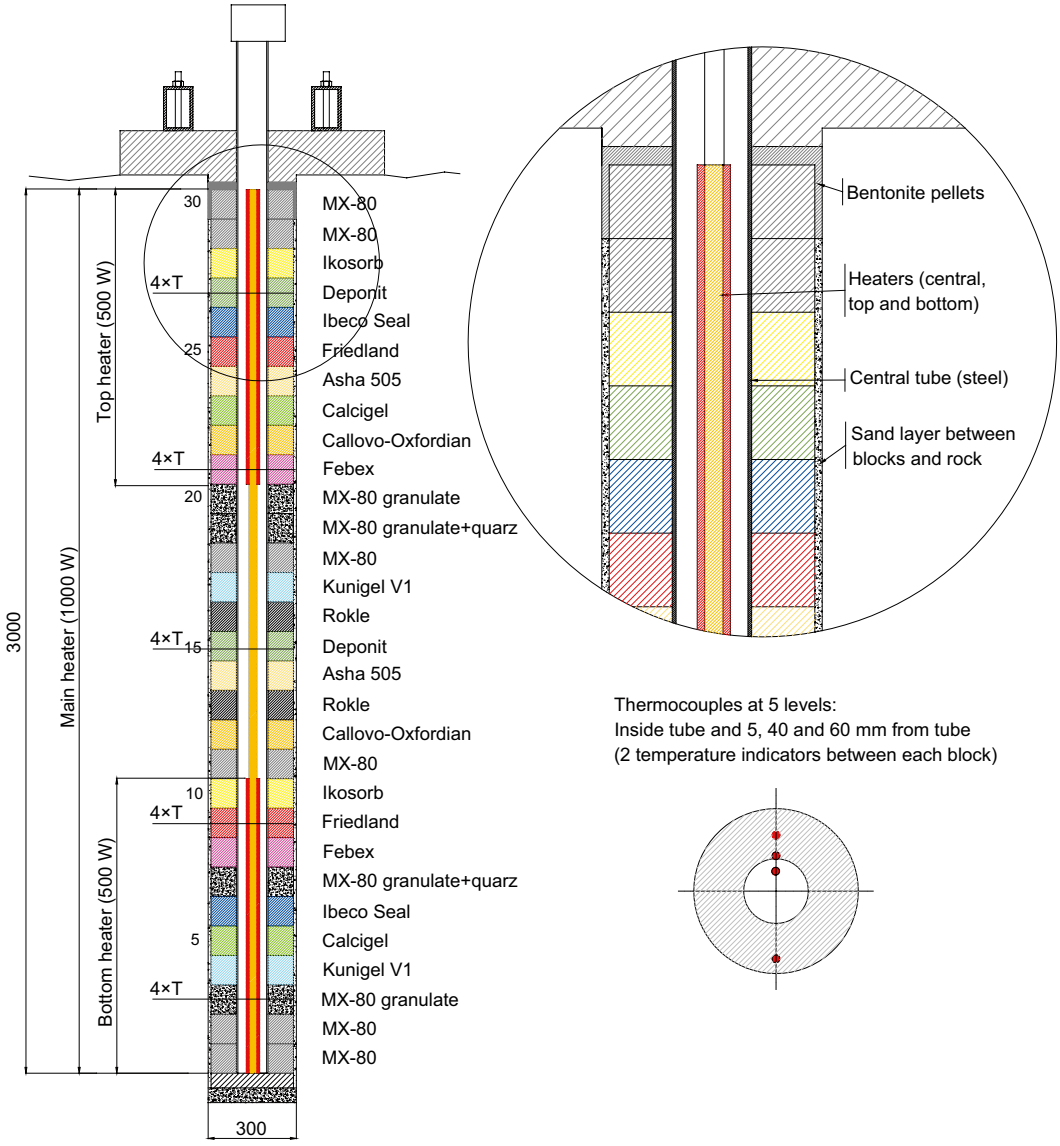

Figure 6-2. *Schematic view of the test layout for the ABM experiment. The drawing shows the block positions in test package 1, the thermocouple positions and the heaters.*

6.3 Standard investigations of reference materials

6.3.1 General

A number of standard geotechnical properties of the reference materials were determined in the laboratory. The results are compiled in Table 6-1.

Water contents

The water contents of the eleven as-delivered raw materials were determined. The water content is defined as mass of water per mass of dry substance. The dry mass is obtained by drying the wet specimen at 105°C for 24 hours.

Liquid limit

The liquid limit of a soil is the water content where the properties of the soil changes from plastic to liquid. The liquid limit was determined with the fall-cone method.

Swelling capacity

One gram of the dry test material is poured down very carefully into a glass cylinder filled with de-ionized water. The volume occupied by the swelled clay is recorded after 24 hours to provide the volumetric swelling capacity. The swelling capacity depends mainly on the montmorillonite content of the material.

Grain density

The grain density of the materials was determined by using volumetric flasks. After determining the volume of the flasks very carefully, dried material was mixed with 1 M NaCl solution (in order to prevent swelling of the bentonite). When the mass of the solids, the total volume, the total mass (solids and flask) and the density of the liquid is known, it is possible to calculate the grain density of the material. The method is described in detail in Karnland et al. (2006).

In the calculations of the degree of saturation, the grain density determined in this investigation has been used except for two materials, MX-80 and Deponit CAN. The grain density for these two materials has been determined several times e.g. in Karnland et al. (2006) and are established since long time. The grain density used for MX-80 is 2,780 kg/m^3 and for Deponit CAN 2,750 kg/m^3.

Table 6-1. Compilation of results from standard investigations of the reference material.

Material	Water content %	Free swelling ml	Liquid limit %	Grain density kg/m^3
MX-80	12.9	17.0	545	2,735
Calcigel	8.2	4.0	119	2,695
Ikosorb	15.6	6.2	326	2,740
Rokle	11.5	3.0	116	2,940
Kunigel	7.8	9.7	462	2,681
Febex	14.7	2.4	109	2,735
Callovo Oxfordian	2.4	1.6	–	2,682
Asha 505	12.7	8.8	337	2,869
Friedland	5.2	3.9	68	2,828
Ibeco Seal	14.0	11.2	522	2,753
Deponit CAN	16.8	6.2	160	2,678

6.4 Water content and density determinations

6.4.1 General

The water content and the density were determined in a large number of positions in the material from ABM test package 1. All blocks (the pellets cages were treated separately) were investigated at the B-level i.e. at the middle level, in the south direction if possible. From each block, a slice with a thickness of about 2 cm was cut out. The slice was divided at five radial distances according to Figure 6-3, with samples for both water content and density determinations. The sampling of the four cages containing pellets was done by Urs Mäder, University of Bern/Nagra. Samples were cut out according to the same principal as the blocks but at six radial distances.

6.4.2 Test procedure and evaluation

Water content

Immediately after division the sample was placed in aluminum tin and the bulk mass (m_b) of the sample determined by use of a laboratory balance. The sample was then placed in an oven for 24 h at a temperature of 105°C. The dry mass of the sample (m_s) was determined immediately after take out. From these measurements the water mass (m_w) was calculated:

$$m_w = m_b - m_s \qquad 6\text{-}1$$

and the water content (w) of the sample determined:

$$w = \frac{m_w}{m_s} \qquad 6\text{-}2$$

Bulk density, dry density and degree of saturation

The bulk density was determined by hanging the sample in a thin thread under a balance. The sample was then weighed, first in air (m_b) and then submerged into paraffin oil (m_{bp}). The volume of the sample was then calculated:

$$V = \frac{(m_b - m_{bp})}{\rho_p} \qquad 6\text{-}3$$

where ρ_p is the paraffin oil density. The bulk density of the sample was then calculated:

$$\rho_b = \frac{m_b}{V} \qquad 6\text{-}4$$

After determining the water content and the bulk density of each sample it was possible to calculate the dry density (ρ_d):

$$\rho_d = \frac{\rho_b}{1+w} \qquad 6\text{-}5$$

Since the density of the particles (ρ_s) and the density of the water (ρ_w) are known the degree of saturation (S_r) can be calculated:

$$Sr = \frac{w \cdot \rho \cdot \rho_s}{[\rho_s \cdot [1+w] - \rho]} \frac{}{\rho_w} \qquad 6\text{-}6$$

In the calculations different value of the particle density (ρ_s) have been used for the different materials, see Chapter 6-3.

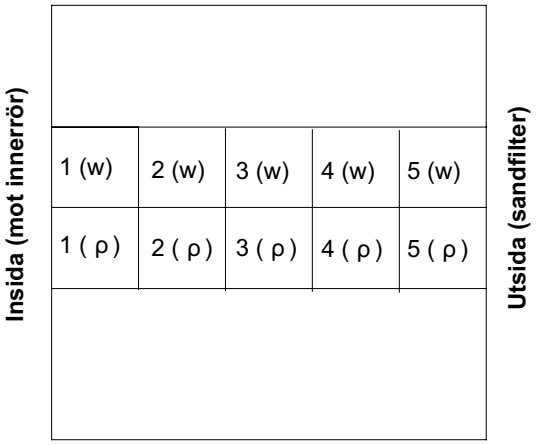

Figure 6-3. *Schematic view of a slice from a block, showing how samples were cut out at different radial distances from the inner block surface.*

6.4.3 Results

The eleven materials tested in the ABM project were before installation compacted to blocks at a compaction pressure of 100 MPa. Depending on the different material properties, different bulk densities of the blocks were reached, see Table 4-2. This means that there will be large differences between the different materials regarding the final saturated density and the water content at saturation. The achieved swelling pressure of each material depends of the block density which means that during the test period some blocks will expand more, preventing swelling of neighboring blocks with lower swelling pressure, until a steady state has been reached.

The determined (water content and bulk density) and calculated values (dry density, void ratio and degree of saturation) for all blocks are provided in Figure 6-4 to 6-6. An example of the water content and density distribution for the MX-80 blocks in the test package is shown in Figure 6-7. In Figure 6-8 to 6-10 overviews of the experiment are provided, showing the radial distribution of water content, dry density and degree of saturation for every block.

The diagrams in Figure 6-11 show the calculated difference in dry density between the installed blocks and the blocks after termination. All blocks has swelled, and by that decreased the density, but the difference between the different materials is large.

Sample ID	Material	Radial distance	Grain density	Water content	Bulk wet density (paraffin oil)	Bulk dry density	Void ratio	Degree of saturation
		mm	g/cm^3	%	g/cm^3	g/cm^3		%
AB101BS1	MX-80	8.5	2.780	31.016	1.965	1.500	0.853	101.035
AB101BS2	MX-80	25.5	2.780	32.083	1.942	1.470	0.891	100.147
AB101BS3	MX-80	42.5	2.780	32.598	1.931	1.456	0.909	99.651
AB101BS4	MX-80	59.5	2.780	33.707	1.917	1.434	0.939	99.759
AB101BS5	MX-80	76.5	2.780	31.842	1.921	1.457	0.908	97.441
AB102BS1	MX-80	8.5	2.780	32.776	1.934	1.457	0.908	100.322
AB102BS2	MX-80	25.5	2.780	32.385	1.936	1.462	0.901	99.883
AB102BS3	MX-80	42.5	2.780	31.864	1.935	1.468	0.894	99.068
AB102BS4	MX-80	59.5	2.780	31.627	1.945	1.478	0.881	99.805
AB102BS5	MX-80	76.5	2.780	31.394	1.946	1.481	0.878	99.456
AB103BS1	MX-80 granulate	7.5	2.780	33.846	1.934	1.445	0.924	101.802
AB103BS2	MX-80 granulate	22.5	2.780	35.488	1.895	1.399	0.988	99.901
AB103BS3	MX-80 granulate	37.5	2.780	35.940	1.890	1.390	1.000	99.926
AB103BS4	MX-80 granulate	52.5	2.780	36.225	1.882	1.381	1.013	99.461
AB103BS5	MX-80 granulate	67.5	2.780	37.498	1.883	1.370	1.029	101.260
AB103BS6	MX-80 granulate	78	2.780	38.426	1.868	1.350	1.060	100.774
AB104BS1	Kunigel V1	8.5	2.681	22.913	2.075	1.688	0.588	104.459
AB104BS2	Kunigel V1	25.5	2.681	23.419	2.052	1.662	0.613	102.469
AB104BS3	Kunigel V1	42.5	2.681	23.792	2.051	1.657	0.618	103.157
AB104BS4	Kunigel V1	59.5	2.681	24.467	2.042	1.641	0.634	103.442
AB104BS5	Kunigel V1	76.5	2.681	25.483	2.078	1.656	0.619	110.434
AB105BS1	Calcigel	8.5	2.695	33.089	1.947	1.463	0.842	105.892
AB105BS2	Calcigel	25.5	2.695	34.438	1.917	1.426	0.890	104.273
AB105BS3	Calcigel	42.5	2.695	34.428	1.915	1.424	0.892	104.017
AB105BS4	Calcigel	59.5	2.695	34.547	1.909	1.419	0.899	103.525
AB105BS5	Calcigel	76.5	2.695	35.626	1.906	1.405	0.918	104.630
AB106BS1	Ibeco Seal	8.5	2.753	33.898	1.927	1.439	0.913	102.167
AB106BS2	Ibeco Seal	25.5	2.753	33.319	1.921	1.441	0.910	100.779
AB106BS3	Ibeco Seal	42.5	2.753	34.551	1.926	1.431	0.924	102.980
AB106BS4	Ibeco Seal	59.5	2.753	35.066	1.916	1.419	0.940	102.653
AB106BS5	Ibeco Seal	76.5	2.753	36.445	1.923	1.409	0.954	105.226
AB107BS1	MX-80 gr-+quarz	7.5	2.741	29.219	1.955	1.513	0.811	98.704
AB107BS2	MX-80 gr-+quarz	22.5	2.741	30.150	1.944	1.493	0.835	98.938
AB107BS3	MX-80 gr-+quarz	37.5	2.741	30.346	1.934	1.484	0.847	98.155
AB107BS4	MX-80 gr-+quarz	52.5	2.741	30.825	1.934	1.478	0.854	98.910
AB107BS5	MX-80 gr-+quarz	67.5	2.741	32.612	1.913	1.443	0.900	99.330
AB107BS6	MX-80 gr-+quarz	78	2.741	33.737	1.898	1.419	0.931	99.278
AB108BS1	Febex	8.5	2.735	32.496	1.918	1.448	0.889	99.933
AB108BS2	Febex	25.5	2.735	32.507	1.916	1.446	0.892	99.699
AB108BS3	Febex	42.5	2.735	33.042	1.913	1.438	0.902	100.140
AB108BS4	Febex	59.5	2.735	33.712	1.907	1.426	0.918	100.478
AB108BS5	Febex	76.5	2.735	32.693	1.902	1.433	0.909	98.414
AB109BS1	Friedland	8.5	2.828	17.554	2.184	1.858	0.522	95.104
AB109BS2	Friedland	25.5	2.828	18.048	2.171	1.839	0.538	94.876
AB109BS3	Friedland	42.5	2.828	18.543	2.174	1.834	0.542	96.713
AB109BS4	Friedland	59.5	2.828	19.670	2.166	1.810	0.562	98.904
AB109BS5	Friedland	76.5	2.828	21.021	2.108	1.742	0.624	95.286
AB110BS1	Ikosorb	8.5	2.740	30.853	1.921	1.468	0.867	97.541
AB110BS2	Ikosorb	25.5	2.740	30.944	1.940	1.482	0.849	99.869
AB110BS3	Ikosorb	42.5	2.740	30.737	1.932	1.478	0.854	98.580
AB110BS4	Ikosorb	59.5	2.740	32.528	1.929	1.456	0.882	101.002
AB110BS5	Ikosorb	76.5	2.740	34.898	1.883	1.396	0.963	99.307

Figure 6-4. *Water content, bulk density, dry density, void ratio and degree of saturation for block 1 to 10.*

Sample ID	Material	Radial distance	Grain density	Water content	Bulk wet density (paraffin oil)	Bulk dry density	Void ratio	Degree of saturation
		mm	g/cm^3	%	g/cm^3	g/cm^3		%
AB111BS1	MX-80	8.5	2.780	32.838	1.933	1.455	0.910	100.303
AB111BS2	MX-80	25.5	2.780	33.485	1.923	1.441	0.930	100.147
AB111BS3	MX-80	42.5	2.780	33.677	1.921	1.437	0.934	100.197
AB111BS4	MX-80	59.5	2.780	34.783	1.910	1.417	0.962	100.507
AB111BS5	MX-80	76.5	2.780	36.852	1.866	1.364	1.039	98.625
AB112BS1	Callovo Oxfordian	8.5	2.682	11.942	2.257	2.016	0.330	97.021
AB112BS2	Callovo Oxfordian	25.5	2.682	12.664	2.252	1.999	0.342	99.380
AB112BS3	Callovo Oxfordian	42.5	2.682	12.798	2.250	1.995	0.345	99.628
AB112BS4	Callovo Oxfordian	59.5	2.682	12.972	2.236	1.979	0.355	97.985
AB112BS5	Callovo Oxfordian	76.5	2.682	14.627	2.202	1.921	0.396	99.061
AB113BS1	Rokle	8.5	2.940	34.611	1.953	1.451	1.027	99.099
AB113BS2	Rokle	25.5	2.940	34.975	1.947	1.442	1.038	99.035
AB113BS3	Rokle	42.5	2.940	35.230	1.938	1.433	1.051	98.546
AB113BS4	Rokle	59.5	2.940	38.674	1.881	1.356	1.168	97.361
AB113BS5	Rokle	76.5	2.940	39.220	1.894	1.360	1.161	99.277
AB114BS1	Asha 505	8.5	2.869	31.441	1.987	1.512	0.898	100.483
AB114BS2	Asha 505	25.5	2.869	31.023	1.947	1.486	0.930	95.663
AB114BS3	Asha 505	42.5	2.869	31.669	1.963	1.491	0.925	98.258
AB114BS4	Asha 505	59.5	2.869	30.971	1.955	1.492	0.922	96.323
AB114BS5	Asha 505	76.5	2.869	35.410	1.925	1.422	1.018	99.784
AB115BS1	Deponit CAN	8.5	2.750	31.330	1.944	1.480	0.858	100.459
AB115BS2	Deponit CAN	25.5	2.750	31.376	1.940	1.476	0.863	100.011
AB115BS3	Deponit CAN	42.5	2.750	31.617	1.944	1.477	0.862	100.826
AB115BS4	Deponit CAN	59.5	2.750	32.541	1.921	1.449	0.897	99.729
AB115BS5	Deponit CAN	76.5	2.750	34.017	1.920	1.433	0.919	101.773
AB116BS1	Rokle	8.5	2.940	32.517	1.978	1.492	0.970	98.560
AB116BS2	Rokle	25.5	2.940	33.028	1.985	1.492	0.970	100.104
AB116BS3	Rokle	42.5	2.940	33.297	1.977	1.483	0.982	99.648
AB116BS4	Rokle	59.5	2.940	34.325	1.958	1.458	1.017	99.259
AB116BS5	Rokle	76.5	2.940	36.499	1.901	1.393	1.111	96.590
AB117BS1	Kunigel V1	8.5	2.681	21.033	2.092	1.729	0.551	102.342
AB117BS2	Kunigel V1	25.5	2.681	21.901	2.070	1.698	0.579	101.434
AB117BS3	Kunigel V1	42.5	2.681	22.102	2.066	1.692	0.585	101.319
AB117BS4	Kunigel V1	59.5	2.681	22.751	2.062	1.680	0.596	102.329
AB117BS5	Kunigel V1	76.5	2.681	23.394	2.043	1.656	0.619	101.335
AB118BS1	MX-80	8.5	2.780	32.839	1.937	1.458	0.906	100.734
AB118BS2	MX-80	25.5	2.780	33.110	1.921	1.443	0.926	99.351
AB118BS3	MX-80	42.5	2.780	33.285	1.923	1.443	0.927	99.854
AB118BS4	MX-80	59.5	2.780	33.816	1.916	1.432	0.941	99.851
AB118BS5	MX-80	76.5	2.780	35.416	1.894	1.399	0.988	99.676
AB119BS1	MX-80 gr-+quarz	7.5	2.741	28.136	1.964	1.532	0.789	97.796
AB119BS2	MX-80 gr-+quarz	22.5	2.741	29.111	1.950	1.510	0.815	97.943
AB119BS3	MX-80 gr-+quarz	37.5	2.741	30.014	1.944	1.495	0.833	98.730
AB119BS4	MX-80 gr-+quarz	52.5	2.741	30.696	1.932	1.479	0.854	98.545
AB119BS5	MX-80 gr-+quarz	67.5	2.741	31.822	1.915	1.453	0.887	98.372
AB119BS6	MX-80 gr-+quarz	78	2.741	31.952	1.919	1.455	0.884	99.031
AB120BS1	MX-80 granulate	7.5	2.780	39.735	1.828	1.308	1.126	98.137
AB120BS2	MX-80 granulate	22.5	2.780	40.713	1.821	1.294	1.148	98.595
AB120BS3	MX-80 granulate	37.5	2.780	41.376	1.809	1.279	1.173	98.061
AB120BS4	MX-80 granulate	52.5	2.780	41.863	1.791	1.263	1.201	96.867
AB120BS5	MX-80 granulate	67.5	2.780	44.309	1.790	1.240	1.241	99.236
AB120BS6	MX-80 granulate	78	2.780	46.075	1.785	1.222	1.275	100.461

Figure 6-5. *Water content, bulk density, dry density, void ratio and degree of saturation for block 10 to 20.*

Sample ID	Material	Radial distance	Grain density	Water content	Bulk wet density (paraffin oil)	Bulk dry density	Void ratio	Degree of saturation
		mm	g/cm^3	%	g/cm^3	g/cm^3		%
AB121BS1	Febex	8.5	2.735	31.321	1.913	1.457	0.878	97.600
AB121BS2	Febex	25.5	2.735	31.642	1.915	1.455	0.880	98.367
AB121BS3	Febex	42.5	2.735	32.179	1.911	1.446	0.891	98.741
AB121BS4	Febex	59.5	2.735	33.048	1.898	1.426	0.918	98.511
AB121BS5	Febex	76.5	2.735	30.271	1.908	1.464	0.868	95.415
AB122BS1	Callovo Oxfordian	8.5	2.682	11.774	2.263	2.025	0.324	97.323
AB122BS2	Callovo Oxfordian	25.5	2.682	12.088	2.277	2.031	0.320	101.157
AB122BS3	Callovo Oxfordian	42.5	2.682	12.285	2.275	2.026	0.324	101.694
AB122BS4	Callovo Oxfordian	59.5	2.682	12.755	2.266	2.010	0.335	102.271
AB122BS5	Callovo Oxfordian	76.5	2.682	13.449	2.242	1.976	0.357	100.987
AB123BS1	Calcigel	8.5	2.695	28.629	1.973	1.534	0.757	101.938
AB123BS2	Calcigel	25.5	2.695	29.642	1.976	1.525	0.768	104.050
AB123BS3	Calcigel	42.5	2.695	29.867	1.973	1.519	0.774	103.949
AB123BS4	Calcigel	59.5	2.695	30.302	1.950	1.497	0.801	101.992
AB123BS5	Calcigel	76.5	2.695	27.828	1.934	1.513	0.781	96.019
AB124BS1	Asha 505	8.5	2.869	30.752	2.006	1.534	0.870	101.421
AB124BS2	Asha 505	25.5	2.869	30.824	1.999	1.528	0.878	100.729
AB124BS3	Asha 505	42.5	2.869	30.331	1.990	1.527	0.879	98.981
AB124BS4	Asha 505	59.5	2.869	31.211	1.978	1.508	0.903	99.182
AB124BS5	Asha 505	76.5	2.869	29.772	1.971	1.519	0.889	96.108
AB125BS1	Friedland	8.5	2.828	14.825	2.267	1.974	0.432	96.970
AB125BS2	Friedland	25.5	2.828	15.385	2.255	1.955	0.447	97.388
AB125BS3	Friedland	42.5	2.828	15.751	2.245	1.940	0.458	97.281
AB125BS4	Friedland	59.5	2.828	16.305	2.229	1.917	0.475	96.978
AB125BS5	Friedland	76.5	2.828	14.474	2.209	1.930	0.465	87.950
AB126BS1	Ibeco Seal	8.5	2.753	28.998	1.978	1.534	0.795	100.402
AB126BS2	Ibeco Seal	25.5	2.753	29.329	1.976	1.528	0.802	100.645
AB126BS3	Ibeco Seal	42.5	2.753	29.789	1.967	1.516	0.816	100.490
AB126BS4	Ibeco Seal	59.5	2.753	30.794	1.954	1.494	0.843	100.551
AB126BS5	Ibeco Seal	76.5	2.753	27.231	1.967	1.546	0.780	96.064
AB127BS1	Deponit CAN	8.5	2.750	28.842	1.994	1.547	0.777	102.066
AB127BS2	Deponit CAN	25.5	2.750	28.878	1.988	1.543	0.783	101.466
AB127BS3	Deponit CAN	42.5	2.750	29.394	1.978	1.529	0.799	101.211
AB127BS4	Deponit CAN	59.5	2.750	30.346	1.967	1.509	0.822	101.512
AB127BS5	Deponit CAN	76.5	2.750	28.748	1.968	1.528	0.799	98.923
AB128BS1	Ikosorb	8.5	2.740	24.120	2.019	1.627	0.684	96.598
AB128BS2	Ikosorb	25.5	2.740	25.408	2.011	1.604	0.708	98.291
AB128BS3	Ikosorb	42.5	2.740	25.789	2.010	1.598	0.715	98.859
AB128BS4	Ikosorb	59.5	2.740	26.116	2.000	1.585	0.728	98.264
AB128BS5	Ikosorb	76.5	2.740	26.911	1.990	1.568	0.747	98.650
AB129BS1	MX-80	8.5	2.780	26.874	2.002	1.578	0.762	98.073
AB129BS2	MX-80	25.5	2.780	27.173	2.023	1.591	0.747	101.088
AB129BS3	MX-80	42.5	2.780	28.456	2.004	1.560	0.782	101.202
AB129BS4	MX-80	59.5	2.780	28.933	1.993	1.546	0.798	100.765
AB129BS5	MX-80	76.5	2.780	29.941	1.975	1.520	0.829	100.432
AB130BS1	MX-80	8.5	2.780	28.699	1.989	1.545	0.799	99.856
AB130BS2	MX-80	25.5	2.780	30.444	1.973	1.513	0.838	101.050
AB130BS3	MX-80	42.5	2.780	31.560	1.953	1.485	0.873	100.538
AB130BS4	MX-80	59.5	2.780	31.836	1.930	1.464	0.899	98.435
AB130BS5	MX-80	76.5	2.780	32.665	1.915	1.444	0.926	98.109

Figure 6-6. *Water content, bulk density, dry density, void ratio and degree of saturation for block 21 to 30.*

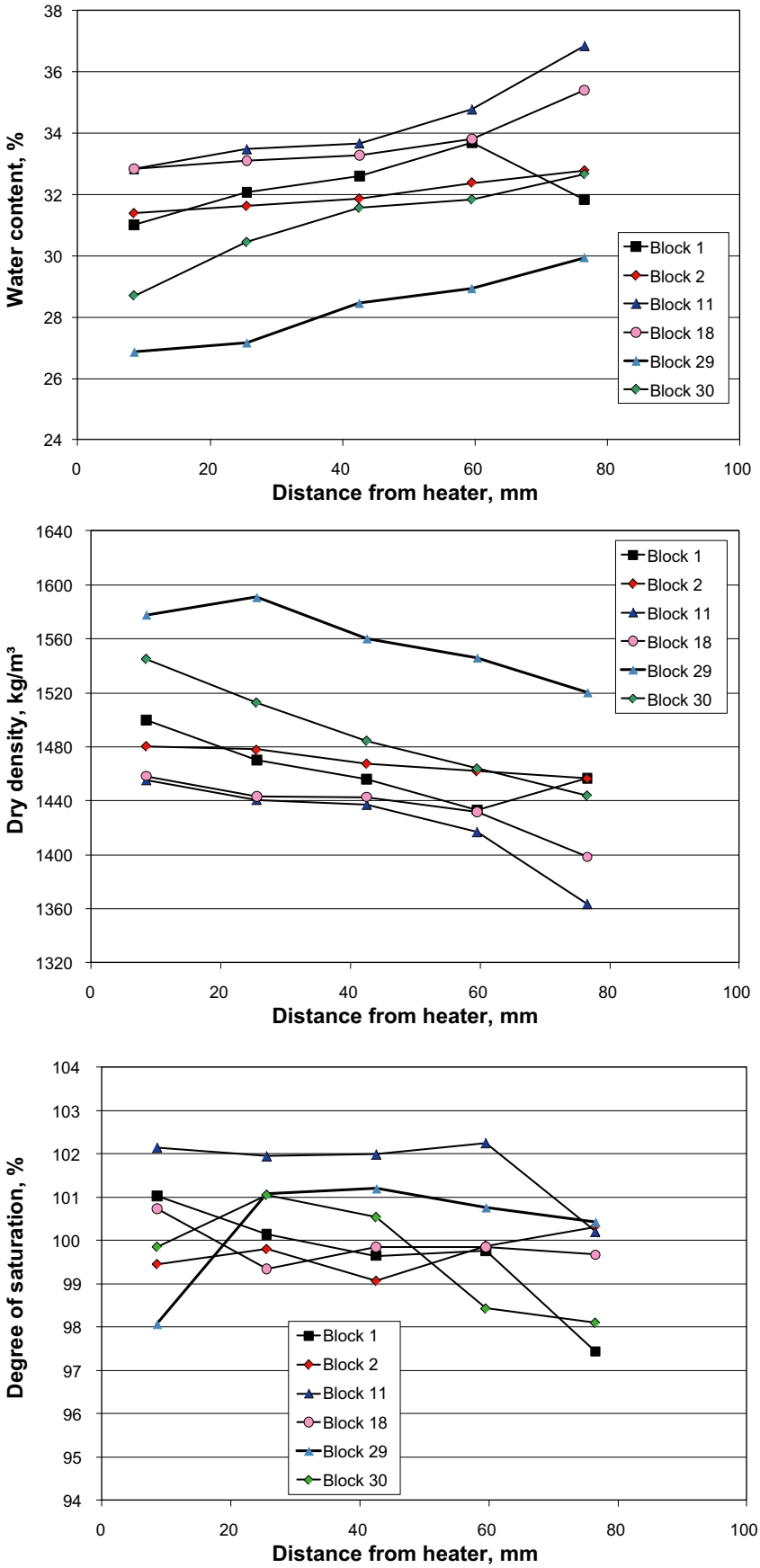

Figure 6-7. *Water content (upper), dry density (middle) and degree of saturation (lower) plotted as function of the radial distance from the inner mantel surface of the blocks made of MX-80 material.*

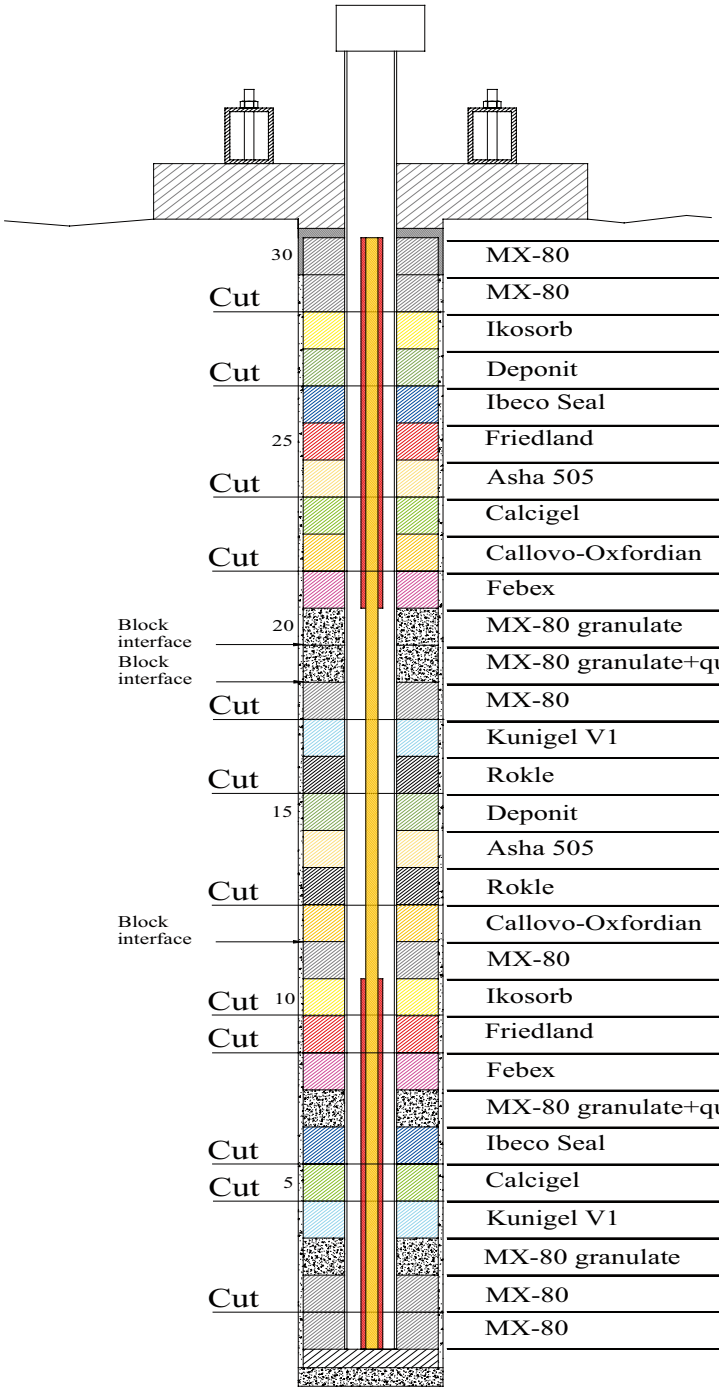

	1	2	3	4	5
MX-80	28.7	30.4	31.6	31.8	32.7
MX-80	26.9	27.2	28.5	28.9	29.9
Ikosorb	24.1	25.4	25.8	26.1	26.9
Deponit	28.8	28.9	29.4	30.3	28.7
Ibeco Seal	29.0	29.3	29.8	30.8	27.2
Friedland	14.8	15.4	15.8	16.3	14.5
Asha 505	30.8	30.8	30.3	31.2	29.8
Calcigel	28.6	29.6	29.9	30.3	27.8
Callovo-Oxfordian	11.8	12.1	12.3	12.8	13.4
Febex	31.3	31.6	32.2	33.0	30.3
MX-80 granulate	39.7	40.7	41.4	41.9	44.3	46.0
MX-80 granulate+quarz	28.1	29.1	20.0	30.7	31.8	31.9
MX-80	32.8	33.1	33.3	33.8	35.4
Kunigel V1	21.0	21.9	22.1	22.8	23.4
Rokle	32.5	33.0	33.3	34.3	36.5
Deponit	31.3	31.4	31.6	32.5	34.0
Asha 505	31.4	31.0	31.7	31.0	35.4
Rokle	34.6	35.0	35.2	38.7	39.2
Callovo-Oxfordian	11.9	12.7	12.8	13.0	14.6
MX-80	32.8	33.5	33.7	34.8	36.9
Ikosorb	30.9	30.9	30.7	32.5	34.9
Friedland	17.6	18.0	18.5	19.7	21.0
Febex	32.5	26.6	33.0	33.7	32.7
MX-80 granulate+quarz	29.2	30.2	30.3	30.8	32.6	33.7
Ibeco Seal	33.9	33.3	34.6	35.1	36.4
Calcigel	33.1	34.4	34.4	34.5	35.6
Kunigel V1	22.9	23.4	23.8	24.5	25.5
MX-80 granulate	33.8	35.5	35.9	36.2	37.5	38.4
MX-80	31.4	31.6	31.9	32.4	32.8
MX-80	31.0	32.1	32.6	33.7	31.8

Figure 6-8. *Radial water content distribution (%) for all blocks in test package 1. Most of the samples were taken in the south direction.*

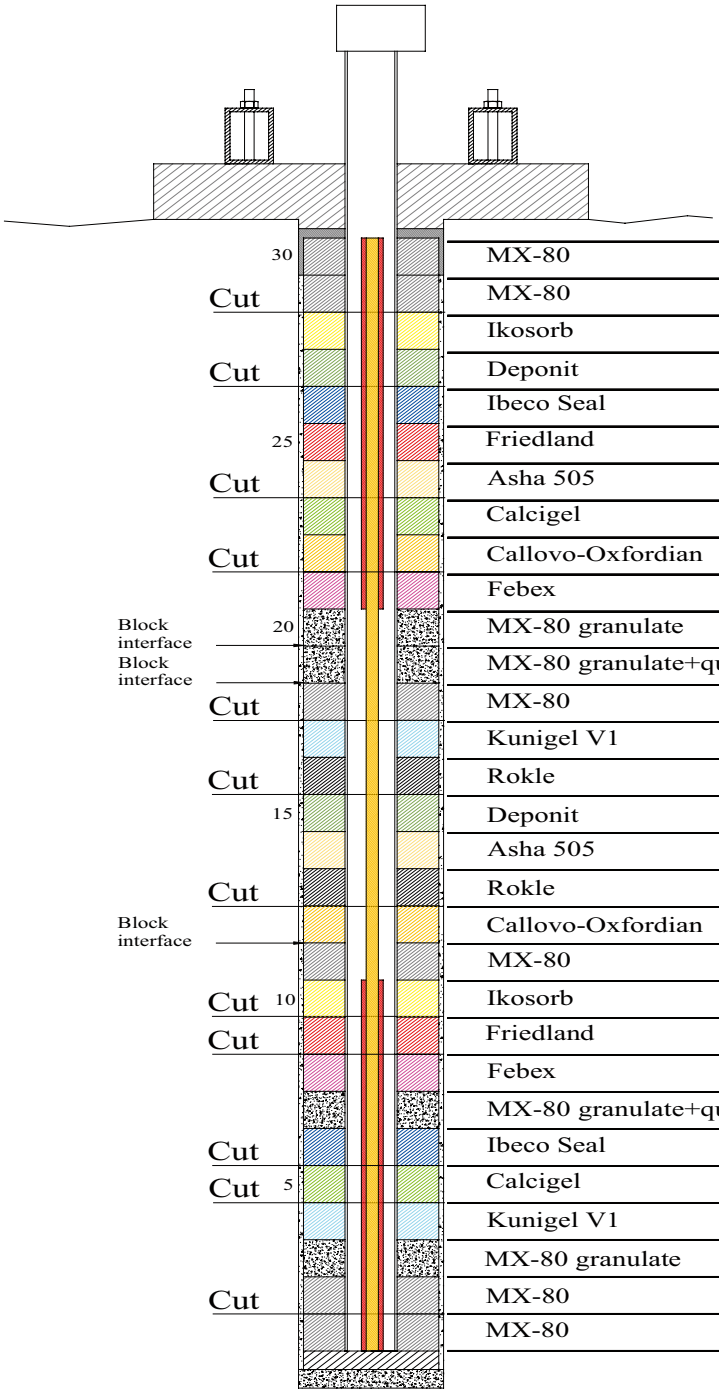

	1	2	3	4	5
MX-80	1545	1513	1485	1464	1444
MX-80	1578	1591	1560	1546	1520
Ikosorb	1627	1604	1598	1585	1568
Deponit	1547	1543	1529	1509	1528
Ibeco Seal	1534	1528	1516	1494	1546
Friedland	1974	1955	1940	1917	1930
Asha 505	1534	1528	1527	1508	1519
Calcigel	1534	1525	1519	1497	1513
Callovo-Oxfordian	2025	2031	2026	2010	1976
Febex	1457	1455	1446	1426	1464
MX-80 granulate	1308	1294	1279	1263	1240	1222
MX-80 granulate+quarz	1532	1510	1495	1479	1453	1455
MX-80	1458	1443	1443	1432	1399
Kunigel V1	1729	1698	1692	1680	1656
Rokle	1492	1492	1483	1458	1393
Deponit	1480	1476	1477	1449	1433
Asha 505	1512	1486	1491	1492	1422
Rokle	1953	1947	1938	1881	1894
Callovo-Oxfordian	2016	1999	1995	1979	1921
MX-80	1455	1441	1437	1417	1364
Ikosorb	1921	1940	1932	1929	1883
Friedland	1858	1839	1834	1810	1742
Febex	1448	1513	1438	1426	1433
MX-80 granulate+quarz	1513	1493	1484	1478	1443	1419
Ibeco Seal	1439	1441	1431	1419	1409
Calcigel	1463	1426	1424	1419	1405
Kunigel V1	1688	1662	1657	1641	1656
MX-80 granulate	1445	1399	1390	1381	1370	1350
MX-80	1481	1478	1468	1462	1457
MX-80	1500	1470	1456	1434	1457

Figure 6-9. *Radial dry density distribution (kg/m^3) for all blocks in test package 1. Most of the samples were taken in the south direction.*

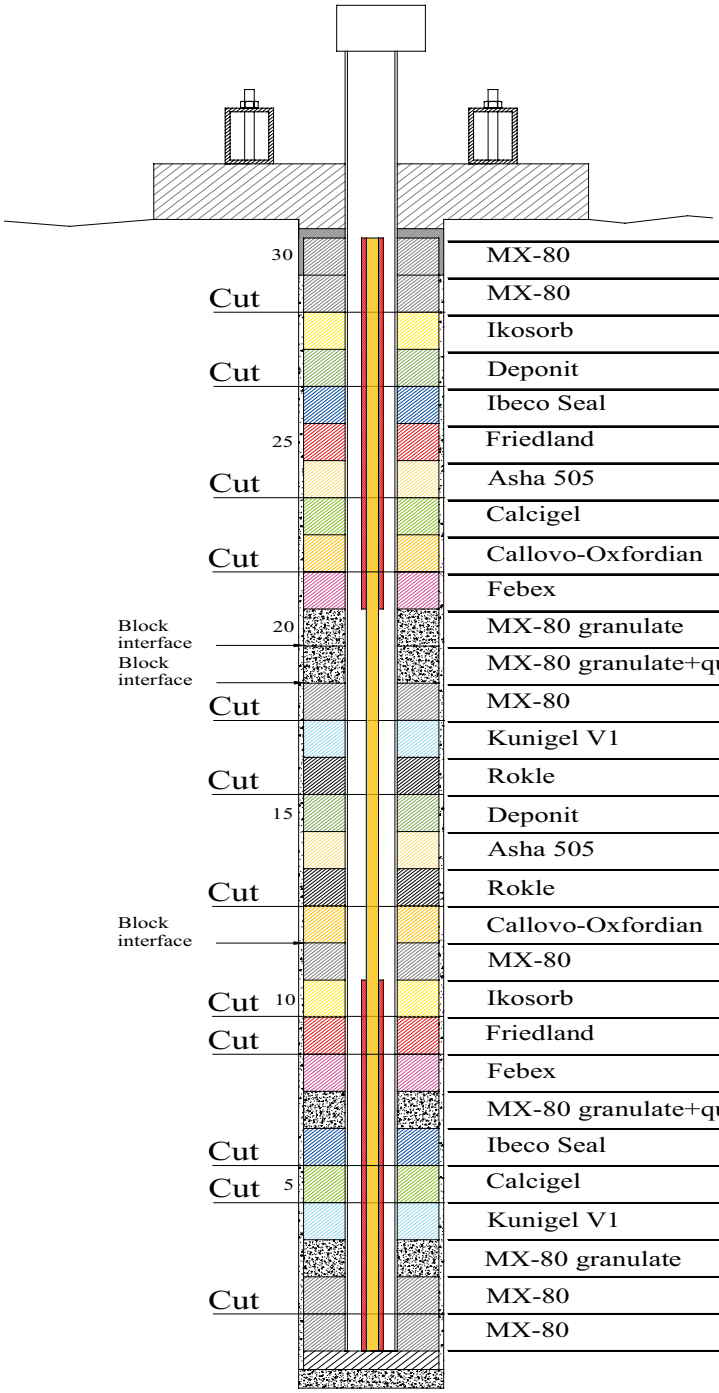

	1	2	3	4	5
MX-80	99.9	101.0	100.5	98.4	98.1
MX-80	98.1	101.1	101.2	100.8	100.4
Ikosorb	96.6	98.3	98.9	98.3	98.6
Deponit	102.1	101.5	101.2	101.5	98.9
Ibeco Seal	100.4	100.6	100.5	100.6	96.1
Friedland	97.0	97.4	97.3	97.0	87.9
Asha 505	101.4	100.7	99.0	99.2	96.1
Calcigel	101.9	104.0	103.9	102.0	96.0
Callovo-Oxfordian	97.3	101.2	101.7	102.3	101.0
Febex	97.6	98.4	98.7	98.5	95.4
MX-80 granulate	98.1	98.6	98.1	96.9	99.2	100.5
MX-80 granulate+quarz	97.8	97.9	98.7	98.5	98.4	99.0
MX-80	100.7	99.4	99.9	99.9	99.7
Kunigel V1	102.3	101.4	101.3	102.3	101.3
Rokle	98.6	100.1	99.6	99.3	96.6
Deponit	100.5	100.0	100.8	99.7	101.8
Asha 505	100.5	95.7	98.3	96.3	99.8
Rokle	99.1	99.0	98.5	97.4	99.3
Callovo-Oxfordian	97.0	99.4	99.6	98.0	99.1
MX-80	100.3	100.1	100.2	100.5	98.6
Ikosorb	97.5	99.9	98.6	101.0	99.3
Friedland	95.1	94.9	96.7	98.9	95.3
Febex	99.9	99.7	100.1	100.5	98.4
MX-80 granulate+quarz	98.7	98.9	98.1	98.9	99.3	99.3
Ibeco Seal	102.2	100.8	103.0	102.7	105.2
Calcigel	105.9	104.3	104.0	103.5	104.6
Kunigel V1	104.5	102.5	103.2	103.4	110.4
MX-80 granulate	101.8	99.9	99.9	99.5	101.3	100.8
MX-80	100.3	99.9	99.1	99.8	99.5
MX-80	101.0	100.1	99.7	99.8	97.4

Figure 6-10. *Radial degree of saturation distribution (%) for all blocks in test package 1. Most of the samples were taken in the south direction.*

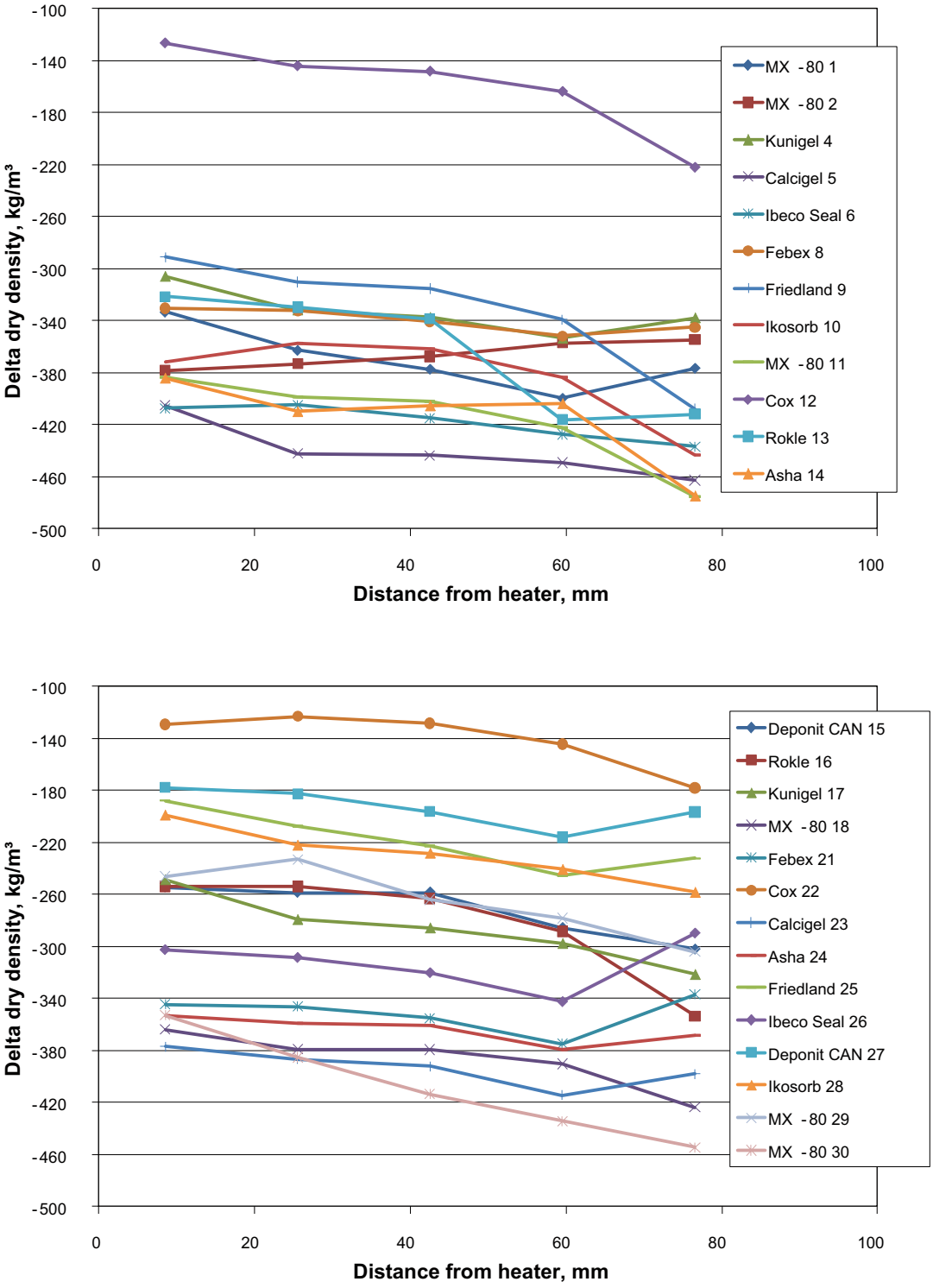

Figure 6-11. *The diagrams show radial distribution of the calculated differences in dry density between the installed blocks and after termination. The upper diagram shows the result for block 1 to14 and the lower for block 15 to 30.*

6.5 Swelling pressure and hydraulic conductivity

6.5.1 Test procedur

The swelling pressure and hydraulic conductivity were determined for three of the materials, MX-80, Deponit CAN and Asha 505. Measurements have been made both on material taken from different positions in the test parcel but also on reference material saved from the block production. Five special designed test cells were used, see Figure 6-12.

In the test cell, the sample is confined by a steel cylinder with the inner diameter of 35 mm and stainless steel filters at the top and bottom. The height of the samples was in most cases about 15 mm but in addition some tests with a height of 8 mm also were performed. The axial force from the sample due to the swelling pressure was measured by a transducer positioned between the piston and the upper lid.

The test series includes totally twenty-three tests, see Table 6-2:

1. **Reference materials**. Totally ten tests were made. These samples were prepared using material saved from the block production. The air dry material was compacted to a certain density and then placed in the test cell.
2. **Package material**. Totally thirteen tests were made. The main part of the samples were drilled and sawn out to fit the test cells, see Figure 6-13. In order to compare the preparation technique one sample was prepared by crushing and drying material and then re-compact it to a density close to the original.

All tests were performed using formation water from borehole KA2598A which also was used for the artificial saturation of the test parcels in field (test parcel 1 and 2).

The compacted, or trimmed, sample was placed in the test cell which then was assembled. In order to avoid problems with trapped air, filters and tubes were evacuated by use of a vacuum pump and water was then let in, filling up all empty voids in the test cell. The water uptake was during saturation monitored indirectly by the force transducer. After about one week stable conditions were reached and a water pressure of 500 kPa was applied in the bottom filter in order to percolate the sample with water. The volume of the percolated water was measured daily by measuring the position of the water meniscus in the tube leading out from the upper filter. The hydraulic conductivity was measured during about one week and then the water pressure was reduced to zero. After a certain time of recovery the test was terminated. Each sample was split in two halves and the bulk density and the water content were determined according to the technique described in Section 6.1. The degree of saturation, the void ratio and the dry density could then be calculated.

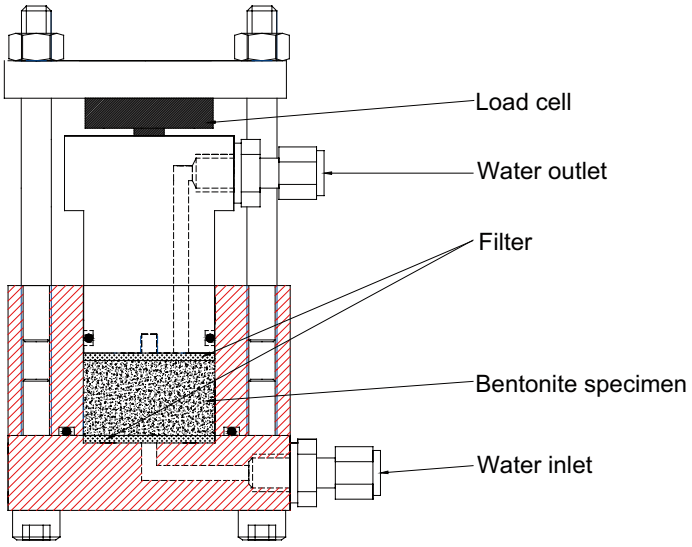

Figure 6-12. *Schematic showing an .*

Figure 6-13. *Preparation of samples for measuring the swelling pressure and the hydraulic conductivity. The samples were drilled out and then sawn out from the block pieces.*

The swelling pressure P_s was calculated from the measured force at zero water pressure according to:

$$P_s = \frac{F}{A} \qquad 6\text{-}7$$

where F is the axial force (N) and A is the sample area acting on the piston (m^2). The accuracy of the measurements depends on the force transducer which is calibrated by use of special standard rings (SP calibrated).

The hydraulic conductivity was evaluated from the percolated water volume according to Darcy's lag:

$$k = \frac{V \cdot l}{A \cdot h \cdot t} \qquad 6\text{-}8$$

Where V is the percolated volume (m^3), l is the sample length (m), A is the sample area (m^2), h is the water pressure difference over the sample (mvp) and t is the time (s).

6.5.2 Results

A compilation of the results from the measurements is provided in Table 6-2. The denominations of samples taken from the test parcel are done according to the system described in Section 6.2. The results are also presented in diagrams, two for each tested material, where the swelling pressure and hydraulic conductivity is plotted versus the dry density of each sample; see Figure 6-14 to 6-16.

The scatter in density of the trimmed sample depends probably on the preparation technique and is not directly related to the previous field conditions.

Table 6-2. Results from measurements of swelling pressure and hydraulic conductivity.

Denomination	Material	Remark	Preparation	Water content %	Dry density kg/m^3	Swelling pressure kPa	Hydraulic conductivity m/s
MX-80 ref1	MX-80	Reference	powder	36.5	1374	1621	3.5E-13
MX-80 ref2	MX-80	Reference	powder	31.9	1472	3519	1.8E-13
MX-80 ref3	MX-80	Reference	powder	27.3	1567	5559	1.2E-13
MX-80 ref4	MX-80	h=8 mm	powder	38.1	1351	1541	3.8E-13
AB102BE2b	MX-80	Inner	trimmed	35.4	1413	1453	2.0E-13
AB102BE8b	MX-80	Outer	trimmed	39.2	1327	1043.0	3.0E-13
AB102BE2b	MX-80	Inner, h=8 mm	trimmed	36.8	1401	1305	2.0E-13
AB102BE2b	MX-80	Inner, h=8 mm	crushed	35.5	1401	1674	3.8E-13
Dep. CAN ref1	Deponit CAN	Reference	powder	31.9	1469	3990	1.6E-13
Dep. CAN ref2	Deponit CAN	Reference	powder	43.4	1262	936	1.5E-12
Dep. CAN ref3	Deponit CAN	Reference	powder	35.3	1409	2815	3.0E-13
AB115BN2b	Deponit CAN	Inner	trimmed	35.8	1407	1334	2.9E-13
AB115BN8b	Deponit CAN	Outer	trimmed	38.7	1349	1113	3.7E-13
AB127BN2b	Deponit CAN	Inner	trimmed	34.3	1457	1953	1.7E-13
AB127BN8b	Deponit CAN	Outer	trimmed	32.9	1467	2436	1.6E-13
Asha ref1	Asha 505	Reference	powder	33.0	1494	3163	3.7E-13
Asha ref2	Asha 505	Reference	powder	42.7	1304	780	2.4E-12
Asha ref3	Asha 505	Reference	powder	35.7	1406	1783	6.8E-13
AB114BN2b	Asha 505	Inner	trimmed	34.1	1443	816	6.4E-13
AB114BN8b	Asha 505	Outer	trimmed	38.7	1371	924	6.9E-13
AB124BE2b	Asha 505	Inner	trimmed	34.1	1457	960	5.0E-13
AB124BE5b	Asha 505	Middle	trimmed	32.9	1483	1404	2.9E-13
AB124BE8b	Asha 505	Outer	trimmed	35.0	1439	1657	3.3E-13

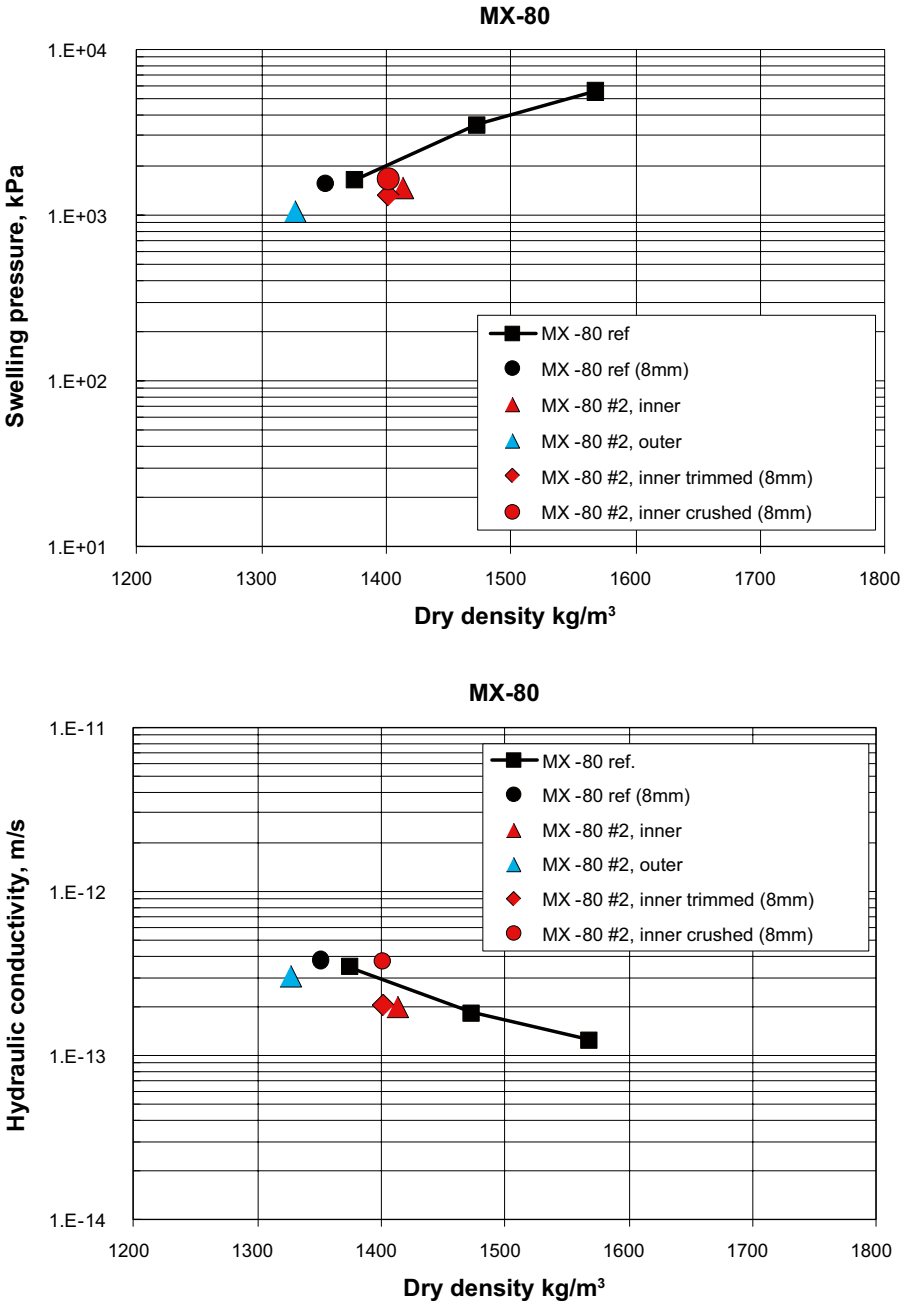

Figure 6-14. *Swelling pressure (upper) and hydraulic conductivity (lower) plotted versus dry density for the MX-80 samples.*

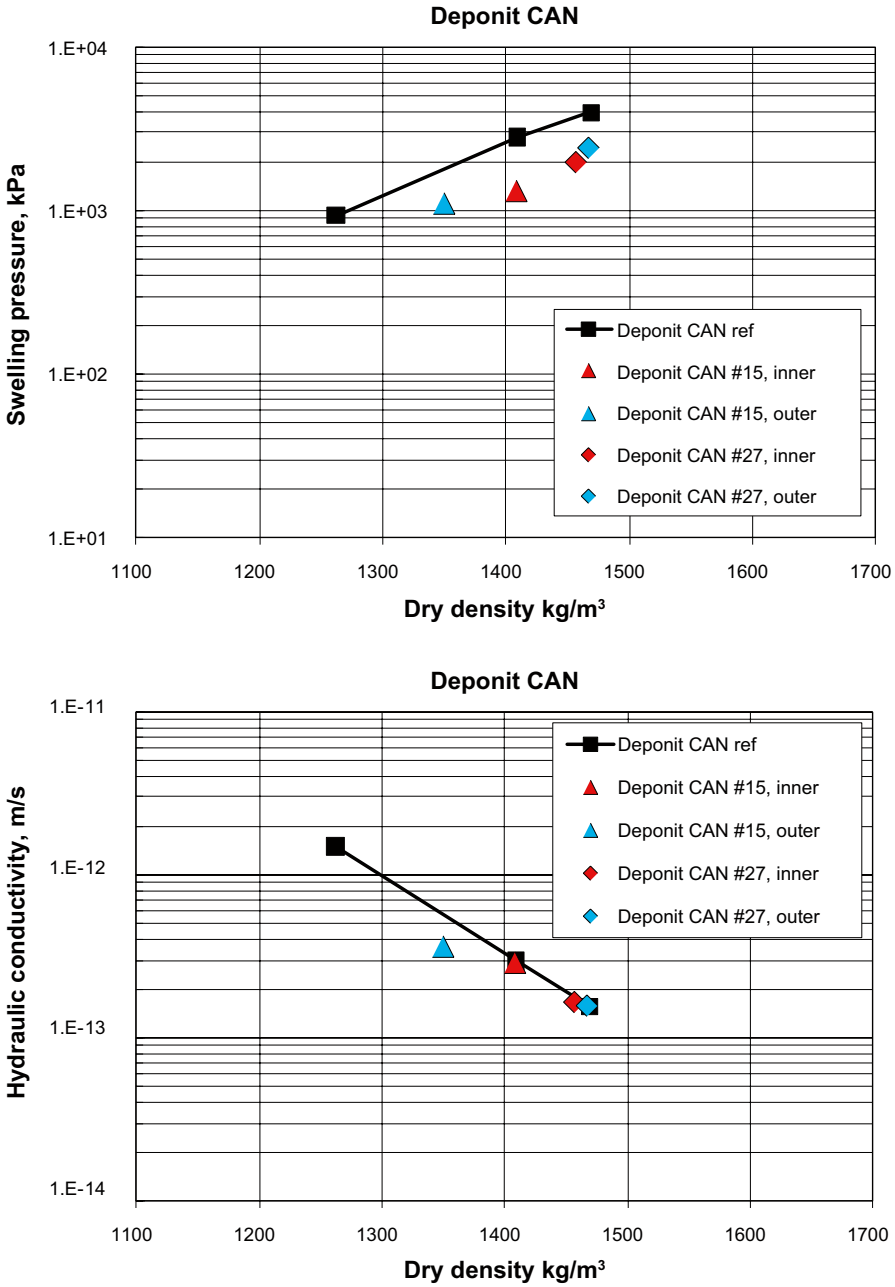

Figure 6-15. *Swelling pressure (upper) and hydraulic conductivity (lower) plotted versus dry density for the Deponit CAN samples.*

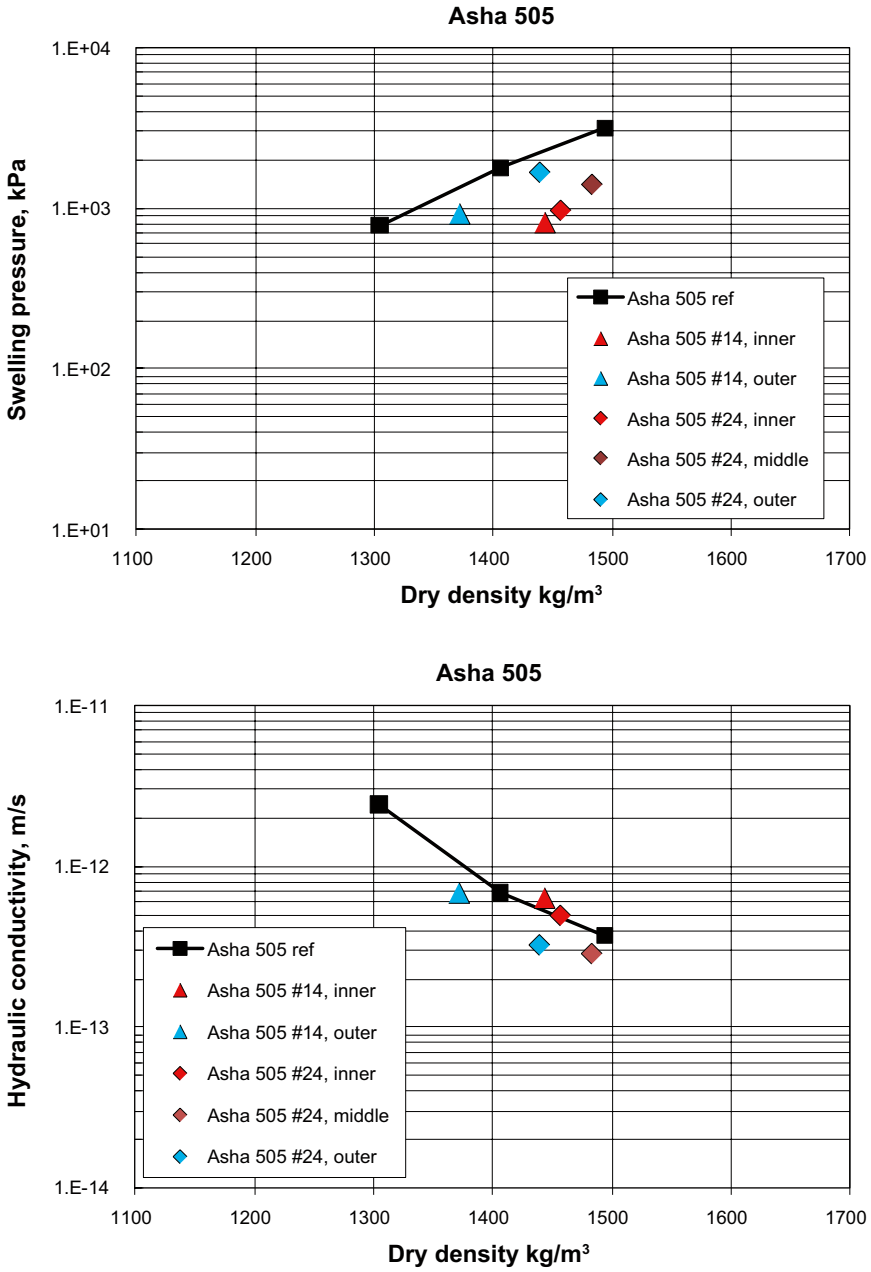

Figure 6-16. *Swelling pressure (upper) and hydraulic conductivity (lower) plotted versus dry density for the Asha 505 samples.*

6.6 Unconfined compression tests

6.6.1 General

The unconfined compression test is an experimentally simple method where a specimen is compressed axially with a constant rate of strain with no radial confinement or external radial stress.

The cylindrical specimen is compressed to shear failure and when aiming at determination of shear strength it is important to allow for the shear failure to develop without boundary effects at the end surfaces of the specimen and the dimensions should therefore be a height which is double the size of the diameter. However, with the height equal to the diameter and with lubricated end surfaces the effects of the boundaries are minimized and the maximum deviator stress has been shown to be a good measure of the shear strength (Dueck et al. 2010).

6.6.2 Test procedure and evaluation

Three test series were run, one for each of the materials used. Each test series included samples from the field experiment and corresponding reference material. The specimens from the field experiment were prepared both as drilled specimens and as ground (dried, ground and re-compacted) specimens.

The diameter of the test samples was minimized in order to get spatial resolution of the test parcel and to ensure full water re-saturation. The diameter and the height were for all specimens 20 mm. Groundwater (filtered) from the ABM test site was used for saturation.

Three types of bentonites were tested; MX-80, Asha and Deponit CAN. MX-80 specimens were taken from block #2 and the reference material MX-80 02R, Asha specimens from block #14 and the reference material Asha 14R and the Deponit CAN specimens were taken from blocks #15 and #27 and the reference material CAN 15R and CAN 27R, respectively. Since the reference material Asha 14R contained large grains some extra reference tests were made with ground reference material Asha 14R. At least six specimens from each of the bentonites from the field experiment were drilled from different positions of the block used.

The field exposed material was retrieved as large sectors and for each material a slice from such sector was taken for the unconfined compression tests. In such slice all radii were represented, i.e. all radii from the heater (0 mm) to the rock (100 mm).

Equipment

All specimens were saturated in a special designed device of steel before the shear test. The specimens were placed in a mechanical press according to Figure 6-17 where a constant rate of deformation was applied to the specimen. The end surfaces were lubricated to minimize the end effects of the specimens. During the tests the deformation and the applied force were measured by means of a load cell and a deformation transducer. All transducers were calibrated prior to the shearing of one series and checked afterwards.

Preparation of specimens

Cylindrical specimens were prepared for all tests but different preparation techniques were used. The specimens were either prepared from the field exposed material by drilling and trimming cylindrical specimens or prepared in a compaction device from powder to cylindrical specimens. All specimens were prepared to the same dimensions; 20 mm in diameter and 20 mm in height

All specimens were placed in a saturation device were they were saturated with groundwater from the ABM test site applied after evacuation of air from the filters and tubes. After saturation during 2 weeks the specimens were removed from the saturation device at least 12 h before the shearing, while protected against evaporation.

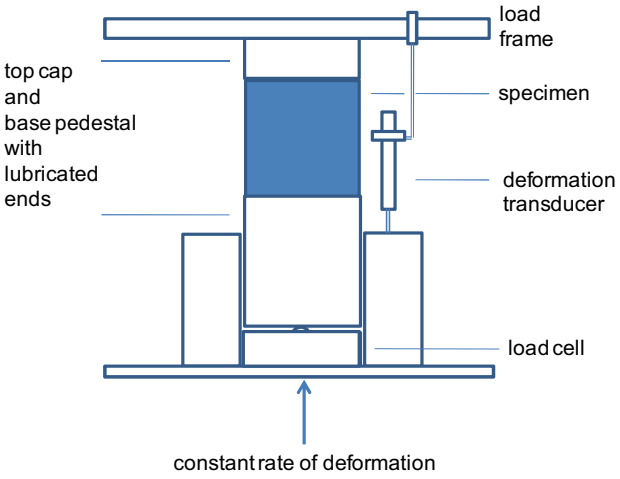

Figure 6-17. *Set-up for the unconfined compression test.*

Test procedure

The specimens were placed in the mechanical press and the compression started and continued at a constant deformation rate of 0.8%/min, i.e. 0.16 mm/min. During shearing the specimens were surrounded by a protective plastic sheet to prevent evaporation. After failure the water content and density were determined according to Section 6.4.2.

Evaluated variables

The specimens were considered as undrained during shearing and no volume change was taken into account. The deviator stress q (kPa) and the strain ε (%) were derived from Equation 6-9 and 6-10, respectively.

$$q = \frac{F}{A_0} \cdot \left(\frac{l_0 - \Delta l}{l_0}\right) \tag{6-9}$$

$$\varepsilon = \frac{\Delta l}{l_0} \cdot 100 \tag{6-10}$$

where

F = applied vertical load (kN)

A_0 = original cross section area (m^2)

l_0 = original length (m)

Δl = change in length (m)

The results were corrected for initial problems with the contact surface in that decreasing the strain with the intercept on the x-axis, strain, of the tangent to the stress-strain curve taken at a stress of 500 kPa.

6.6.3 Results

All test results in terms of maximum deviator stress q_{max} and corresponding strain ε are given for MX-80, Asha and Deponit CAN specimens in Tables 6-3 to 6-5. The results are given with the actual dry density ρ_d, water content w and degree of saturation S_r.

Results from the specimens from the field experiment are shown as deviator stress versus strain in Figures 6-18 to 6-20 where the legends show "*Test ID_ dry density(kg/m³)_distance from heater (mm)*". The letter G after the distance denotes the material being dried, ground and re-compacted before the saturation.

Table 6-3 Test results from unconfined compression tests on MX-80, block #2.

Sample ID	Test ID	Type of material	Preparation[1]	Dry density ρ_d (kg/m^3)	Water content w (%)	Degree of saturation S_r (%)	Maximum deviator stress q_{max} (kPa)	Strain at qmax e (%)
MX-80 02R	AB102UC01	MX-80	compacted	1,310	39.0	97	557	11.4
MX-80 02R	AB102UC02	MX-80	compacted	1,468	30.8	96	1,586	8.4
MX-80 02R	AB102UC03	MX-80	compacted	1,625	24.9	98	3,556	8.2
MX-80 02R	AB102UC04	MX-80	compacted	1,338	38.2	99	705	11.4
MX-80 02R	AB102UC05	MX-80	compacted	1,495	30.1	97	1,688	9.3
MX-80 02R	AB102UC06	MX-80	compacted	1,634	24.3	96	3,669	7.5
AB102BE2b	AB102UC07	MX-80	drilled	1,445	33.7	101	1,289	6.0
AB102BE3b	AB102UC08	MX-80	drilled	1,419	34.7	100	1,017	6.0
AB102BE5b	AB102UC09	MX-80	drilled	1,429	33.6	99	1,211	7.6
AB102BE6b	AB102UC10	MX-80	drilled	1,446	33.2	100	1,313	7.5
AB102BE8b	AB102UC11	MX-80	drilled	1,405	35.2	100	1,016	7.1
AB102BE1b	AB102UC12	MX-80	drilled	1,457	32.6	100	1,434	6.1
AB102BE1b	AB102UC13	MX-80	ground and compacted	1,522	29.2	98	1,791	11.2
AB102BE3b	AB102UC14	MX-80	ground and compacted	1,529	29.5	100	1,759	10.5
AB102BE7b	AB102UC15	MX-80	ground and compacted	1,527	29.0	98	1,781	10.9
AB102BE9b	AB102UC16	MX-80	ground and compacted	1,518	30.0	100	1,759	10.8

[1] The preparation also included saturation with filtered water from the ABM test site.

Table 6-4 Test results from unconfined compression tests on Asha, block #14.

Sample ID	Test ID	Type of material	Preparation[1]	Dry density ρ_d (kg/m^3)	Water content w (%)	Degree of saturation S_r (%)	Maximum deviator stress q_{max} (kPa)	Strain at qmax e (%)
Asha 14R	AB114UC01	Asha	compacted	1,272	41.3	94	384	3.9
Asha 14R	AB114UC02	Asha	compacted	1,415	35.4	99	1,111	4.0
Asha 14R	AB114UC03	Asha	compacted	1,540	29.6	98	2,345	5.1
Asha 14R	AB114UC04	Asha	compacted	1,636	25.4	97	3,900	3.9
Asha 14R	AB114UC05	Asha	ground and compacted	1,527	30.9	101	2,372	7.0
Asha 14R	AB114UC06	Asha	ground and compacted	1,622	27.2	102	4,365	6.4
AB114BE8b	AB114UC07	Asha	drilled	1,365	37.9	98	680	3.7
AB114BE7b	AB114UC08	Asha	drilled	1,388	36.8	99	596	2.4
AB114BE5b	AB114UC09	Asha	drilled	1,428	34.8	99	900	3.1
AB114BE3b	AB114UC10	Asha	drilled	1,447	33.9	99	1,116	3.0
AB114BE1b	AB114UC11	Asha	drilled	1,448	34.1	100	710	1.8
AB114BE1b	AB114UC12	Asha	drilled	1,432	34.7	99	775	2.1
AB114BE1b	AB114UC13	Asha	ground and compacted	1,499	30.9	97	1,901	4.7
AB114BE1b	AB114UC14	Asha	ground and compacted	1,501	31.0	97	1,865	5.2
AB114BE4b	AB114UC15	Asha	ground and compacted	1,496	30.9	96	1,778	4.5
AB114BE9b	AB114UC16	Asha	ground and compacted	1,512	30.9	99	2,122	6.9
Asha 14R	AB114UC17	Asha	compacted	1,440	34.5	100	1,271	5.0
Asha 14R	AB114UC18	Asha	compacted	1,524	30.3	98	2,207	4.6
Asha 14R	AB114UC19	Asha	compacted	1,608	27.2	100	3,434	5.0

[1] The preparation also included saturation with filtered water from the ABM test site.

Table 6-5 Results from unconfined compression tests on Deponit CAN, blocks #15 and #27.

Sample ID	Test ID	Type of material	Preparation[1]	Dry density ρ_d (kg/m^3)	Water content w (%)	Degree of saturation S_r (%)	Maximum deviator stress q_{max} (kPa)	Strain at qmax e (%)
CAN 15R	AB115UC01	Dep CAN	compacted	1,330	38.4	99	854	9.3
CAN 15R	AB115UC02	Dep CAN	compacted	1,501	30.6	101	2,294	9.3
CAN 15R	AB115UC03	Dep CAN	compacted	1,655	24.0	100	5,784	6.1
CAN 27R	AB127UC04	Dep CAN	compacted	1,354	37.9	101	864	9.5
CAN 27R	AB127UC05	Dep CAN	compacted	1,488	30.5	99	2,096	9.5
CAN 27R	AB127UC06	Dep CAN	compacted	1,613	25.7	100	4,157	7.9
AB115BN1b	AB115UC07	Dep CAN	drilled	1,380	36.8	102	1,250	4.2
AB115BN5b	AB115UC08	Dep CAN	drilled	1,433	33.7	101	1,268	2.5
AB115BN3b	AB115UC09	Dep CAN	drilled	1,440	33.9	102	1,426	2.6
AB115BN6b	AB115UC10	Dep CAN	drilled	1,402	35.7	102	1,497	4.3
AB115BN8b	AB115UC11	Dep CAN	drilled	1,347	38.6	102	864	4.8
AB127BN5b	AB127UC12	Dep CAN	drilled	1,520	30.0	102	2,659	3.0
AB127BN7b	AB127UC13	Dep CAN	drilled	1,505	30.8	102	2,551	3.8
AB127BN1b	AB127UC14	Dep CAN	drilled	1,509	30.9	103	2,641	3.4
AB127BN1b	AB127UC15	Dep CAN	drilled	1,503	31.1	103	2,565	3.5
AB115BN5b	AB115UC16	Dep CAN	drilled	1,432	34.3	102	946	1.4
AB115BN1b	AB115UC17	Dep CAN	ground and compacted	1,527	29.8	102	2,343	8.2
AB115BN7b	AB115UC18	Dep CAN	ground and compacted	1,505	30.7	102	1,955	11.1
AB127BN1b	AB127UC19	Dep CAN	ground and compacted	1,569	27.6	101	3,005	10.0

[1] The preparation also included saturation with filtered water from the ABM test site.

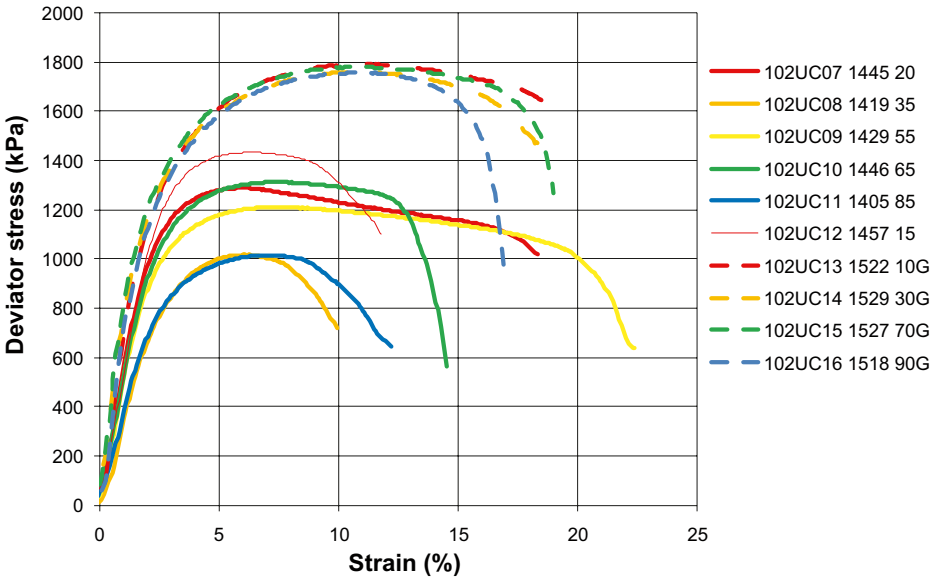

Figure 6-18. *Deviator stress versus strain from specimens of MX-80 from #2. The colors red, orange, yellow, green and blue represent the distances 0–20, 21–40, 41–60, 61–80 and 81–100 mm, respectively. Broken lines represent ground material. The legend shows: Test ID_dry density (kg/m3)_distance from heater (mm).*

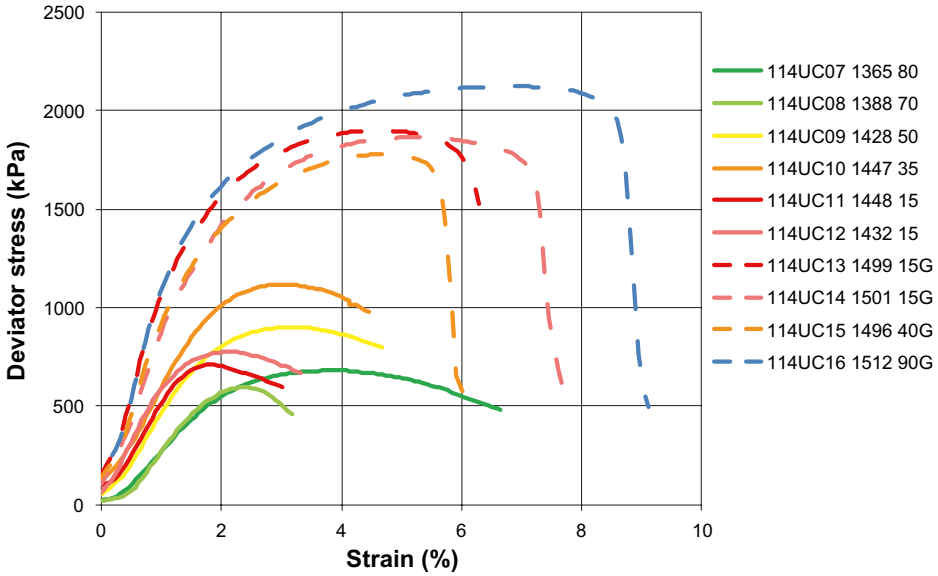

Figure 6-19. *Deviator stress versus strain from specimens of Asha from #14. The colors red, orange, yellow, green and blue represent the distances 0–20, 21–40, 41–60, 61–80 and 81–100 mm, respectively. Broken lines represent ground material. The legend shows: Test ID_dry density (kg/m3)_distance from heater (mm).*

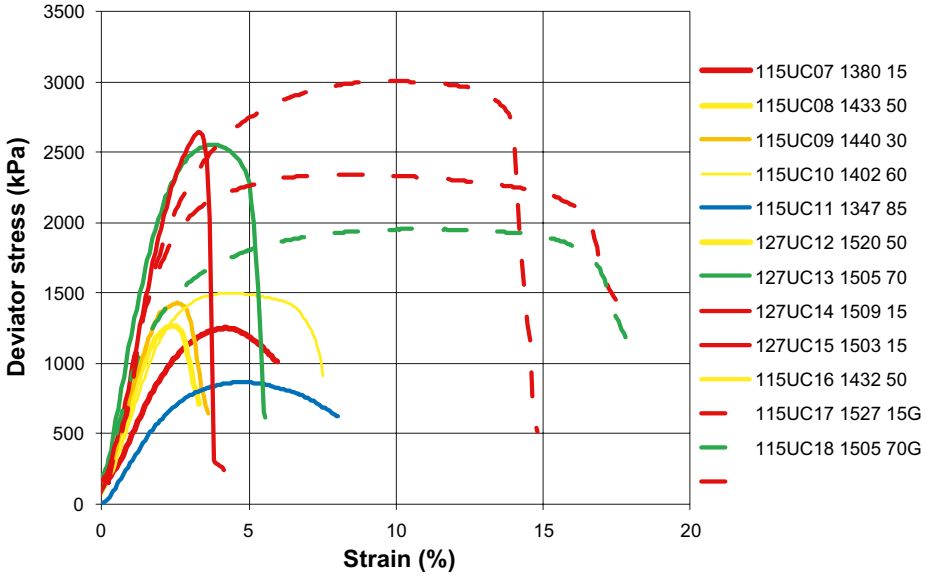

Figure 6-20. *Deviator stress versus strain from specimens of Deponit CAN from #15 and #27. The colors red, orange, yellow, green and blue represent the distances 0–20, 21–40, 41–60, 61–80 and 81–100 mm, respectively. Broken lines represent ground material. The legend shows: Test ID_dry density (kg/m3)_distance from heater (mm).*

All results plotted as maximum deviator stress q_{max} and corresponding strain ε versus dry density are shown for MX-80, Asha and Deponit CAN specimens in Figures 6-21 to 6-22, Figures 6-23 to 6-24 and Figures 6-25 to 6-26, respectively.

In the diagrams below the colors refer to the positions of the ABM1 field experiment. From the warmest to the coldest the colors red, orange, yellow, green and blue represent the distance intervals 0–20, 21–40, 41–60, 61–80, 81–100 mm, respectively from the heater. The reference tests are marked with black or brown markers. The labels denote the material, the distance (mm) from the heater and the letter G denotes the ground specimen.

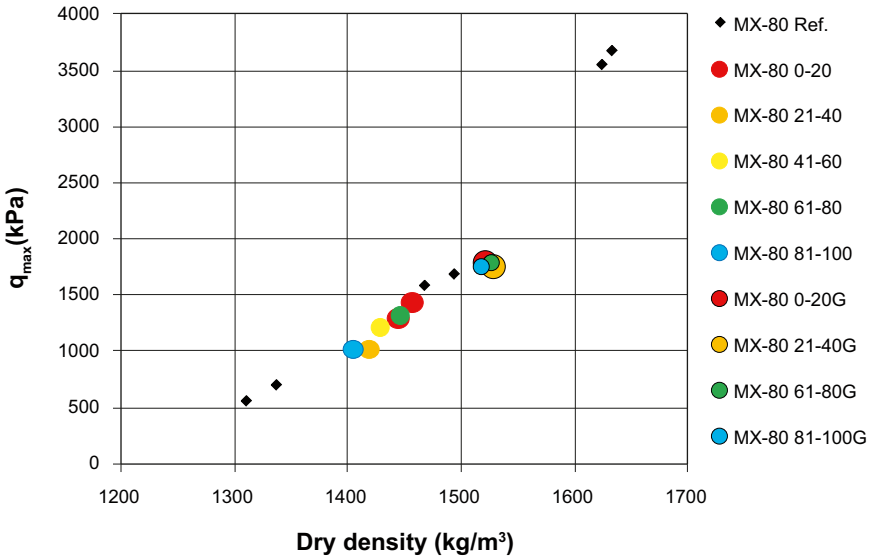

Figure 6-21. *Maximum deviator stress versus dry density. Test results from the specimens of MX-80 from #2. The colors red, orange, yellow, green and blue represent the distances 0–20, 21–40, 41–60, 61–80 and 81–100 mm, respectively. The black diamonds represent reference tests. In the labels G denotes ground specimens.*

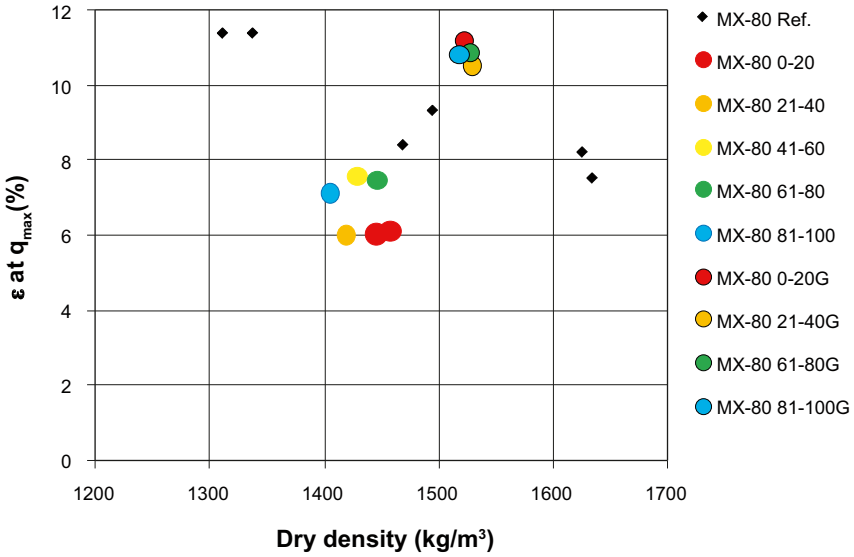

Figure 6-22. *Strain versus dry density. Test results from the specimens of MX-80 from #2. The colors red, orange, yellow, green and blue represent the distances 0–20, 21–40, 41–60, 61–80 and 81–100 mm, respectively. The black diamonds represent reference tests. In the labels G denotes ground specimens.*

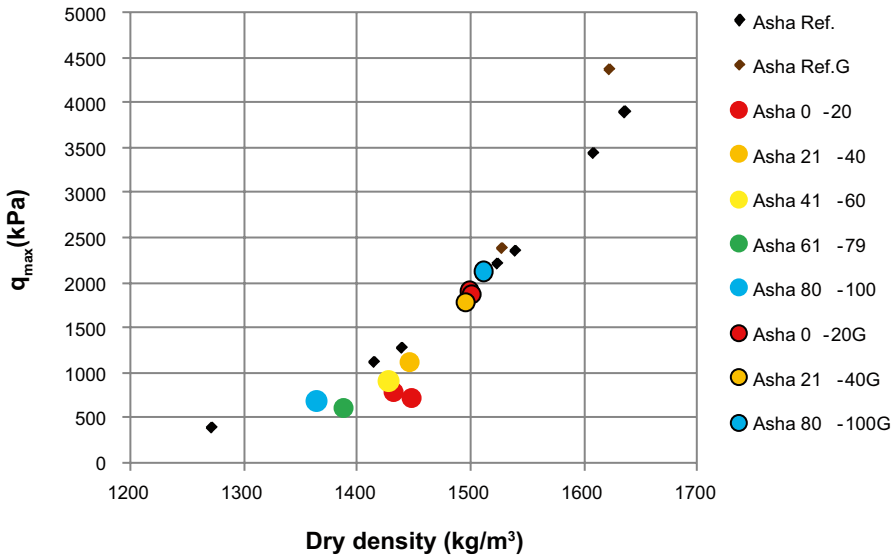

Figure 6-23. *Maximum deviator stress versus dry density. Test results from the specimens of Asha from #14. The colors red, orange, yellow, green and blue represent the distances 0–20, 21–40, 41–60, 61–80 and 81–100 mm, respectively. The black and brown diamonds represent reference tests. In the labels G denotes ground specimens.*

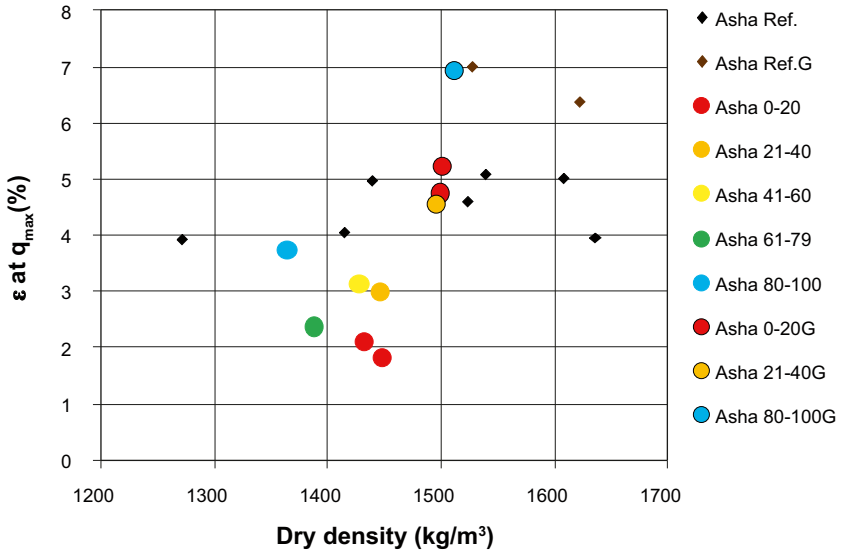

Figure 6-24. *Strain versus dry density. Test results from the specimens of Asha from #14. The colors red, orange, yellow, green and blue represent the distances 0–20, 21–40, 41–60, 61–80 and 81–100 mm, respectively. The black and brown diamonds represent reference tests. In the labels G denotes ground specimens.*

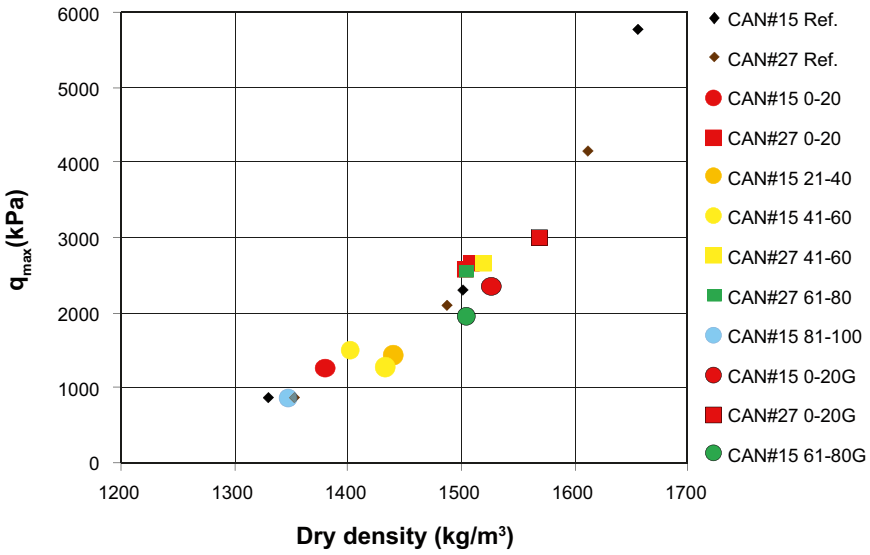

Figure 6-25. *Maximum deviator stress versus dry density. Test results from the specimens of Deponit CAN from #15 and #27. The colors red, orange, yellow, green and blue represent the distances 0–20, 21–40, 41–60, 61–80 and 81–100 mm, respectively. The black and brown diamonds represent reference tests. In the labels G denotes ground specimens.*

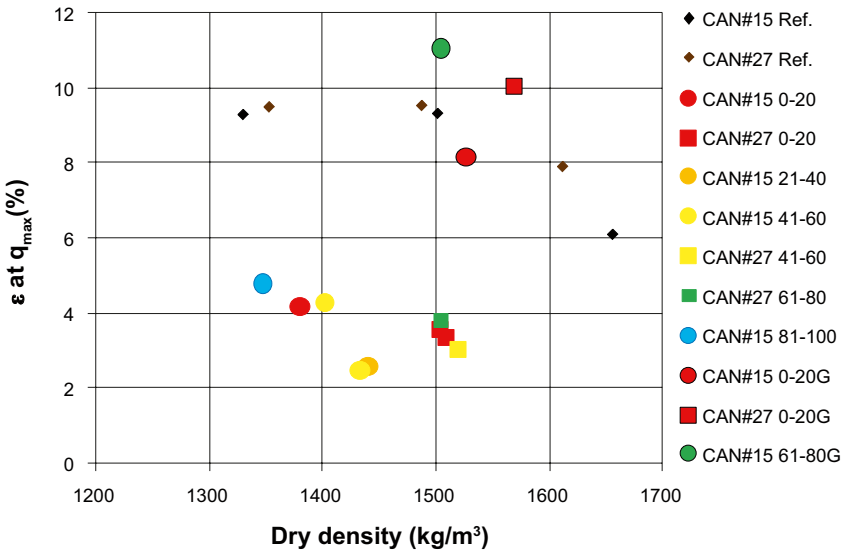

Figure 6-26. *Strain versus dry density. Test results from the specimens of Deponit CAN from #15 and #27. The colors red, orange, yellow, green and blue represent the distances 0–20, 21–40, 41–60, 61–80 and 81–100 mm, respectively. The black and brown diamonds represent reference tests. In the labels G denotes ground specimens.*

Reduced strain at failure, i.e. less strain than the reference specimens was seen on all specimens drilled from the field experiment, particularly from the innermost part. On the other hand, ground material from the field experiment showed strain of the same size or larger than the references.

Regarding the maximum deviator stress q_{max} no large deviations from the references were seen on drilled specimens of MX-80 and Deponit CAN. However, a larger scatter than else was noted in the results from the Deponit CAN specimens. Decreased q_{max} was seen on the drilled specimens of Asha taken 0 to 80 mm from the heater. Concerning maximum deviator stress resulting from the ground specimens the results from Asha specimens did not deviate from the corresponding references while slightly less q_{max} was seen on the ground specimens of MX-80 and Deponit CAN.

Unconfined compression tests on MX-80 samples from block #29 of the ABM1 field experiment were presented by Dueck (2010). The results are shown in Figure 6-27 with results from tests on MX-80 specimens from block #2 from comparable distances from the heater, also shown in Figures 6-21 and 6-22. The results from the two blocks follow the same trends and no obvious difference in the results from the two blocks was seen.

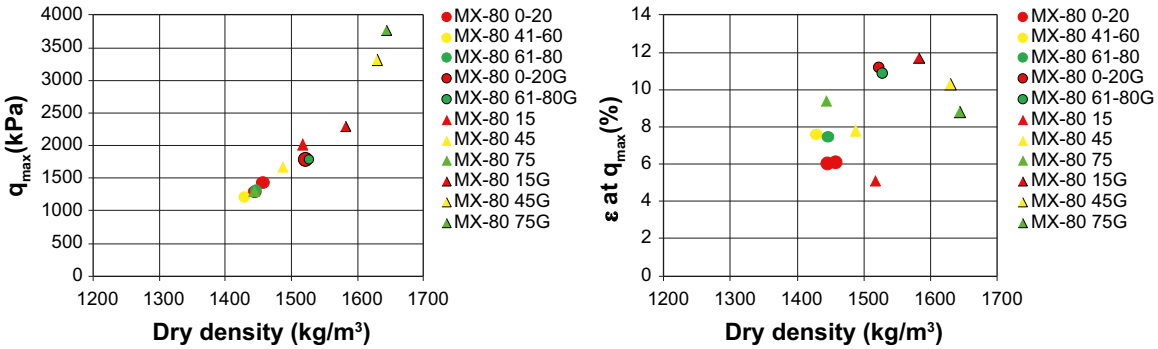

Figure 6-27. *Maximum deviator stress and strain versus dry density for specimens of MX-80 from block #2 (circles) and block #29 (triangles). The results from #2 are also shown in Figures 6-21 and 6-22 and the results from #29 are taken from Dueck (2010). The colors red, orange, yellow, green and blue represent the distances 0–20, 21–40, 41–60, 61–80 and 81–100 mm, respectively. In the labels G denotes ground specimens.*

7 Chemical and mineralogical analyses – reference materials

7.1 General

The chemical and mineralogical characterization of the buffer materials were performed in two campaigns, one initial for the reference clays and a second one at excavated material from the test parcel number 1. The initial characterisation of the clays gave information regarding the wide spread in properties within and between the different clays, but was also used to test different analytical methods towards each other, and in some cases the reliability or variability of a certain method on a specific material. In the project several international groups were also involved, making comparisons between different laboratories possible, which were found to be fruitful.

7.2 Cation exchange capacity (CEC) using the Cu-tri method – reference materials

7.2.1 Method

Smectites (eg. montmorillonite) which are the swelling clay minerals in bentonites are ion exchangers. This means that the mineral is composed by two parts, one stationary which is the silicate structure, and one rather mobile part, which are the counter ions. The two most common counter ions are Na^+ and Ca^{2+}, giving Na- and Ca-bentonite respectively. Almost all bentonites have mixed cation populations and Mg^{2+} and K^+ are also common, however usually not as the dominating cations. The higher the charge of the silicate structure, the more counter ions are present and the higher the cation exchange capacity (CEC) of the smectite is. Consequently the more smectite there is in the bentonite, the higher the CEC will be of the bentonite. Hence CEC of a bentonite is a combined function of the amount of montmorillonite and the montmorillonite surface charge.

The CEC was determined for the bulk clays using the Cu(II)-triethylenetetramine complex according to Meier and Kahr (1999). A clay sample (60 ± 5 mg) was dispersed in deionised water (9 ml) followed by addition of the Cu-complex (1 ml; 45 mM), and left on a vibrating table for 30 minutes. After centrifugation the supernatant was analysed using a spectrophotometer (620 nm, 1 cm cuvette) to determine the concentration of the Cu-complex using a calibration curve. The CEC was calculated as the sum of the Cu-ions absorbed from the solutions in relation to the clay dry mass (a separate sample was taken to get the water content, drying at 105°C for 24 h). The CEC is expressed as cmol(+)/kg which is a factor of 100 times larger compared to eq/kg.

7.2.2 Results

Most clays have rather high CEC values which is typical for bentonites. Friedland and Callovo-Oxfordian has much lower CEC values which is compatible with their different origin. In order to properly compare two samples the determination should probably be done by a single person at the same moment. Homogeneity differences have to be rouled out as well.

Table 7-1. Cation exchange capacity of the reference clays in cmol(+)/kg.

Bentonite	2007-02-22	2007-08-02	2010-01-13	2010-01-14	CEC-average
Asha 505	79.8	89.2	93.5	92.0	88.6
Calcigel	62.2	64.4	71.7	66.2	66.1
Callovo-Oxfordian	6.8		10.1	11.1	9.3
Callovo-Oxfordian (acid treated)		17.1			17.1
Dep CAN	81.0	79.6	84.2	82.0	81.7
Febex	100.9	93.5	99.8	90.2	96.1
Friedland	22.0	26.3		24.0	24.1
Ibeco seal	89.7	87.0	88.0	90.6	88.8
Ikosorb	98.7	90.5	85.9	87.6	90.7
Kunigel	67.1	63.2	63.8	75.6	67.4
MX80	84.3	82.4	80.5	73.7	80.2
Rokle	61.1	62.6	68.5	66.0	64.6

7.3 Anion analysis

7.3.1 Method

In the bentonites various water soluble minerals or salts may be present. These salts may influence the behaviour of the bentonite and may also react differently to temperature gradients, as some salts are higher in solubility at low temperatures and others at high temperatures. The cations in bentonite are present both in the smectites as counter ions and in salt with anions. The counter ions of the smectites are analysed separately (EC), the cations are indirectly seen in the element analyses, and hence as a complement to these analysis to detect soluble salts the anion analysis is very efficient.

A sample of clay (0.5 g) was thoroughly mixed with deionised water (50 ml), dispersed with ultrasonic sound (30 minutes), put on a shake board over night and allowed to equilibrate with the water for one week. The dispersed clay was centrifuged at maximum speed for 30 – 60 minutes, and the supernatant was filtered using a 0.5µm filter and the filtrate was analysed using ion-chromatography (IC, Äspö chemistry lab). The amounts of anions are expressed in relation to the dry weight of the clay (105°C, 24 h). Worth noticing is that 1,000 ppm in this case corresponds to mass and is 1/1,000 = 0.1 wt%.

7.3.2 Results

In most cases the level of sulphate is higher than the chloride level. Ikosorb, Friedland and Asha 505 has 0.2–0.3 wt% chloride. MX-80, IbecoSeal, Deponit CA-N and Friedland have 0.3–0.5 wt% sulphate, the most likely source is gypsum which is a water soluble hydrated calcium sulphate. Fluoride and bromide are very low in all cases.

Table 7-2. Extracted antions from the reference clays in ppm (by weight).

Clay	F (ppm)	Br (ppm)	Cl (ppm)	SO_4 (ppm)
Asha 505	20.2	18.4	2,988	1,043
Calcigel	19.4	0.0	64	388
Callovo-oxfordian	12.6	0.0	76	922
Deponit CA-N	23.4	0.0	744	4,112
Febex	29.1	0.0	652	516
Friedland	16.2	0.0	1,939	5,181
Ibeco Seal	15.7	0.0	255	3,046
Ikosorb	27.1	9.2	3,106	1,051
Kunigel	14.3	0.0	51	1,500
MX80	16.8	0.0	156	3,610
Rokle	45.0	0.0	48	140

7.4 Citrate-Bicarbonate-Dithionite extraction

7.4.1 Method

In bentonite clays various poorly crystalline or amorphous metal oxides may be present, most commonly from Fe, Si and Al. It is important to characterise these for several reasons: (i) due to their relatively high solubility may be more reactive compared to well crystallised minerals, (ii) as they are poorly crystalline or amorphous they are normally not identified in the X-ray diffractograms, and hence may be difficult to find, and (iii) to properly determine the iron content of the montmorillonite one has to remove these free oxides as they also are in the size of clay minerals and cannot be separated gravimetrically by settling.

A clay sample (200 mg) was dispersed in a solution of Na-citrate and Na– bicarbonate (8 ml 0.3 M Na-citrate and 1.0 ml 1 M $NaHCO_3$). The solution was heated to 80°C and Na-dithionite was added (200 mg solid). The mixture was stirred constantly for 1 min and occasionally for 15 min. The solution was kept heated for approximately 30 minutes. A solution of saturated NaCl was added (2 ml) followed by centrifugation. After centrifugation the supernatant was filtered (0.5 µm) and the supernatant was diluted (1:10) and later analysed using ICP-AES /MS. The numbers are given in relation to dry clay (105°C, 24 h).

7.4.2 Results

In almost all cases the extractable iron content was lower in mass % in previously reported results from the clay fractions (Karnland et al. 2006) compared to the bulk clay, which was expected. Elevated amounts of Mn in Rokle indicates presence of undetected Mn-phase. Rather high soluble Si in Calcigel and Rokle, compare with kunigel (low value but a lot of quartz) indicates the presence of amorphous silica.

Table 7-3. Mass percent of Fe, Si, Al and Mn the clays extracted by the CBD method.

Clay	Fe	Si	Al	Mn
Asha505	2.028	0.143	0.087	0.012
Calcigel	0.247	0.468	0.028	0.010
Callovo-Oxfordian	0.084	0.032	0.011	0.003
DepCAN	0.352	0.239	0.057	0.029
Febex	0.073	0.126	0.018	0.004
Friedland	0.306	0.073	0.021	0.001
IbecoSeal	0.105	0.148	0.018	0.010
Ikosorb	0.037	0.091	0.018	0.002
Kunigel	0.074	0.080	0.025	0.042
MX80	0.125	0.176	0.016	0.004
Rokle	3.541	0.390	0.075	0.127

7.5 Chemical data and evolved gas analysis

7.5.1 Method

The elemental analysis of the bulk clays were done at Acmelab, Canada (ISO 9002 accredited laboratory). The clay was fused with lithium metaborate followed by dissolution with dilute nitric acid prior to analysis using inductively coupled plasma using atomic emission spectroscopy (AES) or mass spectroscopy (MS) for detection. Loss on ignition (LOI) was determined gravimetrically by ignition to 1,000°C to allow the release of volatiles.

The evolved gas analysis was done with a Leco machine to determine the sulfur and organic carbon content. The determination is done by temperature programmed heating of the sample combined with an elemental sensitive detector (C or S) eg. IR detector for CO_2. The CO2 released below 550°C was classified as organic carbon.

7.5.2 Results

Table 7-4. Elemental analysis of the reference clays.

Analyte:	SiO_2	Al_2O_3	Fe_2O_3	MgO	CaO	Na_2O	K_2O	TiO_2	P_2O_5
Unit:	%	%	%	%	%	%	%	%	%
MDL:	0.01	0.01	0.04	0.01	0.01	0.01	0.01	0.01	0.001
Sample									
Callovo-oxfordian	44.97	13.4	5.4	2.26	12.81	0.4	2.62	0.72	0.097
Asha 505	46.48	20.64	12.16	2.01	0.84	1.97	0.14	1.01	0.091
Calcigel	54.67	17.54	5.05	3.37	2.94	0.47	1.16	0.41	0.096
Dep CAN	52.01	17.15	4.64	3.11	5.07	0.78	0.90	0.71	0.143
Febex	53.36	16.84	3.88	4.1	1.92	1.08	0.99	0.44	0.09
Friedland	56.89	18.01	6.93	1.95	0.51	0.99	2.82	0.9	0.107
Ibecoseal	55.09	17.75	3.8	3.83	3.14	2.75	1.28	0.39	0.11
Ikosorb	53.5	21.02	2.56	2.15	1.72	2.13	1.15	0.26	0.06
Kunigel	69.5	13.74	1.85	2.15	1.75	2.37	0.25	0.14	0.044
MX80	59.58	18.9	3.91	2.56	1.39	1.95	0.60	0.2	0.085
Rokle	43.74	13.35	13.69	1.96	3.25	0.26	1.00	3.87	0.719

Analyte:	MnO	Cr_2O_3	Ni	Sc	LOI	Sum	Ba	Be	Co
Unit:	%	%	PPM	PPM	%	%	PPM	PPM	PPM
MDL:	0.01	0.002	20	1	0.1	0.01	1	1	0.2
Sample									
Callovo-oxfordian	0.04	0.014	51	16	16.7	99.4	203	2	16.3
Asha 505	0.05	0.038	90	56	14.4	99.89	54	< 1	59.9
Calcigel	0.03	0.005	28	15	14.1	99.87	205	2	6.2
Dep CAN	0.07	0.003	< 20	14	14.5	99.05	900	1	11.5
Febex	0.04	0.002	25	12	17.3	100.06	134	2	5.7
Friedland	0.03	0.017	64	17	10.4	99.56	304	2	15.8
Ibecoseal	0.09	0.006	22	7	11.4	99.65	777	3	5.2
Ikosorb	0.01	< 0.002	25	4	14.9	99.47	1,444	8	2.8
Kunigel	0.06	< 0.002	< 20	8	7.7	99.58	1,089	1	1
MX80	0.02	0.014	< 20	7	10.5	99.67	321	2	2.7
Rokle	0.16	0.012	59	33	17.3	99.33	594	3	47.6

Table 7-4 continued.

Analyte:	Cs	Ga	Hf	Nb	Rb	Sn	Sr	Ta	Th
Unit:	PPM	PPM	PPM	PPM	PPM	PPM	PPM	PPM	PPM
MDL:	0.1	0.5	0.1	0.1	0.1	1	0.5	0.1	0.2
Sample									
Callovo-oxfordian	8.1	16.3	4.7	14.9	104.2	2	353.2	0.9	7.7
Asha 505	0.3	20.2	2	10.3	7.3	< 1	127.6	0.6	2.1
Calcigel	5.3	21.7	8	20.9	59.6	5	69.7	1.5	15.8
Dep CAN	12.7	18.1	4.2	8.6	65.1	2	124.2	0.7	11.4
Febex	4.6	21.5	6.3	17.6	42.4	8	212.5	1.6	15.5
Friedland	12.3	24.5	5.7	20.2	149.3	5	229.4	1.5	14.3
Ibecoseal	4	19.8	5.2	12.1	46.8	3	294.6	0.9	16.2
Ikosorb	4	23	7.1	24.8	47.3	6	196.6	2.2	45.1
Kunigel	1.4	17.2	5.2	6.7	9.8	3	179	0.6	10.8
MX80	1	27.7	8.5	28.7	17.8	9	278.3	3.1	38
Rokle	3	24	10.7	126.5	52.1	4	357.7	7.5	13.2

Analyte:	U	V	W	Zr	Y	La	Ce	Pr	Nd
Unit:	PPM	PPM	PPM	PPM	PPM	PPM	PPM	PPM	PPM
MDL:	0.1	8	0.5	0.1	0.1	0.1	0.1	0.02	0.3
Sample									
Callovo-oxfordian	2.3	125	1.4	154	25.5	30.1	55.5	6.88	26
Asha 505	0.7	189	< 0.5	72.2	30.8	11.3	22.4	2.96	13.2
Calcigel	3.4	45	1.1	253.3	46.3	45.1	93	11.13	43.2
Dep CAN	5.8	150	0.9	145.4	20.1	28.1	57.1	6.81	26
Febex	1.4	39	0.9	187.9	27	34.4	75.8	9.05	33.5
Friedland	4.2	202	2.3	201.9	31.3	42.2	86.8	10.45	37.9
Ibecoseal	6.3	71	0.9	167.2	28.1	38.6	76.7	9.02	33.7
Ikosorb	5.7	35	2.3	219.3	31.6	62.3	113.9	12.75	44
Kunigel	2.6	< 8	< 0.5	132.4	48.9	25.2	57.6	7.12	28.6
MX80	13.1	16	< 0.5	201.1	43.7	52.3	109.7	13.27	50.4
Rokle	1.4	389	2.1	391	33.4	90.3	186.1	22.33	85.4

Analyte:	Sm	Eu	Gd	Tb	Dy	Ho	Er	Tm	Yb
Unit:	PPM	PPM	PPM	PPM	PPM	PPM	PPM	PPM	PPM
MDL:	0.05	0.02	0.05	0.01	0.05	0.02	0.03	0.01	0.05
Sample									
Callovo-oxfordian	4.47	1.07	3.94	0.6	3.99	0.77	2.2	0.32	2.33
Asha 505	2.94	1.18	3.94	0.6	4.36	1.09	2.91	0.42	2.86
Calcigel	7.98	1.34	7.88	1.12	7.36	1.58	4.29	0.69	4.42
Dep CAN	4.69	1.36	4.41	0.57	3.64	0.72	2.13	0.36	2.05
Febex	6.53	1.13	6.03	0.87	5.5	1.07	2.84	0.47	2.73
Friedland	6.88	1.54	6.33	0.85	5.23	1.11	3.12	0.49	3.19
Ibecoseal	6.22	1.4	5.27	0.76	4.81	1	2.78	0.43	2.79
Ikosorb	7.26	1.34	5.63	0.82	5.2	1.18	3.14	0.51	3.4
Kunigel	6.33	0.69	6.66	1.07	7.54	1.7	5.06	0.75	5.54
MX80	10.18	0.82	9.59	1.37	8.62	1.65	4.36	0.66	4.07
Rokle	13.14	3.75	10.53	1.16	6.78	1.17	2.99	0.42	2.42

Table 7-4 continued.

Analyte:	Lu	Mo	Cu	Pb	Zn	Ni	As	Cd	Sb
Unit:	PPM	PPM	PPM	PPM	PPM	PPM	PPM	PPM	PPM
MDL:	0.01	0.1	0.1	0.1	1	0.1	0.5	0.1	0.1
Sample									
Callovo-oxfordian	0.35	0.1	12.8	9.8	48	31.5	7.4	< 0.1	< 0.1
Asha 505	0.41	< 0.1	129.9	0.8	123	44.7	< 0.5	< 0.1	< 0.1
Calcigel	0.66	< 0.1	10.7	22.3	54	15.2	5.2	0.1	< 0.1
Dep CAN	0.32	1	21.2	14	47	5.1	7.8	0.2	0.1
Febex	0.39	< 0.1	5.4	17.6	13	4.7	6	< 0.1	0.2
Friedland	0.46	0.2	23.7	16.2	64	30.7	10.2	0.2	0.2
Ibecoseal	0.41	0.6	14.5	22	51	4.1	4.3	0.2	0.1
Ikosorb	0.5	0.1	1.7	10.1	8	0.9	1.7	< 0.1	< 0.1
Kunigel	0.85	1.4	2.7	12.3	59	1.3	1.9	0.1	< 0.1
MX80	0.56	3.1	4.2	39.7	100	3.6	14.2	0.3	0.7
Rokle	0.35	0.3	165.9	7.3	128	28.6	5.7	0.2	< 0.1

Analyte:	Bi	Ag	Au	Hg	Tl	Se	TOTAL C	C/ORG	TOTAL S
Unit:	PPM	PPM	PPB	PPM	PPM	PPM	%	%	%
MDL:	0.1	0.1	0.5	0.01	0.1	0.5	0.02	0.02	0.02
Sample									
Callovo-oxfordian	0.2	< 0.1	< 0.5	0.02	< 0.1	< 0.5	3.7	0.69	0.68
Asha 505	< 0.1	< 0.1	< 0.5	< 0.01	< 0.1	< 0.5	0.08	< 0.02	0.06
Calcigel	0.3	< 0.1	0.5	0.03	0.3	< 0.5	0.43	< 0.02	0.03
Dep CAN	< 0.1	< 0.1	0.5	0.34	1.9	< 0.5	0.89	0.03	0.7
Febex	0.4	< 0.1	1.4	< 0.01	< 0.1	< 0.5	0.15	< 0.02	0.04
Friedland	0.3	< 0.1	1	0.04	0.1	1.7	0.73	0.29	0.53
Ibecoseal	0.3	< 0.1	< 0.5	0.07	0.4	< 0.5	1.21	0.45	0.24
Ikosorb	0.3	< 0.1	4.1	< 0.01	0.1	< 0.5	0.31	0.04	0.11
Kunigel	0.2	< 0.1	1.2	0.01	0.3	< 0.5	0.43	0.05	0.33
MX80	1	0.1	0.6	0.01	0.4	< 0.5	0.3	0.11	0.24
Rokle	0.1	< 0.1	6.1	0.04	< 0.1	< 0.5	0.49	0.21	0.05

7.6 X-ray Powder diffraction on reference materials

7.6.1 Method

Bentonite is mainly composed by crystalline phases, minerals. The probably most used and powerful technique to identify crystalline phases is powder X-ray diffraction. The technique relies on long range order in the crystals, and hence the lower the crystallinity the weaker the XRD peaks of the phase becomes. Glass which is amorphous scatters X-rays in a very diffuse way, while quartz shows very distinct peaks. Montmorillonite has lower crystallinity compared to quartz, and hence the reflections are broader (this is also a particle size effect). A coarser grained mineral may not scatter completely randomly and in two dimensional diffractograms it is possible to separate single reflections from single mineral grains (eg. quartz which is hard to crush, or other coarse grained minerals such as feldspar and calcite that also has preferred orientation) from complete rings coming from randomly oriented fine grained phases (eg. clay minerals). Clay minerals normally show high orientation in reflection measurements, however in these transmission measurements the level of orientation was very low (indicated by the highly symmetrical diffraction rings).

The reference clays were studied using synchrotron X-rays. This is beneficial for several reasons but also has some drawbacks. The most beneficial parts are: (i) the high intensity and brilliance of the beam, making it possible to do fast measurements with high signal/noise ratio, (ii) the availability of different wavelengths, hence it is possible to minimise fluorescence radiation from the sample which is a problem with Cu-Kα and iron rich samples, (iii) generally lower wavelengths are used, and hence problems with sample absorption is decreased and (iv) the design of the apparatus is open for modifications making it possible to optimise the experimental conditions to the angular interval of interest. The drawbacks are mainly: (i) availability is low, (ii) the use of several wavelengths makes it more complicated to import data to software and more difficult to compare data from different campaigns, (iii) the level of experience needed to make the measurement and evaluate the data is higher compared to conventional XRD. The MAR detector gave two dimensional diffractograms, which after integration gave one dimensional data for standard treatment.

The data was collected at beamline I711 at MAX-Lab, Lund University. Typical measure time was 20–30 seconds. The clays were crushed in an agate mortar prior to measurement. The measurements were done in transmission mode using filled capillaries. The integrated intensity, scattering angle and width of the recorded diffraction rings were evaluated using the software Fit2d (A.P. Hammersley, ESRF). The minimum scattering angle that was measured was approximately $2\theta = 1.7°$, depending on the exact position of the beam stop in each experiment. This corresponded to a maximum observable d-spacing of 38 Å.

Below examples are given on how the minerals were identified. The purpose of this is also to give a hint to the reader about the problems in identifying each of these main minerals.

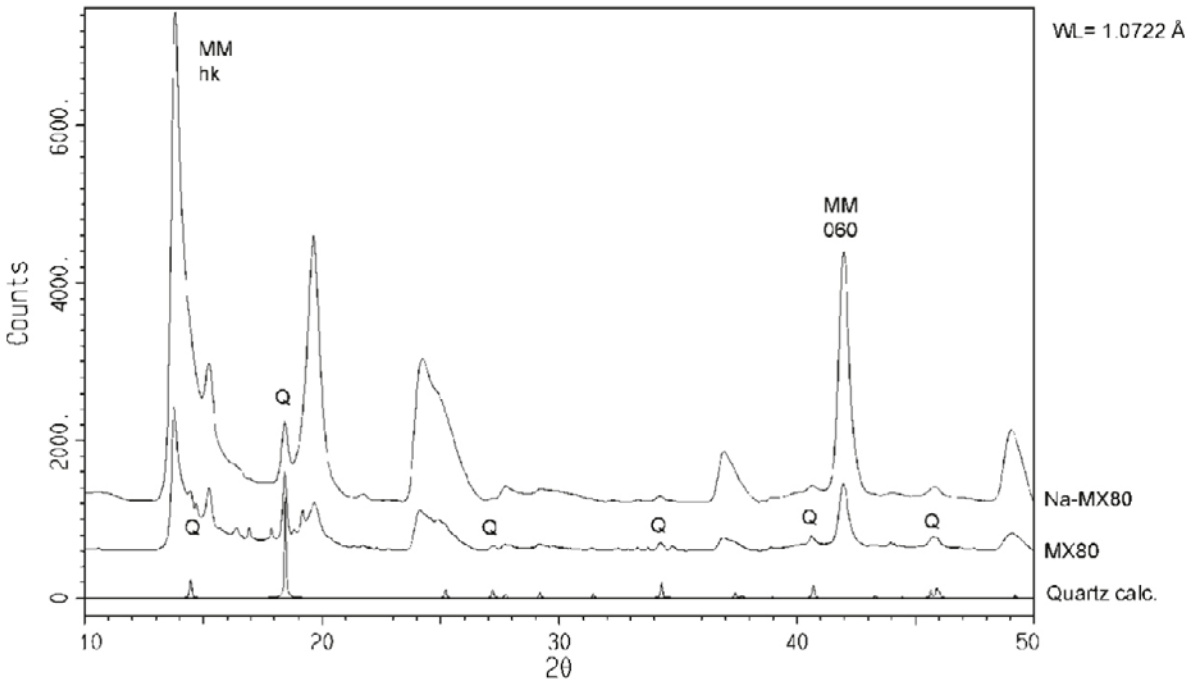

Figure 7-1. *Example of identification of quartz. Powder X-ray diffractograms of Na-MX80 (montmorillonite, MM), MX80 and quartz (Q; calculated). MAR detector.*

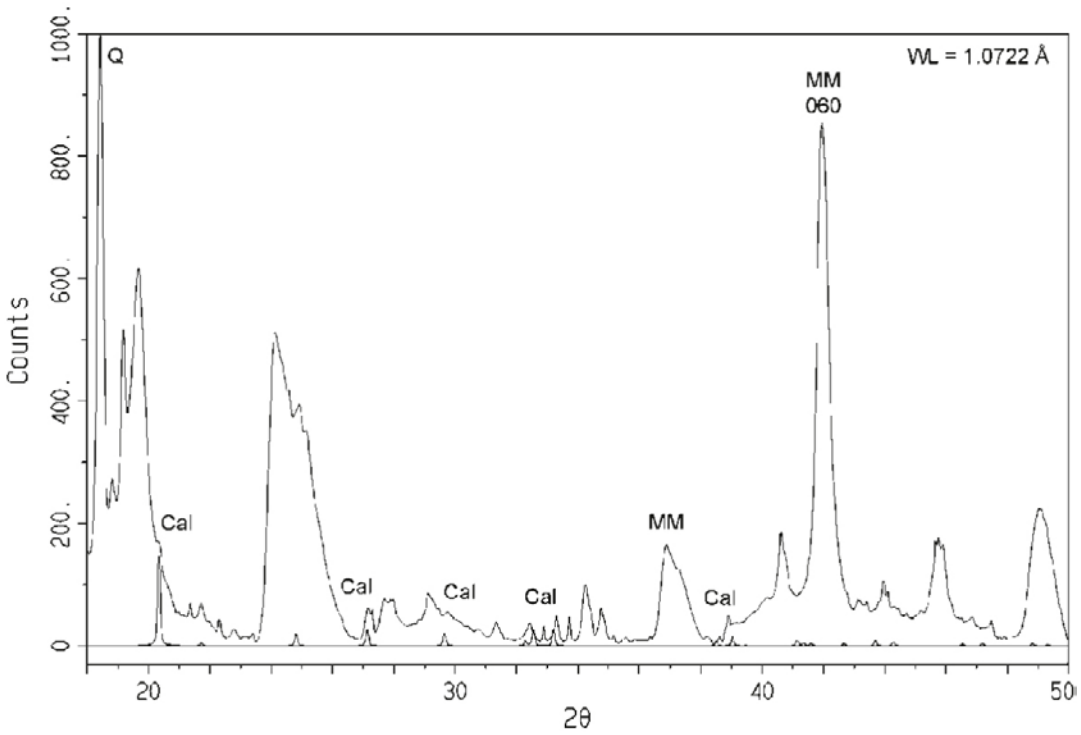

Figure 7-2. *Example of identification of calcite. Powder X-ray diffractograms of MX80 and calcite (Cal; calculated). MM is montmorillonite. MAR detector.*

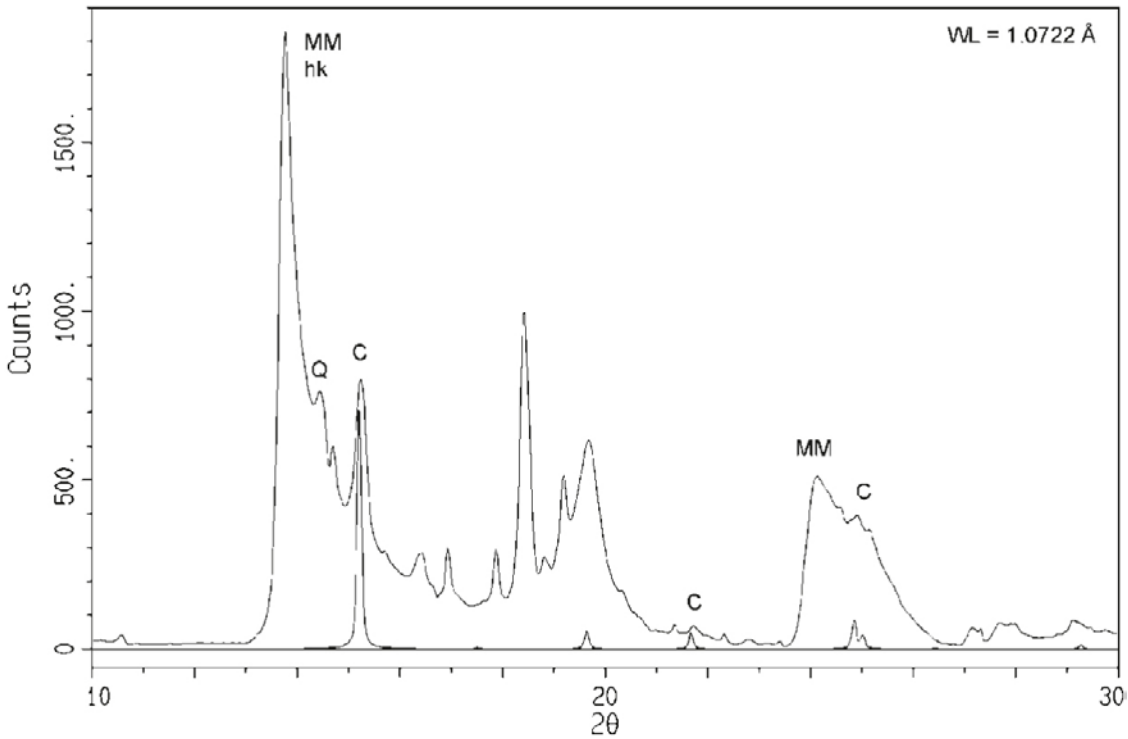

Figure 7-3. *Example of identification of cristobalite. Powder X-ray diffractograms of MX80 and cristobalite (C; calculated). MM is montmorillonite. MAR detector.*

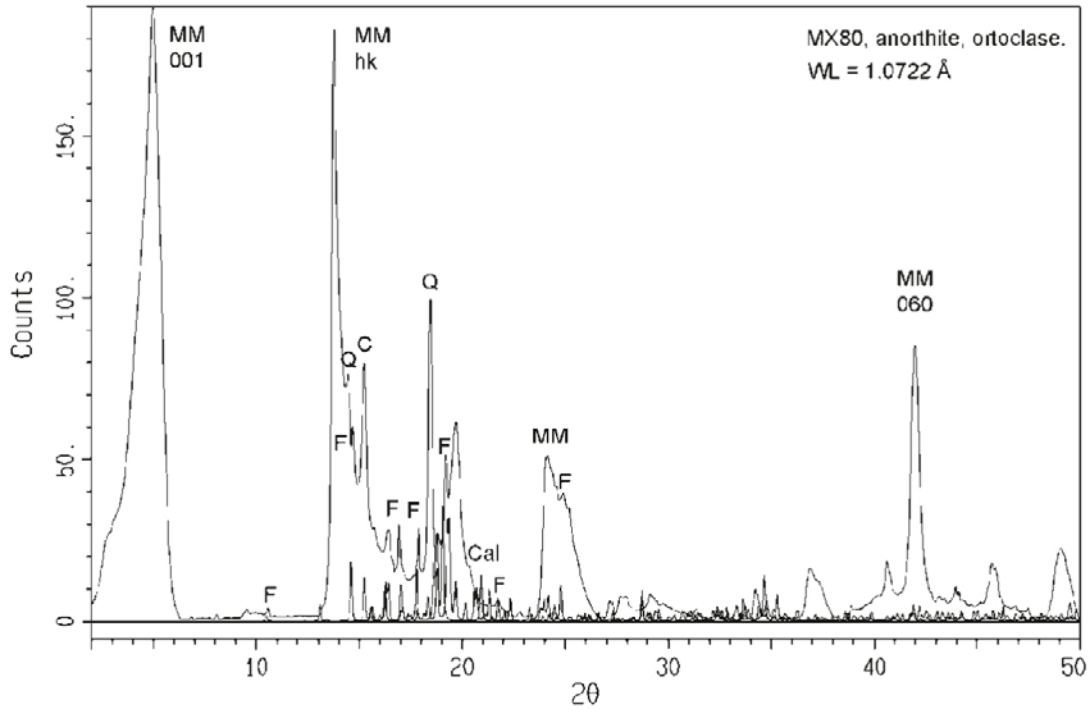

Figure 7-4. *Example of identification of feldspars (F). Powder X-ray diffractograms of MX80, anorthite (calculated) and orthoclase (calculated). MM is montmorillonite. MAR detector.*

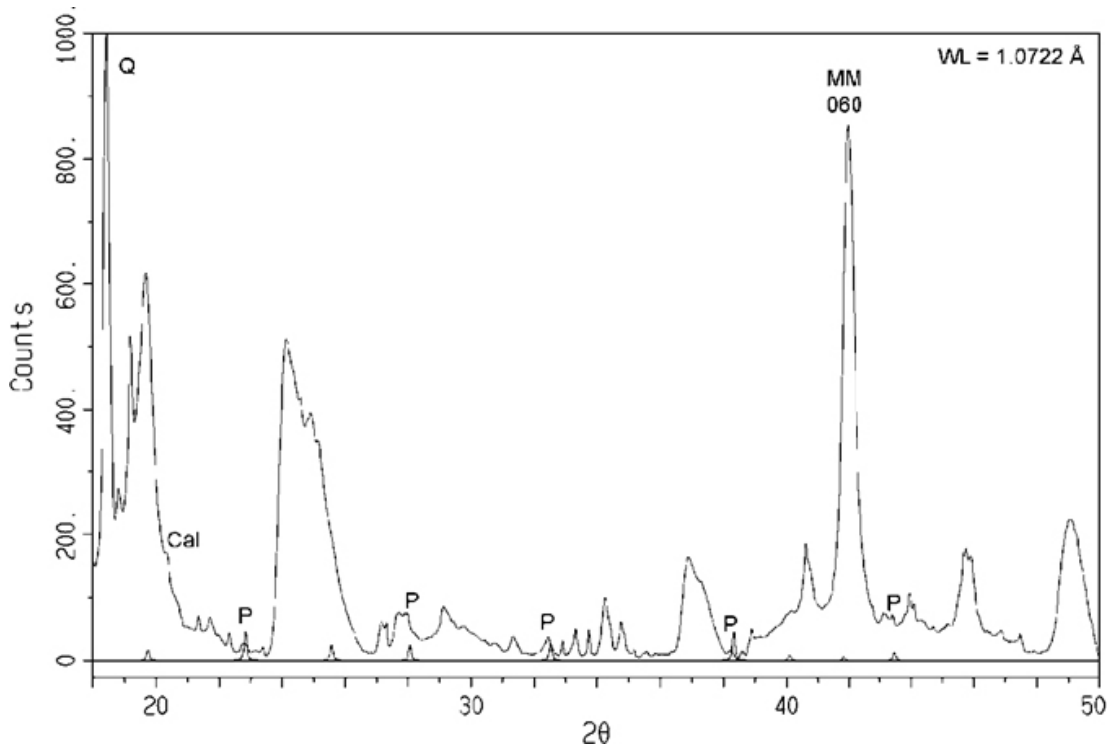

Figure 7-5. *Example of identification of pyrite. Powder X-ray diffractograms of MX80 and pyrite (P; calculated). MM is montmorillonite.*

7.6.2 Results

The identified minerals found in the different bentonites can be seen in Table 7-5. The presence is given semi-quantitatively as ++, +, – or -- to indicate if the level is high, medium, low or on the limit of detection. A parenthesis was added if the identification was uncertain.

The presence of rutile (and or anatase) in Rokle is compatible with the elevated Ti content, as well as the apatite is compatible with the elevated P content. Goethite is identified in the three clays with the most iron. The Friedland clay have rather high K content wich is in agreement with the identified illite. The high Ca found in Callovo-oxfordian and in Dep CAN can be addressed to the calcite phase. Sulfur in DepCAN and Callovo-oxfordian is likely from the pyrite. COX and Friedland are known to contain illite-smectite mixed layers, we could not successfully identify these phases. More work is needed to study these phases in greater detail.

Table 7-5. Minerals identified in the clays using XRD.

	Kunigel	DepCAN	Rokle	Calcigel	COX	IbecoSeal	MX80	Asha 505	Friedland	Febex	Ikosorb
Smectite	++	++	++	++	(-)	++	++	++	+	++	++
Muscovite/illite			--	-	+		--		+		--
Quartz	++	-	-	+	++	-	-		+	-	(-)
Cristobalite		-				-	+			-	+
Feldspare	-			-			-				
Calcite	-	++	-	-	++	-	--			+	-
Dolomite		-		(-)	-		--		(-)		-
Pyrite	-	-			-	--	--		-	--	--
Siderite					(-)				-		(--)
Gypsum		--					--				
Goethite			-					-	(-)		
Apatite			(-)								
Rutile			-								
Kaolinite			--	--	+			+	+		

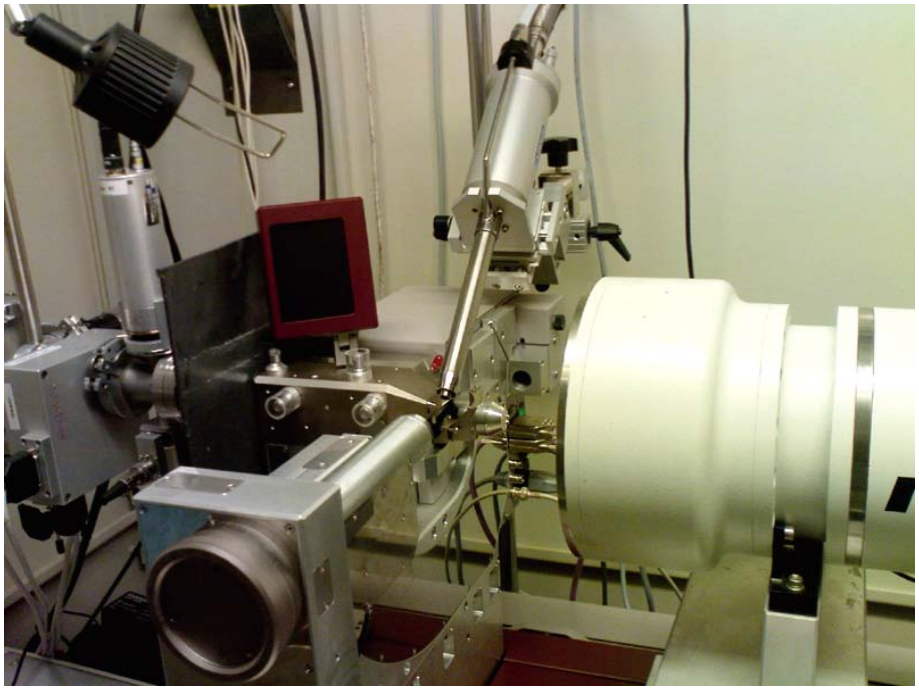

Figure 7-6. *The beam comes from the left.The MAR detector to the right. The sample holder in the front. A cryostate is also available to control the temperature if necessary.*

2D images from the MAR detector

The two dimensional diffractograms gave textural information such as orientation effects (unsymmetric diffraction rings) also separated complete diffraction rings from single crystal diffraction spots, with the origin in larger sized grains often of a harder material such as quartz. The single crystal reflexes never comes from the clay minerals and may be useful in some cases for identification. The main conclusions are that there are no large orientation effects in the diffractograms (indicated by the highly symmetrical diffraction rings), and some clays such as Rokle and Calcigel seems to have more hard minerals compared (more difficult to homogenize) to eg. Asha 505, which was the only clay free from quartz. If the clay sample is oriented one can think of it as a mica crystal (although much less extreme). Hence the x-rays are scattered unequally in space depending on then angle between the x-ray beam, the crystal and the detector. By choosing appropriate location of the detector one may sample only basal reflections (this is most common in clay science) or only the in-plane reflections. With a two dimensional detector one gets both and you may choose what data to integrate.

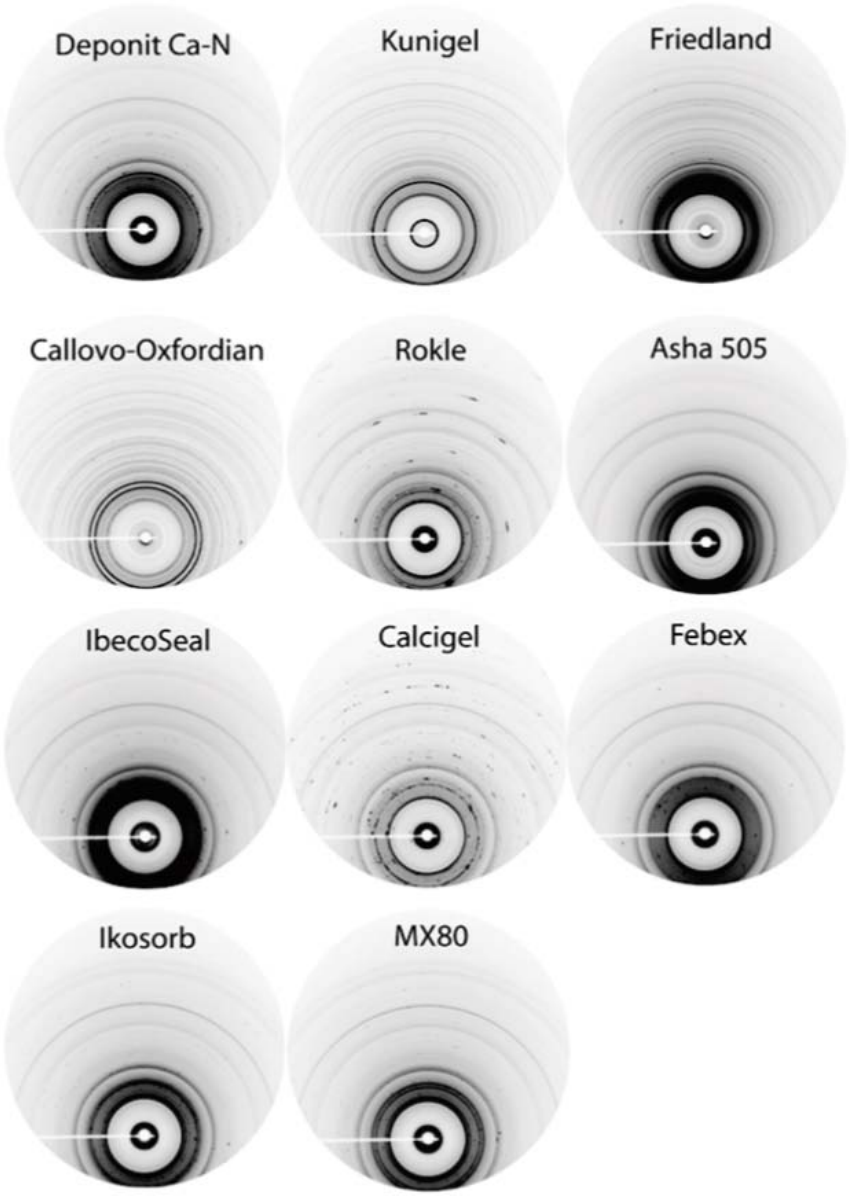

Figure 7-7. *Two dimensional diffractograms.*

Integrated x-ray diffractograms

The clay was crushed in an agate mortar and filled a capillary. The capillary was moved in the X-ray beam in such a way that several X-ray diffractograms were recorded on different material in the capillary (the stepwise movement was 1 mm, and the beam size was 0.5 mm). This indicates the variability of a small amount of crushed and homogenized clay. Even though the particles are very small, the volume of the sample is very small compared to reflection mode, hence one gets more scattering.

One main conclusion is that the repeatability of the measurement is very good. Most of the materials are rather homogenous at this scale. The variability in measurement would be larger in a non area sensitive detector, which is more sensitive towards larger grains and orientation effects.

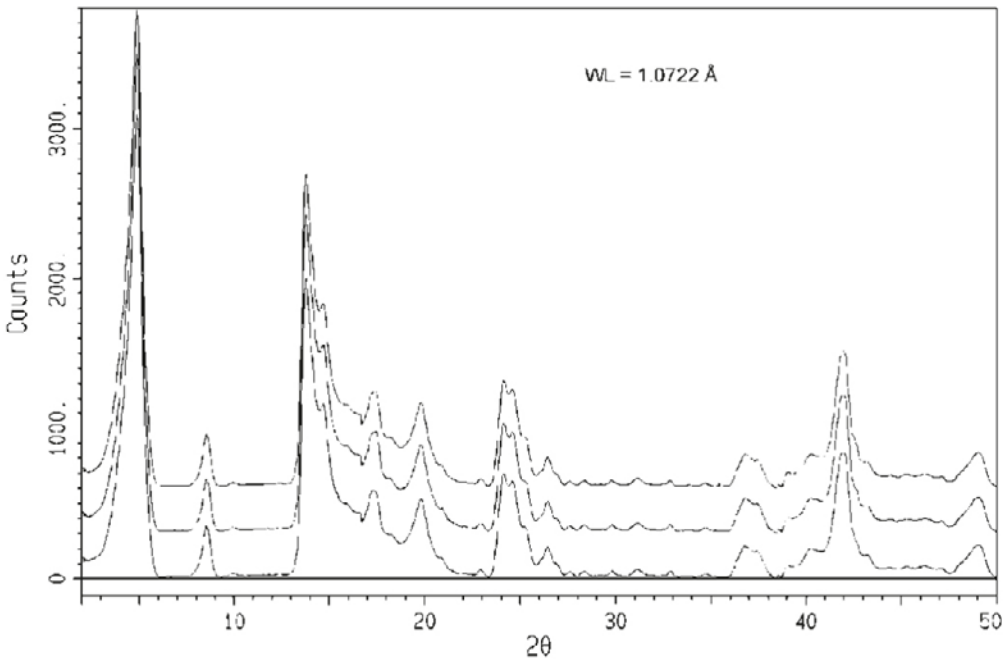

Figure 7-8. *Powder X-ray diffractograms of Asha 505. Three consecutive captures at different positions in the same material.*

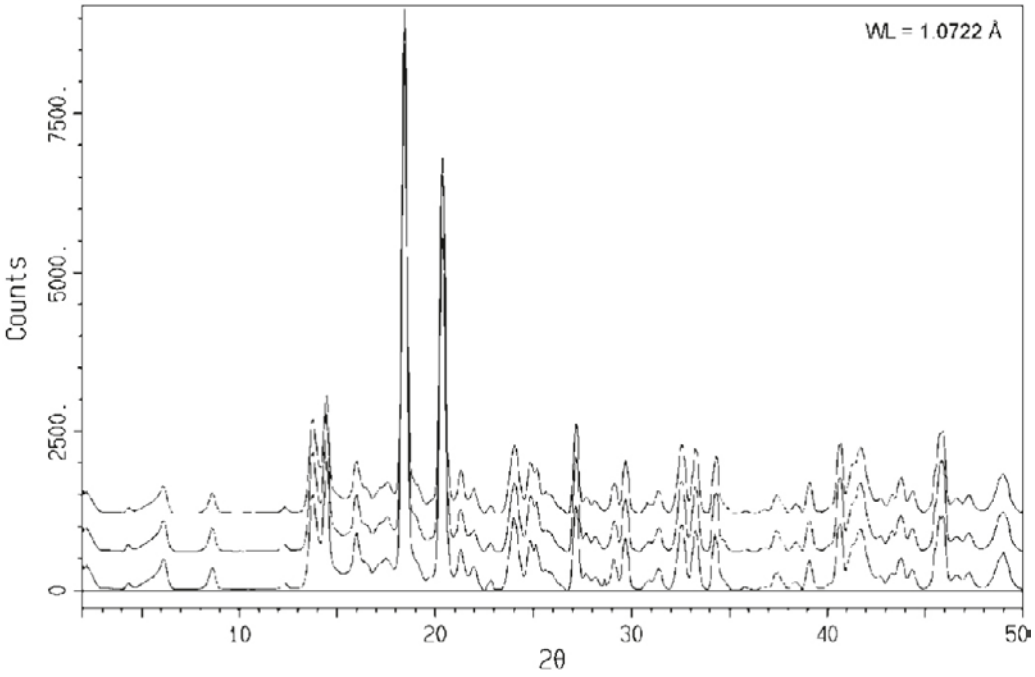

Figure 7-9. *Powder X-ray diffractograms of Callovo-Oxfordian. Three consecutive captures at different positions in the same material.*

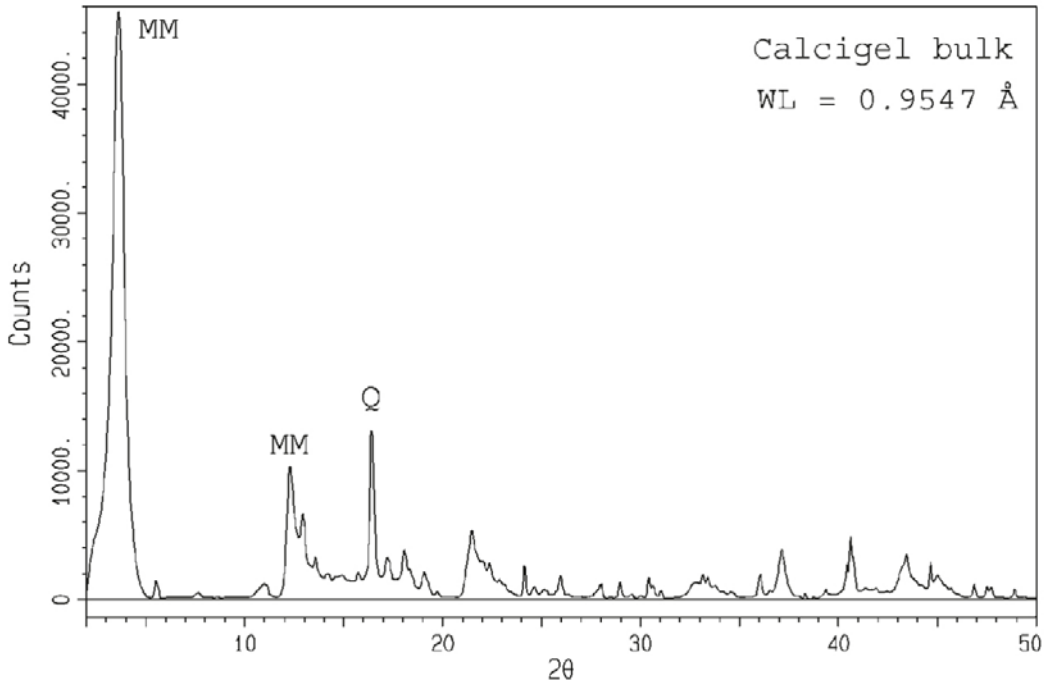

Figure 7-10. *Powder X-ray diffractogram of Calcigel.*

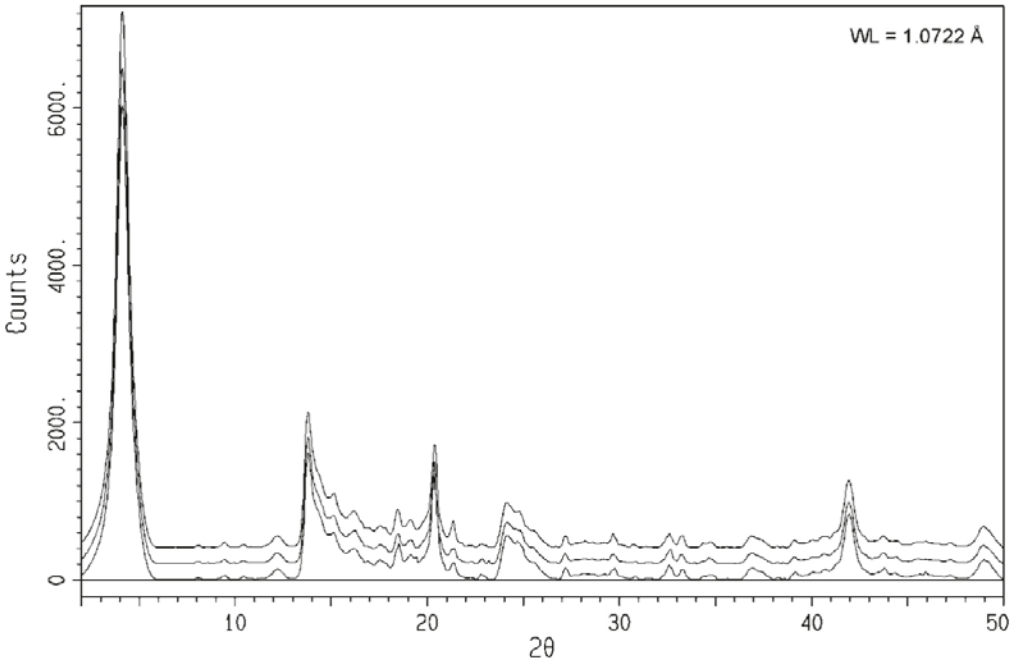

Figure 7-11. *Powder X-ray diffractograms of Deponit CA-N. Three consecutive captures at different positions in the same material.*

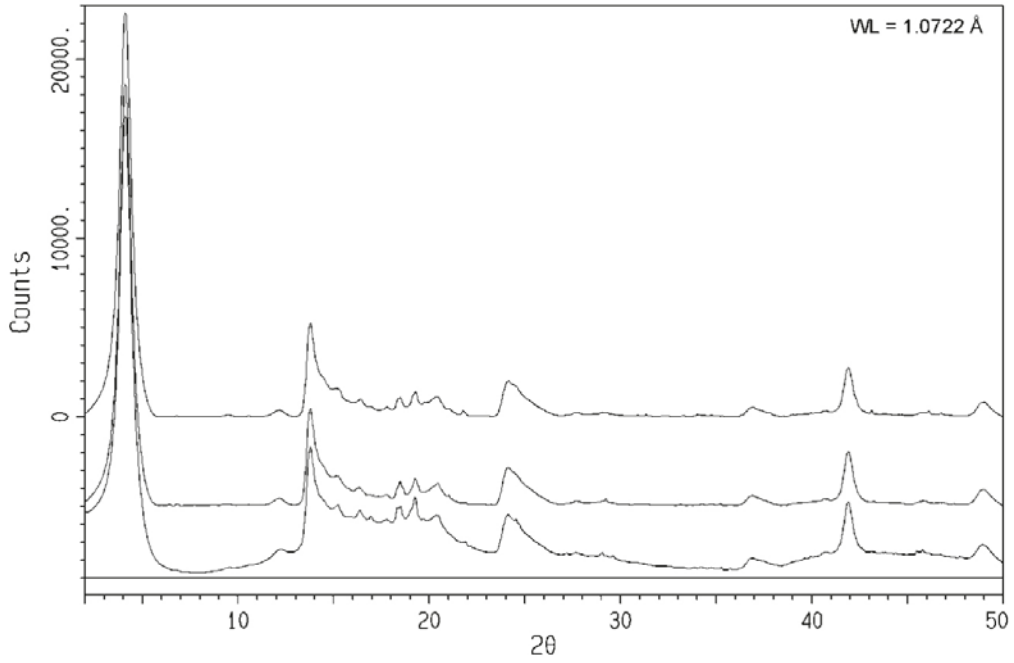

Figure 7-12. *Powder X-ray diffractograms of Febex. Three consecutive captures at different positions in the same material.*

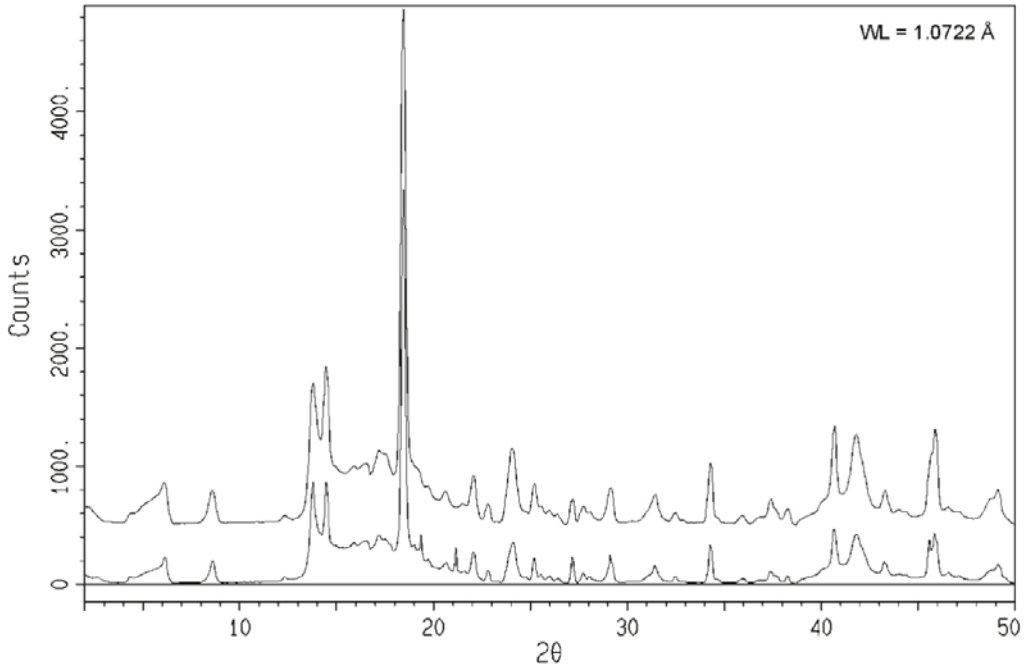

Figure 7-13. *Powder X-ray diffractograms of Friedland. Two consecutive captures at different positions in the same material.*

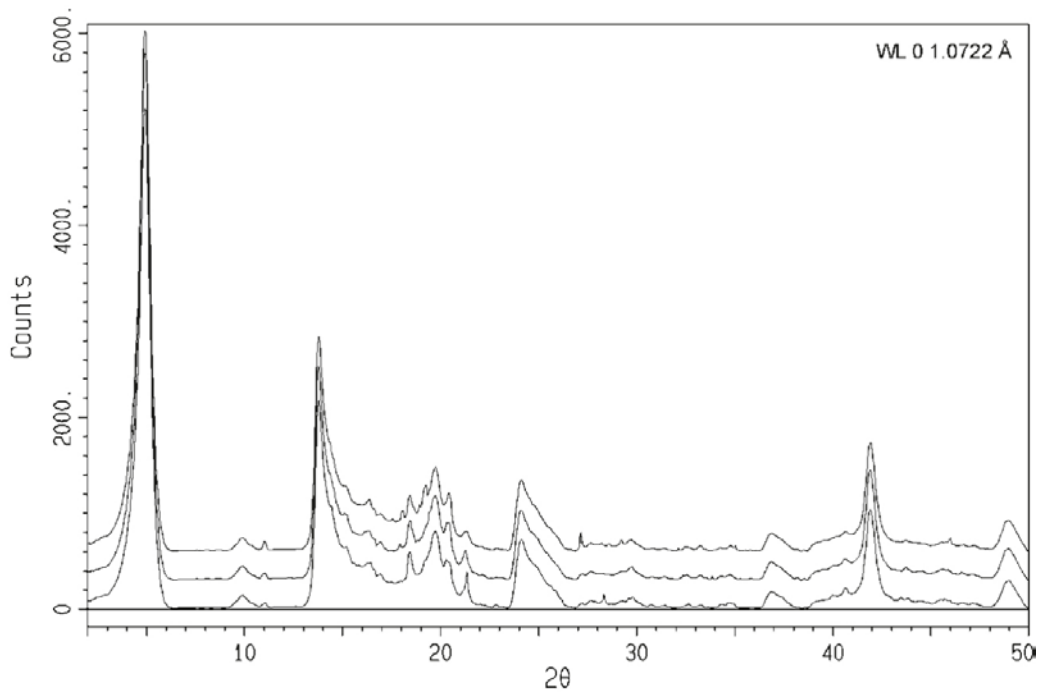

Figure 7-14. *Powder X-ray diffractograms of IbecoSeal. Three consecutive captures at different positions in the same material.*

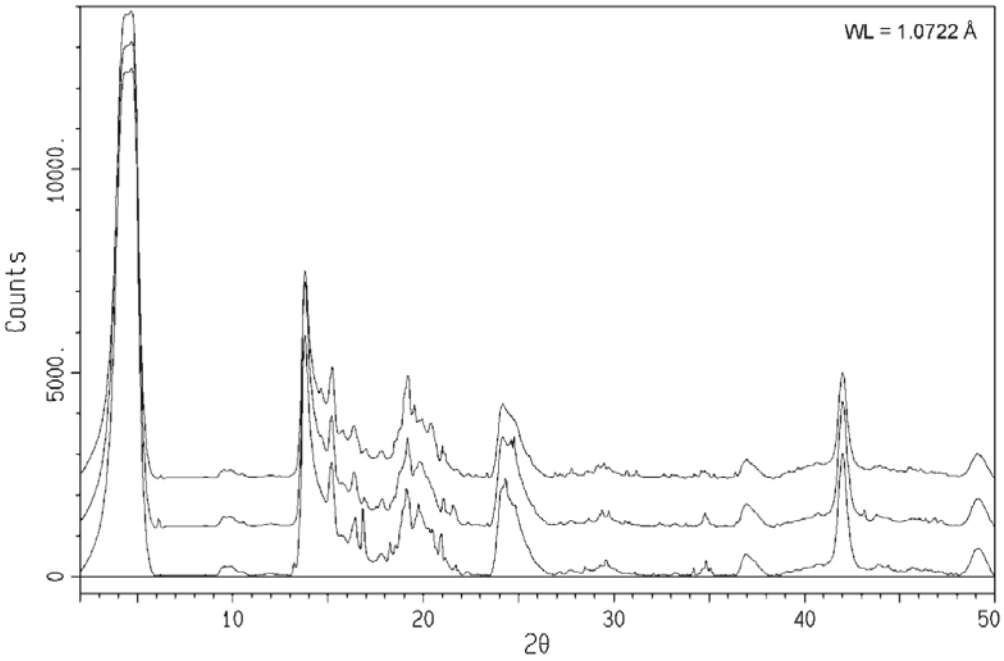

Figure 7-15. *Powder X-ray diffractograms of Ikosorb. Three consecutive captures at different positions in the same material.*

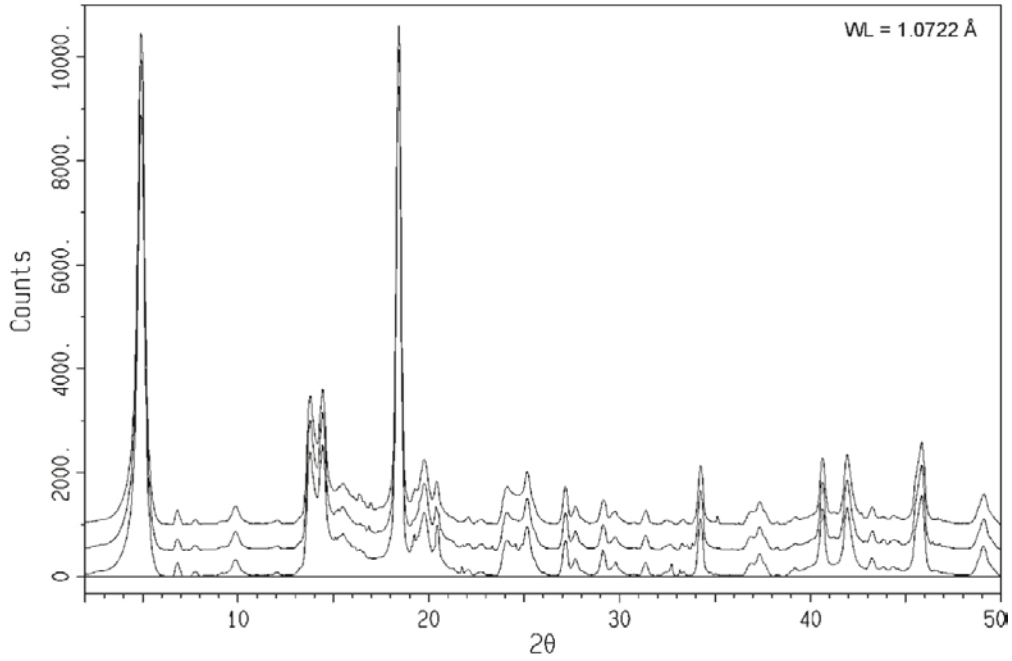

Figure 7-16. *Powder X-ray diffractograms of Kunigel. Three consecutive captures at different positions in the same material.*

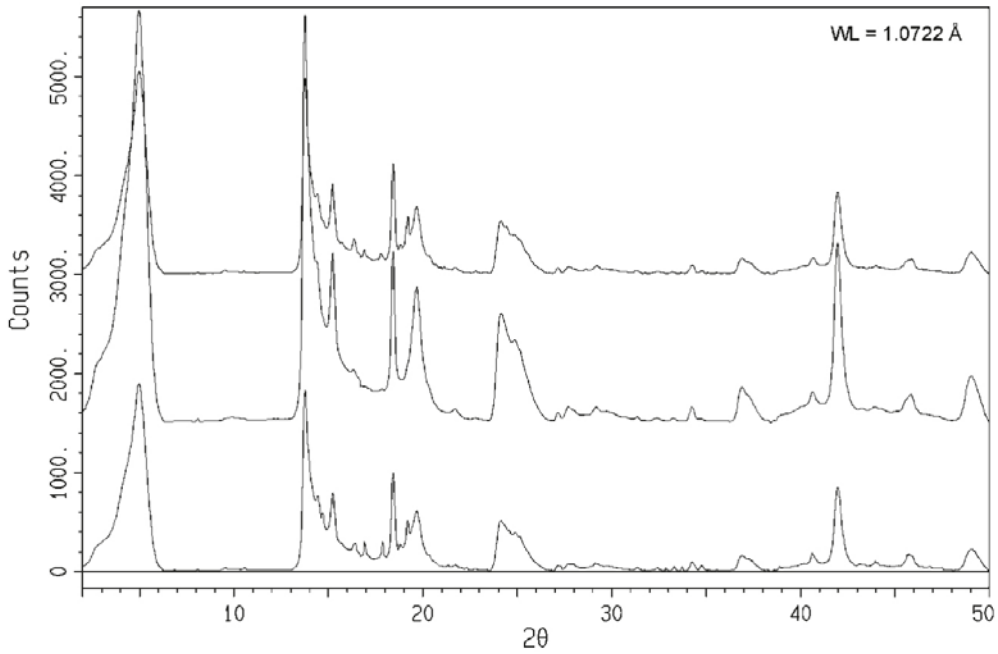

Figure 7-17. *Powder X-ray diffractograms of MX-80. Three consecutive captures at different positions in the same material.*

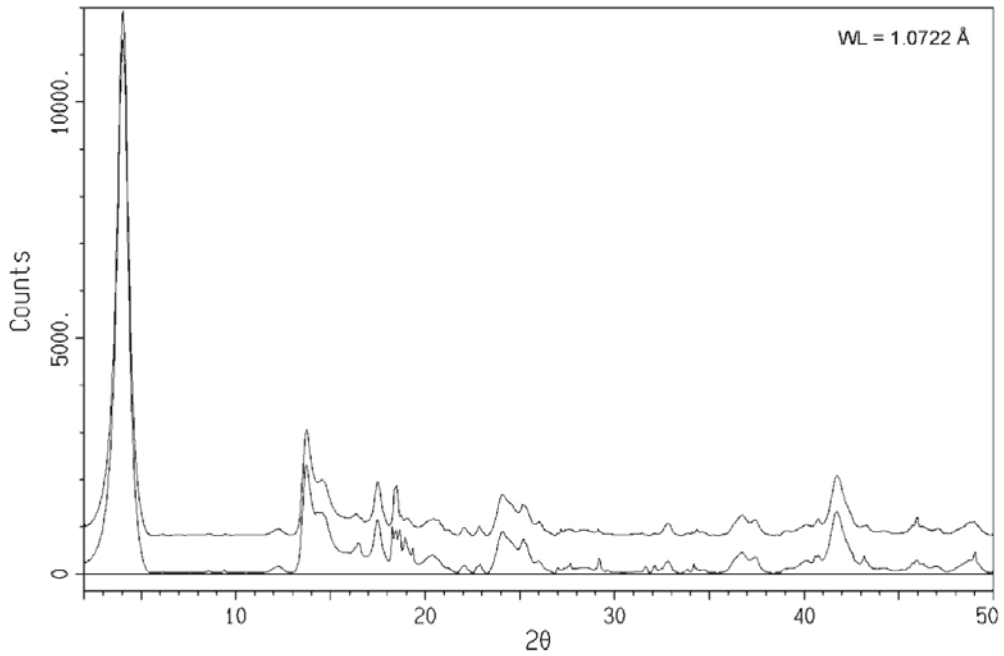

Figure 7-18. *Powder X-ray diffractograms of Rokle. Two consecutive captures at different positions in the same material.*

Close up of the 060 region

Smectites can be either dioctahedral (eg. montmorillonite) or trioctahedral (eg. saponite), or in other words either two or three metal atoms are present in the octahedral layer in each smectite unit cell. The number of cations in the octahedral layer have an impact on the unit cell b-axis dimension. One of the montmorillonite reflections, d(060), gives a measure of the dimensions of the b-axis and hence gives information whether the smectite is dioctahedral (reflection at 1.50 Å) or trioctahedral (1.52–1.55 Å, Moore and Reynolds 1997, p 245). Things are complicated by the presence of quartz which also has reflections in the angular interval.

The main conclusion is that the majority of the included clays are dominated by dioctahedral smectite, however some of the clays are more complex and may also include trioctahedral clay minerals.

Mg – clay fractions (< 2µm) with ehylene glycol

The basal spacing of smectites varies with the water content, and at ambient conditions the basal spacing is approximately 12 Å if the clay is saturated with mono valent ions and 15 Å for divalent ions. Highly indicative for Mg saturated smectites is a basal spacing of approximately 16.9 Å basal spacing when saturated with ethylene glycol (Moore and Reynolds 1997, p 241).

The main conclusion is that all the analysed clays, smectite is the dominant clay mineral. However other clay minerals are present in lower contents and may also be present as interstratifications in the smectite structures. The Callovo-oxfordian clay was not included as it is not a bentonite.

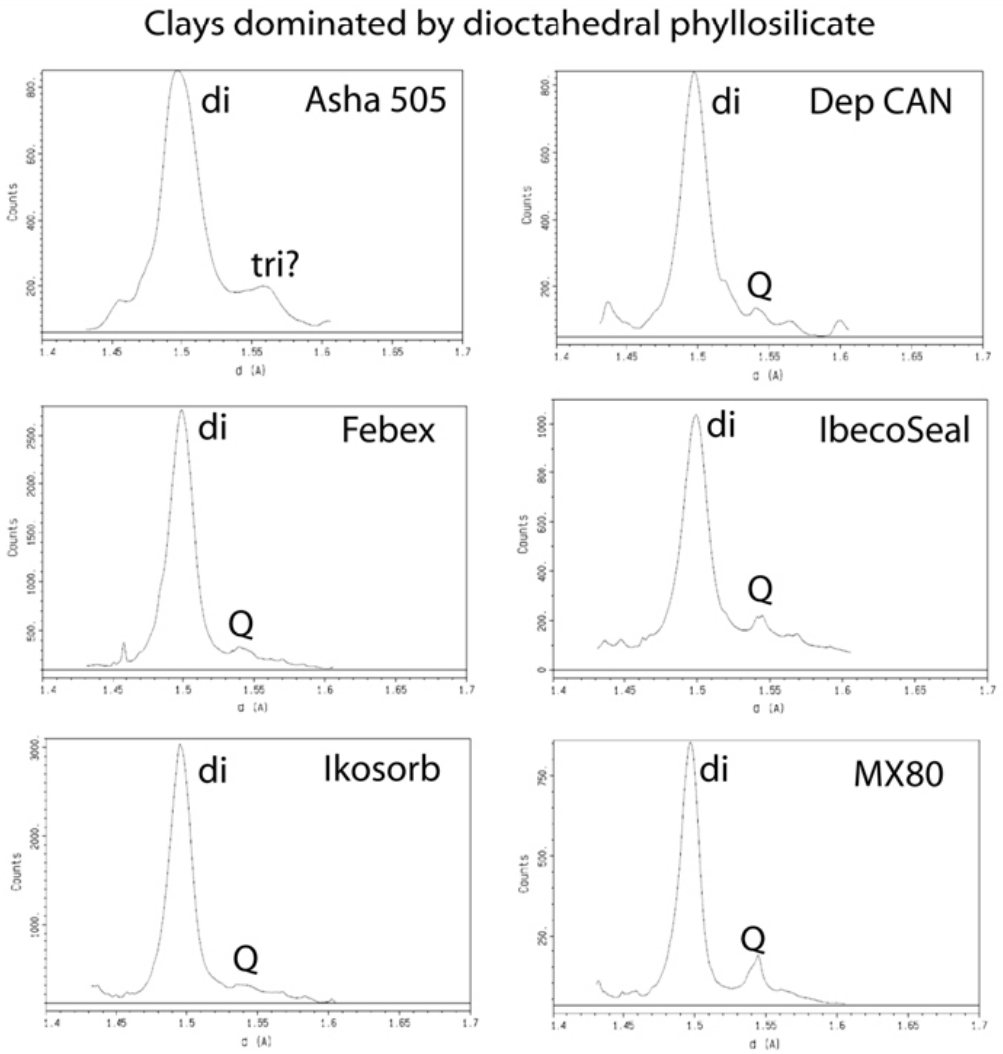

Figure 7-19. *Powder X-ray diffractogram of the 060 region with clays dominated by dioctahedral phyllosilicate. Note that the x-axis scale is distance in Å. MAR detector.*

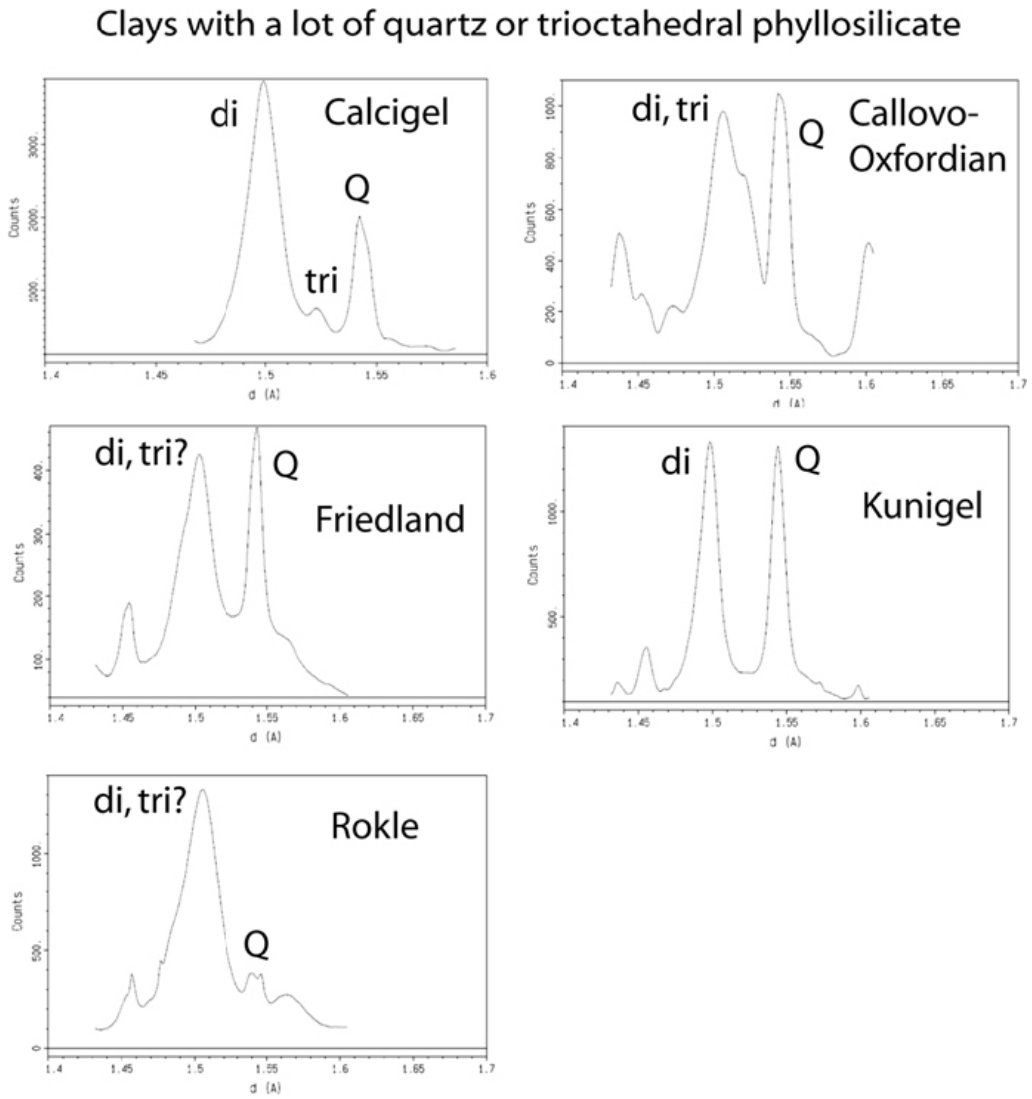

Figure 7-20. *Powder X-ray diffractogram of the 060 region with clays with mixed di- and possible tri-octahedral phyllosilicates and/or quartz. Note that the x-axis scale is distance in Å. MAR detector.*

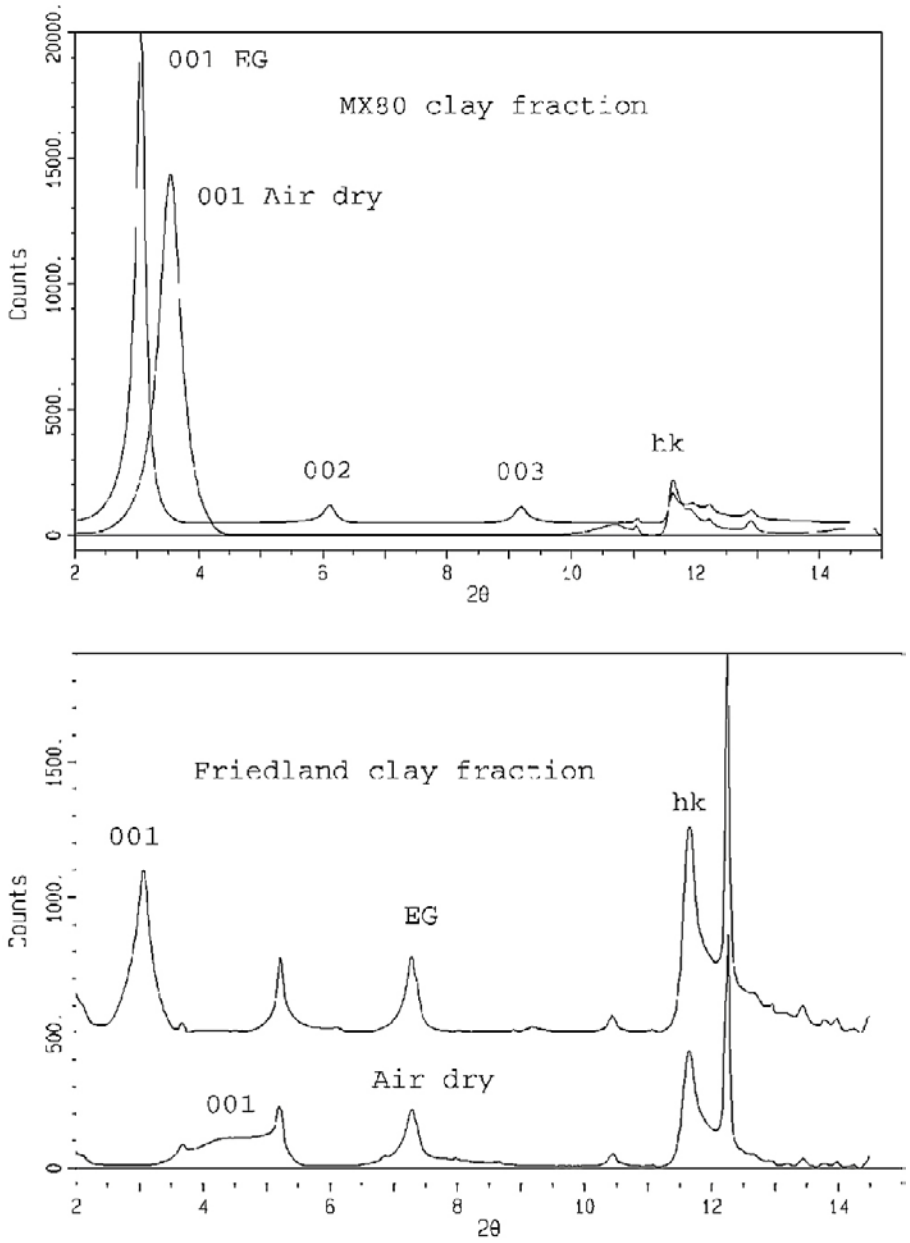

Figure 7-21. *XRD patterns of Mg-saturated clay fractions of MX80 and Friedland both as air dry and ethylene glycol (EG) saturated. The 001 indicates the highest basal spacing observed for the smectite, however in the air dry sample it is likely a lower order reflection. Wavelength = 0.907 Å.*

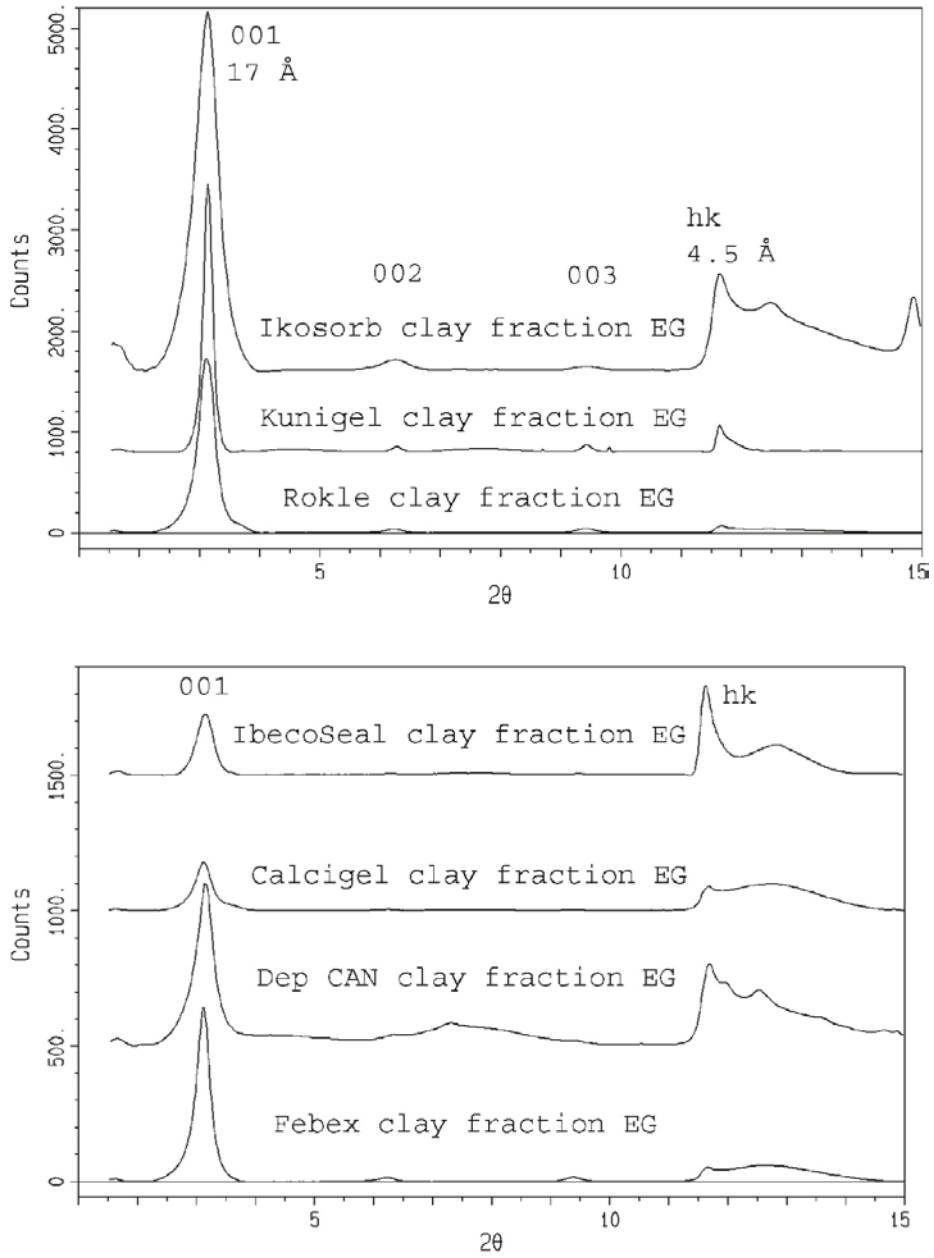

Figure 7-22. *XRD patterns of Mg-saturated clay fractions of Ikosorb, Kunigel, Rokle, IbecoSeal, Calcigel, DepCAN and Febex as ethylene glycol (EG) saturated. Wavelength = 0.9081 Å.*

8 Chemical and mineralogical analyses – material from test package 1

8.1 General

The bentonite blocks from the AB1 package had been stored in evacuated and welded bags of aluminum laminate in air-tight barrels since the retrieval in 2009. In March 2010 sampling was made of eleven of the blocks for analyses of exchangeable cations and water-soluble salts. Later it was decided to supplement these analyses with determinations of the cation exchange capacity, mineralogy and silicate chemistry, performed on the bulk material of four selected blocks. Table 8-1 summarizes the different bentonites and their position in the test package (block number 01 in the bottom), the radial position of the samples (cf Figure 4-1) and the type of analyses that have been performed. Some data on the reference bentonites were already available through earlier work (cf. Chapter 7).

The doughnut-shaped blocks had an inner diameter of 10 cm and an outer diameter of 30 cm. Five contiguous samples were taken along the block radius in the B-level of blocks 2 (MX-80), 5 (Calcigel), 24 (Asha 505) and 27 (Deponit CAN) and three noncontiguous samples were taken from a central (1), middle (5) and peripheral (9) position in the B-level of the remaining seven blocks (Table 8-1). Each sample represents approximately 2 cm of the radius.

Table 8-1. The analytical test protocol for characterization of the bulk bentonites/clays of package 1.

Block no	Radial position	Bentonite	Analyses	Notes
02	1, 3, 5, 7, 9	MX-80	EA, CEC, EC, WS, XRD	
02		Ref MX-80	CEC, EC, WS, XRD	EA performed 2009
05	1, 3, 5, 7, 9	Calcigel	EA, CEC, EC, WS, XRD	
05		Ref Calcigel	CEC, EC, WS, XRD	EA performed 2009
10	1, 5, 9	Ikosorb	EC, WS	
10		Ref Ikosorb	EC, WS	
16	1, 5, 9	Rokle	EC, WS	
16		Ref Rokle	EC, WS	
17	1, 5, 9	Kunigel	EC, WS	
17		Ref Kunigel	EC, WS	
21	1, 5, 9	Febex	EC, WS	
21		Ref Febex	EC, WS	
22	2, 5, 9[a]	COX[b]	EC, WS	[a] inner cm missing
22		Ref COX	EC, WS	
24	1, 3, 5, 7, 9	Asha 505	EA, CEC, EC, WS, XRD	
24		Ref Asha 505	CEC, EC, WS, XRD	EA performed 2009
25	1, 5, 9	Friedland	EC, WS	
25		Ref Friedland	EC, WS	
26	1, 5, 9	Ibeco	EC, WS	
26		Ref Ibeco	EC, WS	
27	1, 3, 5, 7, 9	Deponit CAN	EA, CEC, EC, WS, XRD	
27		Ref Dep CAN	CEC, EC, WS, XRD	EA performed 2009

EA=element analysis of the bentonite, CEC= cation exchange capacity, EC=exchangeable cations, WS= water-soluble salts, XRD=x-ray diffraction analysis

Sampling was made at normal laboratory conditions without any precautions to avoid oxidation of the samples. A rim of corrosion products at the interface between the Fe-tube and the bentonite was removed by scraping off a ~2-mm thick layer, but this material was sampled and analysed separately in some of the blocks with special precautions taken to prevent oxidation. These results are presented in Section 8.7. The outer mantle surface of the blocks was contaminated with sand added at the installation in the slot between the buffer and the borehole wall. The sand-contaminated layer was removed and discarded prior to the sampling. Bentonite stored since the manufacturing of the blocks was used as reference materials.

Individual samples were labeled with the block number, the vertical level within the block (A, B or C), the compass direction in the borehole and the radial position according to Figure 4-1. A suffix **b** or **c** indicates wether the sample consists of the bulk material or the clay fraction, but in this initial study of the AB1 package only the bulk materials have been analysed. The samples were not subjected to any pre-treatments prior to analysis, apart from drying at 60°C and grinding.

8.2 Aqueous leachates

8.2.1 Method

The anions of soluble salts were determined in water extracts of the bulk bentonite. The dried (105°C) and ground bentonite was dispersed in deionised water (solid:solution ratio 1:100) by ultrasonic treatment for 30 minutes and stirring overnight. The suspension was left for 5 days at room temperature to allow equilibration and sedimentation of the coarse matter. After phase separation by centrifugation and filtration (0.8 and 0.2 µm syringe filters Acrodisc PF), major anions (F^{-}, Cl^{-}, SO_4^{2-}, NO_3^{-} PO_4^{3-}) were determined by use of ion chromatography (IC) at the Department of Ecology, Lund University.

A comparison of the results for Cl^{-} and SO_4–S of the reference samples, obtained by two different laboratories (Clay Technology AB and SKB's Äspö Laboratory), gives some idea about the repeatability of the method (Figure 8-1).

8.2.2 Results

The content of water soluble F, Cl, SO_4-S, NO_3-N PO_4-P is given in Table 8-2. Focus has been laid on chloride and sulfate, which are the major anions of salts in all the bentonites examined.

The distribution of chloride (Figure 8-2) indicates that the wetting with and equilibration against the groundwater (composition given in Table 5-1) resulted in laterally and vertically smoothed and more or less constant concentrations. Hence, the most Cl-rich bentonites/clays (Asha 505, Friedland and Ikosorb) display a loss in chloride, whereas the other bentonites have gained chloride during the field test. This is illustrated also in Figure 8-3, which shows the vertical chloride distribution within the package before (i.e. the chloride concentration of the references) and after the 1-year test. The latter values are given as the average concentration of the three or five samples analysed from each block.

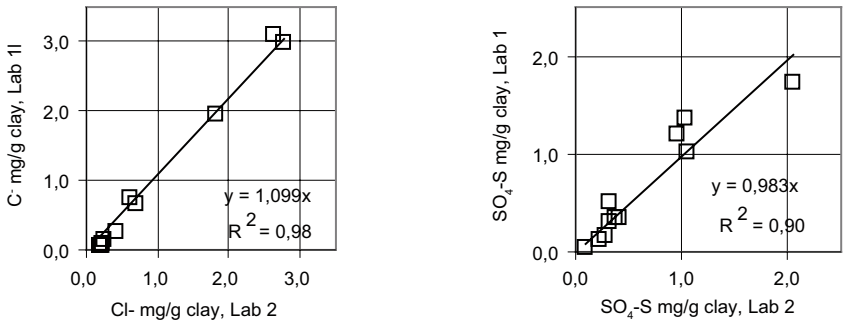

Figure 8-1. *Comparison of the results for water-soluble Cl^{-} and SO_4-S of the reference samples, obtained by two different laboratories (Clay Technology AB and SKB's Äspö Laboratory).*

Table 8-2. Major anions (mg/g dry clay) extracted by dispersion of the bentonite in deionised water using a solid:liquid ratio of 1:100.

SICADA code	Block no	Position	Bentonite	F	Cl	NO_3-N	PO_4-P	SO_4-S
				mg/g dry clay				
AB102BW1b	Block 2	1	MX-80	0.008	0.99	0.021	0.000	0.64
AB102BW3b	Block 2	3	MX-80	0.015	1.11	0.020	0.000	1.45
AB102BW5b	Block 2	5	MX-80	0.018	1.15	0.018	0.000	1.41
AB102BW7b	Block 2	7	MX-80	0.018	1.17	0.019	0.000	1.42
AB102BW9b	Block 2	9	MX-80	0.069	1.28	0.017	0.000	1.33
AB102Rb	Ref		MX-80	0.013	0.26	0.034	0.000	0.96
AB105BW1b	Block 5	1	Calcigel	0.031	1.20	0.013	0.000	0.23
AB105BW3b	Block 5	3	Calcigel	0.030	1.34	0.004	0.000	0.29
AB105BW5b	Block 5	5	Calcigel	0.016	1.09	0.010	0.000	0.19
AB105BW7b	Block 5	7	Calcigel	0.020	1.53	0.005	0.000	0.27
AB105BW9b	Block 5	9	Calcigel	0.024	1.56	0.015	0.000	0.18
AB105Rb	Ref		Calcigel	0.038	0.21	0.016	0.029	0.22
AB110BW1b	Block 10	1	Ikosorb	0.018	0.82	0.017	0.000	0.27
AB110BW5b	Block 10	5	Ikosorb	0.030	0.84	0.013	0.000	0.22
AB110BW9b	Block 10	9	Ikosorb	0.037	1.11	0.017	0.000	0.26
AB110Rb	Ref		Ikosorb	0.038	2.63	0.025	0.000	0.37
AB116BW1b	Block 16	1	Rokle	0.047	1.32	0.016	0.031	0.26
AB116BW5b	Block 16	5	Rokle	0.054	1.29	0.018	0.053	0.26
AB116BW9b	Block 16	9	Rokle	0.075	1.75	0.021	0.055	0.34
AB116Rb	Ref		Rokle	0.051	0.19	0.015	0.006	0.09
AB117BW1b	Block 17	1	Kunigel	0.009	0.83	0.017	0.000	0.50
AB117BW5b	Block 17	5	Kunigel	0.012	0.82	0.019	0.000	0.48
AB117BW9b	Block 17	9	Kunigel	0.028	0.92	0.020	0.000	0.52
AB117Rb	Ref		Kunigel	0.010	0.20	0.013	0.000	0.32
AB121BW1b	Block 21	1	Febex	0.021	1.20	0.011	0.000	0.22
AB121BW5b	Block 21	5	Febex	0.025	1.15	0.011	0.007	0.15
AB121BW9b	Block 21	9	Febex	0.034	1.31	0.012	0.000	0.16
AB121Rb	Ref		Febex	0.081	0.69	0.016	0.000	0.27
AB122BW1b	Block 22	2	COX	0.010	0.89	0.011	0.000	1.25
AB122BW5b	Block 22	5	COX	0.010	0.88	0.000	0.000	1.08
AB122BW9b	Block 22	9	COX	0.016	0.98	0.010	0.000	0.54
AB122Rb	Ref		COX	0.009	0.23	0.013	0.000	0.32
AB124BW1b	Block 24	1	Asha 505	0.018	1.06	0.013	0.000	0.47
AB124BW3b	Block 24	3	Asha 505	0.017	1.03	0.013	0.000	0.26
AB124BW5b	Block 24	5	Asha 505	0.013	1.11	0.014	0.000	0.24
AB124BW7b	Block 24	7	Asha 505	0.064	1.37	0.015	0.000	0.25
AB124BW9b	Block 24	9	Asha 505	0.046	1.35	0.019	0.000	0.24
AB124Rb	Ref		Asha 505	0.016	2.77	0.027	0.000	0.41
AB125BW1b	Block 25	1	Friedland	0.009	0.70	0.000	0.000	1.77
AB125BW5b	Block 25	5	Friedland	0.020	0.86	0.000	0.000	0.78
AB125BW9b	Block 25	9	Friedland	0.023	0.94	0.013	0.000	0.39
AB125Rb	Ref		Friedland	0.023	1.82	0.018	0.000	2.04
AB126BW1b	Block 26	1	Ibeco	0.017	0.92	0.013	0.000	0.38
AB126BW5b	Block 26	5	Ibeco	0.034	0.96	0.013	0.000	0.26
AB126BW9b	Block 26	9	Ibeco	0.027	1.11	0.015	0.000	0.27
AB126Rb	Ref		Ibeco	0.005	0.43	0.024	0.000	1.06
AB127BW1b	Block 27	1	Dep CAN	0.010	1.06	0.012	0.000	2.65
AB127BW3b	Block 27	3	Dep CAN	0.011	0.90	0.000	0.000	1.60
AB127BW5b	Block 27	5	Dep CAN	0.018	1.07	0.013	0.000	0.95
AB127BW7b	Block 27	7	Dep CAN	0.014	1.03	0.009	0.000	1.35
AB127BW9b	Block 27	9	Dep CAN	0.033	1.23	0.012	0.000	0.72
AB127Rb	Ref		Dep CAN	0.030	0.61	0.012	0.020	1.03

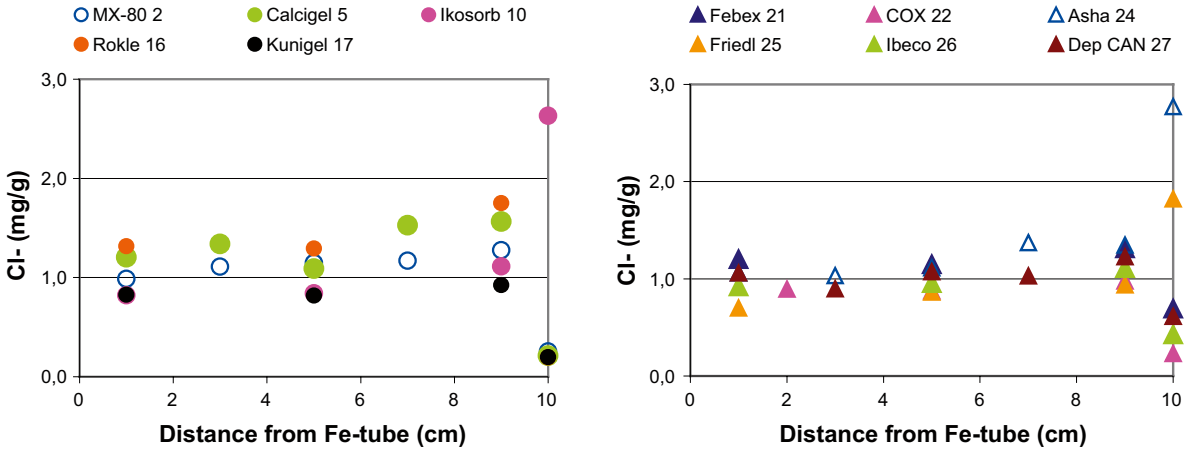

Figure 8-2. *The radial distribution of Cl^- in water extracts of the bentonite from the lower (left) and upper (right) part of the ABM package 1. The reference samples are plotted at the position 10 cm. The type of bentonite and the position of the block in the package are indicated in the legend.*

The post-test sulfate distribution displays no consistent or regular pattern. The Friedland clay has the largest inventory of soluble sulfate minerals of all the clays, followed by the Ibeco, Deponit CAN and MX-80 bentonites. After the test a clear sulfate maximum can be seen at the heater in block 25 Friedland and 27 Deponit CAN along with a more or less clear depletion in the peripheral parts of the blocks (Figure 8-4), indicating a lateral transfer of sulfate. The XRD-data for Deponit CAN, indicating anhydrite formation at the heater, are in support of this. In contrast, sulfate seems to have accumulated in the middle part of block 2 of MX-80 in the bottom of the parcel, whereas block 26 Ibeco has lost most of its initial sulfate content and block 22 COX (clay-stone) gained sulfate, suggesting also a vertical transfer between the blocks.

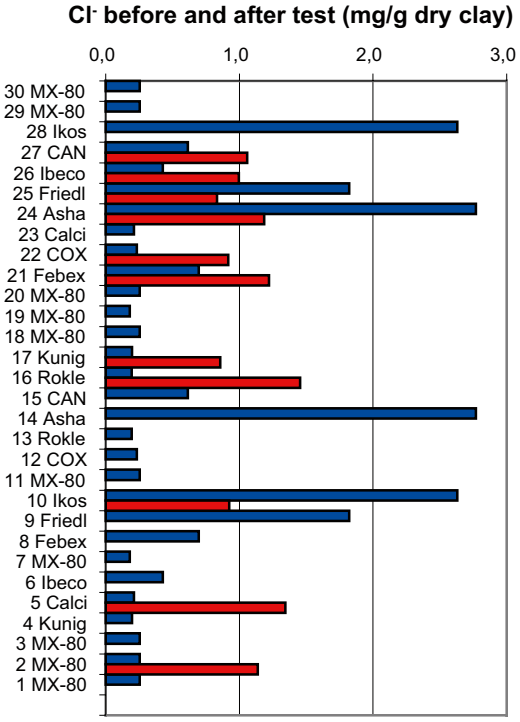

Figure 8-3. *The Cl concentration in individual blocks of package 1 before (blue) and after (red) the field test.*

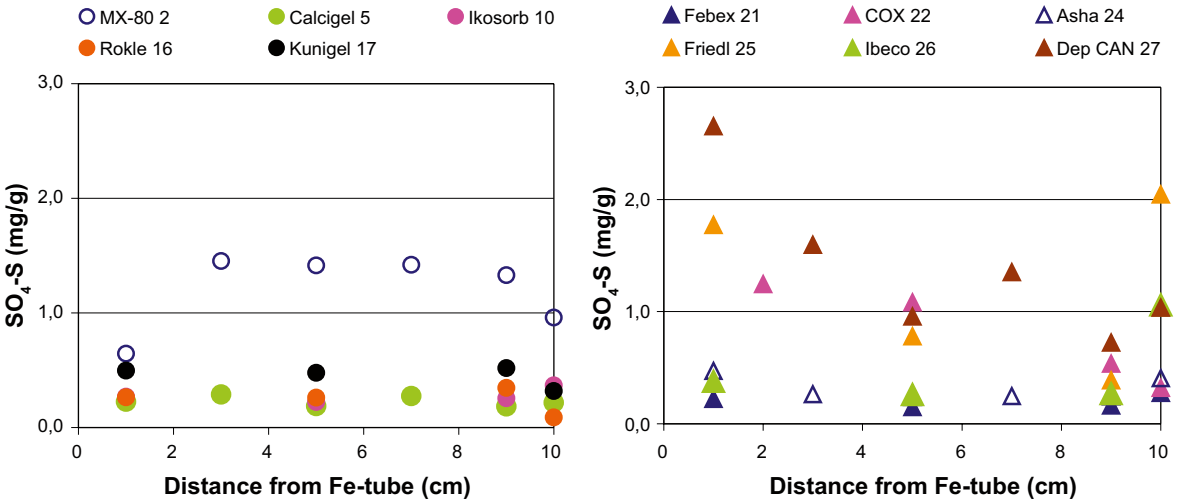

Figure 8-4. The radial distribution of SO_4-S in water extracts of the bentonite from the lower (left) and upper (right) part of package 1. The reference samples are plotted at the position 10 cm.

8.3 Exchangeable cations

8.3.1 Method

The exchangeable cations were extracted into alcoholic ammonium chloride solution (0.15 M NH_4Cl in 80% ethanol) according to a procedure originally recommended for CEC determinations of gypsiferous/calcareous soils (e.g. Belyayeva 1967, Jackson 1975). An alcoholic solution is used to minimize dissolution of gypsum and calcite, which are soluble in aqueous solutions. Ideally, i.e. when there is a minimum of easily soluble salts, such as chlorides and carbonates of alkali metals, the sum of cations extracted should be equivalent to the CEC of the sample.

0.8 g of the ground sample was shaken for 30 minutes in approximately one third of a total volume of 50 ml of the extractant. After centrifugation the supernatant was collected. This treatment was repeated three times. After evaporation of the alcohol and adjustment of volume with deionised water, the concentration of Ca, Mg, Na and K was determined by use of an ICP-AES equipment at the Department of Ecology, Lund University. The water content of the bentonite was determined for a separate sample.

8.3.2 Results

The data on the exchangeable cations extracted by exchange with ammonium in alcoholic solution are compiled in Table 8-3.

As can be expected, the saturation with a Na-Ca type groundwater has resulted in replacement of some sodium by calcium in all those bentonites that were initially Na-dominated. However, the plots of the cation distribution (Figure 8-5) indicate a significant compositional difference in the exchangeable cation pool between the upper and lower parts of the package. Whereas lateral gradients within the blocks are insignificant (cf. Table 8-3), a vertical gradient in the relative cation distribution has developed during/after the field experiment (Figure 8-6). From block 21 and upwards, calcium has become the predominant interlayer cation due to replacement of sodium first of all, but also of magnesium (e.g. block 21 and 27). In inititally Na-dominated clays, such as Asha 505 in block 24, (initial Na-saturation 66%), the exchange is significant enough to be clearly indicated both in the bulk chemistry of the bentonite (Table 8-5) and by a change in the spacing of the first order basal reflection of the smectite (cf. XRD data in Section 8.6).

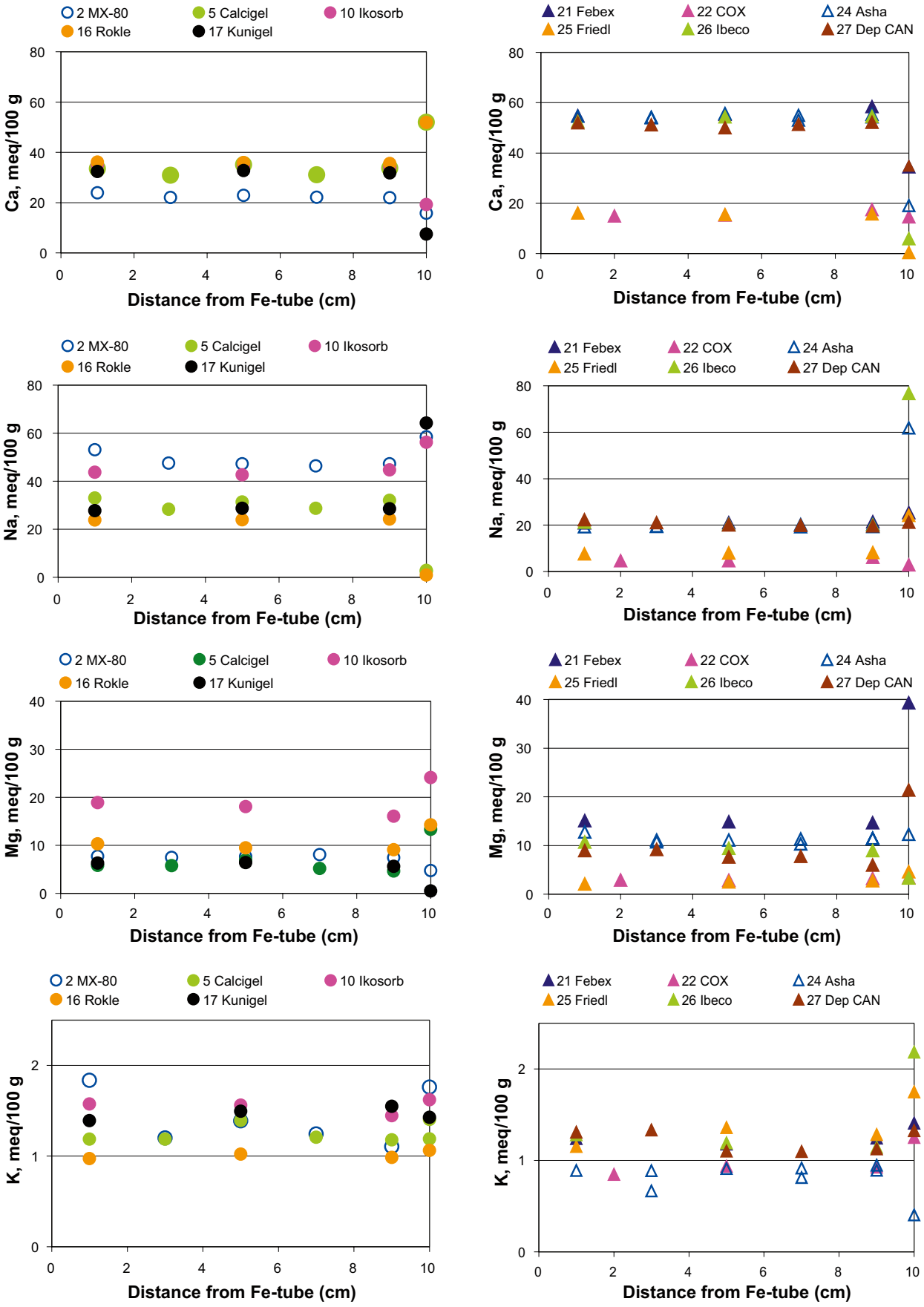

Figure 8-5. Exchangeable Ca, Na, Mg and K. Reference samples plotted at the position 10 cm.

The available data for the lower and middle part of the package are too scanty to provide a complete picture of the relative cation distribution, but supplementary unpublished data (R. Dohrmann pers. com) confirm that from block 11 and downwards, Na comprises between 40 and 60% of the cation pool. This means that calcium to a large extent has been replaced by sodium in the initially Ca-dominated bentonite Calcigel in block 5, and, again, the exchange is clearly indicated both in the bulk chemistry (Table 8-5) and in the XRD-characteristics of the smectite (cf. Section 8.6).

Dissolution/precipitation reactions which involved various calcium minerals (cf. Section 8.2 and 8-5) must have exerted significant control on the porewater chemistry but at the present stage of the investigation no unambiguous explanation can be given of this differentiated equilibration of the exchangeable cation pool within the upper and lower part of the bentonite package.

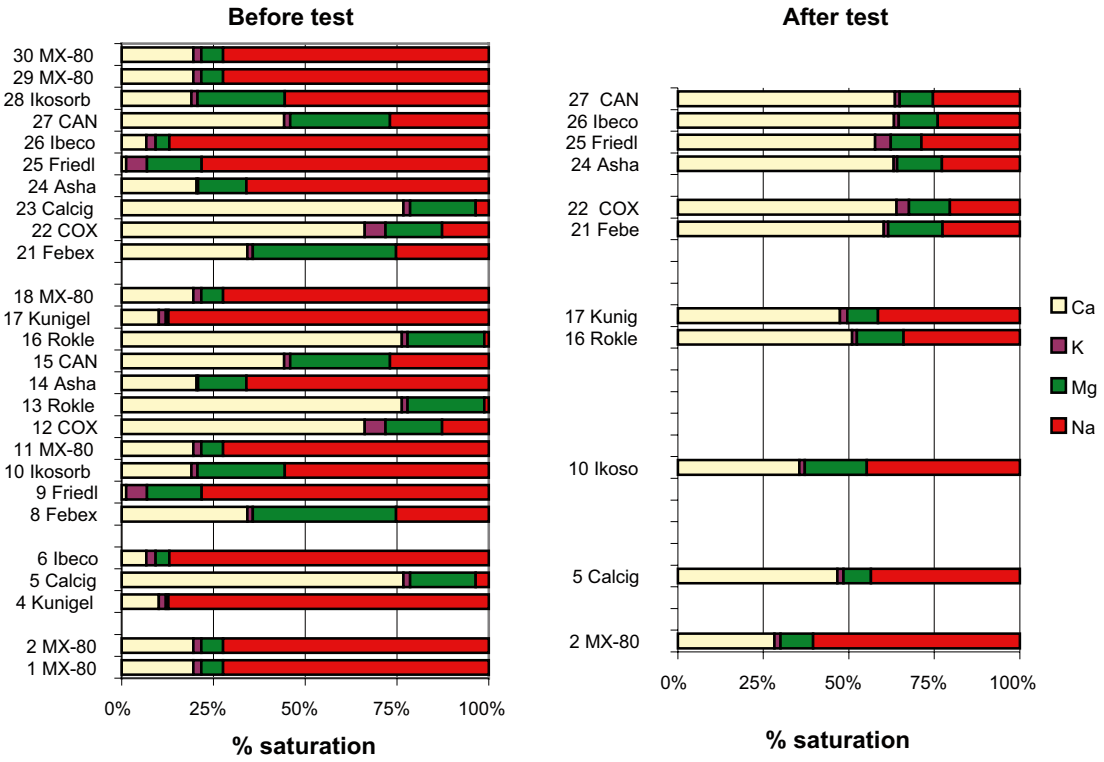

Figure 8-6. *Relative cation distribution in package 1 before (left; all blocks except those consisting of MX-80 granulate+sand) and after the 1 year test.*

Table 8-3. Exchangeable cations extracted by exchange with NH_4^+ in alcoholic solution.

SICADA code	Bentonite	Ca		K		Mg		Na		Σ cations
		meq/100 g	%	meq/100 g	%	meq/100 g	%	meq/100 g	%	meq/100 g
AB102BW1b	MX-80	24	28	1.8	2.1	7.7	8.9	53	61	86
AB102BW3b	MX-80	22	28	1.2	1.5	7.5	9.6	47	61	78
AB102BW5b	MX-80	23	29	1.4	1.8	7.7	9.7	47	60	79
AB102BW7b	MX-80	22	28	1.2	1.6	8.0	10.4	46	60	78
AB102BW9b	MX-80	22	28	1.1	1.4	7.4	9.5	47	61	78
AB102Rb	MX-80	16	20	1.8	2.2	4.7	5.9	58	72	81
AB105BW1b	Calcigel	33	46	1.2	1.6	5.8	7.9	33	45	73
AB105BW3b	Calcigel	31	47	1.2	1.8	5.7	8.7	28	43	66
AB105BW5b	Calcigel	35	47	1.4	1.9	6.9	9.3	31	42	75
AB105BW7b	Calcigel	31	47	1.2	1.8	5.2	7.8	29	43	66
AB105BW9b	Calcigel	34	47	1.2	1.7	4.6	6.5	32	45	72
AB105Rb	Calcigel	52	75	1.4	2.0	13.3	19.2	3	4	69
AB105Rb	Calcigel	52	77	1.2	1.8	12.1	17.9	2	4	68
AB110BW1b	Ikosorb	35	35	1.6	1.6	18.9	19.1	44	44	99
AB110BW5b	Ikosorb	35	36	1.6	1.6	18.0	18.6	43	44	97
AB110BW9b	Ikosorb	34	35	1.4	1.5	16.0	16.7	45	46	96
AB110Rb	Ikosorb	19	19	1.6	1.6	24.1	23.8	56	56	101
AB116BW1b	Rokle	36	51	1.0	1.4	10.3	14.4	24	33	71
AB116BW5b	Rokle	36	51	1.0	1.5	9.5	13.5	24	34	70
AB116BW9b	Rokle	36	51	1.0	1.4	9.1	13.0	24	35	70
AB116Rb	Rokle	52	76	1.1	1.6	14.2	20.9	1	1	68
AB117BW1b	Kunigel	32	48	1.4	2.1	6.3	9.3	28	41	68
AB117BW5b	Kunigel	33	47	1.5	2.2	6.4	9.2	29	41	69
AB117BW9b	Kunigel	32	47	1.5	2.3	5.6	8.3	29	42	68
AB117Rb	Kunigel	7	10	1.4	1.9	0.5	0.7	64	87	74
AB121BW1b	Febex	55	60	1.2	1.3	15.1	16.4	21	23	92
AB121BW5b	Febex	55	60	1.2	1.3	14.8	16.1	21	23	92
AB121BW9b	Febex	58	61	1.2	1.3	14.6	15.3	21	22	96
AB121Rb	Febex	34	34	1.4	1.4	39.3	39.1	25	25	100
AB122BW2b	COX	15	64	0.8	3.7	2.9	12.4	5	20	23
AB122BW5b	COX	15	65	0.9	4.0	2.8	12.0	5	19	24
AB122BW9b	COX	17	63	0.9	3.3	3.2	11.6	6	22	28
AB122Rb	COX	15	66	1.3	5.7	3.4	15.4	3	13	22
AB124BW1b	Asha 505	55	62	0.9	1.0	12.7	14.6	19	22	88
AB124BW3b	Asha 505	54	63	0.7	0.8	11.1	13.0	19	23	85
AB124BW3b	Asha 505	54	63	0.9	1.0	10.7	12.6	19	23	85
AB124BW5b	Asha 505	56	63	0.9	1.0	11.1	12.6	20	23	88
AB124BW7b	Asha 505	53	63	0.8	1.0	11.4	13.5	19	23	84
AB124BW7b	Asha 505	55	64	0.9	1.1	10.3	11.9	20	23	86
AB124BW9b	Asha 505	54	63	0.9	1.0	11.4	13.3	19	22	86
AB124BW9b	Asha 505	55	63	0.9	1.1	11.5	13.0	20	23	88
AB124Rb	Asha 505	19	20	0.4	0.4	12.3	13.1	62	66	94
AB125BW1b	Friedland	16	60	1.2	4.3	2.1	7.7	8	28	27
AB125BW5b	Friedland	15	57	1.4	5.0	2.5	9.3	8	29	27
AB125BW9b	Friedland	16	56	1.3	4.6	2.7	9.7	8	29	28
AB125Rb	Friedland	0	1	1.7	5.6	4.6	14.9	24	78	31
AB126BW1b	Ibeco	52	61	1.3	1.5	10.7	12.5	21	25	86
AB126BW5b	Ibeco	54	64	1.2	1.4	9.4	11.0	20	24	85
AB126BW9b	Ibeco	54	64	1.1	1.3	8.9	10.6	20	24	85
AB126Rb	Ibeco	6	7	2.2	2.5	3.3	3.8	77	87	88
AB127BW1b	Dep. CAN	52	61	1.3	1.5	9.0	10.6	22	26	85
AB127BW3b	Dep. CAN	51	62	1.3	1.6	9.2	11.1	21	25	83
AB127BW5b	Dep. CAN	50	63	1.1	1.4	7.6	9.7	20	25	79
AB127BW7b	Dep. CAN	51	64	1.1	1.4	7.8	9.7	20	25	80
AB127BW9b	Dep. CAN	52	66	1.1	1.4	6.0	7.6	20	25	79
AB127Rb	Dep. CAN	35	44	1.3	1.7	21.4	27.2	21	27	79

8.4 Cation exchange capacity (CEC)

8.4.1 Method

The cation exchange capacity (CEC) was determined by exchange with copper(II)triethylenetetramine following the procedure of Meier and Kahr (1999) modified according to Ammann et al. (2005) to ensure complete exchange. The ground sample (~400 mg) was dispersed in 50 ml deionised water by ultrasonic treatment and shaking until complete dispersion. 20 ml of ~15 mM Cu(II)-triethylenetetramine solution was added to the suspension, which was left to react for 30 minutes on a vibrating table. After centrifugation the absorbance at 620 nm of the supernatant was measured using a spectrophotometer (Shimadzu) and CEC calculated on the basis of the uptake of Cu by the clay. The water content of the clay was determined for a separate sample dried at 105°C to a constant weight. All CEC determinations were at least duplicated.

8.4.2 Results

Data on the CEC of the bulk samples of block 2 MX-80, block 5 Calcigel, block 24 Asha 505 and block 27 Deponit CAN are listed in Table 8-4 and plotted in Figure 8-7. Although changes in relation to the references are close to the resolution of the method, a tendency of increasing CEC towards the heater can be seen in particular in block 5 and block 27. The starting material of these blocks contained carbonates, which partly have dissolved in the samples proximal to the heater. Therefore, a small increase in CEC can be expected as an effect of a diminished dilution by carbonates. On the other hand, the incorporation of corrosion products of iron (cf. Section 8.5) in the bentonite would be expected to lower the CEC of samples closest to the

Table 8-4. CEC of the bulk bentonite from blocks 2 MX-80, 5 Calcigel, 24 Asha 505 and 27 Deponit CAN, determined by exchange with the Cu-trien complex

Sicada code	Bentonite	CEC_1 meq/100 g	CEC_2 meq/100 g	CEC_3 meq/100 g	CEC_{mean} meq/100 g
AB102BW1b	MX-80	86.0	86.4		86.2
AB102BW3b	MX-80	85.7	86.5		86.1
AB102BW5b	MX-80	85.0	85.5		85.2
AB102BW7b	MX-80	86.1	84.9		85.5
AB102BW9b	MX-80	83.7	85.2		84.4
AB102Rb	MX-80	84.6	84.5	83.5	84.2
AB105BW1b	Calcigel	67.2	67.0		67.1
AB105BW3b	Calcigel	65.6	66.7		66.2
AB105BW5b	Calcigel	65.5	66.1		65.8
AB105BW7b	Calcigel	65.6	65.2		65.4
AB105BW9b	Calcigel	64.6	63.7		64.1
AB105Rb	Calcigel	64.6	64.2		64.4
AB124BW1b	Asha 505	87.7	86.9	87.4	87.3
AB124BW3b	Asha505	87.2	86.0		86.6
AB124BW5b	Asha 505	85.2	88.2		86.7
AB124BW7b	Asha 505	87.8	86.6	85.2	86.5
AB124BW9b	Asha 505	86.6	84.3	84.8	85.2
AB124 Rb	Asha 505	85.3	86.2	86.6	86.0
AB127BW1b	Dep CAN	84.1	83.6		83.8
AB127BW3b	Dep CAN	81.3	82.7		82.0
AB127BW5b	Dep CAN	80.1	81.3		80.7
AB127BW7b	Dep CAN	80.6	80.8		80.7
AB127BW9b	Dep CAN	80.9	81.6		81.2
AB127Rb	Dep CAN	80.7	80.4		80.5

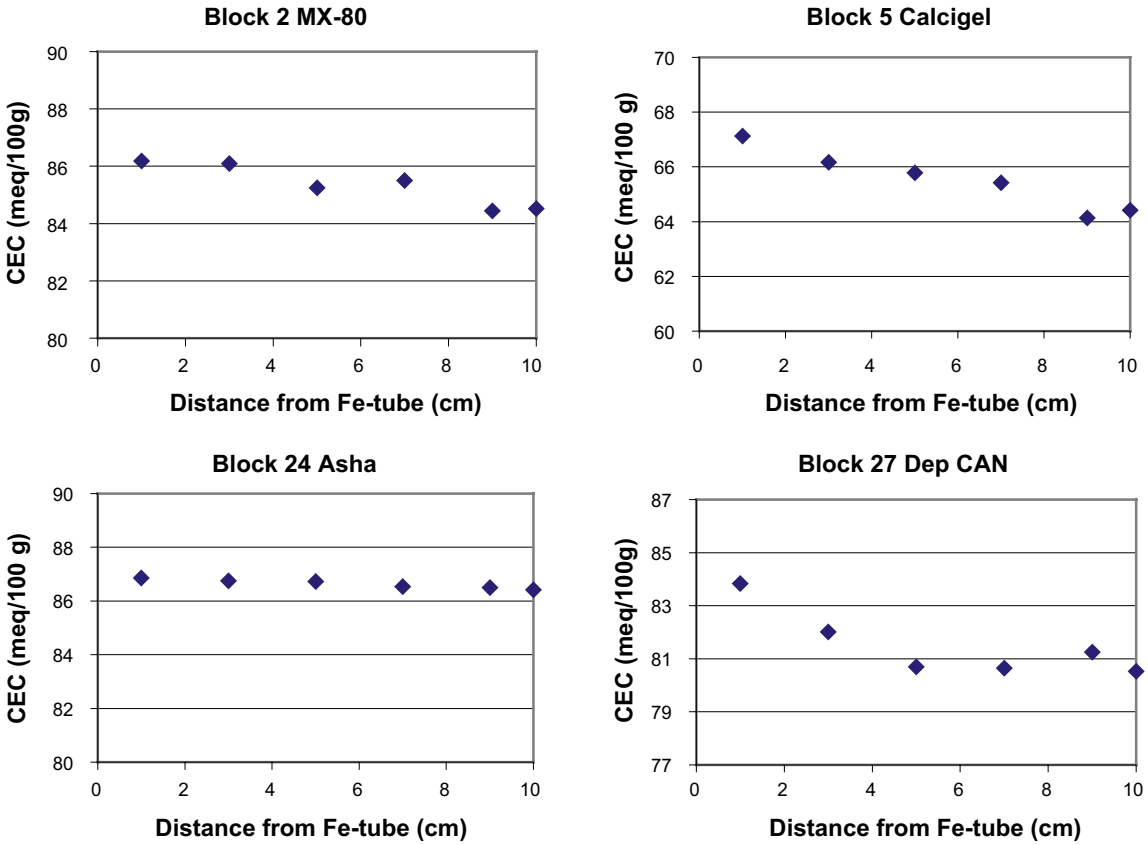

Figure 8-7. *CEC of the bulk bentonites from block 2 MX-80, block 5 Calcigel, block 24 Asha 505 and block 27 Deponit CAN. The values of the references are plotted at the position 10 cm*

Fe-tube due to the dilution effect. However, charged hydroxylated surfaces of iron oxides/hydroxides that may have formed in the clay, can contribute to the CEC depending on the pH, i.e. under conditions more alkaline than the pH of the zero point of charge, cations can be attracted to the charged surfaces of iron oxyhydroxides (Taylor 1987).

8.5 Chemical composition of the bulk bentonites

8.5.1 Methods

The chemical composition of the bulk bentonite was determined at an ISO 9001 accredited laboratory (ACME Analytical Laboratories, Vancouver, Canada). After digestion of the samples using standard techniques for silicate analysis ($LiBO_2/Li_2B_4O_7$ fusion/dilute nitric acid digestion) major, minor and trace elements were determined using ICP-AES and ICP-MS.

Loss on ignition (LOI) was determined as the difference in weight of the samples dried at 105°C and after ignition at 1,000°C.

Total carbon and total sulfur were determined at the same laboratory by evolved gas analysis. The sample was combusted in a Leco furnace, equipped with IR-detectors for CO_2 and SO_2. Acid-soluble carbon was determined as CO_2 evolved on direct treatment with hot 15% HCl.

8.5.2 Results

The chemical composition of the bulk samples from block 2 MX-80, block 5 Calcigel, block 24 Asha 505 and block 27 Deponit CAN is given in Table 8-5.

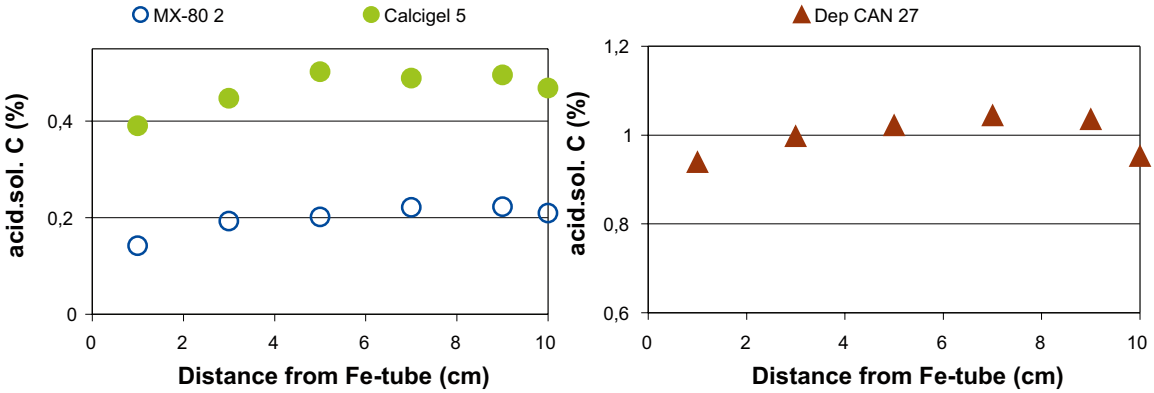

Figure 8-8. *The radial distribution of acid-soluble carbon in the MX-80 (block 2), Calcigel (block 5) and Deponit CAN (block 27) bentonites. Acid-soluble carbon of the Asha 505 samples is close to or below the detection limit and therefore omitted. The reference samples are plotted at the position 10 cm.*

Carbon and sulfur

Special attention is paid to the carbonate and sulfate minerals because of their temperature-dependant solubility, which makes their behaviour susceptible to non-isothermal conditions and hydration gradients, i.e. conditions that will prevail during the water saturation of a bentonite buffer. The abundance of carbonate minerals varies significantly among the reference bentonites/clays. Thus, carbonates are trace constituents (< 1.5%) in e.g. Asha 505, MX-80 and Febex but one of the major components (25%) in e.g. COX (cf. Section 7). The values given within parentheses are the maximum amount if all acid-soluble carbon is allocated to $CaCO_3$, but in addition to calcite, other carbonate minerals, such as dolomite and siderite, exist in some of the clays.

The post-test distribution of acid soluble carbon in the blocks examined (Figure 8-8) indicates carbonate dissolution closest to the heater in the carbonate-bearing bentonites MX-80, Calcigel and Deponit CAN, as was observed also in the 5-year long field test LOT A2 (Karnland et al. 2009). The acid-soluble carbon content of the Asha 505 samples (block 24) is close to or below the detection limit and the data are not included in Figure 8-8.

Total sulfur in the analysis of the bulk samples includes water-soluble sulfate minerals, such as gypsum,$CaSO_4 \cdot 2H_2O$ and anhydrite $CaSO_4$, and insoluble minerals, such as sulphides (e.g. pyrite FeS_2) and, possibly, barite ($BaSO_4$). In the reference sample of MX-80 the water-extracted sulfate fraction makes up almost half of the total inventory of sulfur. In Deponit CAN, which is one of the clays with highest total sulfur content, the major fraction exists as insoluble minerals, probably Fe-sulphides. Both Asha 505 and Calcigel are very low in sulfur, with total S contents close to or below the detection limit. Tendencies in the total sulfur distribution after the field test in Figure 8-9 thus reflect changes in one or both of the sulfur fractions (cf. Figure 8-5). The quantity of the insoluble fraction has been estimated as the difference between total (Table 8-5) and water-extractable sulfur (Table 8-2).

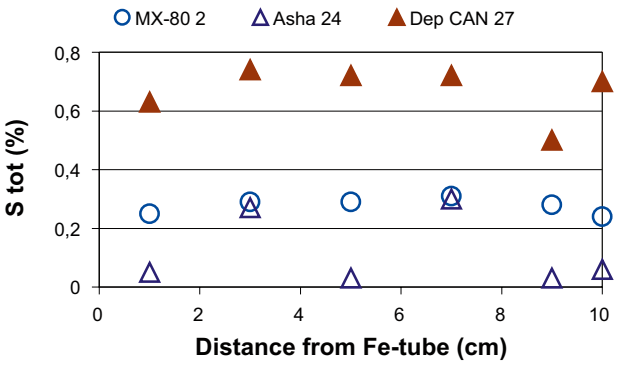

Figure 8-9. *The radial distribution of total sulfur in block 2 MX-80, 24 Asha 505 and 27 Deponit CAN. Total sulfur is below the detection limit in most of the samples of block 5 Calcigel, which has been omitted. The reference samples are plotted at the position 10 cm.*

Table 8-5. Chemical composition of the bulk bentonites MX-80, Calcigel, Asha 505 and Deponit CAN, in blocks 2, 5, 24 and 27, respectively, and the corresponding reference samples. Major, minor and trace elements by ICP-AES and -MS, S and C by evolved gas analysis. DL=detection limit.

Sample id	SiO_2	Al_2O_3	Fe_2O_3	MgO	CaO	Na_2O	K_2O	TiO_2	P_2O_5	MnO	Cr_2O_3	LOI	Sum	TOT/C	TOT/S	CO_3-C	Sc	Mo	Cu	Pb	Zn	Ni
	%	%	%	%	%	%	%	%	%	%	%	%	%	%	%	%	ppm	ppm	ppm	ppm	ppm	ppm
DL	0.01	0.01	0.04	0.01	0.01	0.01	0.01	0.01	0.01	0.01	0.002	5.1	0.01	0.02	0.02	0.02	1	0.1	0.1	0.1	1	0.1
AB1 02BW 1b (MX-80)	62.34	19.74	4.41	2.35	1.21	2.05	0.59	0.15	0.06	0.01	0.007	6.9	99.85	0.26	0.25	0.134	6	2	4.4	39.2	85	3.6
AB1 02BW 3b (MX-80)	62.82	19.92	3.9	2.37	1.66	1.9	0.57	0.15	0.06	0.02	0.007	6.5	99.83	0.29	0.29	0.183	6	1.5	4	38.7	111	3.3
AB1 02BW 5b (MX-80)	62.66	19.92	3.86	2.33	1.74	1.9	0.55	0.15	0.07	0.02	0.006	6.6	99.84	0.32	0.29	0.191	6	1.8	3.9	39.3	90	3.2
AB1 02BW 7b (MX-80)	60.69	19.48	3.82	2.33	1.73	1.87	0.55	0.15	0.06	0.02	0.005	9.1	99.84	0.31	0.31	0.205	6	1.9	3.9	36.8	94	3.2
AB1 02BW 9b (MX-80)	61.67	19.41	3.81	2.31	1.7	1.84	0.55	0.15	0.06	0.02	0.009	8.3	99.85	0.32	0.28	0.207	6	1.9	4.1	37	76	3.2
AB1 02 Rb (MX-80)	59.58	18.9	3.91	2.56	1.39	1.95	0.6	0.2	0.09	0.02	0.014	10.5	99.67	0.30	0.24	0.190	7	3.1	4.2	39.7	100	3.6
AB1 05BW 1b (Calcigel)	56.98	17.55	5.93	3.5	2.19	1.39	1.29	0.43	0.09	0.04	0.004	10.4	99.83	0.52	< .02	0.355	14	0.3	8.9	17.6	54	12.3
AB1 05BW 3b (Calcigel)	55.46	17.63	5.33	3.36	2.46	1.37	1.28	0.43	0.1	0.04	0.007	12.4	99.86	0.42	< .02	0.398	15	0.2	9.7	17.5	50	13.1
AB1 05BW 5b (Calcigel)	55.83	17.74	5.31	3.28	2.56	1.36	1.28	0.42	0.1	0.04	0.006	12	99.86	0.42	< .02	0.45	15	0.2	8.9	18.8	52	13.6
AB1 05BW 7b (Calcigel)	57.53	17.62	5.28	3.27	2.57	1.37	1.28	0.44	0.08	0.04	0.004	10.3	99.83	0.43	0.03	0.447	14	0.4	9.5	19.1	56	14.9
AB1 05BW 9b (Calcigel)	57.45	17.62	5.39	3.25	2.59	1.39	1.28	0.43	0.09	0.04	0.004	10.3	99.83	0.45	< .02	0.453	14	0.4	10	20.1	59	16.1
AB1 05 Rb (Calcigel)	54.67	17.54	5.05	3.37	2.94	0.47	1.16	0.41	0.1	0.03	0.005	14.1	99.87	0.43	0.03	0.41	15	< 0.1	10.7	22.3	54	15.2
AB1 24BW 1b (Asha 505)	47.91	21.77	13.27	2.05	1.78	0.67	0.11	1.14	0.07	0.05	0.047	11	99.86	0.04	0.05	0.011	63	< 0.1	88.2	1	150	47.9
AB1 24BW 3b (Asha 505)	48.53	21.89	13.41	1.99	1.79	0.67	0.11	1.14	0.07	0.05	0.045	10.2	99.87	0.06	0.27	0.027	62	0.1	122.7	0.9	117	45.2
AB1 24BW 5b (Asha 505)	47.84	21.98	13.87	1.96	1.7	0.67	0.12	1.11	0.08	0.06	0.045	10.4	99.88	0.04	0.03	0.016	63	< 0.1	111.4	1	118	46.9
AB1 24BW 7b (Asha 505)	48.21	22.54	12.58	1.96	1.74	0.69	0.12	1.21	0.06	0.06	0.048	10.6	99.88	0.07	0.30	0.011	66	< 0.1	108.7	0.9	120	47.7
AB1 24BW 9b (Asha 505)	48.83	22.01	13.07	1.93	1.71	0.73	0.21	1.11	0.07	0.05	0.047	10.1	99.88	0.04	0.03	0.014	62	0.2	104.8	1	120	48.6
AB1 24 Rb (Asha 505)	46.48	20.64	12.16	2.01	0.84	1.97	0.14	1.01	0.09	0.05	0.038	14.4	99.89	0.08	0.06	0.016	56	< 0.1	129.9	0.8	123	44.7
AB1 27BW 1b (DepCAN)	53.5	17.54	5.12	3.13	5.46	0.81	0.91	0.73	0.14	0.07	0.004	12.3	99.77	0.81	0.63	0.867	15	0.6	23.9	13.8	120	5.7
AB1 27BW 3b (DepCAN)	53.17	17.34	4.76	3	5.57	0.8	0.93	0.74	0.14	0.07	0.004	13.3	99.78	0.84	0.74	0.916	15	0.7	20.8	12.7	46	5.1
AB1 27BW 5b (DepCAN)	53.52	17.25	4.76	2.93	5.55	0.78	0.93	0.73	0.14	0.07	0.003	13.1	99.78	0.86	0.72	0.941	15	0.7	21.4	12.5	49	5.5
AB1 27BW 7b (DepCAN)	53.22	17.33	4.77	2.89	5.62	0.78	0.94	0.74	0.14	0.07	0.002	13.3	99.77	0.84	0.72	0.96	15	0.7	21.8	12.9	50	5.9
AB1 27BW 9b (DepCAN)	54.12	17.55	4.86	2.88	5.66	0.77	0.94	0.74	0.14	0.07	0.003	12	99.77	0.89	0.50	0.96	15	0.7	21.4	14.1	61	11.4
AB1 27 Rb (Dep CAN)	52.01	17.15	4.64	3.11	5.07	0.78	0.9	0.71	0.14	0.07	0.003	14.5	99.05	0.89	0.70	0.86	14	1	21.2	14	47	5.1

Table 8-5 continued.

Sample id		As	Cd	Sb	Bi	Ag	Au	Hg	Tl	Se	Ba	Be	Co	Cs	Ga	Hf	Nb	Rb	Sn	Sr	Ta	Th	U	V	W
		ppm	ppm	ppm	ppm	ppm	ppm	ppm	ppm	ppm	ppm	ppm	ppm	ppm	ppm	ppm	ppm	ppm	ppm	ppm	ppm	ppm	ppm	ppm	ppm
	DL	0.5	0.1	0.1	0.1	0.1	0.5	0.01	0.1	0.5	1	1	0.2	0.1	0.5	0.1	0.1	0.1	1	0.5	0.1	0.2	0.1	8	0.5
AB1 02BW 1b (MX-80)		12	0.4	0.2	1	0.1	< 0.5	< 0.01	0.3	0.5	309	1	1.5	0.4	26	8.3	29.9	13.8	9	331.7	3	38.8	14.7	9	< 0.5
AB1 02BW 3b (MX-80)		13.6	0.3	0.2	1	0.2	< 0.5	< 0.01	0.2	0.6	330	1	1.8	0.5	26.9	9.2	30.8	13.3	9	335	3.1	38.8	14.5	9	< 0.5
AB1 02BW 5b (MX-80)		13.8	0.3	0.2	1	0.2	< 0.5	< 0.01	0.2	0.6	336	2	1.4	0.4	26.4	8.7	29.0	12.5	10	316	3.3	39.7	14.3	9	< 0.5
AB1 02BW 7b (MX-80)		12.7	0.3	0.2	0.9	0.1	< 0.5	< 0.01	0.2	0.5	337	1	1.3	0.4	28	7.8	28.4	13.2	9	310.2	3.1	39.2	13.2	8	< 0.5
AB1 02BW 9b (MX-80)		12.4	0.3	0.1	0.9	0.1	< 0.5	< 0.01	0.2	0.6	282	2	1.6	0.4	26.5	8.2	27.9	13.1	9	271.2	3	36.2	13.8	< 8	< 0.5
AB1 02 Rb (MX-80)		14.2	0.3	0.7	1	0.1	0.6	0.01	0.4	< 0.5	321	2	2.7	1	27.7	8.5	28.7	17.8	9	278.3	3.1	38	13.1	16	< 0.5
AB1 05BW 1b (Calcigel)		4.3	0.1	< 0.1	0.3	< 0.1	1.4	0.02	0.1	< 0.5	193	3	7.1	5.6	22.8	8.3	22.4	68.5	6	138.6	1.4	17.3	3.4	54	1.1
AB1 05BW 3b (Calcigel)		6.4	0.1	< 0.1	0.3	< 0.1	0.6	0.02	0.2	0.5	213	4	6.6	5.9	21	7.8	21.4	60.2	4	124.1	1.5	17.4	3.5	46	1.2
AB1 05BW 5b (Calcigel)		6.5	0.1	< 0.1	0.3	< 0.1	1.2	0.02	0.2	< 0.5	220	3	6.5	6.1	23.3	8	20.8	63.6	5	125.8	1.6	17.4	3.5	46	1.2
AB1 05BW 7b (Calcigel)		6.2	0.2	< 0.1	0.3	< 0.1	2.1	0.02	0.2	< 0.5	236	3	6.9	6.4	22.5	8	23.3	70.2	5	138.3	1.6	17.8	3.7	55	1.1
AB1 05BW 9b (Calcigel)		6.4	0.1	< 0.1	0.3	< 0.1	1.9	0.02	0.2	< 0.5	225	3	6.8	6.4	22.7	8.2	22.6	69.7	5	142.1	1.4	16	3.4	53	1.4
AB1 05 Rb (Calcigel)		5.2	0.1	< 0.1	0.3	< 0.1	0.5	0.03	0.3	< 0.5	205	2	6.2	5.3	21.7	8	20.9	59.6	5	69.7	1.5	15.8	3.4	45	1.1
AB1 24BW 1b (Asha 505)		1	< 0.1	< 0.1	< 0.1	< 0.1	2.2	< 0.01	< 0.1	0.6	17	< 1	60.5	0.1	18.9	1.8	10.5	5.2	< 1	214.4	0.6	1.8	0.3	215	< 0.5
AB1 24BW 3b (Asha 505)		0.9	< 0.1	< 0.1	< 0.1	< 0.1	1.2	< 0.01	< 0.1	< 0.5	17	< 1	58.9	0.2	20.3	3.2	10.3	5.4	< 1	207.1	0.7	1.4	0.4	213	0.6
AB1 24BW 5b (Asha 505)		1	< 0.1	< 0.1	< 0.1	< 0.1	1.2	< 0.01	< 0.1	< 0.5	22	< 1	62.9	0.2	19.9	2.2	10.1	5.7	< 1	213.9	0.7	1.4	0.3	207	0.6
AB1 24BW 7b (Asha 505)		1.1	< 0.1	< 0.1	< 0.1	< 0.1	1.6	< 0.01	< 0.1	< 0.5	19	< 1	51.8	0.2	19.7	2	10.2	6	< 1	202.4	0.7	1.5	0.4	205	< 0.5
AB1 24BW 9b (Asha 505)		1	< 0.1	< 0.1	< 0.1	< 0.1	0.8	< 0.01	< 0.1	0.6	33	< 1	52.4	0.2	20.2	1.9	10.1	8	< 1	200.3	0.6	1.5	0.5	198	< 0.5
AB1 24 Rb (Asha 505)		< 0.5	< 0.1	< 0.1	< 0.1	< 0.1	< 0.5	< 0.01	< 0.1	< 0.5	54	< 1	59.9	0.3	20.2	2	10.3	7.3	< 1	127.6	0.6	2.1	0.7	189	< 0.5
AB1 27BW 1b (DepCAN)		7.4	0.3	< 0.1	< 0.1	< 0.1	< 0.5	0.43	1.7	0.8	866	1	11.9	11.3	16.6	4	8.2	58.3	2	238.4	0.6	10.9	5.7	151	1.1
AB1 27BW 3b (DepCAN)		9	0.1	< 0.1	< 0.1	< 0.1	< 0.5	0.36	1.7	< 0.5	910	1	10.8	9.8	17.5	4.1	8.3	57.2	1	229.1	0.6	10.1	5.6	146	0.8
AB1 27BW 5b (DepCAN)		9	0.2	< 0.1	< 0.1	< 0.1	0.6	0.39	1.6	< 0.5	877	2	10.3	10.1	16.6	4	7.9	58.5	2	229.2	0.7	10	5.6	146	1
AB1 27BW 7b (DepCAN)		8.5	0.2	< 0.1	< 0.1	< 0.1	< 0.5	0.42	1.5	< 0.5	937	2	11.1	11	17.5	3.6	8.4	57.5	2	232.7	0.6	10.7	5.5	148	1
AB1 27BW 9b (DepCAN)		8.7	0.2	< 0.1	< 0.1	< 0.1	0.6	0.40	1.7	< 0.5	936	1	11.4	11.1	17.3	3.7	8.5	59.3	2	249.2	0.7	11.3	5.7	154	1
AB1 27 Rb (Dep CAN)		7.8	0.2	0.1	< 0.1	< 0.1	0.5	0.34	1.9	< 0.5	900	1	11.5	12.7	18.1	4.2	8.6	65.1	2	124.2	0.7	11.4	5.8	150	0.9

Table 8-5 continued.

Sample id	DL	Zr ppm 0.1	Y ppm 0.1	La ppm 0.1	Ce ppm 0.1	Pr ppm 0.02	Nd ppm 0.3	Sm ppm 0.05	Eu ppm 0.02	Gd ppm 0.05	Tb ppm 0.01	Dy ppm 0.05	Ho ppm 0.02	Er ppm 0.03	Tm ppm 0.01	Yb ppm 0.05	Lu ppm 0.01
AB1 02BW 1b (MX-80)		199.4	42.6	50.6	109.2	12.84	47.5	10.24	0.7	9.21	1.49	8.83	1.59	4.38	0.63	4.27	0.55
AB1 02BW 3b (MX-80)		208.6	42.6	51.4	113.7	12.93	48.4	10.27	0.7	8.97	1.5	8.43	1.59	4.12	0.63	4.27	0.56
AB1 02BW 5b (MX-80)		196.5	41.8	49.2	110	12.46	46.7	10.09	0.66	9	1.47	8.48	1.55	4.27	0.59	4.12	0.54
AB1 02BW 7b (MX-80)		186.3	40.3	49.4	107.7	12.21	45.7	9.77	0.64	8.77	1.44	8.04	1.53	4.19	0.58	4.04	0.53
AB1 02BW 9b (MX-80)		182.2	39.3	47.8	107.1	11.88	45.3	9.71	0.63	8.41	1.39	7.87	1.5	4.11	0.58	3.98	0.51
AB1 02 Rb (MX-80)		201.1	43.7	52.3	109.7	13.27	50.4	10.18	0.82	9.59	1.37	8.62	1.65	4.36	0.66	4.07	0.56
AB1 05BW 1b (Calcigel)		259.7	46.1	45.8	100.5	11.1	43.4	8.12	1.25	7.88	1.33	7.58	1.57	4.47	0.67	4.33	0.67
AB1 05BW 3b (Calcigel)		257.4	41.6	42.3	91.7	10.09	40.6	8.13	1.21	7.44	1.24	7.32	1.49	4.32	0.64	4.4	0.63
AB1 05BW 5b (Calcigel)		252.9	41.6	41.4	89.4	9.98	39.8	8.19	1.19	7.26	1.24	7.37	1.51	4.27	0.61	4.56	0.64
AB1 05BW 7b (Calcigel)		265.4	47.1	46.4	101.3	11.43	43.5	8.14	1.26	7.95	1.32	7.49	1.55	4.41	0.68	4.49	0.68
AB1 05BW 9b (Calcigel)		271.0	45.5	46.3	102.2	11.3	44.1	8.04	1.27	7.82	1.32	7.74	1.55	4.64	0.68	4.31	0.65
AB1 05 Rb (Calcigel)		253.3	46.3	45.1	93	11.13	43.2	7.98	1.34	7.88	1.12	7.36	1.58	4.29	0.69	4.42	0.66
AB1 24BW 1b (Asha 505)		72.8	23.6	8.8	17.6	2.31	9.6	2.5	0.96	3.26	0.59	3.63	0.79	2.36	0.33	2.32	0.34
AB1 24BW 3b (Asha 505)		130.1	25	10.5	21.9	2.72	11.9	2.98	1.05	3.62	0.65	4.06	0.85	2.54	0.35	2.4	0.36
AB1 24BW 5b (Asha 505)		69.7	29	10.3	21.8	2.59	10.6	2.82	1.04	3.78	0.67	4.46	0.99	3.08	0.42	2.78	0.42
AB1 24BW 7b (Asha 505)		69.5	21	8.9	17.6	2.28	10.3	2.36	0.92	3.12	0.54	3.57	0.74	2.21	0.3	2.09	0.29
AB1 24BW 9b (Asha 505)		66.6	26.8	9.4	18.8	2.42	10.4	2.44	0.95	3.4	0.6	3.9	0.88	2.7	0.37	2.48	0.38
AB1 24 Rb (Asha 505)		72.2	30.8	11.3	22.4	2.96	13.2	2.94	1.18	3.94	0.6	4.36	1.09	2.91	0.42	2.86	0.41
AB1 27BW 1b (DepCAN)		144.1	17.9	25.3	53.1	5.92	22.5	4.54	1.14	3.82	0.61	3.46	0.65	2.04	0.28	2.00	0.29
AB1 27BW 3b (DepCAN)		145.0	18.1	24.7	52.7	5.91	22.8	4.37	1.15	3.92	0.59	3.39	0.65	1.91	0.28	2.04	0.28
AB1 27BW 5b (DepCAN)		141.0	18.3	24.2	52.1	5.85	23.9	4.37	1.08	3.85	0.59	3.39	0.65	1.83	0.28	2.02	0.3
AB1 27BW 7b (DepCAN)		142.3	18.3	25	51.4	5.91	23	4.44	1.15	3.98	0.6	3.39	0.64	1.92	0.28	2.07	0.31
AB1 27BW 9b (DepCAN)		148.4	18.4	25.7	53.5	6.07	24.9	4.57	1.18	3.99	0.61	3.62	0.69	1.99	0.28	2.06	0.32
AB1 27 Rb (DepCAN)		145.4	20.1	28.1	57.1	6.81	26	4.69	1.36	4.41	0.57	3.64	0.72	2.13	0.36	2.05	0.32

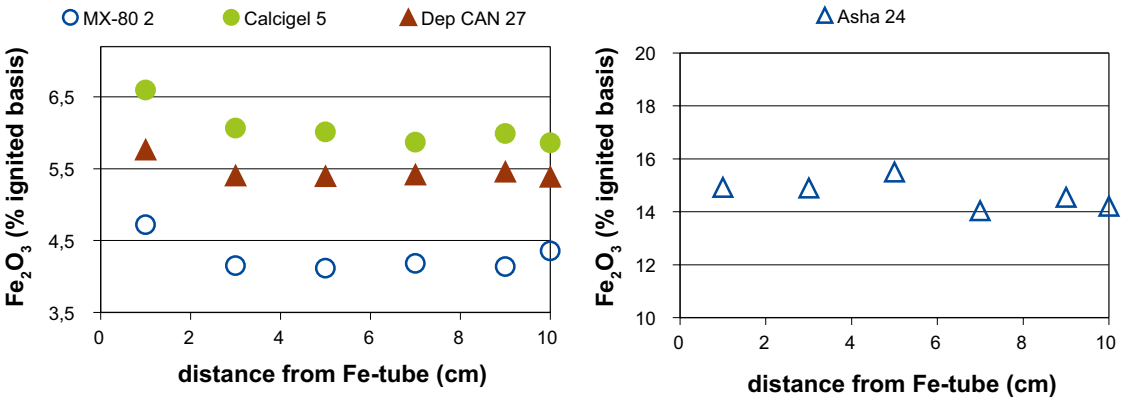

Figure 8-10. *The radial distribution of Fe_2O_3 in block 2 MX-80, block 5 Calcigel, block 24 Asha 505 and block 27 Deponit CAN. The reference samples are plotted at the position 10 cm.*

Sodium, calcium, iron and magnesium

Sodium and calcium emanate from various sources in the bulk bentonites, but the clear contrasting change in the relative proportions of CaO and Na_2O in block 5 Calcigel and 24 Asha 505, respectively, first of all reflects the different equilibrium composition of the exchangeable cation pool in the upper and lower parts of the package (cf. Section 8.3)

The Asha 505 bentonite has significantly higher iron content than any of the other bentonites examined and higher concentrations of several of the other heavy metals (Table 8-5), which reflects the difference in parent rock compositions. No clear trend can be seen in the iron distribution in the Asha 505 bentonite in block 24 after the field test (Figure 8-10 right), whereas the blocks of the less iron-rich bentonites MX-80, Calcigel and Deponit CAN (Figure 8-10 left) display an increase in iron at the Fe-tube, suggesting that iron released by corrosion of the tube has been incorporated into the bentonite. A thin rim of corrosion products was macroscopically visible at the interface between the Fe-tube and the bentonite in several of the blocks but was removed prior to the analyses of the bentonite. The Fe_2O_3-values have been re-calculated on an ignited basis to avoid artefacts that may arise due to variable amounts of volatiles among the samples.

With few exceptions, all samples from all four blocks are depleted in magnesium relative to their reference sample (Figure 8-11). The deficit in magnesium tends to be at a maximum in the peripheral parts, which creates a gradient in magnesium towards the heater. Calcigel and Deponit CAN contain dolomite, which is a possible source of Mg, but since the dissolution of carbonates has been most intense at positions proximal to the heater, carbonate dissolution is an unlikely cause of the peripheral depletion in Mg. Moreover, the Asha 505 bentonite is more or less carbonate-free, and yet the trend in Mg is similar in block 24. A fraction of the magnesium content of the bulk bentonites is exchangeable Mg, and this fraction has decreased in block 5 Calcigel and block 27 Deponit CAN relative the references, but increased in block 2 MX-80 and remained more or less unchanged in block 24 Asha 505. In the LOT A2 field test (Karnland et al. 2009) a transfer of magnesium from the outer to the inner parts of the heated blocks was indicated in both the bulk bentonite and in dialysed, homo-ionic Na-clays. Supplementary analyses of purified and homo-ionic clay fractions would probably provide information about the magnesium behaviour and the sources/sinks also in the various bentonites of the ABM package 1.

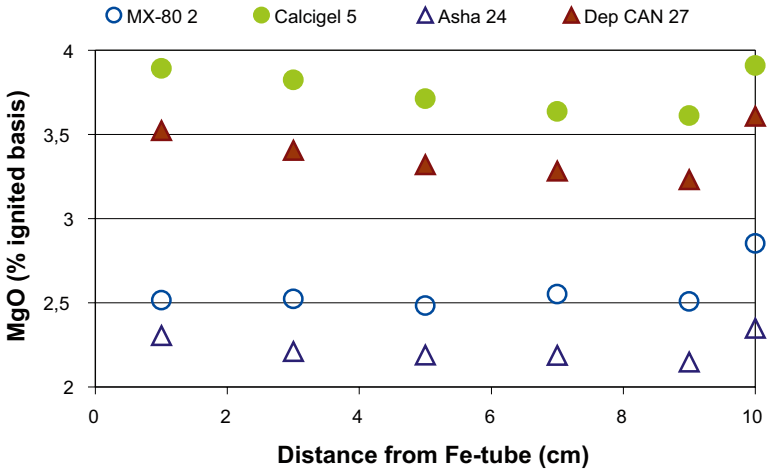

Figure 8-11. *The radial distribution of MgO in block 2 MX-80,block 5 Calcigel, block 24 Asha 505 and block 27 Deponit CAN . The reference samples are plotted at the position 10 cm.*

8.6 X-ray diffraction analysis

8.6.1 Method

The mineralogical composition was determined by X-ray diffraction analysis of randomly oriented powders of the bulk samples The specimens were prepared of the bulk material ground to a grain-size < 10 µm and scanned in the 2θ interval 5–80° with a scanning speed of 1° 2θ/min.

A Philips 1,050 goniometer with fixed divergence, anti-scatter slits and Co-Kα radiation with pulse-high selection and Fe-filter was used for the X-ray scanning, which was carried out at GEUS, Copenhagen.

8.6.2 Results

Block 2 MX-80

The XRD-profiles of random powders of the bulk samples of block 2 MX-80 are shown in Figure 8-12 together with the reference sample. The strongest peaks of the major non-phyllosilicates quartz, cristobalite and feldspars are indicated in Figure 8-12. A variation of the intensity of the feldspar peaks can be seen among the samples, but both the excellent cleavage and the coarse grain-size of the feldspars may give a random variation in the peak intensity. Traces of calcite are generally found in MX-80 and the peak position of the strongest calcite peak is indicated in Figure 8-12. Consistent with the chemical data, which indicate carbonate dissolution at the heater, the calcite peak can be detected only in the outermost block samples. A peak of low intensity at the position of the strongest peak of anhydrite ($CaSO_4$) can be seen in the XRD-profile of sample 3, but cannot unambiguously be attributed to anhydrite.

The position of the first order basal reflection of montmorillonite is approximately 12 – 12.5Å in all samples, which is within the typical range of the monolayer hydrate of Na-montmorillonite and also consistent with the data on the composition of the exchangeable cation pool, showing that the proportion between di- and monovalent cations has changed only slightly in block 2.

In Figure 8-12 also the position of the (060) peak is indicated. This peak is useful for distinguishing between di- and trioctahedral sub-groups of clay minerals because it includes the *b* cell dimension, which is sensitive to the size of the cation and the site occupancy in the octahedral sheet. No change can be seen among the samples and the indicated d-value of 1.49–1.50 Å is typical of the dioctahedral sub-group of smectites, to which montmorillonite belongs.

Block 5 Calcigel

The XRD-profiles of random powders of the bulk samples of block 5 Calcigel are shown in Figure 8-13 together with the reference sample. The strongest peaks of the major non-phyllosilicates quartz, cristobalite, feldspars (K-feldspar and Ca-plagioclase), calcite and dolomite are indicated in Figure 8-13.

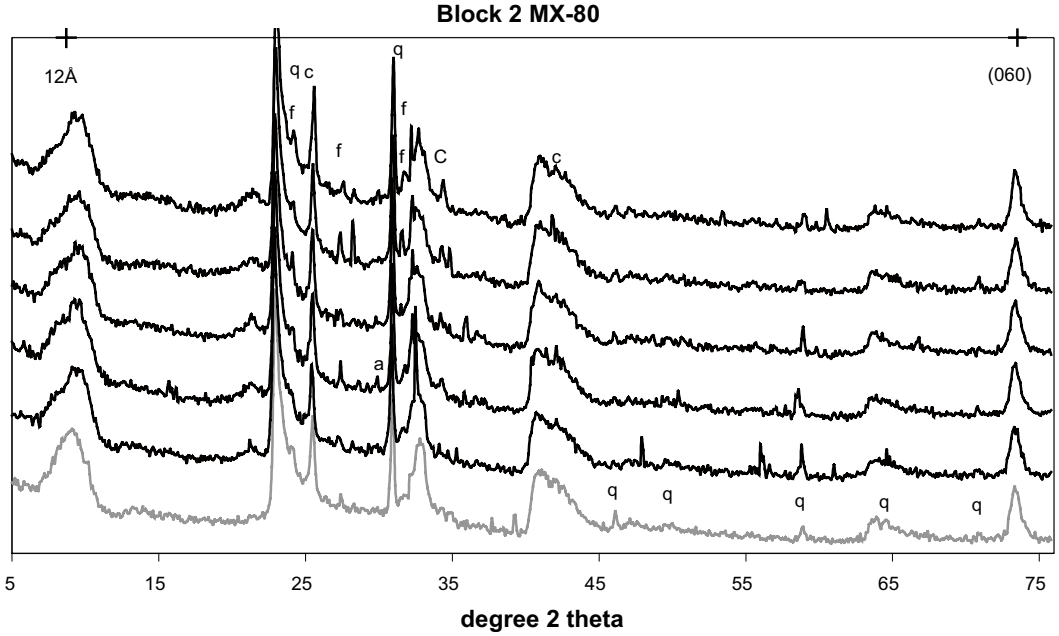

Figure 8-12. *Black curves: XRD-profiles of sample 1 (bottom) to sample 9 (top) from block 2, MX-80. Grey curve: reference sample. The strongest peaks of the major accessory minerals are indicated: a=anhydrite; C=calcite; c=cristobalite; f=feldspars; q=quartz. Random powders of bulk samples. CoKα radiation.*

The Calcigel bentonite also contains a mica mineral, which is aluminous (i.e. of muscovite type) judged by the relative peak intensities of the first and second order basal reflections. In Figure 8-13 also the position of a phyllosilicate with 7Å and 3.5Å basal spacings has been indicated with k?. The most common phyllosilicates producing basal peaks of this spacing are the chlorites and minerals of the kaolin group but the identification requires diagnostic pretreatments followed by X-ray scanning of oriented preparations.

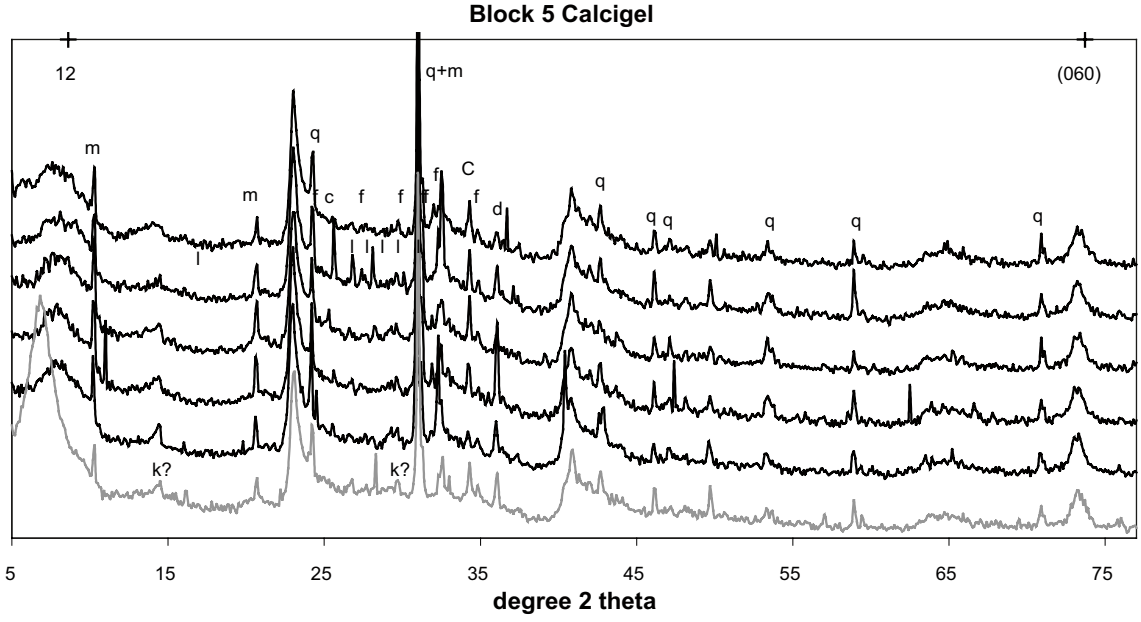

Figure 8-13. *Black curves: XRD-profiles of sample 1 (bottom) to sample 9 (top) from block 5, Calcigel. Grey curve: reference sample. The strongest peaks of the major accessory minerals are indicated: C=calcite; c=cristobalite; d=dolomite; f=feldspars; k?=7Å-phyllosilicate (see text); l=Ca-plagioclase, m=mica; q=quartz. Random powder of bulk samples. CoKα radiation.*

The reference sample has a well-defined first order smectite peak with a spacing of approximately 14.5 Å, which is typical of smectites with divalent interlayer cations with two layers of water molecules (Brindley and Brown 1980). Consistent with the data on the exchangeable cation pool, showing that a large proportion of the divalent cations has been replaced by sodium, the exposed samples have a broad (001) basal reflection which have migrated towards the high angle side.

The d-value of the (060) peak (1.49–1.50 Å) of both the reference and the block samples is typical of the dioctahedral sub-group of smectites. Thus, the available XRD-data give no indication of any significant change of the *b* cell dimension of the smectite.

Block 24 Asha 505

The Asha 505 bentonite has significantly higher content of heavy metals than any of the other bentonites (cf. Table 8-5). As indicated in the XRD-profiles in Figure 8-14, some of the source minerals of the heavy metals exist as discrete, crystalline phases – for instance anatase is the major Ti-bearing mineral and magnetite/maghemite and goethite are the major Fe-bearing accessory minerals. Part of the iron probably also exists as poorly crystalline or X-ray amorphous phases, which are not detectable with the XRD method.

In the XRD-profiles also the strongest basal reflections of a kaolin mineral (7 Å-mineral) are indicated. Kaolinite has been identified in several of the Asha bentonites in previous investigations (e.g. Karnland et al. 2006), but based on the available XRD-data, the identification must be considered tentative, because minerals of the kaolin group cannot be discriminated with certainty from e.g. chlorites without diagnostic pretreatments followed by X-ray scanning of oriented preparations.

The Asha 505 bentonite is poor in free silica minerals, like quartz and cristobalite, and the strongest peak of quartz can be detected only in some of the samples. The same is true for the feldspars.

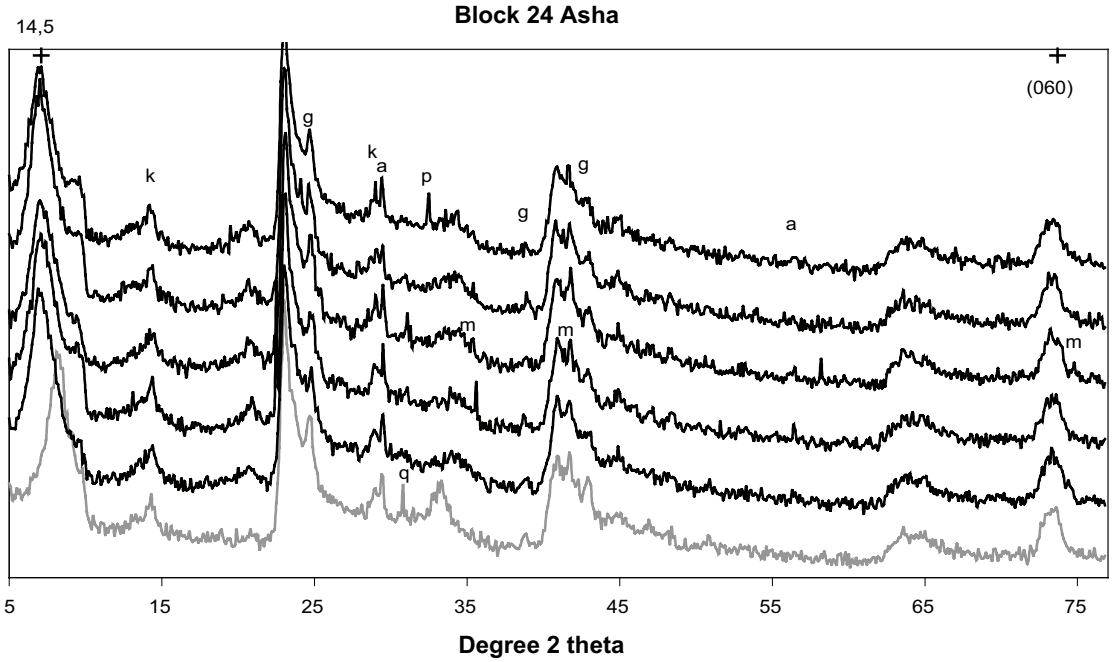

Figure 8-14. *Black curves: XRD-profiles of sample 1 (bottom) to sample 9 (top) from block 24, Asha 505. Grey curve: reference sample. The strongest peaks of the major accessory minerals are indicated: a=anatase (TiO_2); g=goethite (FeOOH); k=kaolin mineral; m=magnetite/maghemite; p=plagioclase; q=quartz. Random powder of bulk samples. CoKα radiation.*

The basal spacing of the first order smectite peak of the reference sample is approximately 12.5 Å, which is typical of the monolayer hydrate of Na-smectites (Brindley and Brown 1980). Consistent with the data on the exchangeable cation pool, showing that the proportion between di- and monovalent cations has changed significantly, the exposed samples have their (001) basal reflection centered around ca. 14.5 Å (Figure 8-14) but the peaks are clearly asymmetrical towards the high-angle side. Peak asymmetri or resolved first order peaks can generally be seen in mixed Na-Ca (Mg) smectite if conditions are such that the interlayers with divalent cations have two layers of water molecules and the Na-layers only one layer of water molecules.

The d-value of the (060) peak ranges from 1.49 to 1.50 Å, which is typical of the dioctahedral subgroup of smectites, to which montmorillonite, beidellite and nontronite belong. Thus, the available XRD-data provide no evidence of any significant change of the cations or site occupancy in the octahedral sheet of the smectite.

Block 27 Deponit CAN

The XRD-profiles of random powders of the bulk samples of block 27 Deponit CAN are shown in Figure 8-15 together with the reference sample. The strongest peaks of the major non-phyllosilicates cristobalite, feldspars, calcite and dolomite are indicated in Figure 8-15. Also the position of the strongest quartz peaks has been indicated in Figure 8-15, although the reference sample examined (cf. also Section 7) appears to be almost free of quartz at the detection limit of the XRD method, considering that the strongest peak can normally be detected already at quartz concentrations below 1%. Fine-grained quartz may, however, show anomalous intensities due to disordering which will decrease the crystalline diffraction (Brindley and Brown 1980).

A weak peak appears in sample 1 (and in sample 3) at the position of the strongest reflection of anhydrite. Based on one single reflection, the identification of anhydrite must be considered tentative, but support is given by the data on water-soluble sulfate, which suggest that sample 1 contains 1.1% $CaSO_4$.

The basal spacing of the first order smectite peak of both the reference and the exposed samples is in the range 14.5–15 Å, which is typical of smectites with predominantly divalent interlayer cations (Mg and Ca) over a wide range of relative humidities (Brindley and Brown 1980).

The major change in the exchangeable cation pool of the exposed samples is replacement of Mg by Ca (cf. Section 8.3) and, accordingly, this exchange of the interlayer cations will have little effect on the basal spacings.

The available XRD-data provide no evidence of any significant change of the cations or site occupancy in the octahedral sheet of the smectite, judged by the position of the (060) peak.

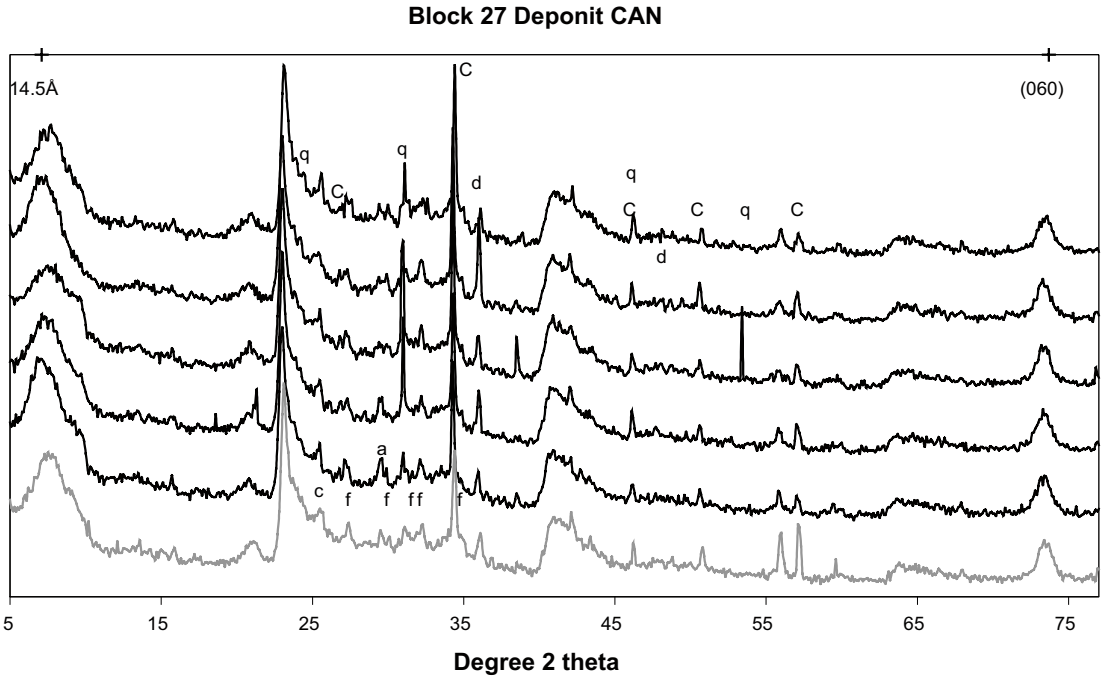

Figure 8-15. *Black curves: XRD-profiles of sample 1 (bottom) to sample 9 (top) from block 27, Deponit CAN. Grey curve: reference sample. The strongest peaks of the major accessory minerals are indicated: a=anhydrite; c=cristobalite; C=calcite; d=dolomite f=feldspars; q=quartz. Random powder of bulk samples. CoKα radiation.*

9 Summary of results and comments

9.1 Hydro-mechanical tests

9.1.1 Standard investigations of the reference materials

The results of the standard tests (water content as delivered, free swelling, liquid limit and grain density) show the large diversity of the materials included in the ABM project. The free swelling varies from a few ml/g (Callovo Oxfordian, Rokle, Febex and Friedland) up to 17 ml/g for MX-80. The same distribution is in the results from the liquid limit which varies between 68% (Friedland) and up to 545% (MX-80). There is also a clear difference between the different materials regarding the grain density. Eight of the tested materials have a grain density between 2,678 and 2,753 kg/m^3 while three of the materials (Asha, Rokle and Friedland) have a grain density between 2,828 and 2,940 kg/m^3.

9.1.2 Water content and density determinations

From the measurements of water content and density of samples taken from the blocks the following conclusions can be drawn:

- The degrees of saturation are very close to 100% in all radial positions and for all materials, see Figure 6-10.
- There is as expected a trend with decreasing densities (and increasing water content) from steel tube to rock, see Figure 6-7, 6-8 and 6-9. The trend is, however rather weak, and the homogenization has for all materials gone far.
- The achieved dry density after compaction to blocks was different for the tested materials. Especially for Friedland, Kunigel and Callovo Oxfordian the density was much higher than for the other materials. This variation in density during emplacement remains also after finishing of the experiment.
- The sampling of the outermost parts, close to the rock, was difficult because of the sand filter. In these parts, the clay and the sand were more or less integrated with each other and this is an explanation for the fact that the measured water content and density at these positions can differ somewhat from the expected.

9.1.3 Swelling pressure and hydraulic conductivity

Swelling pressure and hydraulic conductivity measurements have been made on three materials: MX-80, Asha and Deponit CAN. Totally twenty-three tests have been made (ten on the reference materials and thirteen on specimens taken from the blocks in test package 1).

The results from the tests show that there are no differences between samples from the test parcel and the reference samples regarding the hydraulic conductivity. There is, however, a significant difference in swelling pressure between test parcel material and reference material for two of the investigated materials, Asha 505 and Deponit CAN. The measured swelling pressure for these two materials is lower for material taken from the test parcel. There is also a tendency that the decrease is greater for samples taken from the hottest part i.e. close to the heater.

One explanation for the registered decrease in swelling pressure is, as shown in Chapter 8, that there has been a large redistribution of cations in the test package and this has influenced the physical properties of the materials.

9.1.4 Unconfined compression tests

The results from unconfined compression tests on MX-80, Asha and Deponit CAN specimens from the test package ABM1 blocks #2, #14, #15, #27 and #29 indicate that:

- Reduced strain, i.e. less strain compared to the reference specimens, was observed on re-saturated specimens of all three materials.
- No large deviation in maximum deviator stress compared to the reference specimens was seen on re-saturated specimens of MX-80 and Deponit CAN.
- Decreased maximum deviator stress compared to reference specimens was observed on re-saturated Asha specimens, especially from the innermost position.
- The air-dried, ground, re-compacted and re-saturated material from the field experiment showed strain of the same size or larger than the reference specimens while the maximum deviator stress was of the same size as the references.

9.2 Chemical and mineralogical analyses-reference materials

The repeatability of the CEC measurement was reasonable over time and between lab workers. The scattering in the values was a function of the method, the chemicals used, the lab worker and the inhomogeneity of the clays. Most clays had a rather high CEC values which is typical for bentonites. Friedland and Callovo-Oxfordian was much lower in CEC which is compatible with their different type of clay (not bentonites). In order to properly compare two samples the determination should probably be done by a single person at the same moment, or possibly the procedure have to be more fully documented.

The extractable amount of sulphate and chloride was not negliglible. Ikosorb, Friedland and Asha 505 had 0.2–0.3 wt% chloride. MX-80, IbecoSeal, Deponit CA-N and Friedland had 0.3–0.5 wt% sulphate, the most likely source is gypsum which is a water soluble hydrated calcium sulphate. Fluoride and bromide are very low in all cases.

In almost all cases the extractable iron content was lower in mass % in previously reported results from the clay fractions (Karnland et al. 2006) compared to the bulk clay, which is very reasonable as some iron is also present in the non-clay fraction. Elevated amounts of Mn in Rokle indicates possible presence of undetected Mn-phase. Rather high Si in Calcigel and Rokle (compared to kunigel that is low but high in quartz) possibly indicates the presence of amorphous silica.

The chemical data and evolved gas analysis confirmed the variety in the clays regarding eg. iron content. Kunigel with only 1.9 wt% Fe_2O_3 can be compared to Asha 505 and Rokle with 12.2 and 13.7 wt% respectively. Organic carbon was low in most cases, but higher in Callovo-oxfordian (0.7) and Friedland (0.5) wt%. The total sulfur content was very low (< 0.2 wt%) in Rokle, Ikosorb, Febex, Calcigel, Asha 505, low (< 0.5 wt%) in MX80, Ibecoseal and kunigel, and higher in Friedland (0.53) and Callovo-oxfordian (0.68).

X-ray diffraction was used to show the variability in the crystalline phases of the clay. Most clays were found to be dominated by dioctahedral smectites. Two dimensional diffraction data was also presented to illustrate difficulties in milling the mineral grains appropriately and the consequence of the method that only a very small amount of clay is sampled in this way, hence the scattering increases.

9.3 Chemical and mineralogical analyses-material from test package 1

The distribution of chloride indicates that the wetting with and equilibration against the groundwater resulted in laterally and vertically smoothed and more or less constant concentrations. The post-test sulfate distribution displays no consistent or regular pattern.

As can be expected, the saturation with a Na-Ca type groundwater has resulted in replacement of some sodium by calcium in all those bentonites that were initially Na-dominated. However, the plots of the cation distribution indicate a significant compositional difference in the exchangeable cation pool between the upper and lower parts of the package. Whereas lateral gradients within the blocks are insignificant a vertical gradient in the relative cation distribution has developed during/after the field experiment.

Although changes in relation to the references are close to the resolution of the method, a tendency of increasing CEC towards the heater can be seen in particular in block 5 and block 27. The starting material of these blocks contained carbonates, which partly have dissolved in the samples proximal to the heater. Therefore, a small increase in CEC can be expected as an effect of a diminished dilution by carbonates. On the other hand, the incorporation of corrosion products of iron in the bentonite would be expected to lower the CEC of samples closest to theFe-tube due to the dilution effect. However, charged hydroxylated surfaces of iron oxides/hydroxides that may have formed in the clay, can contribute to the CEC depending on the pH, i.e. under conditions more alkaline than the pH of the zero point of charge, cations can be attracted to the charged surfaces of iron oxyhydroxides.

The post-test distribution of acid soluble carbon in the blocks examined indicates carbonate dissolution closest to the heater in the carbonate-bearing bentonites MX-80, Calcigel and Deponit CAN, as was observed also in the 5-year long field test LOT A2 (Karnland et al. 2009).

No clear trend can be seen in the iron distribution in the Asha 505 bentonite in block 24 after the field test, whereas the blocks of the less iron-rich bentonites MX-80, Calcigel and Deponit CAN display an increase in iron at the Fe-tube, suggesting that iron released by corrosion of the tube has been transported into the bentonite. A thin rim of corrosion products was macroscopically visible at the interface between the bentonite and the iron heater. With few exceptions, all samples from all four blocks are depleted in magnesium relative to their reference sample. The deficit in magnesium tends to be at a maximum in the peripheral parts, which creates a gradient in magnesium towards the heater. Calcigel and Deponit CAN contain dolomite, which is a possible source of Mg, but since the dissolution of carbonates has been most intense at positions proximal to the heater, carbonate dissolution is an unlikely cause of the peripheral depletion in Mg. Moreover, the Asha 505 bentonite is more or less carbonate-free, and yet the trend in Mg is similar in block 24.

With XRD several indications of the presence of anhydrite was found. In MX80 2 a peak of low intensity at the position of the strongest peak of anhydrite ($CaSO_4$) can be seen in the XRD-profile of sample 3, but cannot unambiguously be attributed to anhydrite. In DepCAN 27 a weak peak appears in sample 1 (and in sample 3) at the position of the strongest reflection of anhydrite. Based on one single reflection, the identification of anhydrite must be considered tentative, but support is given by the data on water-soluble sulfate, which suggest that sample 1 contains 1.1% $CaSO_4$.

References

SKB's (Svensk Kärnbränslehantering AB) publications can be found at www.skb.se/publications.

Ammann L, Bergaya F, Lagaly G, 2005. Determination of the cation exchange capacity of clays with copper complexes revisited. Clay Minerals 40, 441–453.

Belyayeva N I, 1967. Rapid method for the simultaneous determination of the exchange capacity and content of exchangeable cations in solonetzic soils. Soviet Soil Science, 1409–1413.

Brindley G W, Brown G, 1980. Crystal structures of clay minerals and their X-ray identification. London: Mineralogical Society. (Mineralogical Society Monograph 5)

Caballero E, Jiménes de Cisneros C, Huertas F J, Huertas F, Pozzuoli A, Linares J, 2005. Bentonites from Cabo de Gata, Almería, Spain: a mineralogical and geochemical overview. Clay Minerals 40, 463–480.

Carlson L, Karnland O, Oversby V M, Rance A, Smart N, Snellman M, Vähänen M, Werme L O, 2007. Physics and Chemistry of the Earth 32, 334–345.

Christidis G E, Scott P W, Marcopoulos T, 1995. Origin of the bentonite deposits of Eastern Milos, Aegean, Greece: geological, mineralogical and geochemical evidence. Clays and Clay Minerals 43, 63–77.

Claret F, Sakharov B A, Drits V A, Velde B, Meunier A, Griffault L, Lanson B, 2004. Clay minerals in the Meuse-Haute Marne underground laboratory (France): possible influence of organic matter on clay mineral evolution. Clays and Clay Minerals 52, 515–532.

Decher A, Bechtel A, Echle W, Friedrich G, Hoernes S, 1996. Stable isotope geochemistry of the bentonites from the island of Milos (Greece). Chemical Geology 129, 101–113.

Dueck A, 2010. Thermo-mechanical cementation effects in bentonite investigated by unconfined compression tests. SKB TR-10-41, Svensk Kärnbränslehantering AB.

Dueck A, Johannesson L-E, Kristensson O, Olsson S, 2010. Report on hydro-mechanical and chemical-mineralogical analyses of the bentonite buffer in Canister Retrieval Test. SKB Technical Report TR-11-07, Svensk Kärnbränslehantering AB.

Elzea J M, Murray H H, 1989. Trace element composition of the Cretaceous Clay Spur bentonite and implications for its alteration history. Abstract of the 9th International Clay Conference, Strasbourg, 28 August – 2 September 1989, 132.

Elzea J M, Murray H H, 1990. Variation in the mineralogical, chemical and physical properties of the Cretaceous Clay Spur bentonite in Wyoming and Montana (U.S.A). Applied Clay Science 5, 229–248.

Eng A, Nilsson U, Svensson D, 2007. Äspö Hard Rock Laboratory. Alternative Buffer Material. Installation report. SKB IPR-07-15, Svensk Kärnbränslehantering AB.

ENRESA, 1998. Bentonite: origin and properties. In FEBEX – Full-scale Engineered Barriers Experiment in crystalline host rock. Publication Technica 01/98, ENRESA, 13–30.

Grim R E, Güven N, 1978. Bentonites – geology, mineralogy and uses. Developments. – in: Developments in Sedimentology, 24., ISBN: 0444416137 Amsterdam, Elsevier.

Henning K-H, Kasbohm J, 1998. Mineralbestand und Genese feinkörniger quartärer und präquartärer Sedimente in Nordostdeutschland unter besonderer Berücksichtigung des „Friedländer Tones". Berichte der DTTG, Bd 6:S, 147–167.

Jackson M L, 1975. Soil chemical analysis: advanced course. 2nd ed. Madison,WI: Parallel Press.

Johannesson L-E, Börgesson L, Sandén T, 1995. Compaction of bentonite blocks. Development of technique for industrial production of blocks which are manageable by man. SKB TR 95-19, Svensk Kärnbränslehantering AB

Karnland O, Olsson S, Nilsson U, 2006. Mineralogy and sealing properties of various bentonites and smectite-rich clay materials. SKB TR-06-30, Svensk Kärnbränslehantering AB.

Karnland O, Olsson S, Dueck A, Birgersson M, Nilsson U, Hernan-Håkansson T, Pedersen K, Nilsson S, Eriksen T E, Rosborg B, 2009. Long term test of buffer material at the Äspö Hard Rock Laboratory, LOT project. Final report on the A2 test parcel. SKB TR-09-29, Svensk Kärnbränslehantering AB.

Kelepertsis A E, 1989. Formation of sulfates at the Thiaphes area of Milos Island: possible precursors of kaolinite mineralization. Canadian Mineralogist 27, 241–245.

Khaled E M, Stucki J W, 1991. Effects of iron oxtidation state on cation fixation in smectites. Soil Science Society of America Journal, 50, 550–554.

Konta J, 1986. Textural variation and composition of bentonite derived from basaltic ash. Clays and Clay Minerals 34, 257–265.

Lantenois S, Lanson B, Muller F, Bauer A, Jullien M, Plancon A, 2005. Experimental study of smectite interaction with metal Fe at low temperature: 1. Smectite destabilization. Clays and Clay Minerals, 53, 597–612.

Martin Vivaldi J L, 1962. The Bentonites of Cabo de Gata (Southeast Spain) and of Guelaya Volcanic Province (North Morocco) Clays and Clay Minerals 1962 11 : 327–357.

Meier L P, Kahr G, 1999. Determination of the cation exchange capacity (CEC) of clay minerals using the complexes of copper(II) ion with triethylenetetramine and tetraethylenepentamine. Clays and Clay Minerals 47, 386–388.

Moore D, Reynolds R C Jr, 1997. X-Ray Diffraction and the Identification and Analysis of Clay Minerals, 2nd ed.: Oxford University Press, New York

Shah N R, 1997. Indian bentonite: focus on the Kutch region. Industrial Minerals 359, 43–47.

Slaughter M, Earley J W, 1965. Mineralogy and geological significance of the Mowry bentonites, Wyoming. New York: Geological Society of America. (Geological Society of America Special Paper 83)

Süd-Chemie Agrimont, 2011. Zusammensetzung und Vorkommen von Bentoniten. Available at: http://agrimont.de/ueber-bentonit/.

Takagi T, 2005. Bentonite in Japan – Geology and industries. *Open file report 425, Geological Survey of Japan.*

Taylor R M, 1987. Non-silicate oxides and hydroxides. In Newman A C D (ed): Chemistry of clays and clay minerals. Harlow: Longman. (Mineralogical Society Monograph 6), 128–201.

Appendix 1

Information report on preparation of bentonite granulate samples 1

According to NAGRA order, no. 905.070.962.09, we produced two bentonite granulate samples of ca. 50 kg each as specified below. We sent the samples on 02.06.06 to the following address :

Anders Eng
Project manager
Swedish Nuclear Fuel and Waste Management Co
Äspö Hard Rock Laboratory
PL 300
SE-572 95 Figeholm
Sweden

Product I

Material : 100% MX80

Particle grain size : binary system 70% 7–15 mm
30% 0.5 1.0 mm

Production conditions:

1. Compaction with roll press, specific compression force 56 kN/cm, compact size ca. 80·20·10 mm.
2. Screening of press product, > 10 mm to be crushed, < 10 mm to be recycled.
3. Crushing of press product with jaw crusher.
4. Screening of comminution product into fractions 7–15 mm, 0.5–1.0 mm.
5. Spheronizing of coarse fraction in IfB-test drum (20 rev.).

Product quality:

- Apparent density of coarse grains (7–15 mm) 2.16 g/cm^3.
- Installation density of binary granulate system 1.243 g/cm^3, (measured under pouring conditions).

Product II

Material : 70% MX80 + 30% quarz (0.1–0.5 mm)

Particle grain size : binary system 70% 7–15 mm
30% 0.5 1.0 mm

Production conditions :

1. Compaction with roll press, specific compression force 64 kN/cm, compact size ca. 80·20·10 mm.
2. Screening of press product, > 10 mm to be crushed, < 10 mm to be recycled.
3. Crushing of press product with jaw crusher.
4. Screening of comminution product into fractions 7–15 mm, 0.5–1.0 mm.
5. Spheronizing of coarse fraction in IfB-test drum (10 rev.).

Product quality:

- Apparent density of coarse grains (7–15 mm) 2.27 g/cm^3.
- Installation density of binary granulate system 1.282 g/cm^3, (measured under pouring conditions).

Appendix 2

PG: Alternative buffer materials

Microbiology

Sara Lydmark and Sara Jägewall

Microbial Analytics Sweden AB

A2.1 Abstract

The Alternative buffer material project (ABM) is presently ongoing at the Äspö Hard Rock Laboratory. The project involves studies of 11 alternative buffer materials which now are being evaluated regarding several parameters, including microbial ones. The microbial abundance was examined in the following different commercial bentonite clays: Asha 505, Calcigel, Callovo Oxfordian, Deponit CA-N, Febex, Friedland, Ibeco Seal M-90, Ikosorb, Kunigel V1, MX-80 and Rokle. Special emphasis was put on the abundance and identity of aerobic heterotrophs and anaerobic sulphate and iron reducers and autotrophic acetogens, because of their abilities to affect the KBS-3 type of storages for nuclear waste in different ways. Microbes in the clay were detected by aerobic plate counts and the most probable number method for anaerobes and examined with PCR, cloning and sequencing. A drastic difference in microbial abundance between the examined materials was observed; Kunigel V1 was close to sterile while Friedland and Ibeco Seal M-90 contained high numbers of all microbes examined. It was found that 200–84,000 g^{-1} aerobic microbes were present in ten of the eleven dry materials, while Kunigel V1 lacked detectable aerobic microorganisms. Iron reducers were detected in all examined materials, ranging from 10 (in Kunigel V1) to 8,000 g^{-1} (in Ibeco Seal M-90). Autotrophic acetogens was detected in the range of 20–60 g^{-1} in the Febex, Friedland and Ibeco Seal materials, and below 10 g^{-1} in the other materials examined. Sulphate reducers were detected in the range of 10–90 g^{-1} in Asha 505, Calcigel, Deponit CA-N, Febex, Friedland and Ibeco Seal M-90, and was below 10 g^{-1} in the other materials. In addition, the temperature tolerance of sulphide- and acetate-producing microorganisms in the dry clays was studied. The dominant part of sulphate reducers and acetogens in the materials thrived in the thermophilic temperature range and grew faster at 50°C than at 20°C. A correlation between produced acetate and sulphide was observed, suggesting that acetogenesis boosted the sulphate-reducing populations in the clay mineral systems. The studies showed that dry clay is a very potent media for long term survival of both aerobic, anaerobic and thermophilic microbes and as it seems from phylogenetic studies, not spore-formers only.

A2.2 Introduction

The project ”Alternative Buffer Materials (ABM)” aims to evaluate and confirm present knowledge of possible buffer materials to be used in the KBS-3 concept for long-term storage of high level radioactive waste (HLRW). The following materials are evaluated: Asha 505, Calcigel, Callovo Oxfordian, Deponit CA-N, Febex, Friedland, Ibeco Seal M-90, Ikosorb, Kunigel V1, MX-80 and Rokle.

This part of the project deals with the microbial presence in these different buffer materials. It is well-known that microbes can survive for a long period of time in bentonite as well as other clays. Often, the microbes can survive as endospores, a non-active resting stage where only the most crucial metabolic processes are on-going in the cell, but there can also be microbes present in dry bentonite without the ability to form endospores (Masurat et al. 2008).

Presence of different kinds of microbes in the buffer material needs to be evaluated for several reasons:

- Microbes can respire oxygen and thus decrease the oxygen content in the buffer much faster than can abiotic processes, which is a good thing for the repository since oxygen is corrosive to the copper canister to be used in the KBS-3 concept. Microbes able to do this are called aerobic microbes and can be detected by cultivation on media containing organic carbon (with a so called CHAB analysis). On the other hand, the presence of aerobic microbes are not solely beneficial for the storage. Many microbes that are able to respire oxygen also have the ability to excrete compounds not favourable for the copper canister. Examples of such compounds are organic acids and bioligands which e.g. can dissolve several radionuclides (Johnsson 2006).
- Other types of microbes previously found in bentonite (Masurat et al. 2008) are the sulphate-reducing microbes (SRB). The SRB can produce sulphide, a compound also highly corrosive to the copper canister: and will thus have to be evaluated in the buffer used in the KBS-3 storage.
- The lack of organic carbon in the buffer materials is often pointed out as a restriction factor for microbial survival in the buffer. However, there are microbes called autotrophic acetogens (AA) able to convert hydrogen gas and carbon dioxide to the organic compound acetate. Acetate can be metabolised by many microbes in the subsurface, not least the SRB. Carbon dioxide can originate from microbial activity and hydrogen gas from iron corrosion. In addition, both gases can be produced geothermically.

- Illitisation of smectite is an unwanted process which decreases the swelling capacity of the buffer. There are studies performed showing that iron-reducing microbes (IRB) can perform what seems to be illitisation in two weeks at atmospheric pressure and room temperature by using the smectite as an iron source (Kim et al. 2004). Obviously, it is important to evaluate the presence and numbers of IRB in the buffer materials.
- All microbes do not thrive in the same temperature. At the start of the storage process of HLRW the temperature in the buffer will be elevated, approaching 90°C. It is thus important to evaluate if microbes present in the buffer material can be active at higher temperatures than the normal ambient rock temperature.

In this project, the microbial abundance was examined in the eleven different commercial bentonite clays. Special emphasis was put on the abundance and identity of aerobic CHAB and anaerobic SRB, AA and IRB, because of their abilities to affect the KBS-3 type of storages for nuclear waste in different ways. Microbes in the clay were enumerated by aerobic plate counts and the most probable number method for anaerobes. The ability of indigenous SRB and AA to grow at elevated temperatures (50°C) was examined for the different materials and the microbes were identified with PCR, cloning and sequencing.

A2.3 Material and methods

A2.3.1 Materials examined

Eleven alternative buffer materials were analysed regarding indigenous microbes. These were Asha 505, Calcigel, Callovo Oxfordian, Deponit CA-N, Febex, Friedland, Ibeco Seal M-90, Ikosorb, Kunigel V1, MX-80 and Rokle.

A2.3.2 Enrichment cultures

From each of the eleven dry materials, a total of 13 enrichment cultures were prepared under anaerobic conditions (Table A2-1). Bacteria from the materials were enriched in anaerobic growth media. Three types of enrichment media were produced (Table A2-1);

1. Sulphate-reducing medium with an organic energy source (lactate).
2. Sulphate-reducing medium with an inorganic energy source (H_2).
3. Medium with neither sulphate nor energy source.

All three media contained a basal salt solution (L^{-1} Analytical Grade Water, AGW): 7 g NaCl, 1g $CaCl_2 \times H_2O$, 0.67 g KCl, 1 g NH_4Cl, 0.15 g KH_2PO_4, 0.5 g $MgCl_2 \times 6H_2O$. In addition, in the sulphate amended media (medium 1 and 2) 3 g $MgSO_4 \times 6H_2O$ L^{-1} AGW was added. The salt solution was autoclaved and cooled under a N_2/CO_2 (80/20%) atmosphere for 1 h. After that the following solutions were added: 10 mL trace element solution, 60 mL 1M $NaHCO_3$ solution, 10 mL yeast extract solution, 10 mL vitamin solution, 1 mL thiamine solution, 1 mL vitamin B_{12} solution, 5 mL iron stock solution, 2 mL resazurin solution, 10 mL cystein-HCl solution, and 10 mL Na_2S solution (Widdel and Bak 1992). In addition, ten mL of 50% lactate solution (L^{-1} AGW) was added to the anaerobic enrichment media with organic energy source (medium 1). The pH was set to 6.5–7.5 and the medium was added in 50 ml aliquots to N_2-filled 120-ml serum flasks sealed with butyl rubber stoppers (Bellco Glass, Vineland, NJ, USA, no. 2048-117800).

Table A2-1. The different enrichment media inoculated with each of the 11 alternative buffer materials.

Medium	Sulphate amended	Energy source	Incubation temperature	n	Used as inocula for quantification of
1	Yes	Organic*	20°C	3	CHAB, SRB
	Yes	Organic*	50°C	3	
2	Yes	Inorganic**	20°C	3	CHAB, AA
	Yes	Inorganic**	50°C	3	
3	No	None	20°C	1	CHAB, IRB

*Lactate, **H_2.

Of these medium flasks six with sulphate- and lactate amended medium (medium 1), six with sulphate amended medium (medium 2) and one without sulphate and energy source (medium 3) was put in an anaerobic box (COY Laboratory Products, Grass Lake, MI, USA) together with each of the buffer materials and an additional set of sterile rubber stoppers (Table A2-1). The serum flasks were opened inside the box and 1 g of buffer material was put under sterile conditions in the anaerobic media in each of the serum flasks. The serum flasks were resealed with new stoppers and removed from the anaerobic box. The serum flasks were sealed with aluminium crimp seals (Bellco Glass, no. 2048-11020) To the sulphate amended media with inorganic energy source (medium 2), H_2 at 2 bars above atmospheric pressure was added.

One enrichment culture for each medium were put in 4°C over-night for the buffer material to disperse in the medium and were after that used as inocula for CHAB, and MPN of SRB, AA and IRB (Table A2-1). After the inoculation these serum flasks were incubated according to Table A2-1 until analysis after three weeks (Table A2-2). All other enrichment cultures were directly incubated according to Table A2-1.

A2.3.3 Quantification of indigenous microbes

As seen above and in Table A2-1, of the in total 13 flasks inoculated from each alternative buffer material, one of each medium was used as inoccula for quantitative microbial analyses:

Culturable heterotrophic aerobic bacteria

From each of the three media, the numbers of cultivable heterotrophic aerobic bacteria (CHAB) was examined.

Petri dishes containing agar with nutrients were prepared for determining the numbers of cultivable heterotrophic aerobic bacteria (CHAB) in the alternative buffer materials. This agar contained 0.5 g L^{-1} of peptone (Merck), 0.5 g L^{-1} of yeast extract (Merck), 0.25 g L^{-1} of sodium acetate (Merck), 0.25 g L^{-1} of soluble starch (Merck), 0.1 g L^{-1} of K_2HPO_4, 0.2 g L^{-1} of $CaCl_2$ (Merck), 10 g L^{-1} of NaCl (Merck), 1 mL L^{-1} of trace element solution (see Table A2-3 D), and 15 g L^{-1} of agar (Merck) (Pedersen and Ekendahl 1990). The medium was sterilized in 1-L batches by autoclaving at 121°C for 20 min, cooled to approximately 50°C in a water bath, and finally distributed in 15-mL portions in 9-cm-diameter plastic Petri dishes (GTF, Göteborg, Sweden).

Ten-times dilution series of enrichment culture samples were made in sterile analytical grade water (AGW) with 0.9 g L^{-1} of NaCl; 0.1-mL portions of each dilution were spread with a sterile rod on the plates in triplicate. The plates were incubated one week at 20°C, after which the number of colony forming units (CFU) was counted; plates with between 10 and 300 colonies were counted, if available. The mean and the standard deviation for the plates from all three kinds of enrichment culture media from each material were calculated.

Most probable number (MPN)

Media for determining the most probable number (MPN) of sulphate-reducing bacteria (SRB), autotrophic acetogens (AA) and iron-reducing bacteria (IRB) in the buffer materials were prepared as follows:

The SRB and AA media contained one type of basal salt solution (L^{-1} AGW): 7 g NaCl, 1g $CaCl_2 \times H_2O$, 0.67 g KCl, 1 g NH_4Cl, 0.15 g KH_2PO_4, 0.5 g $MgCl_2 \times 6H_2O$. For SRB 3 g $MgSO_4 \times 6H_2O$ L^{-1} AGW was additionally added. The IRB medium contained another type of basal solution (L^{-1} AGW): 7 g NaCl, 1g $CaCl_2 \times H_2O$, 0.1 g KCl, 1.5 g NH_4Cl, 0.2 g KH_2PO_4, 0.1 g $MgCl_2 \times 6H_2O$, 0.1 g $MgSO_4 \times 7H_2O$, 0.001 g $Na_2MoO_4 \times 2H_2O$, 0.005 g $MnCl_2 \times 4H_2O$. The basal salt solutions were autoclaved and cooled under a N_2/CO_2 (80/20%) atmosphere for 1 h. After that the following solutions were added for SRB and AA media (Widdel and Bak 1992): 10 mL trace element solution, 60 mL 1M $NaHCO_3$ solution, 10 mL yeast extract solution, 10 mL vitamin solution, 1 mL thiamine solution, 1 mL vitamin B_{12} solution, 5 mL iron stock solution, 2 mL resazurin solution, 10 mL cystein-HCl solution, and 10 mL Na_2S solution. In addition, ten mL of 50% lactate solution (L^{-1} AGW) was added to the SRB medium. For IRB medium the following solutions were added (Widdel and Bak 1992): 1 mL non-chelated

trace element solution, 30 mL 1M $NaHCO_3$ solution, 1 mL yeast extract solution, 1 mL vitamin solution, 1 mL thiamine solution, 1 mL vitamin B_{12} solution and 10 mL of 10% acetate solution. The media were dispensed anaerobically in 9-mL aliquots into 27-mL, sealable anaerobic glass tubes (no. 2048-00150; Bellco Glass), sealed with butyl rubber stoppers and aluminium crimp seals. For IRB, 1 mL of hydrous ferric oxide (HFO), prepared from $FeCl_3$, was added to each culture tube before the basal salt solution.

Inoculations for SRB, AA and IRB were performed using the enrichment cultures as inoccula. After inoculating, the headspaces the AA MPN tubes were filled with H_2 to an overpressure of 2 bars. All MPN tubes were incubated in the dark at 20°C for 8–10 weeks. After incubation, the MPN tubes were analysed by testing for metabolic products (Table A2-2 and in section A2.3.5). The MPN tubes were considered positive if the levels of metabolic products were three times higher than the background in the medium.

The MPN procedures resulted in protocols with tubes that scored positive or negative for growth. The results of the analyses were rated positive or negative compared with control levels. Three dilutions with five parallel tubes were used to calculate the MPN and lower and upper 95% confidence interval of each group, according to the calculations found in Greenberg et al. (1992).

Table A2-2. Analyses performed for the different enrichment media for each of the 11 alternative buffer materials.

Medium	Sulphate amended	Energy source	Incubation temperature	n	Microbial analyses performed
1	Yes	Organic*	20°C	3	CHAB counting, microscopy, sulphide production, SRB MPN
	Yes	Organic*	50°C	3	Microscopy, sulphide production
2	Yes	Inorganic**	20°C	3	CHAB counting, microscopy, sulphide production, acetate production, AA MPN
	Yes	Inorganic**	50°C	3	Microscopy, sulphide production, acetate production
3	No	No	20°C	1	CHAB counting, microscopy, sulphide production, acetate production, ferrous iron production, IRB MPN

*Lactate, **H_2.

A2.3.4 Microscopy

To detect growth in the enrichment cultures, the supernatants from all cultures were , after three weeks of incubation, diluted 50 times in sterile water and 1 ml were filtered onto 0.2 um pore size filters stained black (Osmonics, Minnetonka, MN, US) and stained with acridine orange (10 mg l^{-1}) for 7 min. Bacteria on the filters were observed in an inverted microscope (Nikon Diaphot 300, Teknooptik AB, Göteborg, Sweden) at 1,000 times magnification using blue light (390–490 nm) and photographed.

A2.3.5 Chemical analyses

Sulphide analysis

Sulphide production in the cultures and the SRB MPN tubes were examined using the spectrofotometric copper sulphate method described before (Widdel and Bak 1992). Approximately 1 ml of the supernatant from each enrichment culture was carefully withdrawn with an anaerobic syringe and needle and 0.1 ml was added to 2 ml of 5 mM copper sulphate. If sulphide was present in the sample, a brown precipitate (copper sulphide) was formed. The absorbance of the solution was measured spectrophotometrically (Genesys 10 UV, Thermo electron corporation, Waltham, MA, USA) at λ 480 nm and the concentration was determined with an external standard curve. The sulphide levels in the enrichment cultures were reported as how many times enriched compared to sulphide levels in the non-inoculated growth media.

Acetate analysis

Acetate production in the cultures and the AA MPN tubes were examined using an enzymatic-UV method (Boehringer Mannheim, Mannheim, Germany). A sample from the supernatant from each enrichment culture was carefully withdrawn with an anaerobic syringe and needle. The acetate levels in the enrichment cultures were reported as how many times enriched compared to acetate levels in the non-inoculated growth media.

Ferrous iron analysis

Ferrous iron in the enrichment cultures and the IRB MPN tubes was determined using a DR/2500 spectrophotometer (HACH, Loveland, CO, USA) and the 1,10 phenanthroline method (HACH, method no. 8146).

A2.3.6 Identification of indigenous microbes

Eleven enrichment cultures with extensive sulphide and acetate production were selected for identification using the following molecular techniques: DNA extraction, Polymerase chain reaction, Cloning and Sequencing. Those are shown in Table A2-3 below.

Table A2-3. Enrichment cultures that were cloned and sequenced.

ABM	Cultivation T °C	Source of energy	Cloning vector	Cloning primers	Sequencing primer
Friedland	20	H_2	TOPO pCR2.1	27f/1492r	907r
Friedland	50	H_2	TOPO pCR2.1	27f/1492r	907r
Calcigel	50	Lactate	TOPO pCR2.1	27f/1492r	907r
Calcigel	50	H_2	TOPO pCR2.1	27f/1492r	907r
Ikosorb	50	Lactate	TOPO pCR2.1	27f/1492r	907r
Ikosorb	50	H_2	TOPO pCR2.1	27f/1492r	907r
Febex	20	H_2	TOPO pCR2.1	27f/1492r	907r
Febex	50	H_2	TOPO pCR2.1	27f/1492r	907r
Ibeco Seal M-90	20	H_2	TOPO pCR2.1	27f/1492r	907r
Ibeco Seal M-90	50	H_2	TOPO pCR2.1	27f/1492r	907r
MX-80	50	H_2	TOPO pCR2.1	27f/1492r	907r

DNA extraction

Total genomic DNA was extracted from 1.5 mL of the respective enrichment cultures using the DNeasy Blood&Tissue kit according to the manufacturer's protocol for Gram positive bacteria (Cat. no 69504, QIAGEN, Solna, Sweden). The DNA extractions were then stored in –20°C until it was used in the Polymerase chain reaction (3.6.2).

Polymerase chain reaction (PCR), Cloning and sequencing

The eubacterial primers 27 f and 1492 r were used for the 16S rDNA PCR's (Lane 1991) Each PCR mixture for the bacterial 16S rRNA contained 0.5 µL of each primer solution (10 pmol μL^{-1}), 20 ng of DNA, 12.5 µL 2×iProof Mastermix (Cat. no 172-5310, Bio-Rad Laboratories, Sundbyberg, Sweden) in a final reaction volume of 25 µL. Amplification was carried out on a thermal PCR cycler (MyCycler, Bio-Rad Laboratories). After initial denaturation for 3 minutes at 98°C, 30 cycles were performed with each cycle consisting of 30 s at 98°C, 90 s at 59°C and 90s at 72°C. A final extension step was carried out for 7 min at 72°C. PCR products were visualised on a 1% agarose gel containing Ethidium Bromide (EtBr) (Cat. no 161-0433, Bio-Rad Laboratories, Sunbyberg, Sweden) and the bands were cut out and purified with the Gel Extraction kit according to the manufacturer's protocol (Cat. no 28604, QIAGEN, Solna Sweden). They were then poly-A tailed according to the manufacturer's protocol (Invitrogen, Lidingö Sweden). This was done to secure A-overhang on the PCR products since the DNA polymerase used was a proof-reading enzyme that is not able to add the A's at the ends of the PCR products. The products were cloned into pCR 2.1 using the TOPO TA

Cloning kit before being transformed into Top10F' chemically competent Escherichia coli according to the manufacturer's protocol (Invitrogen, Lidingö, Sweden). Clones were picked and each clone was grown in 1 mL 2×YT medium containing 50 µg mL^{-1} Kanamycin over night. They were then extracted with QIAprep Spin Miniprep kit according to the manufacturer's protocol (QIAGEN, Solna, Sweden). The 16S rDNA gene sequences were then determined by MWG Biotech Sequencing Team (Ebersberg, Germany) using the universal internal 16S rRNA primer 907r and were then aligned with sequences from GenBank using the BLAST tool at NCBI (http://www.ncbi.nlm.nih.gov) based on high BLAST score similarities. The sequences found in the enrichment cultures were also submitted to GenBank and got the Accession numbers listen in Table A2-2. All information about the sequences can be found by using their specific Accession numbers.

A2.3.7 Statistical analyses

Statistical analyses and graphics were performed using STATISTICA software, version 8.0 (Statsoft, Tulsa, OK, USA).

A2.4 Results

A2.4.1 Enrichment cultures

From each of the eleven dry materials, enrichment cultures were prepared under anaerobic conditions and inoculated according to Table A2-1. After three weeks of incubation the sulphide and acetate productions in the enrichment cultures were examined. The enrichment cultures were also examined microscopically. All cultures showing increased levels of sulphide and acetate contained at least 10^6 mL^{-1} microbes in the supernatant, exemplified in Figure A2-1. The 11 materials differed considerably in sulphide after three weeks, both amongst each other and depending on how they were cultured.

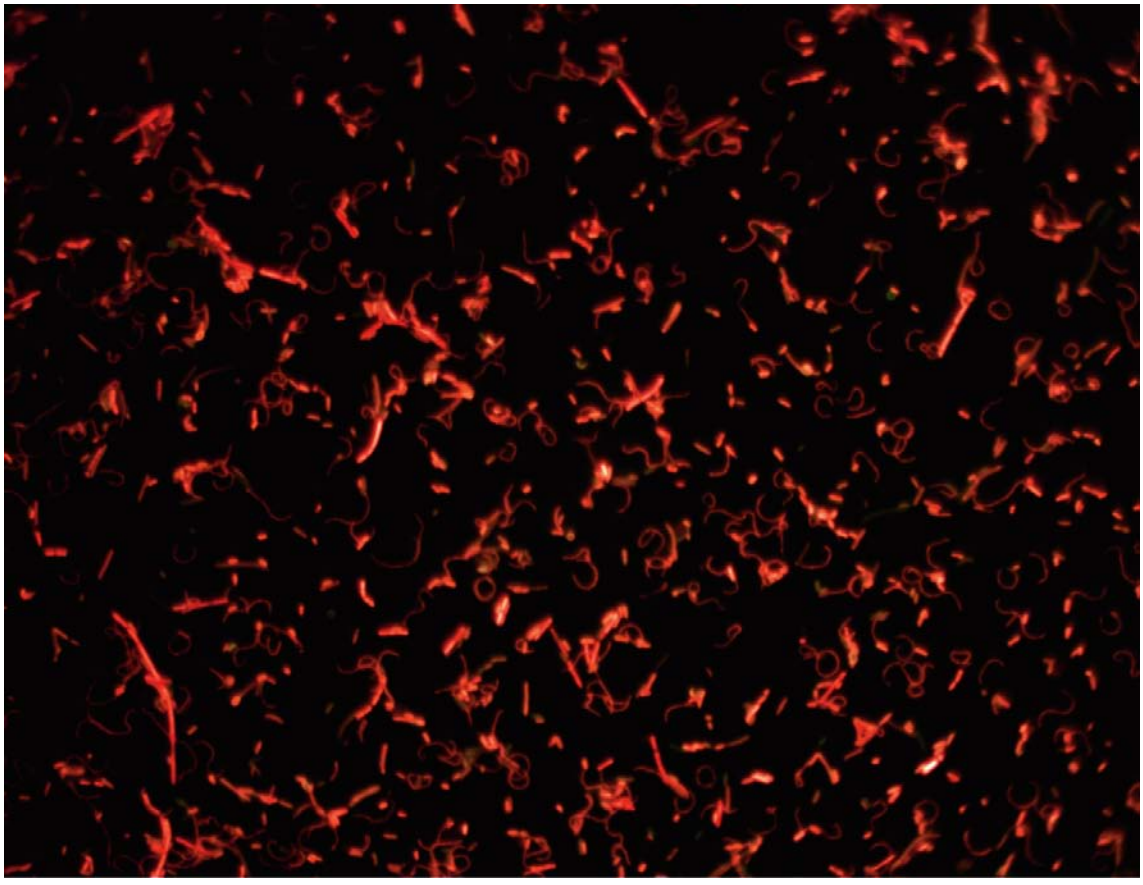

Figure A2-1. *Microbes (stained red) in the supernatant of an enrichment culture inocculated with Friedland clay, incubated in 20°C for three weeks. Lactate was added as an energy source.*

At 20°C and in medium with an organic energy source (lactate), sulphide was enriched the most (nine times) in media inoculated with Friedland clay (Figure A2-1, Figure A2-7). In Febex, Ibeco Seal M-90, Ikosorb and MX-80 inoculated media with added lactate (Figure A2-6, Figure A2-8, Figure A2-9, Figure A2-11), sulphide was enriched up to seven times. In Asha 505, Calcigel, Callovo Oxfordian, Deponite CA-N, Kunigel V1 and Rokle inoculated media with added lactete (Figure A2-2, Figure A2-3, Figure A2-4, Figure A2-5, Figure A2-10, Figure A2-12), sulphide was not enriched.

At 20°C and in medium with an inorganic energy source (H_2), sulphide was again enriched the most in media inoculated with Friedland clay (seven times, Figure A2-7). In Asha 505, Calcigel, Deponite CA-N, Febex, Ibeco Seal M-90 and Ikosorb and MX-80 inoculated media with added H_2 (Figure A2-2, Figure A2-3, Figure A2-5, Figure A2-6, Figure A2-8, Figure A2-9, Figure A2-11), sulphide was enriched up to five times. In Callovo Oxfordian, Kunigel V1 and Rokle inoculated media with added H_2 (Figure A2-4, Figure A2-10, Figure A2-12), sulphide was not enriched. In the same type of medium and at 20°C, acetate was enriched mostly once again in Friedland clay inoculated medium (up to 66 times, Figure A2-7) followed by Ibeco Seal M-90 inoculated medium where acetate was enriched up to 59 times (Figure A2-8). In Asha 505, Deponite CA-N, Febex, and Ikosorb and MX-80 inoculated media acetate was enriched between approximately 30–40 times (Figure A2-2, Figure A2-5, Figure A2-6, Figure A2-9, Figure A2-11), and in Calcigel, Callovo Oxfordian, Kunigel V1 and Rokle inoculated media the enrichment factors were less than 10 (Figure A2-3, Figure A2-4, Figure A2-10, Figure A2-12).

At 50°C and in medium with an organic energy source (lactate), sulphide was enriched the most (34 times) in media inoculated with Ibeco Seal M-90 clay (FigureA2-8). In Calcigel, Febex, Friedland and Ikosorb inoculated media with added lactate (Figure A2-3, Figure A2-6, Figure A2-7, Figure A2-9), sulphide was enriched 7–23 times. In Asha 505, Deponite CA-N, MX-80 and Rokle inoculated media with added lactete (Figure A2-2, Figure A2-5, Figure A2-11, Figure A2-12), sulphide enriched 2–10 times in some of the cultures, and in Callovo Oxfordian and Kunigel V1 inoculated media no sulphide was enriched (Figure A2-4, Figure A2-10).

At 50°C and in medium with an inorganic energy source (H_2), sulphide was enriched the most in media inoculated with Febex clay (32 times, Figure A2-1). In Calcigel, Friedland, Ibeco Seal M-90, Ikosorb and Rokle inoculated media with added H_2 (Figure A2-3, Figure A2-7, Figure A2-8, Figure A2-9, Figure A2-12), sulphide was enriched 5–30 times. In Asha 505, Callovo Oxfordian, Deponite CA-N and MX-80 and Rokle inoculated media with added H_2 (Figure A2-2, Figure A2-4, Figure A2-5, Figure A2-11), sulphide occasionally enriched 3–28 times in some of the cultures, and in Kunigel V1 inoculated medium no sulphide was enriched (Figure A2-10). In the same type of medium and at 50°C, acetate was enriched the most in Ibeco Seal M-90 inoculated medium (up to 135 times, Figure A2-8), followed by Friedland inoculated medium where acetate was enriched up to 132 times (Figure A2-7). In Asha 505, Calcigel, Deponite CA-N, Febex, and Ikosorb, MX-80 and Rokle inoculated media acetate was enriched in all cultures between 5–108 times (Figure A2-2, Figure A2-3, Figure A2-5, Figure A2-6, Figure A2-9, Figure A2-11, Figure A2-12), and in Callovo Oxfordian and Kunigel V1 inoculated medium acetate enriched in some of the cultures between four and 20 times (Figure A2-4, Figure A2-10). Similar results were seen with molecular methods as shown in Table A2-2 and A2-3.

From the results above, it was obvious that acetate and sulphide production correlated. A correlation analysis showed (Figure A2-13) that almost 50% (r^2=0.48, $p > 0.0005$) of the sulphide production in the enrichment cultures was explained by concomitant acetate production.

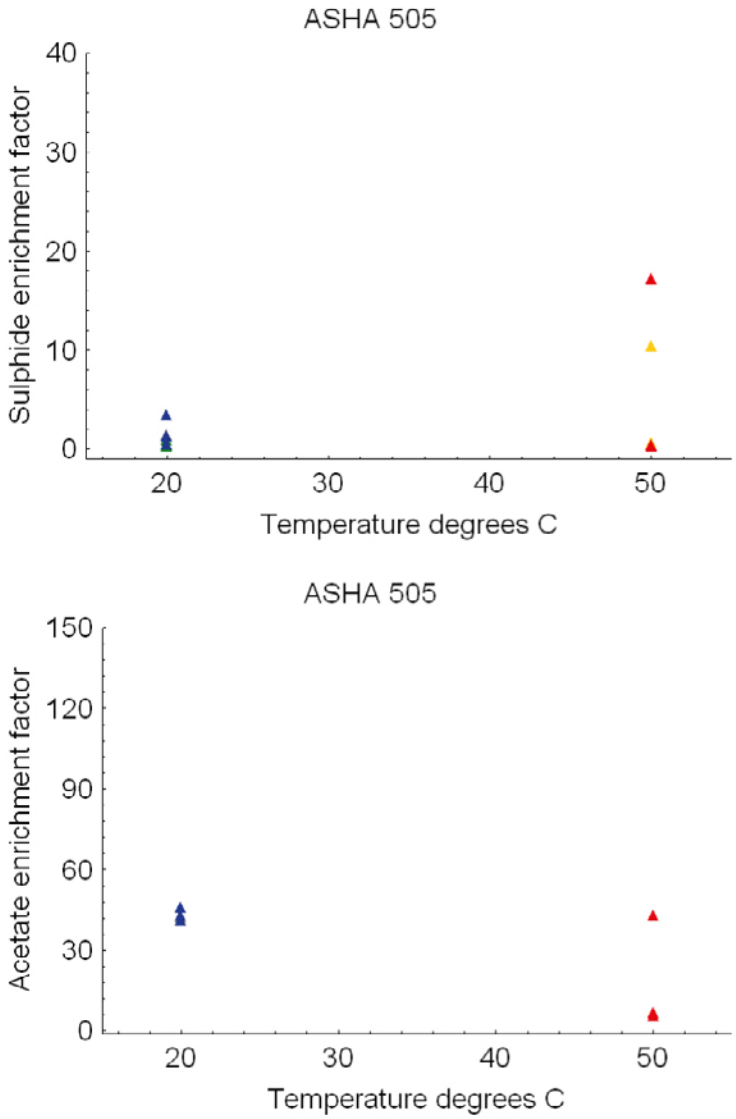

Figure A2-2. *Sulphide and acetate enrichment in the 13 cultures inoculated with the Asha 505 material. The diamonds represent growth conditions as follows: ▲ no added sulphate and energy source, 20°C. ▲ Sulphate and H_2 amended medium, 20°C. ▲ Sulphate and lactate amended medium, 20°C. ▲ Sulphate and H_2 amended medium, 50°C. ▲ Sulphate and lactate amended medium, 50°C.*

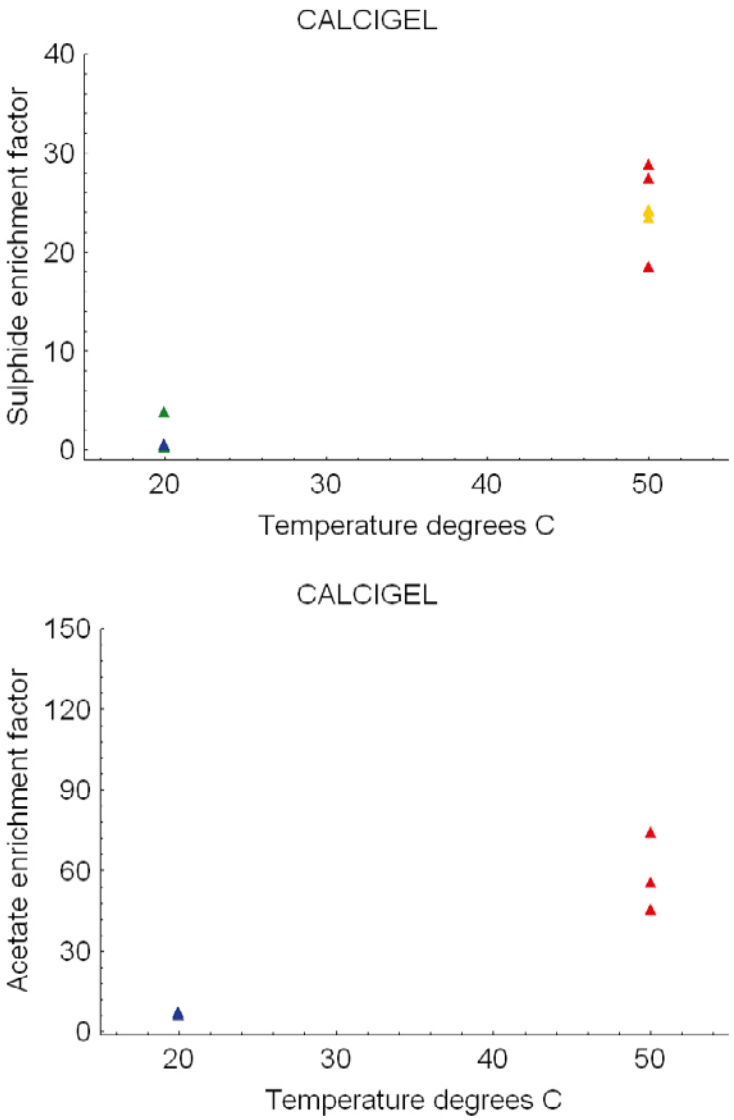

Figure A2-3. *Sulphide and acetate enrichment in the 13 cultures inoculated with the Calcigel material. The diamonds represent growth conditions as follows: ▲ no added sulphate and energy source, 20°C. ▲ Sulphate and H_2 amended medium, 20°C. ▲ Sulphate and lactate amended medium, 20°C. ▲ Sulphate and H_2 amended medium, 50°C. ▲ Sulphate and lactate amended medium, 50°C.*

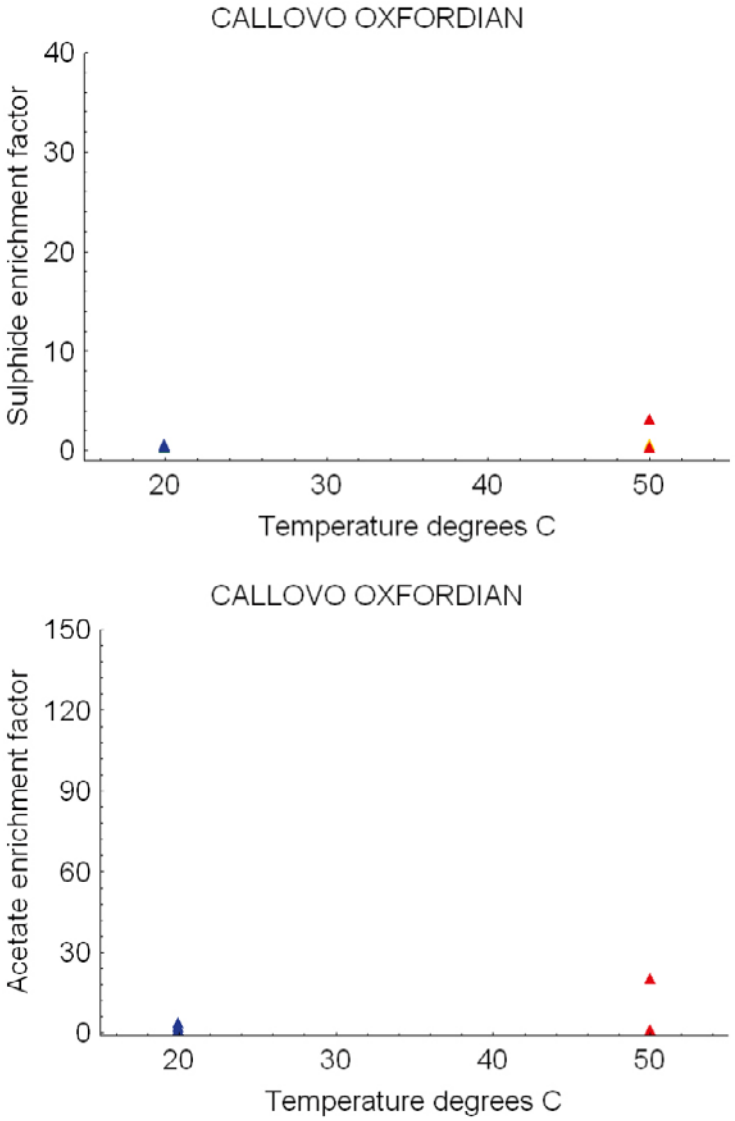

Figure A2-4. *Sulphide and acetate enrichment in the 13 cultures inoculated with the Callovo Oxfordian material. The diamonds represent growth conditions as follows: ▲ no added sulphate and energy source, 20°C. ▲ Sulphate and H_2 amended medium, 20°C. ▲ Sulphate and lactate amended medium, 20°C. ▲ Sulphate and H_2 amended medium, 50°C. ▲ Sulphate and lactate amended medium, 50°C.*

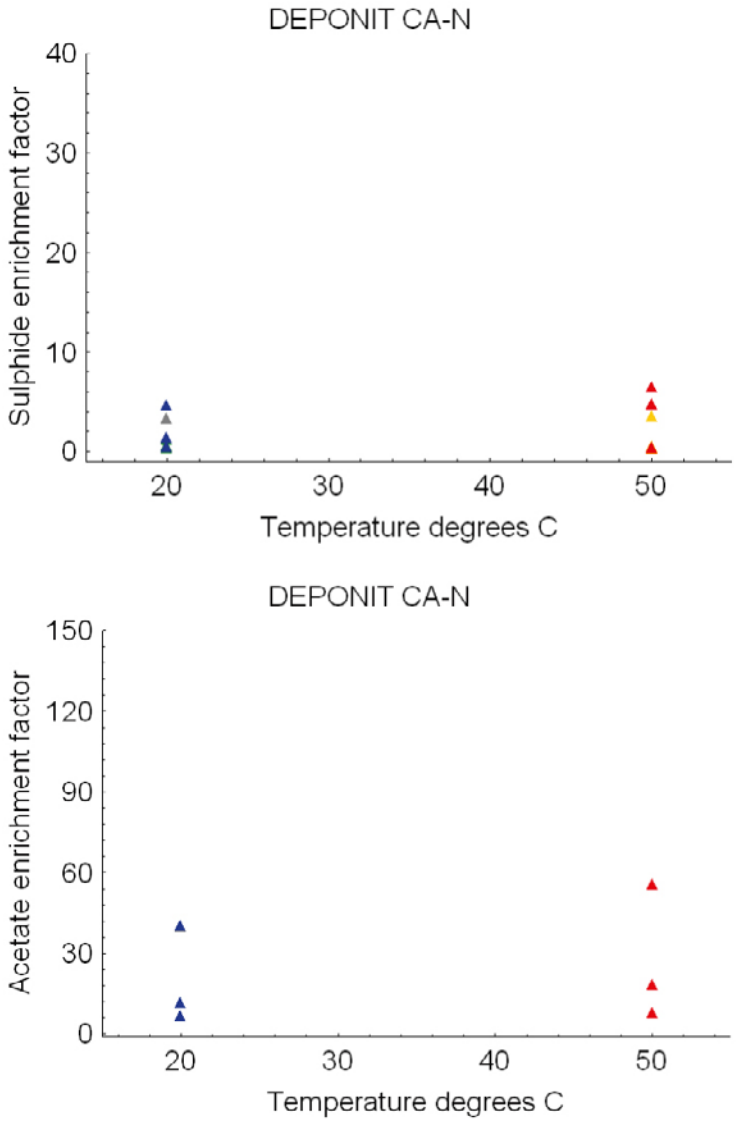

Figure A2-5. *Sulphide and acetate enrichment in the 13 cultures inoculated with the Deponit CA-N material. The diamonds represent growth conditions as follows: ▲ no added sulphate and energy source, 20°C. ▲ Sulphate and H_2 amended medium, 20°C. ▲ Sulphate and lactate amended medium, 20°C. ▲ Sulphate and H_2 amended medium, 50°C. ▲ Sulphate and lactate amended medium, 50°C.*

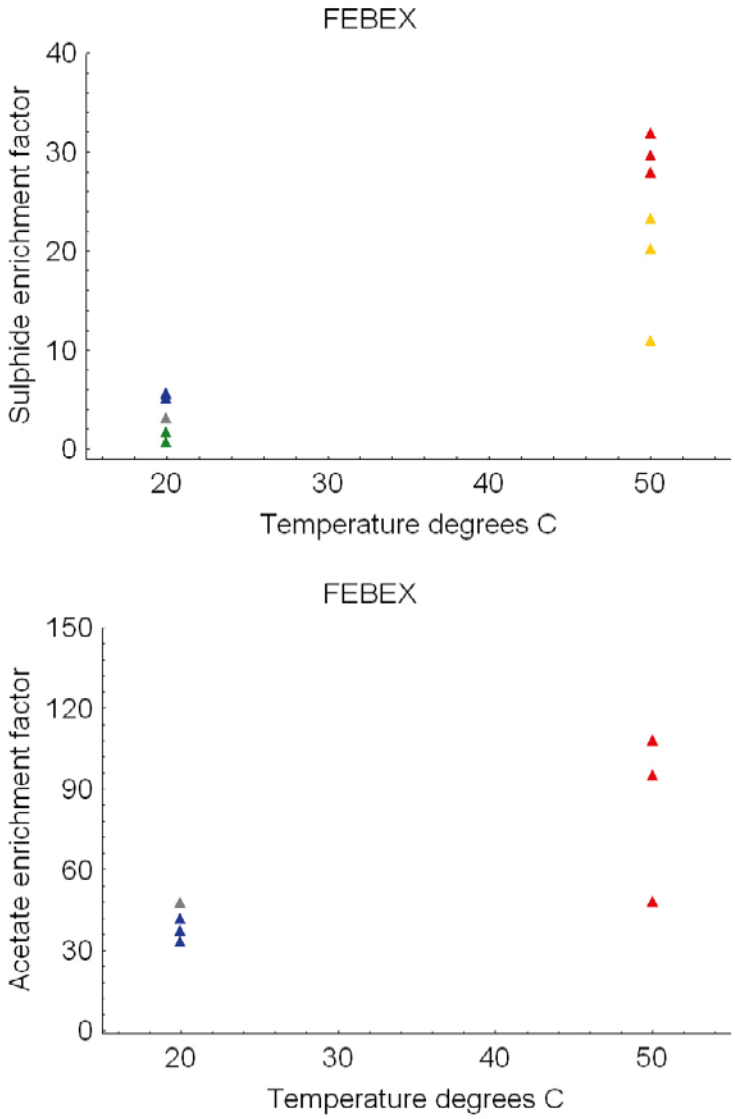

Figure A2-6. *Sulphide and acetate enrichment in the 13 cultures inoculated with the Febex material. The diamonds represent growth conditions as follows: ▲ no added sulphate and energy source, 20°C. ▲ Sulphate and H_2 amended medium, 20°C. ▲ Sulphate and lactate amended medium, 20°C. ▲ Sulphate and H_2 amended medium, 50°C. ▲ Sulphate and lactate amended medium, 50°C.*

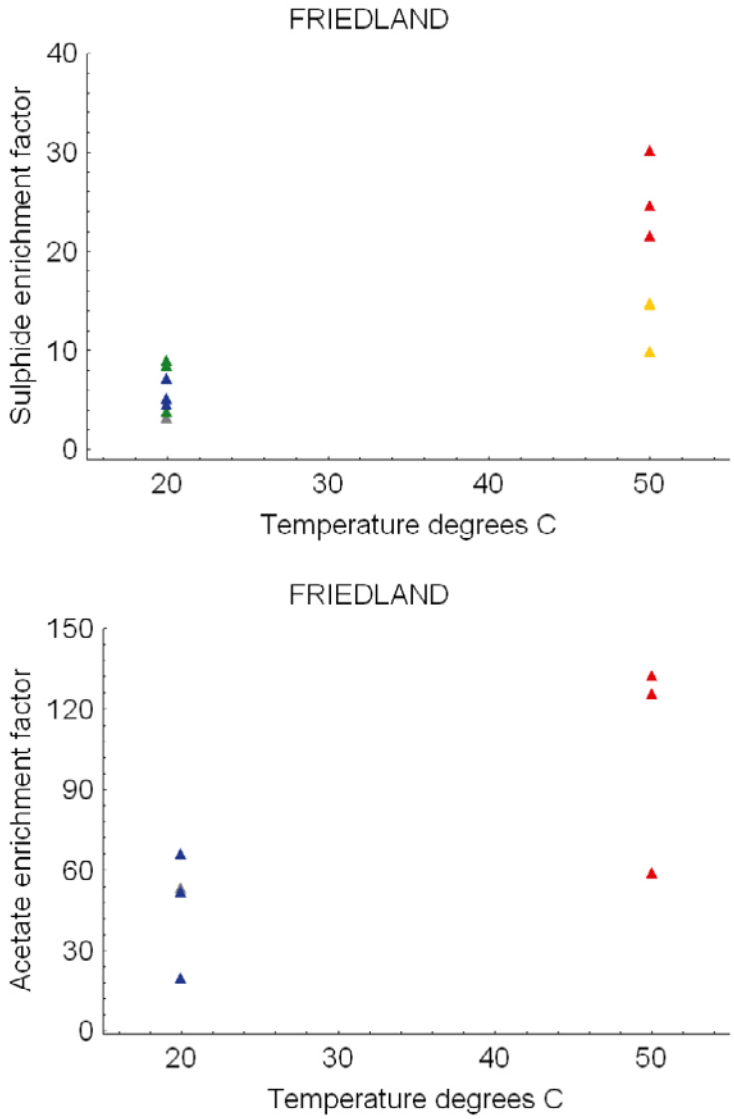

Figure A2-7. *Sulphide and acetate enrichment in the 13 cultures inoculated with the Friedland material. The diamonds represent growth conditions as follows: ▲ no added sulphate and energy source, 20°C. ▲ Sulphate and H_2 amended medium, 20°C. ▲ Sulphate and lactate amended medium, 20°C. ▲ Sulphate and H_2 amended medium, 50°C. ▲ Sulphate and lactate amended medium, 50°C.*

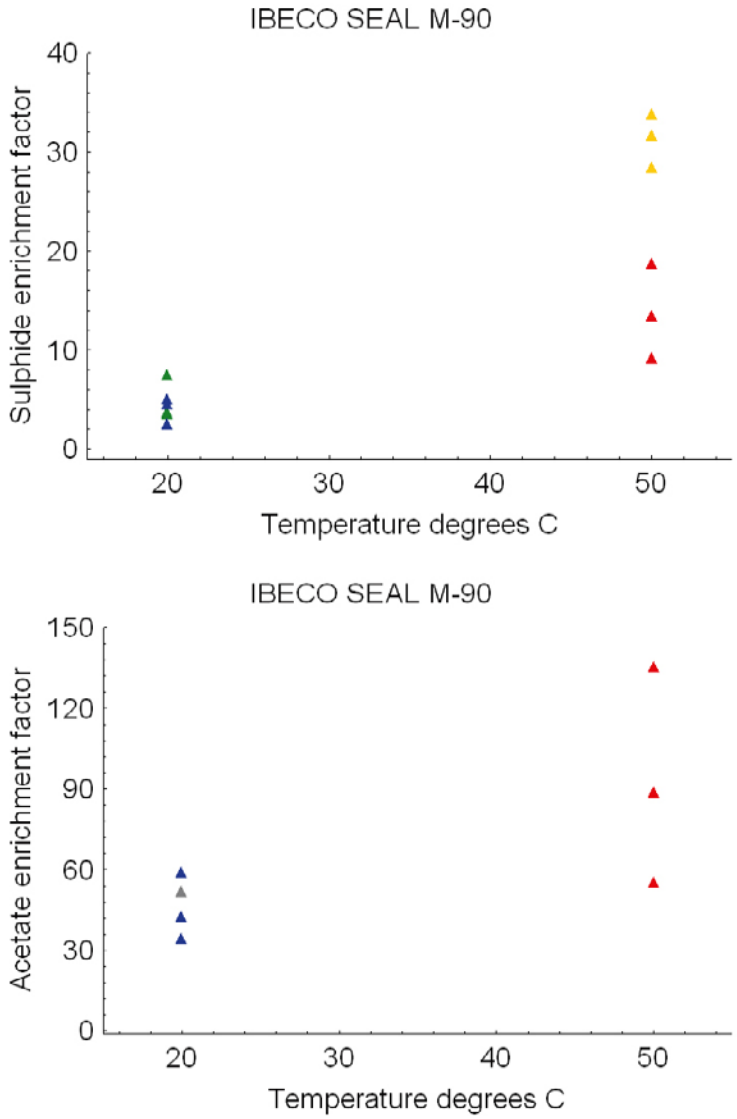

Figure A2-8. *Sulphide and acetate enrichment in the 13 cultures inoculated with the Ibeco Seal M-90 material. The diamonds represent growth conditions as follows: ▲ no added sulphate and energy source, 20°C. ▲ Sulphate and H_2 amended medium, 20°C. ▲ Sulphate and lactate amended medium, 20°C. ▲ Sulphate and H_2 amended medium, 50°C. ▲ Sulphate and lactate amended medium, 50°C.*

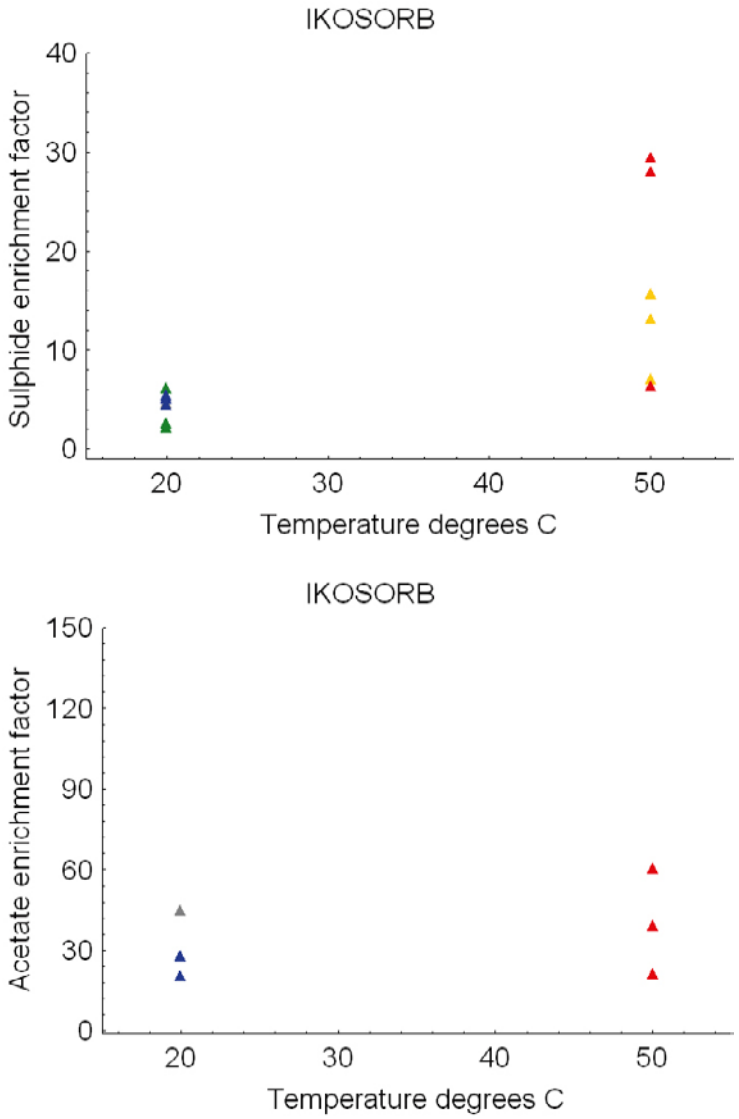

Figure A2-9. *Sulphide and acetate enrichment in the 13 cultures inoculated with the Ikosorb material. The diamonds represent growth conditions as follows: ▲ no added sulphate and energy source, 20°C. ▲ Sulphate and H_2 amended medium, 20°C. ▲ Sulphate and lactate amended medium, 20°C. ▲ Sulphate and H_2 amended medium, 50°C. ▲ Sulphate and lactate amended medium, 50°C.*

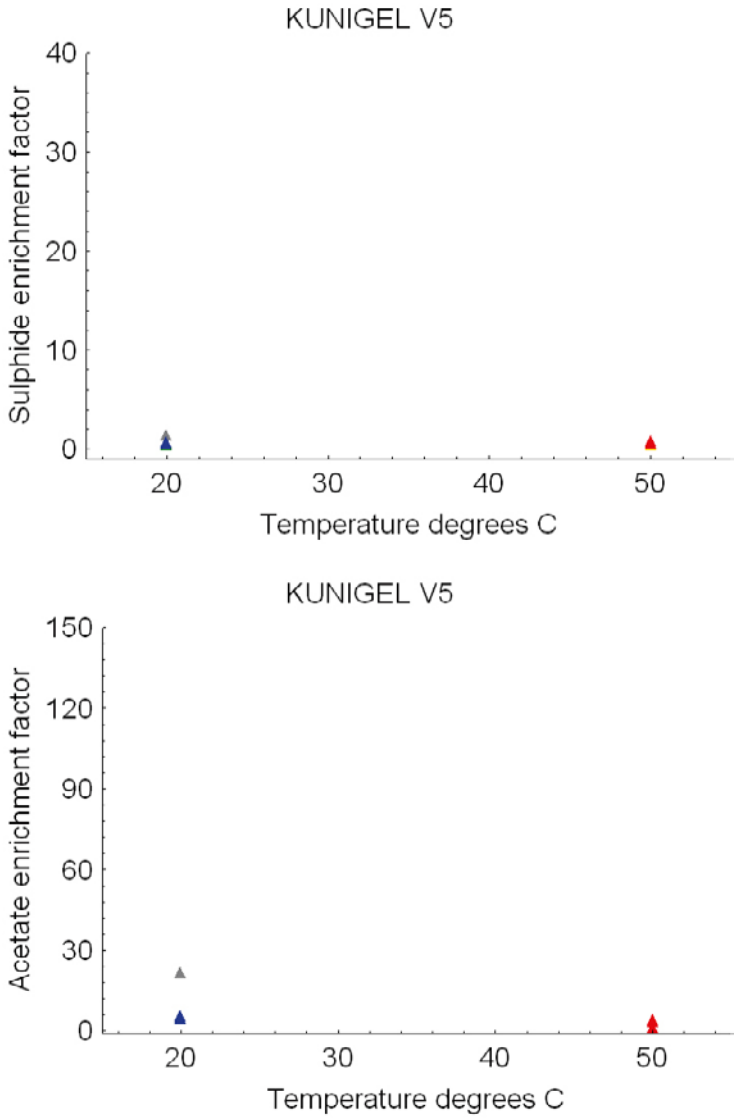

Figure A2-10. *Sulphide and acetate enrichment in the 13 cultures inoculated with the Kunigel V1 material. The diamonds represent growth conditions as follows: ▲ no added sulphate and energy source, 20°C. ▲ Sulphate and H_2 amended medium, 20°C. ▲ Sulphate and lactate amended medium, 20°C. ▲ Sulphate and H_2 amended medium, 50°C. ▲ Sulphate and lactate amended medium, 50°C.*

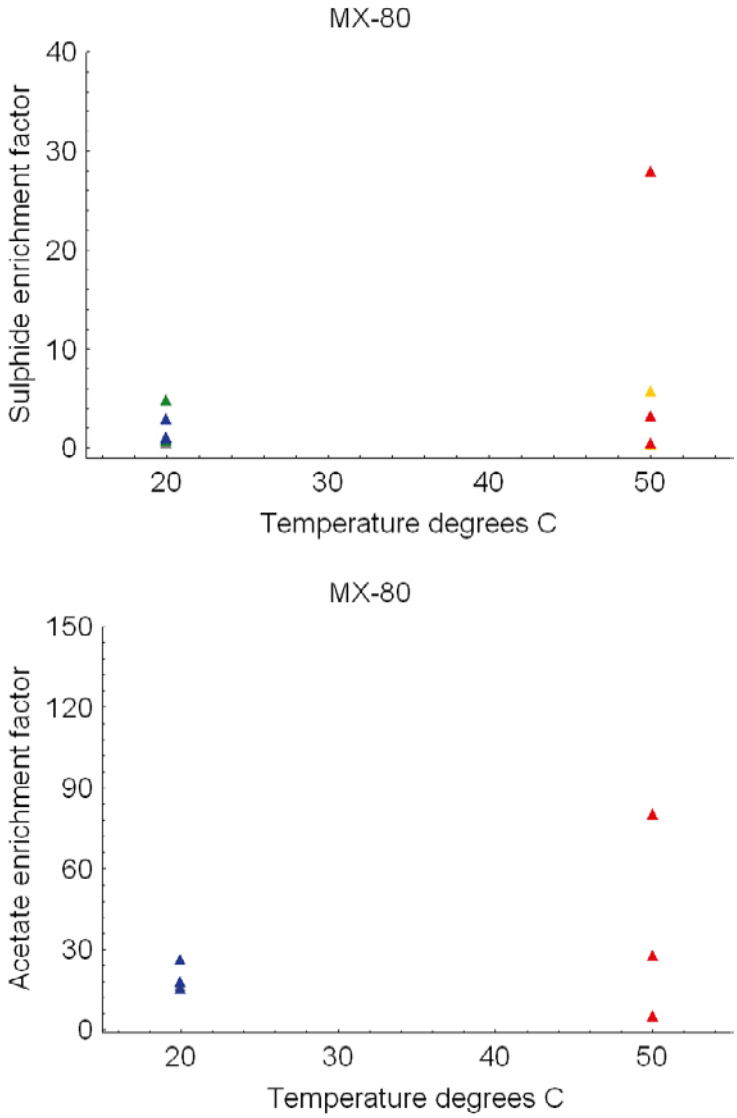

Figure A2-11. *Sulphide and acetate enrichment in the 13 cultures inoculated with the MX-80 material. The diamonds represent growth conditions as follows: ▲ no added sulphate and energy source, 20°C. ▲ Sulphate and H_2 amended medium, 20°C. ▲ Sulphate and lactate amended medium, 20°C. ▲ Sulphate and H_2 amended medium, 50°C. ▲ Sulphate and lactate amended medium, 50°C.*

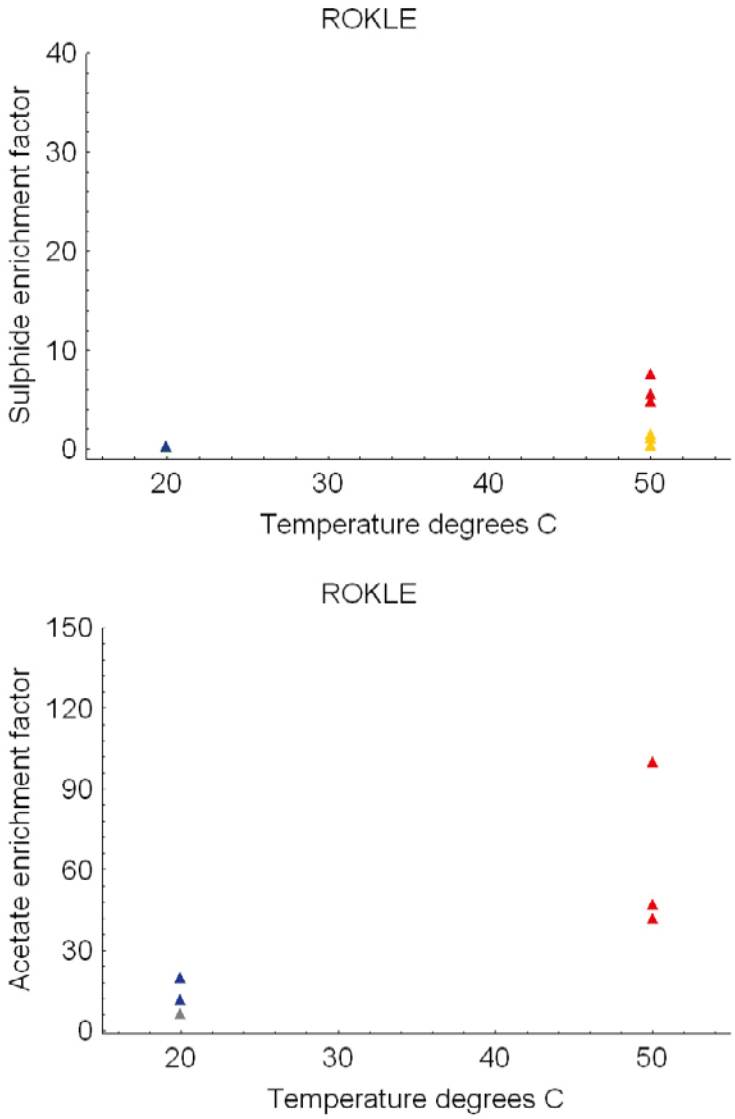

Figure A2-12. *Sulphide and acetate enrichment in the 13 cultures inoculated with the Rokle material. The diamonds represent growth conditions as follows: ▲ no added sulphate and energy source, 20°C. ▲ Sulphate and H_2 amended medium, 20°C. ▲ Sulphate and lactate amended medium, 20°C. ▲ Sulphate and H_2 amended medium, 50°C. ▲ Sulphate and lactate amended medium, 50°C.*

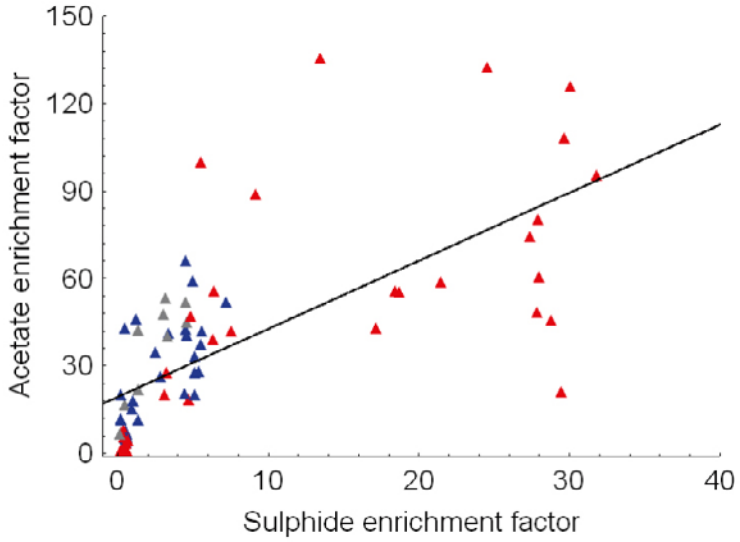

Figure A2-13. *The positive correlation between the sulphide and acetate enrichment factors in all ABM cultures (n=77, r^2=0.48 and p < 0.00005) . The diamonds represent growth conditions as follows: ▲ no added sulphate and energy source, 20°C. ▲ Sulphate and H_2 amended medium, 20°C. ▲ Sulphate and H_2 amended medium, 50°C.*

A2.4.2 Quantification of indigenous microbes

Culturable heterotrophic aerobic bacteria (CHAB)

In Table A2-4, the results from the CHAB analysis are shown. The materials Asha 505 and Febex contained the most CHAB able to grow at 20°C (> 65,000 g^{-1}). The materials Deponit CA-N, Friedland, Ibeco Seal M-90, Ikosorb and MX-80 contained 1,000–6,600 CHAB g^{-1}. Calcigel, Callovo Oxfordian, and Rokle contained 200–400 CHAB g^{-1}, and Kunigel V1 lacked detectable CHAB at 20°C.

Table A2-4. Quantitative analyses of culturable heterotrophic aerobic bacteria (CHAB), sulphate-reducing bacteria (SRB), autotrophic acetogens (AA) and iron-reducing bacteria (IRB) in the eleven ABM materials.

Material	CHAB[a] g^{-1}	MPN SRB[b] g^{-1}	MPN AA[b] g^{-1}	MPN IRB[b] g^{-1}
Asha 505	84,400 ± 109,000	91 (38–409)	< 10	67 (13–170)
Calcigel	420 ± 490	56 (21–152)	< 9	110 (43–410)
Callovo Oxfordian	230 ± 400	< 10	< 11	114 (45–425)
Deponit CA-N	1,000 ± 570	9 (4–44)	< 10	77 (32–207)
Febex	68,600 ± 26,000	10 (5–50)	19 (5–79)	120 (47–448)
Friedland	1,750 ± 880	68 (26–198)	35 (13–106)	6,900 (2,590–22,800)
Ibeco Seal M-90	5,830 ± 4,860	61 (23–178)	63 (24–183)	7,920 (2,970–26,200)
Ikosorb	4,500 ± 4,590	< 10	< 10	117 (46–439)
Kunigel V1	0 ± 0	< 10	< 11	10 (5–56)
MX-80	6,600 ± 1,620	< 10	9 (5–46)	263 (105–895)
Rokle	200 ± 340	9 (5–46)	< 10	110 (45–280)

[a] ± standard deviation, [b] lower and upper 95% confidence interval.

Most probable number (MPN) of sulphate-reducing bacteria (SRB), autotrophic acetogens (AA), and iron-reducing bacteria (IRB)

In Table A2-4, the results from the MPN analyses are shown. The material Asha 505 contained approximately 90 SRB able to grow at 20°C g^{-1}, which was the highest number found in any of the ABM materials. In Freidland, Ibeco seal M-90 and Calcigel, between 55–65 SRB g^{-1} were found. The Deponit CA-N, Febex and Rokle materials contained approximately 10 SRB g^{-1}, and in Callovo Oxfordian, Ikosorb, Kunigel, MX-80 did not contain SRB above the detection limit (< 8–10 g^{-1}).

The most AA were detected in IbecoSeal M-90 (> 60 g^{-1}), followed by Friedland, Febex and MX-80 (9–35 AA g^{-1}). In the remaining ABM materials, AA were not detected above the detection limit (> 10 g^{-1}).

Iron-reducing bacteria able to grow at 20°C g^{-1}were found above the detection limit (approximately > 10 g^{-1}) in all the eleven examined materials. The materials Fridland and Ibeco Seal M-90 was outstanding and contained between 6,900 and 7,900 IRB g^{-1} material. Asha 505, Calcigel, Callovo Oxfordian, Deponit CA-N, Febex, Ikosorb, MX-80 and Rokle contained between approximately 70 and 270 IRB g^{-1}. Kunigel contained 10 IRB 10 g^{-1}.

A2.4.3 Identification of indigenous microbes by molecular metods

Eleven enrichment cultures with sulphide and acetate production were choosen for identification of the microbes present in the cultures. These were:

1. An enrichment cultures inoculated with Friedland clay, growing with hydrogen as energy source and in 20°C.
2. An enrichment cultures inoculated with Friedland clay, growing with hydrogen as energy source and in 50°C.
3. An enrichment cultures inoculated with Ikosorb clay, growing with lactate as energy source and in 50°C.
4. An enrichment cultures inoculated with Ikosorb clay, growing with hydrogen as energy source and in 50°C.
5. An enrichment cultures inoculated with Ibeco Seal M-90 clay, growing with hydrogen as energy source and in 20°C.
6. An enrichment cultures inoculated with Ibeco Seal M-90 clay, growing with hydrogen as energy source and in 50°C.
7. An enrichment cultures inoculated with Febex clay, growing with hydrogen as energy source and in 20°C.
8. An enrichment cultures inoculated with Febex clay, growing with hydrogen as energy source and in 50°C.
9. An enrichment cultures inoculated with Calcigel clay, growing with lactate as energy source and in 50°C.
10. An enrichment cultures inoculated with Calcigel clay, growing with hydrogen as energy source and in 50°C.
11. An enrichment cultures inoculated with MX-80 clay, growing with hydrogen as energy source and in 50°C.

Ten of the eleven clonings worked very well but when the enrichment culture from Febex grown at 20°C did not give any sequence material that were good enough to draw conclusions from..

Table A2-5. Microorganisms found by cloning the enrichment cultures from the different bentonite buffer materials. Different Desulfotomaculum sp. that are sulphate reducing bacteria were found in all different materials and this was the most common bacterium in overall together with different Clostridium and Bacillales.. More information about the sequences behind the accession numbers can be found at GenBank.

ABM	Culture °C	Source of energy	MICANS-ID	Accession number	Most similar NCBI	Identity %	Number of id. clones
Friedland	20	H_2	080213-ABM-Friedland 20-06*	EU732609	*Desulfovibrio africanus* EU659693	99	10/10
Friedland	50	H_2	080213-ABM-Friedland 50-01	EU732610	*Desulfotomaculum sp. Mechi-chi-2001* AY69974	98	3/8
Friedland	50	H_2	080213-ABM-Friedland 50-02	EU732611	Desulfotomaculum geothermicum	85	2/8
Friedland	50	H_2	080213-ABM-Friedland 50-03	EU732612	*Desulfotomaculum sp. NA401* AJ866942	99	3/8
Calcigel	50	Lactate	080212-ABM-Calcigel 1-01	EU732613	*Bacillus bataviensis* AJ542508	100	2/9
Calcigel	50	Lactate	080212-ABM-Calcigel 1-02	EU732614	*Gelria glutamica* AF321086	97	1/9
Calcigel	50	Lactate	080212-ABM-Calcigel 1-05	EU732615	*Gelria glutamica* AF321086	96	1/9
Calcigel	50	Lactate	080212-ABM-Calcigel 1-04*	EU732616	*Bacillus aeolius* AB362281	100	3/9
Calcigel	50	Lactate	080212-ABM-Calcigel 1-06*	EU732617	*Bacillus sp. MDS02* EU236671	95	1/9
Calcigel	50	Lactate	080212-ABM-Calcigel 1-11	EU732618	*Bacillus hackensackii* AY148429	95	1/9
Calcigel	50	H_2	080212-ABM-Calcigel 2-13	EU732619	*Clostridium thermocellum* CP000568	93	3/11
Calcigel	50	H_2	080212-ABM-Calcigel 2-14	EU732620	*Tepidanaerobacter sp. Re1* EU386163	96	3/11
Calcigel	50	H_2	080212-ABM-Calcigel 2-17	EU732621	*Tepidanaerobacter sp. Re1* EU386163	95	3/11
Calcigel	50	H_2	080212-ABM-Calcigel 2-19	EU732622	Uncultured firmicutes bacterium EU194835		1/11
Calcigel	50	H_2	080212-ABM-Calcigel 2-25	EU732623	Uncultured bacterium clone B-13 AB234006	99	1/11
Ikosorb	50	Lactate	080213-ABM-Ikosorb 3-28	EU732624	*Clostridium hastiforne* X80841	94	4/9
Ikosorb	50	Lactate	080213-ABM-Ikosorb 3-30	EU732625	Uncultured bacterium clone CFB-6 AB274495	93	1/9
Ikosorb	50	Lactate	080213-ABM-Ikosorb 3-31	EU732626	*Clostridium sp. EBR-02E-0046* AB186360	96	2/9
Ikosorb	50	Lactate	080213-ABM-Ikosorb 3-32	EU732627	*Peptostreptococcaceae bacterium 19gly3* AF550659		1/9
Ikosorb	50	Lactate	080213-ABM-Ikosorb 3-30	EU732628	*Bacillus thermoamylovorans* L27478	99	1/9
Ikosorb	50	H_2	080213-ABM-Ikosorb 4-39	EU732629	*Clostridium filamentosum* X77847	100	6/12
Ikosorb	50	H_2	080213-ABM-Ikosorb 4-38	EU732630	*Clostridium sp. PML14* EF522948	99	2/12
Ikosorb	50	H_2	080213-ABM-Ikosorb 4-42	EU732631	*Desulfotomaculum halophilum* U88891	89	3/12
Ikosorb	50	H_2	080213-ABM-Ikosorb 4-45	EU732632	*Bacillus thermoamylovorans* L27478	99	1/12
Febex	50	H_2	080213-ABM-Febex 6-49	EU732633	*Desulfotomaculum halophilum* U88891	90	7/12
Febex	50	H_2	080213-ABM-Febex 6-50	EU732634	Uncultured bacterium clone B55 EF558950	98	1/12
Febex	50	H_2	080213-ABM-Febex 6-54	EU732635	*Empedobacter brevis* DQ350833	94	1/12

ABM	Culture °C	Source of energy	MICANS-ID	Accession number	Most similar NCBI	Identity %	Number of id. clones
Febex	50	H_2	080213-ABM-Febex 6-56	EU732636	*Clostridium thermocellum* CP000568	98	1/12
Febex	50	H_2	080213-ABM-Febex 6-57	EU732637	*Bacillus methanolicus* X64465	93	1/12
Febex	50	H_2	080213-ABM-Febex 6-59	EU732638	*Peptostreptococcaceae bacterium 19gly3* AF550659	99	1/12
Ibeco Seal M-90	20	H_2	080213-ABM-Ibeco Seal 7-61	EU732639	*Clostridium sulfidogenes* EF199998	99	4/8
Ibeco Seal M-90	20	H_2	080213-ABM-Ibeco Seal 7-62	EU732640	*Sporotalea proprionica* AM258974	99	2/8
Ibeco Seal M-90	20	H_2	080213-ABM-Ibeco Seal 7-64	EU732641	*Sporotalea proprionica* AM258974	98	2/8
Ibeco Seal M-90	50	H_2	080213-ABM-Ibeco Seal 8-73	EU732642	Uncultured bacterium clone C55 EF558995	99	2/9
Ibeco Seal M-90	50	H_2	080213-ABM-Ibeco Seal 8-74	EU732643	*Desulfotomaculum halophilum* U88891	89	1/9
Ibeco Seal M-90	50	H_2	080213-ABM-Ibeco Seal 8-80	EU732644	*Clostridium sp.EBR-02E-0046* AB186360	99	4/9
Ibeco Seal M-90	50	H_2	080213-ABM-Ibeco Seal 8-82	EU732645	*Desulfotomaculum sp. NA401* AJ866942	99	2/9
MX-80	50	H_2	080214-ABM-MX80 9-86	EU732646	*Desulfotomaculum sp. NA401* AJ866942	99	2/10
MX-80	50	H_2	080214-ABM-MX80 9-87	EU732647	*Clostridium sp.EBR-02E-0046* AB186360	99	1/10
MX-80	50	H_2	080214-ABM-MX80 9-88	EU732648	*Desulfotomaculum sp. Mechichi-2001* AY69974	99	1/10
MX-80	50	H_2	080214-ABM-MX80 9-91	EU732649	*Clostridium ultunae* Z69293	97	1/10
MX-80	50	H_2	080214-ABM-MX80 9-92	EU732650	*Desulfotomaculum halophilum* U88891	89	2/10
MX-80	50	H_2	080214-ABM-MX80 9-93	EU732651	Uncultured bacterium clone C55 EF558995	97	3/10

A2.5 Conclusions

A2.5.1 Difference between the alternative buffer materials

In this study, data concerning indigenous microbes in the eleven alternative buffer reference materials were collected. There was a big difference in to what extent the different dry alternative buffer materials were contaminated with microbes.

Of course, the effects of the microbes will have to be evaluated before conclusions can be drawn but all together, the alternative buffer materials Ibeco Seal M-90, Friedland, and Febex (Figure A2-1, Figure A2-6, Figure A2-7, Figure A2-8, Table A2-4) will have to be regarded as highly inappropriate to use from a bacterial point of view. These materials contained high numbers of all or most microbes analysed in this study as well as microbes with the ability of sulphide production both at 20°C and 50°C. Also the used batches of MX-80, Ikosorb, Asha 505 will have to be regarded as inappropriate as buffer materials because of high numbers of some of the examined microbes (Table A2-4, Figure A2-2, Figure A2-9, Figure A2-11). Calcigel, Rokle, Deponit CA-N (Table A2-4, Figure A2-3, Figure A2-5, Figure A2-12) were cleaner than the aforementioned materials and can be regarded as acceptable buffer materials, even though containing some microbes. The best choise, based on microbe studies solely, were Callovo Oxfordian and Kunigel (Table A2-4, Figure A2-4, Figure A2-10). These materials, especially Kunigel, did almost not contain any microbes, making them suitable as buffer material.

A2.5.2 Iron reduction and illitisation

Previous studies have shown that IRB seem to catalyse illitisation of smectite in a drastic way (Kim et al. 2004). In Table A2-4, the numbers of IRB g^{-1} of each alternative material are presented. As shown, IRB were present in all materials tested, making further studies of IRB in these materials very important if they are to be used. For example, in some materials (i.e. Friedland and Ibeco Seal M-90), almost 7,000–8,000 IRB g^{-1} were detected. In the same time, Friedland contains high amounts of illite compared to other bentonites. Some sequences were found that were most similar to different Uncultured bacteria. It was impossible to say exactly what those bacteria do since that information could not be found yet but it could not be excluded that those are iron-reducers.

A2.5.3 Acetogenesis and H_2 metabolism shows that organic carbon is not necessary

Sometimes, the low amount of organic carbon in the buffer materials is used as an argument for the inability for microbes to thrive in the buffer. However, this study showed that many buffer materials contained AA in the range 1–63 g^{-1} material (Table A2-4). The AA are able to produce acetate from carbon dioxide and hydrogen gas (Figure A2-2, Figure A2–3, Figure A2-5, Figure A2-6, Figure A2-7, Figure A2-8, Figure A2-9, Figure A2-11, Figure A2-12). Acetate can in turn be used by many SRB. In fact, in this study 50% of the sulphide production in media inoculated solely with buffer materials and hydrogen gas could be explained as a consequence of on-going acetogenesis (Figure A2-13).

Acetogens were also found by molecular methods. Bacteria belonging to the genus Clostridium were found throughout the enrichment cultures. *Clostridium thermocellum* was an anaerobic, thermophilic spore forming bacterium found in Calcigel grown at 50°C with H_2 as the energy source and also in Febex under the same conditions. It is capable of directly converting a cellulosic substrate into ethanol and acetate . It had an optimal growth temperature of 60–64°C (Freier et al. 1988). *Clostridium sp. EBR-02-E-0046* is another spore forming thermophile that has been shown to be very similar to *Clostridium thermocellum* and it was also able to convert cellulose directly to ethanol also producing acetate. It had an optimal growth temperature of 55–60°C. Those bacteria were also able to convert cellulose to methane as were archaea that might sometimes live together with those organisms (Shiratori et al. 2006).

Clostridium ultunense was found in MX-80. This was a syntrophic acetate-oxidizing bacterium able to syntrophically oxidize acetate and form methane in stoichiometric amounts. It is spore-forming and rod-shaped and able to utilize formate, glucose, ethylene glycol, cysteine, betaine, and pyruvate. Acetate and sometimes formate were the main fermentation products. It grew optimally at 37°C (Schnürer et al. 1996). Bacteria most similar to different spices of the genus Clostridium dominated the Ikosorb enrichments grown at 50°C both with and without lactate. A bacterium most similar to *Clostridium hastiforne* dominated the enrichment culture with lactate. *Clostridium filamentosum* dominated Ikosorb in the absence of lactate (4.3). Clostridium sp. PML14 was found in Ikosorb grown at 50°C with H_2 as the energy source.

A bacterium 95–96% identical to *Tepidanaerobacter sp. Re1* dominated Calcigel in the absence of lactate. This is a mesophilic syntrophic acetate-oxidizing bacterium (Accession number EU386163).

Sporotalea proprionica dominated Ibeco Seal grown at 20°C together with the sulphate reducer *Clostridium sulfidogenes*. *Sporotalea proprionica* is a spore-forming hydrogen-oxidizing, oxygen-reducing, propionigenic firmicute. It produces acetate (Boga et al. 2007).

A2.5.4 Sulphate reduction under both mesophilic and thermophilic conditions

Sulphide production were detected in the enrichment cultures from several of the alternative buffer materials (Figure A2-2, Figure A2-3, Figure A2-5, Figure A2-6, Figure A2-7, Figure A2-8, Figure A2-9, Figure A2-11, Figure A2-12). The quantitative analyses showed that SRB existed in the different materials in the range of 1–90 g^{-1} (Table A2-4). Interestingly, the sulphide production

in the majority of these materials were higher at 50°C than at 20°C (Figure A2-2, Figure A2-3, Figure A2-6, Figure A2-7, Figure A2-8, Figure A2-9, Figure A2-11). Thus, we quite possibly underestimate the number of SRB in the buffer material by culturing them at 20°C. The molecular studies of SRB show that different SRB are enriched at different temperatures. In the Friedland clay for example, two different types of SRB were found at 20°C and at 50°C (Table A2-5). At 20°C, the SRB *Desulfovibrio africanus* dominated the enrichment. This microbe has previously been found in dry MX-80 bentonite (Masurat et al. 2008) and is thus an important contaminating microbe in dry buffer. *D. africanus* is not known to produce spores, showing that this ability is not crucial for survival in dry clay. At 50°C on the other hand, SRB from the genus *Desulfotomaculum* were found to dominate not only the Friedland enrichment but also Febex and MX-80. In Ibeco Seal M-90 however it dominated together with *Clostridium sp.EBR-02E-0046*. Spices from *Desulfotomaculum* sometimes thrive at temperatures well above 50°C (Widdel 2006). In some enrichments *Desulfotomaculum halophilum* was found. This is as the name indicates a halophilic sulphate reducer (Tardy-Jacquenod et al. 1998). Other sulphate reducers found were *Clostridium sulfidogenes* found in Ibeco Seal grown at 20°C. This is a sulphate reducer able to reduce thiosulfate, sulfur and transiently sulfate (Accession number EF199998).

Bacillales

Bacillus bataviensis are rod-shaped facultatively anaerobic bacteria that were able to reduce nitrate. This spices was able form spores (Heyrman et al. 2004). It has an optimal growth temperature of 30°C but can grow up to 50–55°C. Different spices of Bacillus such as *Bacillus aeolius, Bacillus hackensackii* and *Bacillus sp MDS02* were found to dominate the Calcigel enrichment grown at 50°C with lactate. *Bacillus aeolius* is a thermophile, halophile marine Bacillus (Heyrman et al. 2004). Another Bacillus found in 50°C but in the Ikosorb enrichment was *Bacillus thermoamylovorans*, a moderately thermophilic, facultatively anaerobic, amylolytic bacterium. According to the literature the cells were non-spore forming and rod shaped and the optimum temperature for growth was around 50 degrees C with an upper temperature limit for growth at 58°C (Combet-Blanc et al. 1995).

Bacillus methanolicus is a thermotolerant, methanol-utilizing, endospore-forming methanotroph (Brautaset et al. 2007). It was found in Febex at 50°C without lactate.

Other bacteria found by molecular methods

Another bacterium found (97% id.) was *Gelria glutamica*, an anaerobic, thermophilic, spore-forming, obligate syntrophic bacterium that could grow on lactate and this was also the case in our cultures of Calcigel grown at 50°C where it was found in this study (Table A2-5). The optimal temperature for growth was 50–55 degrees C and growth occurred between 37 and 60°C (Plugge et al. 2002). *Peptostreptococcaceae bacterium* was found in Ikosorb with lactate and in Febex with H_2 as the energy source. Some Uncultured bacterium was also found. The function of those is unclear. *Empedobacter brevis* was a gram-negative aerobic bacterium found in Febex at 50°C.

The sequencing results from the enrichment cultures in this study were an indication of what was present in the different enrichment cultures of bentonite. The sequences from GenBank aligning with our sequences were sometimes far from 100% identical and therefore all unique sequences found in the enrichments were submitted to GenBank. Here they were listed in more detail by separate sequence information pages, with one for each sequence that were unique in this study. Details about the sequences could be studied at GenBank by searching for their Accession numbers listed in Table A2-5.

The enrichments seem to be very specific and even if the different cultures resulted in different spices many of them are very similar. Therefore the bentonitic environment occurs to be limiting the organisms to a few closely related species.

A2.6 References

Boga H I, Ji R, Ludwig W, Brune A, 2007. *Sporotalea propionica* gen. nov. sp. nov., a hydrogen-oxidizing, oxygen-reducing, propionigenic firmicute from the intestinal tract of a soil-feeding termite. Archives of Microbiology 187, 15–27.

Brautaset T, Jakobsen Ø M, Josefsen K D, Flickinger M C, Ellingsen T E, 2007. *Bacillus methanolicus*: a candidate for industrial production of amino acids from methanol at 50°C. Applied Microbiology and Biotechnology 74, 22–34.

Combet-Blanc Y, Ollivier B, Streicher C, Patel B K C, Dwivedi P P, Pot B, Prensier G, García J-L, 1995. *Bacillus thermoamylovorans* sp. nov., a moderately thermophilic and amylolytic bacterium. International Journal of Systematic Bacteriology 45, 9–16.

Freier D, Mothershed C P, Wiegel J, 1988. Characterization of *Clostridium thermocellum* JW20. Applied and Environmental Microbiology 54, 204–211.

Greenberg A E, Clesceri L S, Eaton A D, 1992. Estimation of bacterial density. In Standard methods for the examination of water and wastewater. 18th ed. Washington: American Public Health Association, 9–49.

Heyrman J, Vanparys B, Logan N A, Balcaen A, Rodríguez-Díaz M, Felske A, De Vos P, 2004. *Bacillus novalis* sp. nov., *Bacillus vireti* sp. nov., *Bacillus soli* sp. nov., *Bacillus bataviensis* sp. nov. and *Bacillus drentensis* sp. nov., from the Drentse A grasslands. International Journal of Systematic and Evolutionary Microbiology 54, 47–57.

Johnsson A, 2006. The role of bioligands in microbe-metal interactions: emphasis on subsurface bacteria and actinides. PhD thesis. Göteborg University, Sweden.

Kim J, Dong H, Seabaugh J, Newell S W, Eberl D D, 2004. Role of microbes in the smectite-to-illite reaction. Science 30, 830–832.

Lane D J, 1991. 16S/23S rRNA sequencing. Nucleic acid techniques in bacterial systematics. Stackebrandt E and Goodfellow M eds., John Wiley and Sons, New York, NY, pp. 115–175.

Masurat P, Eriksson S, Pedersen K, 2008. Evidence of indigenous sulphate-reducing bacteria in commercial MX-80 Wyoming bentonite. Applied Clay Science 47, 51–57.

Pedersen K, Ekendahl S, 1990. Distribution and activity of bacteria in deep granitic groundwaters of southeastern Sweden. Microbial Ecology 20, 37–52.

Plugge C M, Balk M, Zoetendal E G, Stams A J M, 2002. *Gelria glutamica* gen. nov., sp. nov., a thermophilic, obligately syntrophic, glutamate-degrading anaerobe. International Journal of Systematic and Evolutionary Microbiology 52, 401–407.

Schnürer A, Schink B, Svensson B H, 1996. *Clostridium ultunense* sp. nov., a mesophilic bacteriumoxidizing acetate in syntrophic association with a hydrogenotrophic methanogenic bacterium. International Journal of Systematic Bacteriology 45, 1145–1152.

Shiratori H, Ikeno H, Ayame S, Kataoka N, Miya A, Hosono K, Beppu T, Ueda K, 2006. Isolation and characterization of a new Clostridium sp. that performs effective cellulosic waste digestion in a thermophilic methanogenic bioreactor. Applied and Environmental Microbiology 72, 3702–3709.

Tardy-Jacquenod C, Magot M, Patel B K C, Matheron R, Caumette P, 1998. *Desulfotomaculum halophilum* sp. nov., a halophilic sulfate-reducing bacterium isolated from oil production facilities. International Journal of Systematic and Evolutionary Microbiology 48, 333–338.

Widdel F, 2006. The genus *Desulfotomaculum*. In The prokaryotes. 3rd ed. New York: Springer, 787–794.

Widdel F, Bak F, 1992. Gram-negative, mesophilic sulphate-reducing bacteria. In Balows A, Truper H G, Dworkin M, Harder W, Schleifer K-Z (eds). The prokaryotes. 2nd ed. New York: Springer-Verlag, 3352–3378.

Appendix 3

Bacterial analyses of three Test Package 1 buffer materials, retrieved in May 2009

Alternative buffer materials

Bacterial analyses of three Test Package 1 buffer materials, retrieved in May 2009.

Sara Lydmark

Microbial Analytics Sweden AB

With contributions from:

Johanna Arlinger, Lena Eriksson, Anna Hallbeck, Maria Hallbeck, Anna Pääjärvi Jörgen Persson and Karsten Pedersen

A3.1 Abstract

The Alternative buffer material (ABM) project is presently ongoing at the Äspö Hard Rock Laboratory. The project involves studies of 11 bentonites (Asha 505, Calcigel, Callovo Oxfordian, Deponit CA-N, Febex, Friedland, Ibeco Seal M-90, Ikosorb, Kunigel V1, MX-80 and Rokle), to be used as possible buffer materials around the copper canister in a KBS-3 repository. The bentonites are now being evaluated regarding several parameters, including microbiology. The 11 betonites were placed underground, water saturated and heated in so called test packages 1–3. In May 2009, the first of the three ABM test packages were lifted from incubation underground and focus has been directed to the following three materials: Asha 505, Deponit CA-N and MX-80. This first test package (TP1) was incubated at a temperature exceeding 130°C closest to the heater. However, farther out in the bentonite the temperature decrease to 90°C and since the highest temperature where life has been proven active is 113°C (or possibly even 121°C), there is a potential for bacterial activity even at these temperatures. This report presents the results from the microbial analysis of TP1. In addition, results on repeated analysis of the raw buffer materials before deposition of Asha 505, Deponit CA-N and MX-80 are presented. Special emphasis was put on the abundance of mesophilic and thermophilic aerobic heterotrophic bacteria and anaerobic sulphate and iron reducers, because of their abilities to affect the KBS-3 type of repository for nuclear waste. Bacteria in the clay were detected by aerobic plate counts and the most probable number method for anaerobes. The repeated analyses on the raw buffer material (RBM) showed that all groups of examined mesophilic bacteria were present in the Asha 505, Deponit CA-N and MX-80 materials. Mesophilic aerobic bacteria were detected in the range of 10^3 g dry weight $^{-1}$ (gdw^{-1}) in Deponit CA-N to 10^5 gdw^{-1} in Asha 505. Mesophilic autotrophic sulphate reducers were detected in the range of 10^1 gdw^{-1}in MX-80 and Asha 505 to 10^2 gdw^{-1} in Deponit CA-N. Mesophilic heterotrophic sulphate reducers were detected in the range of 10^1 gdw^{-1} in Deponit CA-N to 10^2 gdw^{-1} in MX-80. Mesophilic iron reducers were detected in the range of $< 10^1$ gdw^{-1} in Deponit CA-N to 10^2 gdw^{-1} in Asha 505. When it comes to thermophilic bacteria, the groups of examined bacteria were present in some of the ABM materials. Especially Deponit CA-N contained a high number of thermophilic bacteria (in fact up to ten times as many as mesophilic bacteria for iron reducers). Thermophilic aerobic bacteria were detected in the range of $< 10^2$ gdw^{-1} in MX-80 to 10^4 gdw^{-1} in Asha 505. Thermophilic autotrophic sulphate reducers were detected in the range of $< 10^1$ gdw^{-1} in Asha 505 to 10^2 gdw^{-1} in Deponit CA-N. Thermophilic heterotrophic sulphate reducers were detected in the range of $< 10^1$ gdw^{-1} in MX-80 and Asha 505 to 10^2 gdw^{-1} in Deponit CA-N. Thermophilic iron reducers were detected in the range of $< 10^1$ gdw^{-1} in MX-80 and Asha 505 to 10^2 gdw^{-1} in Deponit CA-N. For TP1, it was found that mesophilic aerobic bacteria were present in the range of 10^2–10^3 g^{-1}wet weight (gww^{-1}) in Asha 505, Deponit CA-N and MX-80. All other bacteria were below detection in the materials. Thus, the results in this report show that bacteria with potential corrosive or buffer degradation properties were present in the RBMs and how the same mostly failed to survive after in situ incubation at high swelling pressure and temperatures exceeding 90°C. However, the importance of finding the absolute breakpoint where bacteria survive once again becomes apparent since the ABM experiments are run with temperatures exceeding what will be found in the real repository.

A3.2 Introduction

The project Alternative Buffer Materials (ABM) aims to evaluate and confirm present knowledge of possible bentonites to be used as potential buffer materials in the KBS-3 concept for long-term storage of high level radioactive waste (HLRW). At the start of the storage process of HLRW according to the KSB-3 repository concept the temperature in the buffer will be elevated, approaching 90°C. In the ABM experiments the maximum temperature reaches even further, up to 130°C. Because of the high temperatures, bacteria able to grow at elevated temperatures have gained increased interest in the long time storage of HLRW. Bacteria able to grow at 50°C are called thermophilic, in comparison to bacteria able to grow at 20°C which are called mesophilic. This report deals with the part of the project that investigates bacterial presence in buffer materials specifically from the test package 1 (TP1), lifted on May 11th 2009 and the corresponding raw buffer material (RBM). Focus has been directed to the following three materials: Asha 505, Deponit CA-N and MX-80. It is well-known that bacteria can survive for a long period of time in bentonite as well as in other clays. Recent research has shown that bacteria such as Desulfotomaculum spp. which have the ability to survive as endospores thrive in dry bentonite (Boivin-Jahns et al. 1996, Appendix 2 in this report). An endospore is a non-active resting stage. In addition, there can also be bacteria without the ability to form endospores such as Desulfovibrio africanus present in dry bentonite (Masurat et al. 2010a, Appendix 2 in this report).

Different kinds of bacteria in the buffer material can affect the buffer and the canisters in different ways. This research was focused on three different kinds of bacteria: Cultivable aerobic heterotrophic bacteria (CHAB), sulphate-reducing bacteria (SRB) and iron-reducing bacteria (IRB). Bacteria able to grow in oxygenated environments are called aerobic bacteria and can be detected by cultivation on media containing organic carbon (with a so called CHAB analysis). Bacteria that can respire oxygen and thus decrease the oxygen content in the buffer much faster than abiotic processes could be beneficial for the repository since oxygen itself is corrosive to the copper canister to be used in the KBS-3 concept. However, many bacteria that are able to respire oxygen also have the ability to excrete compounds not favourable for a HLRW repository. Examples of such compounds are organic acids and bioligands which e.g. can mobilize several radionuclides (Johnsson 2006). Other bacteria of interest are the SRB and IRB, which can be detected by most-probable-number (MPN) analyses. During oxidation of either inorganic (i.e. hydrogen gas) or organic compounds the SRB reduces sulphate to sulphide, a compound also highly corrosive to the copper canister. Sulphate-reducing bacteria able to oxidize inorganic compounds are called autotrophic SRB whilst SRB able to oxidize organic compounds are heterotrophic. Both autotrophic SRB (Desulfotomaculum spp.) and heterotrophic SRB (D. africanus) have previously been found in bentonite (Masurat et al. 2010a, Appendix 2 in this report). Presence and survival of SRB will thus have to be evaluated in the buffer used in the KBS-3 repository. Concerning IRB, there are studies performed showing that members of the iron-reducing genus Shewanella seem to be able to perform illitisation in two weeks at atmospheric pressure and room temperature by using the smectite as an iron source (Kim et al. 2004) Illitisation of smectite is an unwanted process which decreases the swelling capacity of the buffer. Consequently, it is important to evaluate the presence and numbers of IRB in the buffer materials.

In this project, the bacterial abundance was examined in three different RBM twice with one year time laps between sampling and analysis and in buffer material that had been included in the TP1. Special emphasis was put on the abundance and identity of aerobic CHAB and anaerobic SRB and IRB, because of their abilities to affect the KBS-3 type of storages for HLRW. The ability of the bacteria to survive and grow in the different materials when incubated at elevated temperatures (50°C) was examined as well as the ability to grow when incubated at room temperature. This was done to evaluate if bacteria present in the buffer material can be active at higher temperatures as well as the normal ambient rock temperature. The samples were taken at locations in the bulk of the TP1, to eliminate the possibility to mistake bacteria introduced during the lifting for bacteria surviving in TP1.

A3.3 Material and methods

A3.3.1 Materials examined

Raw buffer material

Three RBM, Asha 505, Deponit CA-N and MX-80, were analysed to confirm the results from 2008 and add information about the bacteria present indigenous in the materials.

Test package 1

Three alternative materials retrieved from TP1 sampled 11th and 12th May were analysed regarding bacterial presence. These were Asha 505 (block 14), Deponit CA-N (block 27) and MX-80 (block 2).

A3.3.2 Sampling

Raw buffer material

Of the RBM, approximately 0.1 g dry weight^{-1} (gdw^{-1}) aliquots were weighed inside the anaerobic box and used for CHAB analyses as well as heterotrophic SRB, autotrophic SRB and IRB MPN analyses. To favour bacteria with different growth ranges, the CHAB and MPN analyses were performed at 20°C to detect mesophilic bacteria and 50°C to detect thermophilic bacteria. The analyses were initiated in August 2009.

Test package 1

Immediately after sampling *in situ*, the blocks were laminated in sterile aluminium and vacuum sealed (as described in Sandén and Nilsson 2009). The pieces were transported to the laboratory of Microbial Analytics Sweden AB. Upon arrival, they were immediately put in an anaerobic box (COY laboratory products, Grass Lake, MI, USA).

By means of a sterile hammer, knife, chisel and a ruler, sampling was performed inside the anaerobic box during June and July 2009: Eight pieces of approximately 0.1 g wet weight^{-1} (gww^{-1}) each were sampled under sterile conditions at the following distances from the center of the three blocks; 1 cm, 3 cm, 5 cm, 7 cm and 9 cm. Two pieces were used for determinations of the number of cultivable heterotrophic aerobic bacteria (CHAB) in the TP1. Six of the pieces were used for most-probable-number (MPN) analyses of heterotrophic sulphate-reducing bacteria (heterotrophic SRB), autotrophic sulphate-reducing bacteria (autotrophic SRB) and iron-reducing bacteria (IRB). As for the RBM, samples were incubated at 20°C and 50°C, which favoured bacteria with different growth ranges.

A3.3.3 Growth media

Cultivable heterotrophic aerobic bacteria

Per litre medium 0.5 g peptone (Merck, VWR, Stockholm, Sweden), 0.5 g yeast extract (Merck), 0.25 g sodium acetate (Merck), 0.25 g soluble starch (Merck, VWR), 0.1 g K_2HPO_4 (Merck, VWR), 0.2 g $CaCl_2$ (Merck), 10 g NaCl (Merck, VWR), 1 mL trace element solution (see Pedersen and Ekendahl 1990) and 15 g agar (Merck). The solution was autoclaved at 121°C for 20 min and dispensed in 20 mL aliquots in Petri dishes after cooling to about 60°C. Dilution tubes with liquid CHAB medium (i.e. without agar) was also prepared, dispensed in 9 ml-aliquots in 27-mL anaerobic tubes and sealed with blue butyl rubber stoppers and aluminum crimp seals.

Heterotrophic sulphate-reducing bacteria

The heterotrophic SRB medium was prepared as described in Hallbeck and Pedersen (2008) and were after preparation anaerobically dispensed in 9 mL aliquots in 27 mL anaerobic tubes and sealed with blue butyl rubber stoppers (no. 2048-117800; Bellco Glass) and aluminum crimp seals (no. 2048-11020; Bellco Glass).

Autotrophic sulphate-reducing bacteria

The autotrophic SRB medium was prepared as described in Hallbeck and Pedersen (2008), with the exception that no lactate was added to the medium. The medium was after preparation anaerobically dispensed in 9 mL aliquots in 27 mL anaerobic tubes and sealed with blue butyl rubber stoppers and aluminum crimp seals.

Iron-reducing bacteria

The IRB medium was prepared as described in Hallbeck and Pedersen (2008), with the exception that no lactate was added to the medium. The medium was after preparation anaerobically dispensed in 9 mL aliquots in 27 mL anaerobic tubes and sealed with blue butyl rubber stoppers and aluminum crimp seals.

A3.3.4 Inoculation

Inside the anaerobic box, the samples of approximately 0.1 gdw^{-1} of each RBM and the samples from TP1 were added to two tubes of each of liquid dilution CHAB medium, heterotrophic SRB medium, autotrophic SRB medium and IRB medium. The tubes were resealed with blue butyl rubber stoppers and aluminum crimp seals. The tubes were removed from the anaerobic box and the buffer material was left at 4°C overnight to disintegrate the buffer materials.

A3.3.5 Analyses of cultivable heterotrophic aerobic bacteria

In the CHAB analyses, ten-fold dilutions in three steps of the buffer material dissolved at 4°C overnight were made in liquid CHAB medium. 0.1-mL portions of each dilution were spread with a sterile rod on the CHAB plates in triplicate. The plates were incubated overnight or one week depending on if they were incubated in 50°C or 20°C. After incubation, the number of colony forming units (CFU) was counted and plates with between 10 and 300 colonies were counted, if available. The mean and the standard deviation for the plates from all three kinds of enrichment culture media from each material were calculated in Excel (Microsoft Corporation, Redmond, WA, USA).

A3.3.6 Analyses of most-probable-numbers of anaerobic bacteria

MPN analyses of heterotrophic SRB, autotrophic SRB and IRB at two different temperatures, 20 and 50°C were performed. The buffer material disintegrated at 4°C overnight was used in respective MPN analysis. The sample was first diluted in ten-fold dilutions in three steps. From each dilution 1 mL was inoculated under anaerobic conditions into five replicates of the respective growth media. To the autotrophic SRB, hydrogen gas was added to an overpressure of 1 bar. The MPN tubes were then incubated three and eight weeks depending on if they were growing in 50 or 20°C.

After incubation, the MPN tubes were analysed by testing for metabolic products. The MPN tubes were considered positive if the levels of metabolic products were three times higher than the background in the medium. Sulphide production in the SRB MPN tubes was measured using the $CuSO_4$ method according to Widdel and Bak (1992) on a UV–visible spectrophotometer (Genesys10UV, VWR, Stockholm, Sweden). Samples were extracted through the rubber stopper using a 1 mL syringe equipped with a 0.6×25 mm needle. Ferrous iron in the IRB MPN tubes was determined using a DR/2500 spectrophotometer (HACH, Loveland, CO, USA) and the 1,10 phenanthroline method (HACH, method no. 8146).

The MPN procedures resulted in protocols with tubes that scored positive or negative for growth. Three dilutions with five parallel tubes were used to calculate the MPN and lower and upper 95% confidence interval of each group, according to the calculations found in Greenberg et al. (1992).

A3.4 Results

A3.4.1 Cultivable heterotrophic aerobic bacteria and most-probable-numbers of anaerobic bacteria in the raw buffer materials

Mesophilic bacteria

All examined bacteria were detected in the RBM in the mesophilic growth range (Table A3-1). Mesophilic CHAB were detected in RBM in the range of 10^3 gdw^{-1} in Deponit CA-N to 10^5 cells gdw^{-1} in Asha 505. Heterotrophic SRB were most abundant in MX-80 (130 cells gdw^{-1}) whilst autotrophic SRB were most abundant in Deponit CA-N (190 cells gdw^{-1}) and IRB most abundant in Asha 505 (110 cells gdw^{-1}).

Thermophilic bacteria

As shown in Table A3-2, the presence of thermophilic bacteria in RBM was different compared to mesophilic bacteria (Table A3-1). Except from thermophilic CHAB, which was present in highest amounts in Asha 505 (10^4 gdw^{-1}, Table A3-2) most thermophilic bacteria were found in the Deponit CA-N buffer material where heterotrophic and autotrophic SRB were in the order of 10^2 and IRB 10^3 gdw^{-1}. Deponit CA-N is without question the ABM material with most potential for presence of thermophilic bacteria.

Table A3-1. Growth of mesophilic bacteria in the examined raw buffer materials.

Material	Incubation temperature (°C)	CHAB ± stdev (gdw^{-1})	SRB het (gdw^{-1})	SRB aut (gdw^{-1})	IRB (gdw^{-1})
MX-80	20	34,000 ± 11,000	130	40	40
Asha 505	20	200,000 ± 24,000	40	40	110
Deponit CA-N	20	2,400 ± 1,600	15	190	< 10

Table A3-2. Growth of thermophilic bacteria in the examined raw buffer materials.

Material	Incubation temperature (°C)	CHAB ± stdev (gdw^{-1})	SRB het (gdw^{-1})	SRB aut (gdw^{-1})	IRB (gdw^{-1})
MX-80	50	< 100	< 10	17	< 10
Asha 505	50	15,000 ± 2,300	< 10	< 10	< 10
Deponit CA-N	50	1,200 ± 2,100	230	130	1,100

A3.4.2 Temperature span in test package 1

To accelerate degenerative processes of the buffer material, the temperature during incubation in the rock in TS1 was considerably higher than will be in the HRLW repository. The temperature reached 130°C instead of the maximal 90°C expected under authentic repository conditions. The maximum temperatures in the specific locations in block no 2 (MX-80), block no 14 (Asha 505) and block no 27 (Deponit CA-N) analysed regarding bacterial abundance in this study are given in Table A3-3. Temperature sensors were not installed at distances above 6 cm from the heater, which means that the temperature probably is several degrees lower than the maximum temperature value given in Table A3-3.

Table A3-3. Measured maximum temperatures in the examined alternative buffer materials in test package 1.

Material and block	Distance to heater (cm)	Temperature span (°C)
MX-80 *block no 2*	1	110–100
	3	< 90
	5	< 90
	7	< 90
	9	< 90
Asha 505 *block no 14*	1	130–120
	3	115–105
	5	105–95
	7	< 100
	9	< 100
Deponit CA-N *block no 27*	1	115–110
	3	100–95
	5	< 90
	7	< 90
	9	< 90

A3.4.3 Cultivable heterotrophic aerobic bacteria and most-probable-numbers of anaerobic bacteria in in test package 1

Mesophilic bacteria

As revealed in Table A3-4, mesophilic CHAB were found at 1–3 cm from the heater in block 2 (MX-80) and at 1 cm from the heater in block 14 (Asha 505). The numbers of CHAB in these locations were determined to be 10^2–10^3 gww^{-1}. The standard deviations were fairly high, which is normal for analysis result of this order of magnitude. Regarding heterotrophic and autotrophic SRB and IRB, all analysed locations in block 2, block 14 and block 27 (Deponit CA-N) contained less than < 10 cells gww^{-1}.

Thermophilic bacteria

In Table A3-5, the results from the bacterial analyses in the thermophilic temperature range are shown. All CHAB analyses as well as MPN analyses of heterotrophic and autotrophic SRB and IRB of thermophilic bacteria were below the detection limit of 10^2 and 10^1 cells gww^{-1}, respectively.

Table A3-4. Growth of mesophilic bacteria in the examined alternative buffer materials in test package 1.

Material and block	Distance to heater (cm)	Temperature span (°C)	CHAB ± stdev (gww^{-1})	SRB het (gww^{-1})	SRB aut (gww^{-1})	IRB (gww^{-1})
MX-80 *block no 2*	1	110–100	500 ± 900	< 10	< 10	< 10
	3	< 90	4,300 ± 6,800	< 10	< 10	< 10
	5	< 90	< 100	< 10	< 10	< 10
	7	< 90	< 100	< 10	< 10	< 10
	9	< 90	< 100	< 10	< 10	< 10
Asha 505 *block no 14*	1	130–120	700 ± 1,200	< 10	< 10	< 10
	3	115–105	< 100	< 10	< 10	< 10
	5	105–95	< 100	< 10	< 10	< 10
	7	< 100	< 100	< 10	< 10	< 10
	9	< 100	< 100	< 10	< 10	< 10
Deponit CA-N *block no 27*	1	115–110	< 100	< 10	< 10	< 10
	3	100–95	< 100	< 10	< 10	< 10
	5	< 90	< 100	< 10	< 10	< 10
	7	< 90	< 100	< 10	< 10	< 10
	9	< 90	< 100	< 10	< 10	< 10

Table A3-5. Growth of thermophilic bacteria in the examined alternative buffer materials in test package 1.

Material and block	Distance to heater (cm)	Temperature span (°C)	CHAB ± stdev (gww^{-1})	SRB het (gww^{-1})	SRB aut (gww^{-1})	IRB (gww^{-1})
MX-80 *block no 2*	1	110–100	< 100	< 10	< 10	< 10
	3	< 90	< 100	< 10	< 10	< 10
	5	< 90	< 100	< 10	< 10	< 10
	7	< 90	< 100	< 10	< 10	< 10
	9	< 90	< 100	< 10	< 10	< 10
Asha 505 *block no 14*	1	130–120	< 100	< 10	< 10	< 10
	3	115–105	< 100	< 10	< 10	< 10
	5	105–95	< 100	< 10	< 10	< 10
	7	< 100	< 100	< 10	< 10	< 10
	9	< 100	< 100	< 10	< 10	< 10
Deponit CA-N *block no 27*	1	115–110	< 100	< 10	< 10	< 10
	3	100–95	< 100	< 10	< 10	< 10
	5	< 90	< 100	< 10	< 10	< 10
	7	< 90	< 100	< 10	< 10	< 10
	9	< 90	< 100	< 10	< 10	< 10

A3.5 Discussion

A3.5.1 Mesophilic and thermophilic bacteria in the raw buffer material

MPN analyses on the RBM were performed for several reasons. Firstly, verification of the results from 2008 was important to see if one year of storage of the RBM influenced the bacterial composition and survival. Table A3-1 shows the results from the bacterial analyses on RBM of MX-80, Asha 505 and Deponit CA-N performed in 2009 in the mesophilic temperature range. All examined groups of mesophilic bacteria, i.e. CHAB, autotrophic and heterotrophic SRB and IRB were detected. The mesophilic bacteria that were cultivable from the RBM of MX-80, Asha 505 and Deponit CA-N were approximately the same from 2008 to 2009 (Table A3-6) The aerobic bacterial CHAB populations were about 10^3–10^5 gdw^{-1}, and the anaerobic SRB and IRB were found in the range 10^1–10^2 gdw^{-1} (Table A3-1, Table A3-6). Clearly, mesophilic bacteria with abilities of oxygen depletion, sulphide production and potential enhanced illitisation were present in the materials to start with and in addition they survived a year of storage. Since the RBM were dry, it is obvious that these bacteria have found

a strategy to overcome the dry conditions, e.g. by sporulation. Thus, it can be assumed that these bacterial numbers will stay approximately the same for a long period of time. Consequently, the buffer material used in a possible KBS-3 repository will contain bacteria with potential degenerative properties.

Quantitative bacterial analyses on the RBM were also performed to examine the presence of thermophilic bacteria in MX-80, Asha 505 and Deponit CA-N. Since the buffer in a HLRW repository will be exposed to temperatures up to 90°C, the abundance of these bacteria is extremely important to examine. In general, thermophilic bacteria are gaining increased interest in the safety analysis of HLRW repositories. Since such a repository will produce heat for up to 10,000 years, the thermophilic bacteria are probably a group that should be considered carefully. The thermophilic MPN analyses performed on the RBM of MX-80, Asha 505 and Deponit CA-N show interesting results (Table A3-2). The presence of thermophilic CHAB was lower, $< 10^1$ to 10^4 gdw^{-1} compared to 10^3 to 10^5 gdw^{-1} mesophilic CHAB. Also, the presences of thermophilic anaerobic bacteria were lower in the MX-80 and the Asha 505 materials compared to mesophilic bacteria. Thermophilic autotrophic SRB (17 gdw^{-1}, Table A3-2) were detected in MX-80, but otherwise no thermophilic bacteria were present in the MX-80 or Asha 505 materials. The situation was the opposite in Deponit CA-N. Here, the number of thermophilic autotrophic SRB were 20 times higher and the number of thermophilic IRB 100 times higher than the mesophilic autotropic SRB and IRB (Table A3-1, Table A3-2). Obviously, Deponit CA-N seems to be a worse choice than MX-80 and Asha 505 as an alternative buffer taking only microbiology into account.

Table A3-6. Comparison of results from the mesophilic bacterial analyses of the raw buffer materials in 2008 and 2009.

Material	CHAB 2008 (gdw^{-1})	CHAB 2009 (gdw^{-1})	SRB het 2008 (gdw^{-1})	SRB het 2009 (gdw^{-1})	IRB 2008 (gdw^{-1})	IRB 2009 (gdw^{-1})
MX-80	6,600	34,000	< 10	130	260	40
Asha 505	84,000	200,000	90	40	70	110
Deponit CA-N	1,000	2,400	10	15	80	< 10

A3.5.2 High temperatures in the TP1

The highest temperature in which life has been proven to exist is to date 113°C (Blöchl et al. 1997). One paper suggests that iron-reducing bacteria can survive at 121°C (Kashefi and Lovley 2003). Life at these temperatures requires high enough pressure for the water not to boil. Giving these prerequisites, there are several reasons why it obvious that viable bacteria in the in situ incubated ABM materials are very important to look for:

- Dry clays often contain heat resistant-bacteria and or spores (Boivin-Jahns et al. 1996, Appendix 2 in this report).
- The temperature in the TP1 were high, reaching 130°C (Table A3-3) However, at a fem centimetres from the actual heater the temperature can be lower than 90°C and thus providing a real potential for thermophilic bacteria to exist there.
- The TP1 was incubated under pressure, which might exclude boiling of water despite the high temperature.

A3.5.3 Scarce growth in the TP1

The present part of the ABM project aimed to find out if bacteria, both mesophilic and thermophilic, are able to survive in the materials after storage underground and with temperatures reaching up to 130°C.

The worst case scenario, where we would find as substantial populations of CHAB, SRB and IRB in TP1 as in the RBM, was fortunately proven to be wrong. The bacterial growth in TS1 was very scarce and the, from a biological point of view, extreme temperatures (90–130°C, Table A3-3) were reflected in the low numbers of viable bacteria (Table A3-4 and Table A3-5). The only type of bacteria found was CHAB, which were found in the order of 10^2–10^3 gww^{-1} in the retrieved TP1 samples (Table A3-4). These CHAB were all mesophilic. The scarce survival of bacteria in TP1was expected taking the high temperatures in account. It is more remarkable that mesophilic CHAB could be detected in material exposed to these high temperatures at all. The thermophilic bacteria did not appear in the TP1 (Table A3-5 which was expected because of the extreme temperatures.

In addition to the high temperature, the bacteria need to resist the large swelling pressure provided by the buffer material to survive. Exactly how large the pressure was in TS1 has to be evaluated when appropriate experimental data are available. At temperatures around 20°C, a low but yet significant SRB activity has been reported even at swelling pressures approaching 2,000 kg m^{-3} (Masurat et al. 2010b) and examinations of bentonite in the SKB project "The Long Term Test of Buffer Material (LOT)" showed bacteria in bentonite able to withstand temperatures up to 70°C (Karnland et al. 2009). If looking at the KBS-3 concept as a whole, the importance of finding the absolute breakpoint for temperature and density where bacteria survive becomes apparent since the ABM experiments are run at temperatures exceeding what will be found in the real HLRW repository.

A3.6 Conclusions

The main conclusions presented in this report are:

- Bacteria able to grow at 20°C, mesophilic bacteria, with potentials of oxygen depletion, sulphide production and IRB in a HLRW repository of the KBS-3 type were detected in raw buffer material of MX-80, Asha 505 and Deponite CA-N (Table A3-1). One year of storage did not influence the survival of these significantly (Table A3-6). The oxygen-depleting bacteria ranged from 10^3 to 10^5 gdw^{-1} and the sulphide-producing and IRB bacteria were found in the range from 10^1 to 10^2 gdw^{-1}.
- Since the buffer in a HLRW repository will be exposed to temperatures up to 90°C, the abundance of bacteria surviving at these temperatures is important to study. The presence of these so called thermophilic bacteria in the raw buffer material of MX-80, Asha 505 and Deponit CA-N were thus examined (Table A3-2). In general, the presence of thermophilic CHAB was lower than mesophilic CHAB, ranging from $< 10^1$ to 10^4 gdw^{-1}. Also, the presences of thermophilic anaerobic bacteria were lower in the MX-80 and the Asha 505 materials. However, the situation was the opposite in Deponit CA-N. Here, the numbers of thermophilic sulphide-producing and IRB bacteria were 20–100 times higher than their mesotrophic relatives (Table A3-1, Table A3-2). Obviously, Deponit CA-N can be regarded as a bad choice as an alternative buffer material taking only microbiology into account.
- Fortunately, the bacterial growth in TP1 was very scarce and the, from a biological point of view, extreme temperatures (90–130°C, Table A3-3) was reflected in low numbers of surviving bacteria (Table A3-4 and Table A3-5). The only type of bacteria found was mesotrophic CHAB, which were found in the order of 10^2–10^3 gww^{-1}.
- However, it has to be considered that the ABM experiments are run at temperatures 40°C over the maximum temperature expected in a real HLRW repository. Previous bentonite studies have shown that bacteria can survive both high swelling pressures and high temperatures in bentonite (Masurat et al. 2010b, Karnland et al. 2009). The extremely important task of finding the absolute breakpoint for temperature combined with density where degenerative bacteria survive remains.

A3.7 References

Boivin-Jahns V, Ruimy R, Bianchi A, Daumas S, Christen A, 1996. Bacterial diversity in a deep-subsurface clay environment. Applied and Environmental Microbiology 62, 3405–3412.

Blöchl E, Rachel R, Burggraf S, Hafenbradl D, Jannasch H W, Stetter K O, 1997. Pyrolobus fumarii, gen. and sp. nov., represents a novel group of archaea, extending the upper temperature limit for life to 113 degrees C. Extremophiles 1, 14–21.

Greenberg A E, Clesceri L S, Eaton A D, 1992. Estimation of bacterial density. In Standard methods for the examination of water and wastewater. 18th ed. Washington: American Public Health Association, 9–49.

Hallbeck L, Pedersen K, 2008. Characterization of microbial processes in deep aquifers of the Fennoscandian Shield. Applied Geochemistry 23,1796–1819.

Johnsson A, 2006. The role of bioligands in microbe-metal interactions: emphasis on subsurface bacteria and actinides. PhD thesis. Göteborg University, Sweden.

Karnland O, Olsson S, Dueck A, Birgersson M, Nilsson U, Hernan-Håkansson T, Pedersen K, Nilsson S, Eriksen T E, Rosborg B, 2009. Long term test of buffer material at the Äspö Hard Rock Laboratory, LOT project. Final report on the A2 test parcel. SKB TR-09-29, Svensk Kärnbränslehantering AB, Appendix 1.

Kashefi K, Lovley D, 2003. Extending the upper limit for life. Science 301, 934.

Kim J, Dong H, Seabaugh J, Newell S W, Eberl D D, 2004. Role of microbes in the smectite-to-illite reaction. Science 30, 830–832.

Masurat P, Eriksson S, Pedersen K, 2010a. Evidence of indigenous sulphate-reducing bacteria in commercial MX-80 Wyoming bentonite. Applied Clay Science 47, 51–57.

Masurat P, Eriksson S, Pedersen K, 2010b. Microbial sulphide production in compacted Wyoming bentonite MX-80 under in situ conditions relevant to a repository for high-level radioactive waste. Applied Clay Science 47, 58–64.

Pedersen K, Ekendahl S, 1990. Distribution and activity of bacteria in deep granitic groundwaters of southeastern Sweden. Microbial Ecology 20, 37–52.

Sandén T, Nilsson U, 2009. Log book: Lifting and a first divisioon in field, May 11 and 12, 2009. Svensk Kärnbränslehantering AB. /är detta ett refererbart dokument? var är det sparat?/